Characterisation of cell walls at the feeding site of *Meloidogyne incognita*

Refik Bozbuga

Submitted in accordance with the requirements for the degree of Doctor of Philosophy (Ph.D.)

The University of Leeds
Faculty of Biological Sciences
School of Biology

February, 2017

Acknowledgements

I would like to thank my supervisor Prof. Peter E. Urwin for his guidance, contributions, advice and support.

I would also thank to Prof. J. Paul Knox from the cell wall lab as my second supervisor and for the antibodies supplied from his lab. I also would like to thank Dr. Catherine J. Lilley for help and support, and other lab members.

This project was funded by the Islamic Development Bank Merit Scholarship Programme for High Technology (MSP), some part of the tuition fee was funded by the Faculty of Biological Sciences at University of Leeds and bench fee was funded from Prof. Peter E. Urwin.

Abstract

Meloidogyne incognita induces a unique feeding structure, termed giant cells, by reprogramming plant cells in the feeding site within host plant roots. The nematode modifies the function of cells including giant cell wall composition. Characterisation of pectin, hemicellulose and glycoproteins of giant cell walls formed in different hosts was analysed. In addition the role of cell-wall genes in nematode feeding site development was also analysed.

In situ analysis was performed to determine the presence and distribution of giant cell wall components; cell wall elements were quantified using enzyme linked immunosorbent assay in nematode feeding sites on different host plants *Arabidopsis thaliana* (Brassicaceae), *Vigna angularis* (*Fabaceae*) and *Zea mays* (Poaceae). The cell wall compositions in the *M. incognita* feeding site were observed by comparison with uninfected root tissues. There were distinct responses in terms of detection of cell wall polysaccharides in the nematode feeding site of the different hosts. Modifications of cell wall polysaccharides in giant cells formed in Arabidopsis were minor compared to uninfected sections. By contrast, analysis of the giant cell wall formed in *Vigna angularis* revealed decreased amounts of mannan, xylan, galactan, processed arabinan, arabinogalactan protein and extensin. In *Zea mays*, xyloglucan, methyl esterified pectic homogalacturonan, galactan, arabinogalactan proteins increased in abundance in giant cell walls.

Arabidopsis plants that carried mutations in cell-wall related genes were analysed. Mutants for genes important in the formation of hemicellulose (*GLZ1, MSR1* and *MUR3*) together with those of the pectin related genes *BGAL5* and *RGXT1* all resulted in smaller gall development together with a concomitant reduction in nematode size in addition to a reduction in the number of nematodes recovered. Conversely mutation of the pectin-related genes *ARAD1* and *ARAD2* or the glycoprotein-related genes led to increased susceptibility to the nematodes.

Table of Contents

List of Tables

List of Figures

List of Abbreviations

AGPs	Arabinogalactan proteins
ATR FT-IR	Attenuated Total Reflectance Fourier-Transform Infrared
AX	Arabinoxylan
bp	base pairs
Ca^{2+}	Calcium ion
CAZy	Carbohydrate Active enZYmes
cDNA	Complementary DNA
CESA	Cellulose synthases
CO_2	Carbon Dioxide
Col-0	Arabidopsis Columbia ecotype (wild)
CSC	Cellulose synthesis complex
CSL	Cellulose synthesis like
Ct	Threshold cycle
CTAB	Hexadecyltrimethylammonium bromide
CWA	Cell wall apposition
CWDE	Cell wall degrading enzymes
°C	Degrees in centigrade
DAMPs	Damage associated pathogen patterns
De-PHG	De-esterified pectic homogalacturonan
Dha	3-deoxy-D-lyxo-heptulosaric acid
DNA	Deoxyribonucleic acid
DNase	Deoxyribonuclease
dNTP	Deoxynucleotide
dpi	Days post infection
EDTA	Ethylenediaminetetraacetic acid
EGTA	Ethylene glycol tetra acetic acid
ELISA	Enzyme linked immunosorbent assay
En	Endodermis
ET	Ethylene
EtOH	Ethanol
EXP	Expansin protein

FITC	Fluorescein isothiocyanate
g	Gram
GC	Giant cell
GEBD	Genome expressed browser server
GF/A	Glass microfiber filter
GH	Glycoside hydrolase
Gly	Glycine
Glyp	Glycoprotein
GRP	Glycine-rich protein
h	Hour
HG	Homogalacturonan
HRGP	Hydroxyproline-rich glycoprotein
Hyp	Hydroxyproline
J2	Second stage juvenile nematode
J3	Third stage juvenile nematode
J4	Forth stage juvenile nematode
JA	Jasmonic acid
JIM	John Innes Monoclonal
kb	Kilo base
KOH	Potassium hydroxide
LM	Leeds Monoclonal
M	Molar
MAMP	Microbial associated molecular patterns
MePHG	Methyl-esterified pectic homogalacturonan
min	Minute
ml	millilitres
MLG	Mixed linkage glucan
mM	Millimolar
mRNA	Messenger RNA
NASC	Nottingham Arabidopsis Stock Centre
PAMP	Pathogen associated molecular patterns
PBS	Phosphate-buffered saline
PCR	Polymerase chain reaction

PGIPs	Polygalacturonase-inhibiting proteins
PGs	Polygalacturonases
Ph	Phloem
PIPES	Piperazine-N,N′-bis(2-ethanesulfonic acid)
PPN	Plant parasitic nematodes
PRP	Proline-rich proteins
qRT-PCR	Quantitative reverse transcriptase PCR
RG-I	Rhamnogalacturonan-I
RG-II	Rhamnogalacturonan-II
RKN	Root-knot nematode
RNA	Ribonucleic acid
ROS	Reactive oxygen species
RPM	Rotations per minute
sec	Seconds
TAE	Tris-acetate-EDTA
TAIR	The Arabidopsis information sources
T-DNA	Transfer DNA
UV	Ultraviolet
µ	Micro
µg	Microgram
µL	Microliter
µm	Micrometre
VC	Vascular cylinder
WAKs	Wall-associated kinases
WT	Wild type
Xy	Xylem vessels

Chapter 1

General Introduction

1 General Introduction

1.1 The plant cell wall

Plants are essential organisms in the terrestrial biosphere, and human life is highly dependent on plants and subsequently plant cell walls, as a carbon source for the human food chain, fossil fuels, pulp, wood, paper, cotton, linen, gums, and chemical feedstocks (Albersheim et al., 2011). The plant cell wall is a partly-rigid and complex structure that plays a part in all plant biology (Albersheim et al., 2011, Heredia et al., 1995). Plant cell walls have many functions; determining cell shape, providing mechanical strength, carbohydrate storage, signalling, a metabolic role and the recognition of responses (Albersheim et al., 2011, Albersheim et al., 1994, Kaczkowski, 2003). The plant cell wall also plays an important role in plant cell growth and acts as a barrier against many different pathogens and herbivores (McNeil et al., 1984, Caffall and Mohnen, 2009). In general, the plant cell wall consists of cellulose, hemicelluloses, pectic substances, lignin, proteins and enzymes (Heredia et al., 1995). It is usually classified as either primary (growing cells) or secondary (thickened structures) where the primary cell wall is composed of polysaccharides and structural proteins and the secondary cell wall contains extra cellulose and lignin (Albersheim et al., 2011). The primary cell wall is typically composed of 20% cellulose microfibrils, 70-80% non-cellulosic polysaccharides and 10% structural glycoproteins (McNeil et al., 1984, Albersheim et al., 1994). The secondary cell wall is formed after the primary cell wall (Heredia et al., 1995) and has different ratios of constituents compared to the primary wall (Murugesan et al., 2015). The secondary cell walls composed of mainly cellulose, xylan and glucomannan (hemicellulose), lignin (Mellerowicz and Sundberg, 2008, Kumar et al., 2016, Murugesan et al., 2015), are accompanied by other polysaccharides (Mellerowicz et al., 2001) and glycoprotein (Girault et al., 2000). Cellulose and glucuronoxylans are major components of the secondary cell walls of dicots and glucuronoxylans may be involved in morphogenesis of lignified secondary cell walls (Reis and Vian, 2004). The pectin (galactose) is found during the secondary cell wall formation (Gorshkova et al., 2009). Secondary cell wall has less protein than primary cell walls (Keller, 1993). The secondary cell walls may consist of three-layer S1, S2 and S3 wall structures (Reis and Vian, 2004) where the direction of the cellulose microfibrils differs between the layers (Murugesan et al., 2015). The S1 (transverse), S2

(longitudinal) and S3 (abrupt reorientation) are formed from the reorientation of microfibrils (Mellerowicz et al., 2001). The secondary cell wall increases the cell wall strength and cell wall rigidity of plant cell wall and may resist negative pressures in plant tissues (Cosgrove and Jarvis, 2012), and it is the deposition of carbohydrate storage (Murugesan et al., 2015).

1.1.1 Composition of the plant cell wall

Plant cell wall molecules can be classified into major biochemical groups: cellulose, hemicellulose, pectic polysaccharides, other cell wall polysaccharides (such as mixed linkage glucan, β(1→3)-D-glucan etc.), proteins, glycoproteins, lignin, suberin, cutin, waxes and silica (Albersheim et al., 2011).

1.1.1.1 Cellulose

Cellulose is the main essential component of plant cell walls (Taylor, 2008). Cellulose has been studied for many years but a lot of different aspects, including cell wall biosynthesis, have not been fully understood (Cosgrove, 2014, Basu et al., 2016). The amount of cellulose in primary walls varies depending on the plant species and particular organ: grasses (monocotyledon) contain between 6-10% in cell walls of leaves and 20-40% in stems, however, for dicotyledon plants such as Arabidopsis, a leaf cell wall contains 15% cellulose with 6-33% in the stems (Caffall and Mohnen, 2009). Cellulose is a polysaccharide with the formula $C_6H_{10}O_5$, consisting of many linear chains of β(1→4) linked D-glucose units, and it is the most stable polysaccharide in the plant cell wall (Albersheim et al., 2011). The number of glucose units in cellulose chains differs between secondary and primary cell walls, reaching 8000 in primary cell walls but up to 15000 in secondary cell walls (Brown, 2004). These β(1→4) linked D-glucose chains form the cellulose microfibrils. Around 36 glucan chains held together by hydrogen bonds (Cosgrove, 2014). But the real number of β(1→4) linked D-glucose chains has been doubtful with a suggested range between 30-50 β(1→4) linked glucan chains forming the cellulose microfibril alignment (Albersheim et al., 2011). Cellulose biosynthesis, which involves the formation of cellulose synthases complexes in the plasma membrane and the subsequent polymerisation of glucose into β(1→4) glucan chains, is a complex process (Slabaugh et al., 2014, Reiter, 2002). Cellulose synthase enzymes are

secreted to the plasma membrane as part of rosette-type structures (McFarlane et al., 2014) each comprising six hexagonally arranged particles (Cosgrove, 2005, Mutwil et al., 2008) that act together to carry out cellulose chain elongation and lateral aggregation of the chains into a crystalline microfibril (McFarlane et al., 2014).

1.1.1.2 Hemicellulose

Hemicelluloses are complex heteropolymers comprising glucose, mannose, or xylose with a β(1→4) linked structure (Scheller and Ulvskov, 2010). They are bound to cellulose microfibrils by hydrogen bonds to arrange the matrix structure of the plant cell wall (Leroux et al., 2011). Hemicelluloses are structurally similar to cellulose (Leroux et al., 2011) but they can be branched or modified with other sugars (Figure 1.1) and have shorter chains. Hemicellulose comprises about 1/5 of the biomass in plants (Albersheim et al., 2011, Scheller and Ulvskov, 2010). Cellulose synthesis like (CSL) genes may be involved in the biosynthesis of hemicellulose (Leroux et al., 2011) that, unlike cellulose, takes place in the Golgi apparatus. The hemicellulose group of polysaccharides includes heteromannan, xylan, xyloglucan and mixed linkage glucan (Scheller and Ulvskov, 2010, Leroux et al., 2011).

Heteromannans

Heteromannans, of which galactoglucomannan, mannan, galactomannan and glucomannan are all sub-groups, contain mannosyl residues (Scheller and Ulvskov, 2010). Galactoglucomannan and galactomannan have β(1→4) linked mannose and glucose, although glucomannan and mannan contain pure β(1→4) linked mannose (Pauly et al., 2013). The mannans and galactomannans which were abundant in early land plants, and still occur in walls of some algae and mosses, might be the oldest of the hemicelluloses (Scheller and Ulvskov, 2010). The activated nucleotide sugars GDP-mannose, UDP-galactose and GDP-glucose are involved in the synthesis of heteromannans (Pauly et al., 2013). A member of the cellulose synthase-like gene family is involved in glucomannan synthesis (Leroux et al., 2011). The biological functions of mannan are cell wall rigidity, tissue differentiation and cell wall signalling (Pauly et al., 2013).

Xylans

Xylans are the main hemicellulose of monocot cell walls making up 15-20% of the dry weight (Varner and Lin, 1989) and they are also the major hemicellulose in the secondary cell walls of dicots (Rennie and Scheller, 2014). Xylans have a backbone of β-(1→4)-linked xylose residues (Varner and Lin, 1989) that is commonly substituted with α-(1→2)-linked glucuronosyl and 4-*O*-methyl glucuronosyl residues giving rise to glucuronoxylan in secondary walls of dicots (Rennie and Scheller, 2014). In general, xylans abundant in the primary cell walls of grasses contain numerous arabinose residues attached to the backbone and are termed glucuronoarabinoxylans which can create xylose or ferulic acid substitutes (Rennie and Scheller, 2014) (Figure 1.1c). The feruloylated glucuronoarabinoxylans are found exclusively in the cell wall of commelinid monocots amongst seed-bearing plants (Scheller and Ulvskov, 2010). Arabinoxylan (AX) which may reach up to 70% of endosperm walls in grasses, consists of arabinose with acetyl substitutions (Pauly et al., 2013).

Xyloglucan

Xyloglucan comprises 20-25% of the cell wall dry weight in dicot plants whereas only 2-5% in the cell wall of grasses (Varner and Lin, 1989, Scheller and Ulvskov, 2010). Xyloglucan binds the cellulose microfibrils to form a cellulose-xyloglucan network in plant cell wall (Pauly and Keegstra, 2016). The structure of xyloglucan consists of a glucan backbone (β(1→4) linked O-glucosyl residues) with side chains (Varner and Lin, 1989). The variation of xylosyl with glycosyl and nonglycosyl substitutions in xyloglucan plays functional and taxonomic roles in plants (Scheller and Ulvskov, 2010). Xyloglucan structure varies depending on the plant species and cell type (Pauly and Keegstra, 2016) and the xyloglucan type, XXXG (three-xylosyl-residues per glucosyl-residue pattern) is common among most plants, but *Poaceae* and *Solanaceae* families have an XXGG (two-xylosyl-residues with two glucosyl-residues) pattern (Leroux et al., 2011).

The *CSLC* genes which belong to the cellulose synthesis-like-gene family are involved in forming the xyloglucan backbone (Leroux et al., 2011) whilst specific glycosyltransferases add the side-chains. For example, the Arabidopsis genes *XXT1*

and *XXT2* which encode xylosyltransferases are involved in xyloglucan biosynthesis in this species (Cavalier et al., 2008).

Xyloglucan is involved in a cross-linking network with microfibrils bound by hydrogen bonds (Cosgrove, 2005), changing the cellulose architecture and cell wall rigidity (Scheller and Ulvskov, 2010). Deficiency of xyloglucan results in decreased cell wall extensibility (Chanliaud et al., 2004). It may also play roles in cell wall elongation, cell wall mechanics and cell wall growth (Pauly et al., 2013).

Mixed Linkage Glucans (MLGs)

MLGs are specifically found in the Poales and also in *Equisetum* (Pauly et al., 2013). They are β(1→4) linked glucans which contain several single β(1→3) linkages (Carpita, 1996, Scheller and Ulvskov, 2010) (Figure 1.1b). The 20% of dry mass in mesophyll tissue of maize is MLGs (Pauly et al., 2013) that are predominantly found in older stems, and developmentally regulated and vary during the cell elongation (Vega-Sanchez et al., 2013). Although all other hemicelluloses contain side chains which are added by glycosyltransferases, MLGs lack side chains (Leroux et al., 2011). MLG is bonded to cellulose like other hemicelluloses (Kiemle et al., 2014) and is involved in cell wall strengthening (Kido et al., 2015). MLG may play a structural role, but the mechanisms of MLG synthesis have not been fully understood (Pauly et al., 2013).

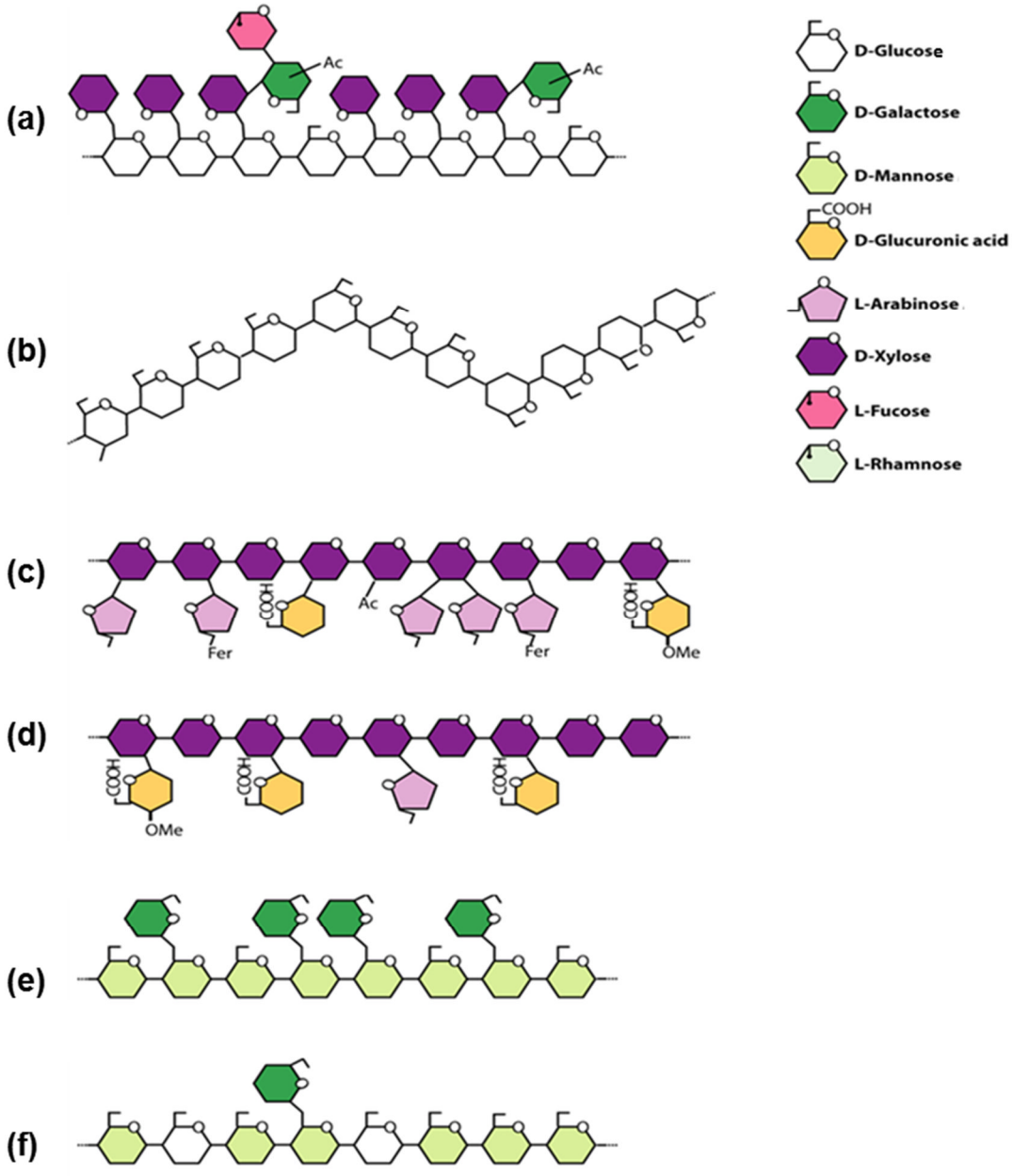

Figure 1.1 Hemicellulose structures in the plant cell wall. Hemicellulose structure can vary depending on different tissue and plant species. (a) Xyloglucan backbone substituted side chains structure in pea and Arabidopsis. (b) Mixed linkage ß-glucan is found typically in Poales such as maize. (c) Glucuronoarabinoxylan is found in commelinid monocots such as banana. (d) A typical dicotyledon structure: glucoroxylan. (e) A typical fabaceace seeds: galactomannan. (f) The conifer wood is a good example for a typical structure of galactoglucomannan. The figure was modified from Scheller and Ulvskov (2010).

1.1.1.3 Pectin

Pectin is a complex polysaccharide found in plant primary cell walls which has many functions, including plant growth and development (Ridley et al., 2001). Around 30% of cell wall polysaccharides in dicotyledon, gymnosperm, and non-Poales monocotyledon plants are pectic polysaccharides (Caffall and Mohnen, 2009). Pectin and hemicellulose cross-link with cellulose microfibrils and bind with covalent bonds to other cell wall molecular structures (Wei et al., 2009). The pectic polysaccharides are involved in cell wall rigidity, intermediate defence, cell adhesion and stomatal function (Caffall and Mohnen, 2009). Following a pathogen penetration, the pathogen degrades the pectin in order to breakdown the cell wall and oligogalacturonides that are well established part of a signalling cascade that senses wall degradation upon pathogen attack (Ridley et al., 2001). The major groups of pectic polysaccharides - homogalacturonan, rhamnogalacturonan-I, xylogalacturonan and rhamnogalacturonan-II are shown in Figure 1.2. Among these polysaccharides, homogalacturonan and rhamnogalacturonan-I are more abundant than the others (Harholt et al., 2010).

Homogalacturonan (HG)

HG is the most abundant polysaccharide in pectin (Caffall and Mohnen, 2009), and is formed of linear chains of 1,4-linked α-D-galactopyranosyluronic acid residues that are heavily methyl esterified when first incorporated into the cell wall (Harholt et al., 2010). Homogalacturonan is available in the primary cell wall and middle lamella (Patova et al., 2014), and is involved in the cell wall strength (Caffall and Mohnen, 2009), plant development and biotic stress (Senechal et al., 2014).

Rhamnogalacturonan-I (RG-I)

RG-I is a complex and usually branched pectic polysaccharide (Harholt et al., 2010) (Figure 1.2) and has more than 30 different side chains with galactosyl and arabinosyl residues (Varner and Lin, 1989). L-rhamnosyl, L-arabinosyl D-galactosyluronic acid, D-galactosyl and small amounts of L-fucosyl are the main components of rhamnogalacturonan I that the interchanging of 2-linked L-rhamnosyl and 4-linked D-galactosyluronic acid residues are the backbone of rhamnogalacturonan I (McNeil et al., 1984). The nature of the side chains of galactan and arabinan modifications alters the plant cell wall mechanical structure (Bidhendi and Geitmann, 2016).

Additionally, rhamnogalacturonan-I is involved in the tension of the cell wall that may protect against the rain, wind and heavy fruits (Mikshina et al., 2015).

Rhamnogalacturonan-II (RG-II)

Structurally, as the most complex polysaccharide within pectin in higher plants (Perez et al., 2003), rhamnogalacturonan-II contains up to 15 (1→4)-linked-α-D-GalpA units, some of which carry four well-defined side chains, often referred to as A-, B-, C-, and D-side chains (Pabst et al., 2013, Vidal et al., 2000, Glushka et al., 2003). Rhamnogalacturonan-II accounts for 10% of pectic polysaccharides (Harholt et al., 2010) and plays an important role for the growth, development and mechanical structure of plant cell walls (Perez et al., 2003, O'Neill et al., 2004). The complexes of rhamnogalacturonan II- borate support the cell wall strength (Caffall and Mohnen, 2009). The structure of rhamnogalacturonan II is nearly the same among plant families: *Gramineae*, *Leguminoseae*, *Liliaceae*, *Apiaceae*, *Amaryllidaceae*, *Araceae*, *Cucurbitaceae*, *Brassicaceae* (Perez et al., 2003).

Xylogalacturonan

Xylogalacturonan consists of a α-(1→4)-linked D-galacturonic acid backbone with β-D-xylose substitution (Patova et al., 2014). The level of xylose substitution of the backbone varies from 20% to 80% depending on the source (Patova et al., 2014). The xylogalacturonan is available within the pectin in the cell wall and the xylose content is uniformly distributed within the plant (Zandleven et al., 2007). The occurrence of xylogalacturonan in many tissues suggests that it may have several functional properties (Patova et al., 2014).

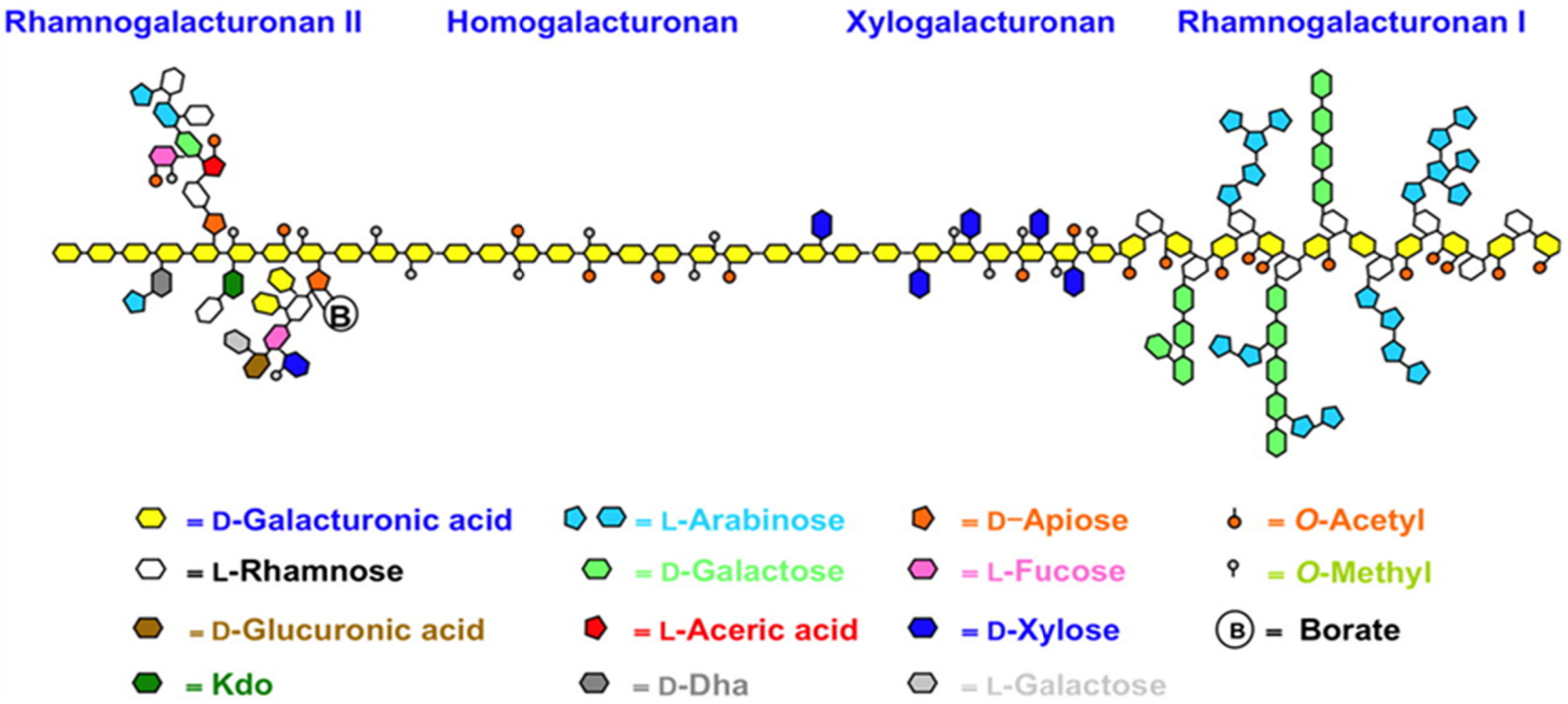

Figure 1.2 The structure of pectin. The pectin backbone is formed of galacturonic acid. Pectic polysaccharides consists of Rhamnogalacturonan II, homogalacturonan, xylogalacturonan and rhamnogalacturonan I. Rhamnogalacturonan and homogalacturonan are more abundant pectic polysaccharides than rhamnogalacturonan II and xylogalacturonan. Kdo, 3-Deoxy-d-manno-2-octulosonic acid; DHA, 3-deoxy-d-lyxo-2-heptulosaric acid. The figure was taken from Harholt et al. (2010).

1.1.1.4 Plant cell wall proteins

The plant cell wall comprises many diverse proteins, proteoglycans and glycoproteins (Albersheim et al., 2011) that can be classified based on amino acid content (Showalter, 1993). Structural proteins are also divided into classes based on repeated sequence motifs which may consist of 2-12 amino acids (Albersheim et al., 2011). The repeated sequence motifs which are augmented by specific amino acids create different classes of proteins termed as hydroxyproline-rich glycoproteins (HRGPs) and glycine-rich proteins (GRPs) and proline-rich proteins (PRPs) (Showalter, 1993, Kieliszewski et al., 1995, Cassab, 1998, Albersheim et al., 2011, Nobre and Evans, 1998). All plant cell wall proteins contain hydroxyproline (Hyp) and they are glycosylated apart from glycine-rich proteins (Cassab, 1998). Cell wall proteins are found in many land plants and algae (Cassab, 1998). Cell wall proteins are indispensable components of plant cell walls and they play many biological roles including alterations of cell wall structure, signalling, cell wall strength, expansion, and cell wall metabolism (Jamet et al., 2006, Albersheim et al., 2011).

Hydroxyproline-rich glycoproteins (HRGPs)

HRGPs have several functions in plant growth (Showalter et al., 2010) and are involved in a cell wall associated plant defence against pathogens and plant cell wall strengthening (Deepak et al., 2010). HRGPs can be categorised as proline-rich proteins (PRPs), arabinogalactan proteins (AGPs) and extensin (Taylor et al., 2012). In addition, AGPs, PRPs and extensin are hyperglycosylated, moderately glycosylated and lightly glycosylated, respectively (Showalter et al., 2010). AGPs and extensin are found in most tissues of plants (Heredia et al., 1995, Jose-Estanyol and Puigdomenech, 2000). AGPs belong to proteoglycans which contains repetitive dipeptide motifs and are found on the plant cell walls (Knoch et al., 2014). The cell differentiation, development and cell-cell interaction can be controlled by AGPs (Jose-Estanyol and Puigdomenech, 2000) and can be involved in plant reproductive process (Pereira et al., 2015). Extensin is Hyp-rich structural glycoproteins with interchanging hydrophilic and hydrophobic motifs (Lamport et al., 2011). The extensin which is found in dicots is rich in hydroxyproline and serine with the mixture of histidine valine, tyrosine and lysine amino acid (Showalter, 1993). Two types (Pex 1 and SerPro4) of extensin are found in monocotyledon species, but extensin related

gene expression is found in meristematic and vascular tissues during wounding of maize (Jose-Estanyol and Puigdomenech, 2000). The extensin is involve in defence response and mediated oxidative cross-linking (Jose-Estanyol and Puigdomenech, 2000).

Glycine-rich proteins (GRPs)

GRPs are other central structural cell wall proteins (Keller, 1993) that have semi-repetitive glycine-rich motifs (Mangeon et al., 2010) and numerous proteins are rich in Glycine 'Gly' amino acid approximately 50-70% (Keller, 1993). They are found both in dicots and monocots (Showalter, 1993). GRPs act as structural role in plant cell wall components and they are involved in the formation of secondary cell walls and the biosynthesis of lignin (Mangeon et al., 2010).

Proline-rich proteins (PRPs)

PRPs are lightly glycosylated and comprise repetitive motif, and absence of Serine amino acid (Cassab, 1998). They are found in different cell types specifically during the development including cortical cells, hypocotyls, seed coats (Keller, 1993), nodulation, normal plant development and germination (Showalter, 1993, Cassab, 1998).

Expansin (EXP)

EXPs are novel cell wall proteins with around 27 kiloDalton molecular weights (Cosgrove, 1998). Expansin is involved in the development plant stages including the growth of root and germination (Marowa et al., 2016), cell wall alteration (Yan et al., 2014), cell growth (Zhao et al., 2012), root hair elongation (Yu et al., 2011), cell wall loosing and cell wall growth and enlargement (Cosgrove, 2005).

1.1.2 Plant cell wall with pathogens

Plant cell walls are the first structural layer that comes in contact with plant pathogens. Pathogens are required to overcome the plant cell wall to reach the interior organelles of the cell. Plant cell walls act as a physical barrier and also a sensory barrier in the defence response (Albersheim et al., 2011). The damage to plant cell walls can be either physical or enzymatic digestions upon pathogen infection. During

damage of cell walls, important changes occur in the cell wall metabolism, then the modification of plant cell wall is visible (Hamann, 2015).

Plant pathogens such as bacteria, fungi and nematodes secrete many plant cell wall degrading enzymes (CWDE) including glucanases, xylosidases, arabinosidases, pectinases, polygalacturonases and glucosidases and following the action of these enzymes, the released oligosaccharides (often described as damage-associate molecular patterns, or DAMPs) may act as elicagpitors for membrane receptors to trigger the plant defence (Hematy et al., 2009). Pathogen molecules themselves, known as microbial/pathogen-associated molecular patterns (MAMPs/PAMPs), are also recognised by cell surface pattern recognition receptors to trigger inducible defence responses including a hypersensitive response and programmed cell death. Some of the plant responses to pathogen infection are specifically associated with reinforcement of the cell wall such as the synthesis of lignin, phenolic complexes and glucan polymers (Vallarino and Osorio, 2012). Successful plant cell wall-associated defences may terminate the pathogen during the early step of pathogen attack (Underwood, 2012).

The diverse cell wall compositions among plant species may be a factor in limiting pathogen host range (Underwood, 2012) and will affect cell wall components involved in host-pathogen interactions (Vorwerk et al., 2004).

The compositions of plant cell walls, cellulose, hemicellulose, pectin and glycoproteins (Albersheim et al., 2011), may be modified by the plant defence to resist the pest and diseases in crops (Santiago et al., 2013). Various roles have been postulated for arabinogalactan proteins: cell division, plant microbe interactions and programmed cell death (Seifert and Roberts, 2007). Changes in xyloglucan endotransglucosylase/hydrolase expression and xyloglucan endo-transglycosylase activity during apple fruit infection by *Penicillium expansum* suggest xyloglucans are involved in host-pathogen interaction (Munoz-Bertomeu and Lorences, 2014).

The complex structures of the plant cell wall need to be modified by plant parasitic nematodes both during the invasion of host roots and to allow feeding, as the plant cell wall is a barrier to reach the nutrient within the cell. Therefore, detailed descriptions of the nematode-plant interactions are discussed in the following section.

1.2 Nematodes

The phylum Nematoda is one of the largest within the Animalia, containing 25,043 nematode species, which have been identified to date (Zhang, 2013). Most nematodes are microscopic organisms that are bilaterally symmetrical-vermiform, unsegmented metazoans (Bird and Bird, 1991) inhabiting a very broad range of environments from the poles to the tropics and are found in freshwater, marine and soil habitats (Nicholas, 1984). They can be classified according to their feeding habits that include free living, plant and animal parasites (Decraemer and Hunt, 2006, Nicholas, 1984). Specifically, nematodes that live mainly in the soil environment can be categorised based on their food source, for example plants, fungi, bacteria, omnivorous, or predatory on other nematodes (Nicholas, 1984).

A free-living nematode species, *Caenorhabditis elegans*, feeds on bacteria and it was the first multicellular organism to have its genome completely sequenced (Consortium, 1998). *C. elegans* has a number of inherent traits that facilitate research that has led to it becoming a model organism for research scientists (Strange, 2006). *C. elegans* has a short life cycle, its body structure is transparent, it has a fast reproductive rate and it is easy and cheap to culture in the laboratory (Hope, 1999). This nematode species has been studied at the molecular level since 1974 and there is a wealth of information on the development and genetics of the animal which has consequently led to a large number of tools, such as characterised mutants being available to the research community (Strange, 2006).

Nematodes can parasitize animals including humans, insects, or plants. Animal parasitic nematodes, which are parasites of many invertebrate and vertebrate animals, attack a range of animal species from mice (Tattersall et al., 1994) to whales (Forbes, 2000). Some species are damaging to human health; for instance, *Ascaris lumbricoides,* a gastrointestinal nematode, infects 900 million people and causes 8,000 deaths and 1,292,000 disabilities a year in the world (Hirst and Stapley, 2000). *Enterobius vermicularis,* an intestinal parasite*,* infects mostly school-aged children and causes perianal itching, anorexia, abdominal pain, irritability, restlessness and insomnia. It is the most common helminth infection in the USA and Western Europe; its prevalence rate in England is 50% in school-aged children (Burkhart and Burkhart, 2005).

1.2.1 Plant parasitic nematodes

Plant parasitic nematodes (PPNs) are an important group in the nematode phylum (Figure 1.3). PPNs consist of 15% of the known nematode species (there are approximately 4,100 species) and they cause extensive damage to crops estimated at $157 billion per annum, globally (Perry and Moens, 2013, Abad et al., 2008). Plant parasitic nematodes can be classified depending on their parasitic strategies and can be broadly divided into ectoparasites and endoparasites (Perry and Moens, 2013).

Ectoparasites

Ectoparasitic nematodes are present on the outer surface of plants and their whole body does not enter the plant roots. Ectoparasites generally feed on the root hairs, epidermal cells and/or deeper tissues. They can be divided into migratory ectoparasites, sedentary ectoparasites and semi-ecto/endo parasites. *Belonolaimus* and *Dolichodorus* are examples of migratory ectoparasites that feed on deeper root cells repeatedly in short feeding bouts, moving along the root system. Generally, black lesions, stubby roots, stunting, wilting plants are visible symptoms of these nematodes. Longidoridae and Trichodoridae families carry plant viruses: nepoviruses and tobraviruses. From the Longidoridae family, *Xiphinema index* is one of the economically damaging plant parasitic nematodes that is a virus-vector species. It causes not only direct effect on the roots of plants such as necrosis, galling and lateral root development but also indirect effects as it transmits a fanleaf virus. Sedentary ectoparasites, as the collective term suggests, do not move along the root but feed from a specific cell or group of cells for several days. All the developmental stages of ectoparasitic nematodes feed on plant roots. The nematode stylet, a hollow protrusible needle-like feeding structure, penetrates into cells causing necrosis and some gall formation (Decraemer and Geraert, 2006).

Endoparasites

Endoparasitic nematodes are divided into two categories, migratory and sedentary endoparasites. Lesion nematodes (*Pratylenchus* spp.), burrowing nematodes (*Radopholus* spp.), rice root nematodes (*Hirschmanniella* spp.), the stem and bulb nematode (*Ditylenchus dipsaci*), bud and leaf nematodes (*Aphelenchoides fragaria* and *Aphelenchoides ritzemabosi*), *Aphelenchoides besseyii* and the pinewood nematode (*Bursaphelenchus xylophilus*) are important species and/or genera of

migratory endoparasitic nematodes. The symptoms of endoparasitic nematodes can vary within plants: enzymatic degradation of host tissue, inducing hormonal imbalance, causing galls, swelling and root lesions. The different life stages of migratory endoparasitic nematodes are found within the plant tissues; however, no permanent feeding site is found within the plant (Duncan and Moens, 2006).

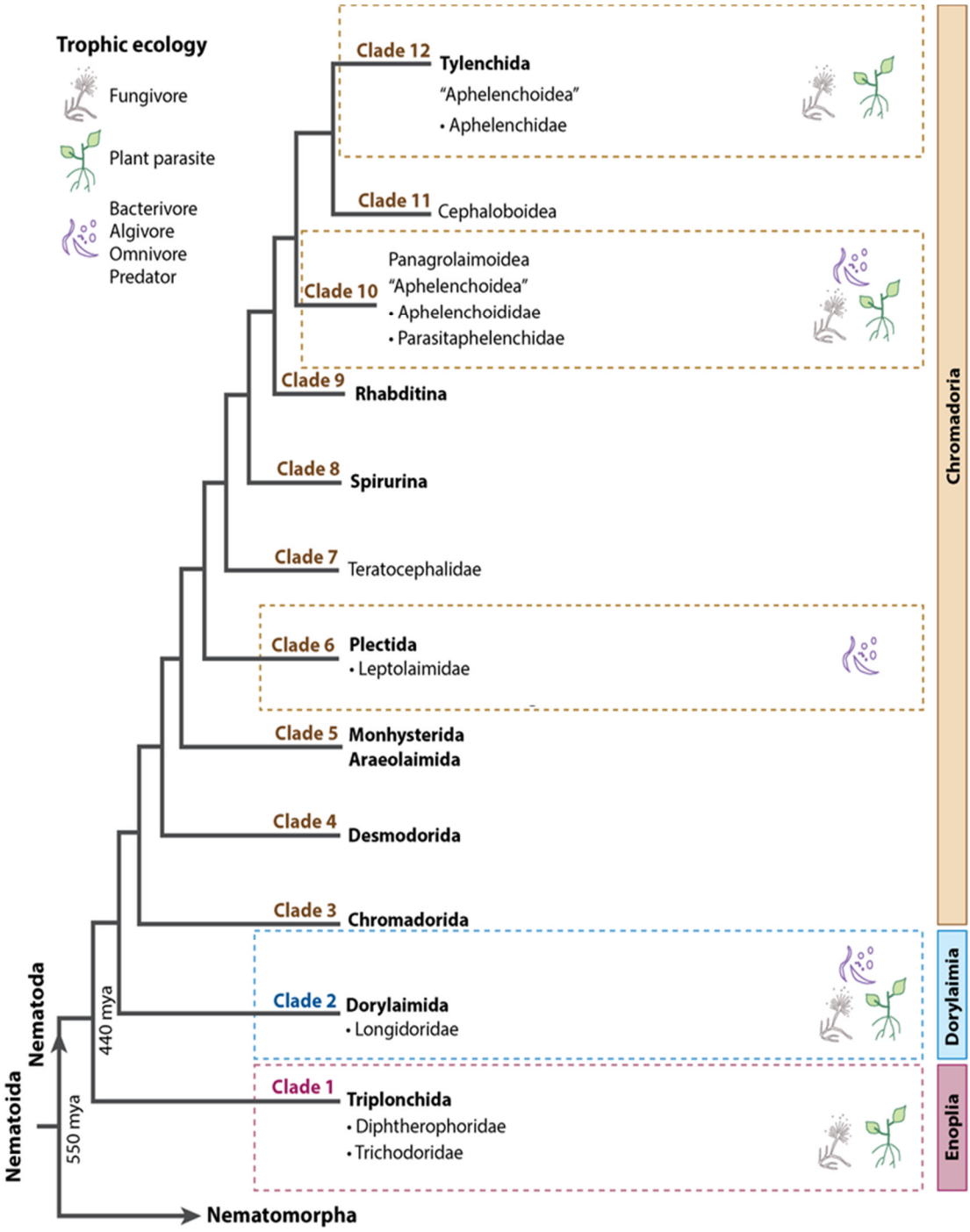

Figure 1.3 Phylogenetic tree of the nematode phylum based on SSU rDNA sequence. Most of the known plant parasitic nematode species are found in Clade 12 (Tylenchida), followed by other clades: Clade 10, Clade 2 and Clade 1, respectively. Figure was modified from Quist et al. (2015).

1.2.2 Sedentary endoparasitic nematodes

Sedentary endoparasitic nematodes are the most economically damaging groups of plant parasitic nematodes and feed from specialised feeding cells that they induce within host plant roots. The second-stage juvenile of sedentary endoparasitic nematodes is the only infective stage that invades root tissues and establishes a permanent feeding site (Perry and Moens, 2013). Females of endoparasitic nematodes do not move from the feeding site and spend their entire adult stage at this site. Life cycle strategies of sedentary plant parasitic nematodes are dissimilar to other nematode groups. Sedentary endoparasitic nematodes can be divided into two main groups based on the feeding site formed (Perry and Moens, 2013): cyst nematodes and root knot nematodes (Perry and Moens, 2013, Wyss and Grundler, 1992).

1.2.2.1 Cyst nematodes

The *Heterodera* and *Globodera* genera contain economically important species of cyst nematodes that cause damage from temperate regions to tropical and subtropical regions. *Heterodora filipjevi* and *H. avenae* affect wheat, barley oat and grass. *H. glycines* affects soybeans and lupins, and *H. sacchari* causes damage to rice, sugarcane and the *Poaceae* family. *Globodera pallida* and *G. rostochiensis* (potato cyst nematodes) cause yield losses to potato, tomato and aubergine (Turner and Rowe, 2006) including damage to 9% of the potato crop in Europe (Jones et al., 2013, Turner and Rowe, 2006).

1.2.2.2 Root knot nematodes

As obligate sedentary plant parasitic nematodes, *Meloidogyne* Göldi, 1982 spp., which are also known as root knot nematodes (RKNs) are significant parasites of higher plants. RKNs are the most economically important group of plant parasitic nematodes in that they cause damage to plants in both direct (crop losses) and indirect ways (quarantine regulations) (Perry and Moens, 2013). For instance, the crop losses caused by RKNs account for 25% in West Africa, 15% in South America and 11% in South Asia. The damage of RKNs appears in various ways such as root galling, root malformation, stunting and wilting (Perry and Moens, 2013). Root knot nematodes have more than 100 species and the most common species are *Meloidogyne incognita*, *M. javanica*, *M. arenaria* and *M. hapla* (Moens et al., 2010).

Although these four are accepted as the major root knot nematode species, some minor species (*M. minor, M. exigua, M. enterolobii, M. fallax, M. paranaensis, M. chitwoodi*) should not be neglected as they can be more and/or equally important depending on crops and regions (Elling, 2013). *Meloidogyne* spp consists of mainly parthenogenetic species and male rate is very low except under stress conditions. The parthenogenetic species generally have large host ranges and *M. incognita* infects almost all plant families in tropical and subtropical regions including cereals, legumes, vegetables, trees and fibre crops. However, some exceptions are apparent such as *M. incognita* race 3 which has a limited host range (Trudgill and Blok, 2001).

Hatching and invasion

Eggs of RKN are placed in gelatinous egg sacs which are located on the galled root surface (Karssen et al., 2013). The *Meloidogyne* female can lay up to 30-40 eggs per day and the total number of eggs may reach up to 770 in a single egg mass (Curtis et al., 2010). Embryogenesis and the first moult occur inside eggs (Jones and Goto, 2011). Hatching happens in suitable conditions, mostly depending on temperature and water availability (Karssen et al., 2013) and hatching is generally not affected by the release of root diffusate, however stimulation may occur (Perry and Wesemael, 2008). For example, the hatching of J2s of *M. chitwoodi* produced on young plants is not affected by root diffusate but a proportion of eggs produced at the end of the growing season do require plant root diffusate to stimulate hatch i.e. hatching is affected by host plant age (Wesemael et al., 2006).

Egg shell permeability allows water and solute transport to trigger the hatching. Chitinase and lipase enzymes, possibly located in the egg fluid, are involved in hatching. Other enzymes may be involved in altering the permeability of the lipid layer of the eggshell (Perry and Clarke, 1981).

Following hatching, second-stage juveniles (J2s) of *M. incognita* move to neighbouring roots. Organic and inorganic compounds which are secreted by plant roots and carbon dioxide attract the J2s (Curtis et al., 2010). Carbon dioxide (CO_2) indicates biological activity within the soil and attracts the root knot nematodes (Rasmann et al., 2012, Curtis et al., 2010). Root diffusate affects the *M. incognita* J2 behaviour, causing the surface of the cuticle to undergo modification. The binding of plant host auxins in *M. incognita* chemosensory organs (nematode amphid) may act

as a signal to orientate the nematode to the plant root (Curtis, 2008). Hatched *Meloidogyne* juveniles can migrate 20 cm in natural soils (14-22% clay and silts), however different soil texture (Prot and Vangundy, 1981) and pore size affect the nematode migration (Eo et al., 2007).

Parasitizing, nutrient uptake and nematode development

Once a root-knot nematode J2 finds a root it enter the plant root by using its stylet mechanically along with cell wall degrading enzymes released from its subventral pharyngeal glands through the stylet (Davis et al., 2004). The J2 migrates intercellularly towards the root tip, and once it reaches the apical meristematic region, it turns until reaching the plant vascular cylinder within the plant roots (Williamson and Gleason, 2003). The J2 embeds its head in the vascular tissue and its body is located on the longitudinal axis of the root in a parallel position, and a permanent feeding site is established from typically between two and twelve vascular parenchymal cells; the nematode now becomes sedentary (Von Mende, 1997). The nematode secretions which are injected through the stylet into these parenchyma cells induce significant alterations (Williamson and Gleason, 2003). Secretions from the nematode dorsal gland have a role in the formation of feeding cells (Davis et al., 2004).

The cells which are selected by the nematode become multinucleate and large and are termed ‘giant cells’ (Bird and Kaloshian, 2003). The repeated nuclei division without cell division result in the multinucleated state of these cells (Jones, 1981). DNA content is increased 14-16 fold in nematode induced cells (Karssen and Moens, 2006) and there is increased volume of the nuclei (Wiggers et al., 1990). Other changes such as increased numbers of ribosomes, denser cytoplasm, morphological changes in the nuclei and alterations of organelles occur to enable the function of giant cells (Endo and Wergin, 1973). The expansion of giant cells during the three weeks following nematode infection results in distortion of the vascular elements in the nematode feeding site (Jones, 1981, Moller et al., 1998). The lateral expansion of giant cells changes the water movement and causes the differentiation of sieve elements and xylem vessels (Bird, 1996). Alongside the development of giant cells, the cortical and pericycle cells proliferate resulting in a gall termed a root-knot (Bird, 1996). Galls are already visible 1-2 days following the nematode infection and gall size can change

depending on host and nematode species (Karsen et al., 2013). Plasmodesmata, which are channels enabling substance transfer between cells (Crawford and Zambryski, 2000), are found in the feeding site of *Meloidogyne*. Such symplasmic connections are seen both between giant cells and neighbouring cells and also between giant cells (Hofmann et al., 2010) although their presence may depend on the developmental stage of the parasitic interaction (Kyndt et al., 2013). The formation of ingrowths in giant cell walls that are adjacent to vascular elements helps to provide an influx pathway for nutrients (Jones, 1981).

Several morphological modifications occur in the second stage of juveniles following the onset of parasitism, such as an increase in size of the dorsal pharyngeal glands. Three moults occur following the initiation of giant cells with the adult female emerging following the last moult (Jones, 1981, Moller et al., 1998). Although most of the root-knot nematode species are facultative or obligate parthenogenetic species (Bird et al., 2009) with males rarely seen, the male number is increased during stress conditions (Snyder et al., 2006, Triantaphyllou, 1973). Although the females are sedentary within the root, the adult males, which are vermiform, leave from the galls (Abad et al., 2003).

The female of *M. incognita* lays eggs within a gelatinous matrix which is generally located on the surface of the galled root. The life cycle of *Meloidogyne spp.* is generally completed in several weeks (Perry et al., 2010). Temperature is one of the most important elements to determine the length of the nematode life cycle. The life cycle of *M. incognita* is completed between 20 and 25 days depending on temperature between 25 and 30 °C, respectively (Ploeg and Maris, 1999). *M. incognita* infected plants have reduced biomass, thinner and smaller leaves, and are stunted with shorter internodes (Fortnum et al., 1991). Additionally, carotenoid and chlorophyll content reduce following the infection of *M. incognita* in sugar beet (Korayem et al., 2012). The root galling and abnormal root growth and alteration of chlorophyll may relate to the nutrient demands of the nematode (Koenning et al., 2004). Some plant parasitic nematodes including *M. incognita* increase the susceptibility of their host plants to other pathogens such as fungal pathogens (Koenning et al., 2004). Furthermore, the monogenic resistance of tomato plants against a fungal pathogen (*Fusarium* wilt) is broken when the plants are also infected by root-knot nematodes (Karssen et al., 2013).

Giant cell walls

Cell wall synthesis is important for thickening the cell wall during giant cell development. Cell wall thickening is not homogeneously distributed in giant cells. The cell wall materials of giant cells are unevenly distributed during the cell wall development (Berg et al., 2009). The giant cell wall thickening varies depending on plant species; horse bean giant cell thickness is greater than pea and clover cell wall thickness (Yousif, 1979). During giant cell wall thickening, cell wall ingrowths typical of transfer cells are apparent and there is an increase in the plasma membrane surface area to facilitate transport of nutrients to the giant cells. Xyloglucan and pectin are homogenously disseminated in the cell walls (Berg et al., 2009).

Although there is a limited description of the cell wall changes that occur during giant cell formation, cell wall modifying proteins play roles on giant cell wall modifications. The cell wall growth, thickening, and loosening are regulated by cell wall modifying proteins. Nematode-derived secreted proteins such as expansins (Qin et al., 2004) may function during the cell enlargement; the expansin repairs the polysaccharide cell wall matrix and causes the enlargement of cells (Cosgrove, 2000). Changes occur in the cell wall during the development of giant cells (Williamson and Gleason, 2003); however, the breaking down of cell walls does not occur during giant cell development (Berg et al., 2009, Jones and Payne, 1978) as it does for the syncytia of cyst nematodes.

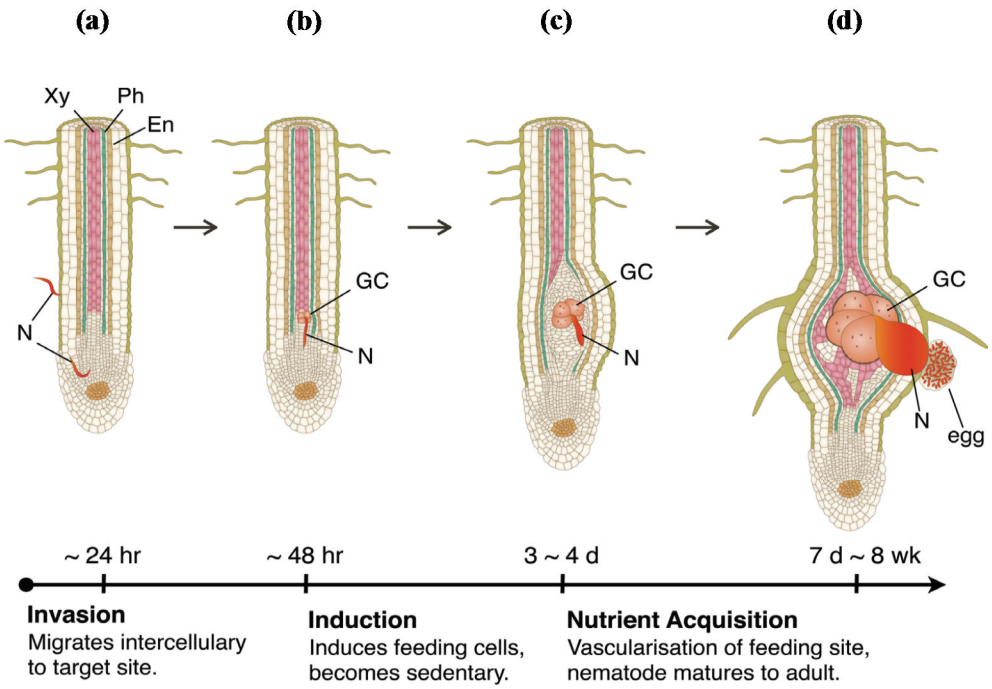

Figure 1.4 Nematode invasion and development of the root-knot nematode feeding site. (a) *Meloidogyne* second-stage juveniles enter just behind the root tip and migrate intercellularly. When they reach the meristematic zone, they turn up to reach the suitable location to create a feeding site within the endodermis in 24 hr. (b) The nematode commences to create the giant cells and become sedentary following the invasion in 48 hours. (c) Giant cells are multinucleated nutrient sinks that supply nutrients to the nematode. The cell modifications in the phloem and xylem network around the feeding site are visible. Giant cell and nematode size increases and root swelling appears between three and four days after invasion. (d) Giant cells reach the final size between two and three weeks and the nematode moults three times to become an adult. The gelatinous egg masses and eggs are visible three to four weeks after invasion in suitable conditions. N, GC, Xy, Ph and En represent the root-knot nematode, giant cells, xylem, phloem and endodermis, respectively. The figure was taken from Bartlem et al. (2014).

1.3 Project overview

The main focus of project was to characterise the composition of giant cell walls, determine how this changes throughout the biotrophic interaction and develop an understanding of the role of different cell wall components in giant cell function. These aims were achieved through *in situ* analysis of the giant cell wall molecular architecture using a range of specific monoclonal antibodies and use of mutant plants to investigate the role of certain cell wall-related genes in giant cell development and function.

Firstly, the distribution of hemicellulose (xyloglucan, mannan, feruloylated xylan), pectin (arabinan, processed arabinan, galactan, methyl-esterified pectic homogalacturonan, de-esterified pectic homogalacturonan) and glycoproteins (arabinogalactan proteins and extensin) in the walls of giant cells and surrounding root cells of infected *Arabidopsis thaliana*, *Vigna angularis* (aduki bean) and *Zea mays* (maize) were investigated. Changes in the relative abundance of these components were documented throughout the parasitic interaction.

Secondly, the abundance of cell wall components in whole galls induced by *M. incognita* on four different hosts was determined by using enzyme-linked immunosorbent assay.

Thirdly, 12 Arabidopsis mutants for a range of different cell wall-related genes have been infected with root-knot nematode and the effect on nematode establishment and development were analysed.

Chapter 2

General Material and Methods

2 General Material and Methods

2.1 Plant culture

Arabidopsis (*Arabidopsis thaliana*), aduki bean (*Vigna angularis*), Potato (*Solanum tuberosum*) and maize (*Zea mays*) were selected to be representative nematode hosts of the *Brassicaceae, Fabaceae, Solanaceae* and *Poaceae* families in the plant kingdom, respectively.

2.1.1 Potato, Bean and Maize culture

The sprouts of chitted potato tubers (*Solanum tuberosum*, 'Desiree') were gently removed without damaging the developing root buds. Single chits were placed into the upper fold of growth pouches (Mega International) and held in position by a paper clip on either side. All pouches were placed in a deep plastic box, separated by polystyrene tiles and tap water was added to supply moisture for root development. Pouch containers were placed in an environmental-regulated chamber (Sanyo) at 20 °C under 16 hour (h) light/8h dark cycle with 30% humidity, and light intensity was calibrated as 140 µmol $m^{-2}s^{-1}$. After root-knot nematode inoculation of 14 days old potato plants, they were moved to a 25 °C growth chamber to provide suitable conditions for nematode infection and development.

Aduki bean and maize seeds stored at 4 °C were placed into growth pouches using the same method described above and they were placed in a growth chamber at 25 °C to allow germination and root growth.

2.1.2 *Arabidopsis thaliana* culture

Seeds of *Arabidopsis thaliana* (L) Heynh, ecotype Columbia-0 (Col-0) were sterilised in the sterile flow cabinet. Around 500-700 seeds were placed in a 1.5 ml microcentrifuge tube to which 200 µl of 70% ethanol was added. After 2 minutes (min), the seeds were centrifuged at 3000 revolutions per minute (rpm) for 30 seconds (sec) and the ethanol was removed. Seeds were incubated for 30 minutes in 10% household bleach, and then washed five times with 200 µl sterile tap water. Finally, 500 µl sterile tap water was added into the tube and placed at 4 °C in order to stratify the seeds and synchronise germination. Arabidopsis seeds were grown in tissue culture on solidified Gamborg's B5 medium: 3.16 g/l Gamborg's B5 medium including vitamins (Duchefa Biochemie, Haarlem, Netherlands) dissolved in ELGA

water with 15 g/l sucrose. The pH value was adjusted to 5.5-5.8 by adding 1M KOH. Then 10 g/l plant agar (Duchefa) was added after pouring the liquid media into bottles, and they were sterilised at 126 °C in an autoclave. Sterilised media was poured into 100 mm square Petri dishes (Sterilin Ltd., Newport, United Kingdom) in a laminar flow hood cabinet. Later, sterilised Arabidopsis seeds which were taken from the refrigerator were sown onto the agar plates (2 seeds for each plate) by using a sterilised toothpick. Plates were labelled and sealed with tape (Micropore^{TM}, 3M Deutschland GmbH, Germany). They were placed into a Sanyo environmental regulated test chamber at 25 °C under 16 h light/8 h dark cycles with 30% humidity conditions and 140 µmol $m^{-2}s^{-1}$ light intensity.

2.2 Root-knot nematodes

2.2.1 Maintenance of root-knot nematode populations

Meloidogyne incognita VW6 population, from University of California Davis was used to infect roots of susceptible tomato (*Solanum lycopersicum* L.) plants, variety Ailsa Craig in the glasshouse. At eight weeks galled tomato roots were chopped into 1 cm length and placed in 22 cm diameter pots filled with compost and a 4 week-old tomato seedling was subsequently planted into the mix. Following labelling, the tomato seedlings were placed in the glasshouse -16 hours light, 8 hours dark conditions. Watering was carried out every three days. Following the inoculation of nematodes, after about eight weeks, roots harbouring mature *M. incognita* egg masses were ready for extraction.

2.2.2 Extraction of second-stage juveniles

The nematode infected roots were gently separated from compost, and soil particles washed from the roots. They were cut into 2-3 cm lengths and roots were placed in a misting chamber at 25 °C. Roots were placed onto tissue paper on a nylon mesh filter, and a funnel was used as supporting material for the filter and samples. A 50 ml tube (Greiner bio-one) was placed under the funnel to collect the second-stage juveniles of root knot nematodes.

2.2.3 Collection of root-knot nematode juveniles

Nematodes accumulated in the bottom of the 50 ml tubes and were collected every 24 hours. The live juveniles were counted under a stereo-binocular microscope (Wild

M5 A model, Switzerland). They were allowed to settle to the bottom of the tube for approximately four hours and the water was replaced with sterile tap water. Tubes were stored in the 10 °C incubator until they were used. These procedures were continued iteratively on every occasion requiring juveniles.

2.2.4 Surface sterilisation of second-stage juveniles (J2s)

For procedures that required sterile nematodes, hatched J2s were pelleted in 1.5 ml microfuge tubes (Axygen, Maxymum Recovery) at 3000 rpm for 30 seconds. They were then put into: 0.1% chlorhexidine digluconate and 0.5 mg/ml hexadecyltrimethylammonium bromide (CTAB) for 32 minutes at room temperature on a rotational mixer. Juveniles were washed in sterile water and subsequently incubated in streptomycin (1 mg/ml) and penicillin (1000 units/ml) sterilising agent for 5 minutes Followed by amphotericin B (50 µg/ml) for five minutes. The final sterilisation step was a five minute incubation in CTAB (0.1 %). Following three washes with sterile tap water containing 0.01% Tween-20, juvenile numbers were optimized at one nematode per 1 µl for inoculation of *Arabidopsis thaliana* plants.

2.3 Immunohistochemical analysis

2.3.1 Collection of root samples

Infected root lengths (approximately 1 cm) harbouring galls were cut with a scalpel and uninfected root sections, were taken from similar location in the root system of uninfected plants. They were placed into the General tubulin buffer in 1.5 microcentrifuge tubes (Sarstedt, Numbrecht). 2x General tubulin buffer; 100 mM piperazine-N, N′-bis (2-ethanesulfonic acid) (PIPES), 10 mM ethylene glycol tetraacetic acid (EGTA) and 10 mM magnesium sulphate, pH 6.9.

2.3.2 Tissue sample fixation

Paraformaldehyde (4%) in General tubulin buffer was used as fixative for immunolabelling. 1 ml aliquots of fixative solution were stored in microcentrifuge tubes at -20 °C. Root segments were placed into micro centrifuge tubes containing fixative. Vacuum infiltration of the fixative was performed for roots of potato, bean and maize using a SpeedVac concentrator for 20 minutes (Savant, Stratech scientific, UK) (Figure 2.1). All samples were incubated in fixative overnight at 4°C.

Phosphate-Buffered Saline (PBS) was prepared with ELGA water, and fixed root samples were washed three times in 1x PBS. The 10x PBS: 1.37 M NaCl, 27 mM KCl, 100 mM Na_2HPO_4, 18 mM KH_2PO_4, pH 7.4.

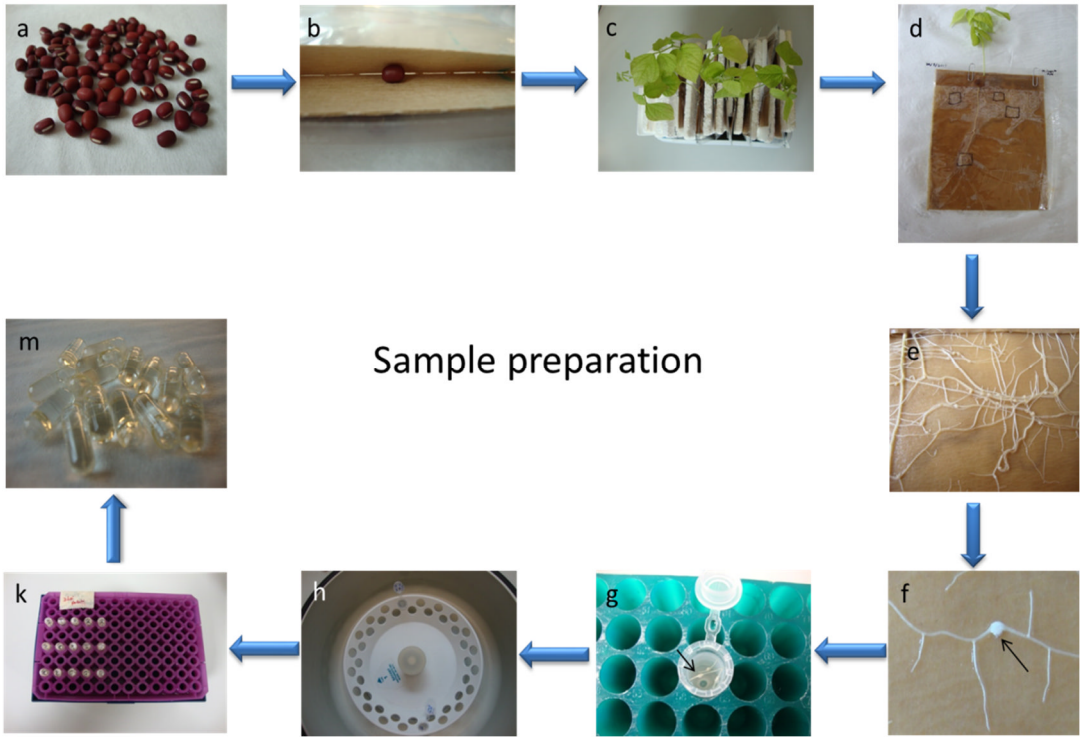

Figure 2.1 Steps of tissue sample preparation for immunohistochemical analysis. The process from germination of seeds, nematode inoculation, collection of root galls, resin embedding in gelatine capsules: (a-b) aduki bean seeds placed into the pouch prior to germination; (c-d) Germinated bean plantlets in pouches; (d) Nematode-inoculated roots of bean with inoculation points marked on the pouch; (e-f) Galls induced in bean roots by *M. incognita*. Arrow indicates a single gall; (g) single-galled root segments were cut and placed in a general tubulin buffer; (h) SpeedVac concentrator; (k-m), resin embedded root segments in gelatine capsules.

2.3.3 Ethanol dehydration and resin embedding of root samples

Following fixation, roots were dehydrated with ethanol at increasing concentrations with different time durations. Ethanol was diluted with ELGA water to create a range of concentrations that were used to wash the section for different duration (Table 2.1) and samples were stored at 4 °C.

After completing the process of ethanol dehydration, resin embedding using LR White resin (R1280, hard grade; Agar Scientific) was accomplished. Samples were incubated in resin diluted with different concentrations of ethanol for different time periods as indicated in Table 2.2. Following completion of the resin embedding process, the gelatine capsules (G29204; Agar Scientific; Size 4, UK) were prepared and filled with 100% resin, a single root sample was inserted into each capsule and placed into a rack (Figure 2.1, k). Capsules which contained resin and root samples were incubated at 37 °C for five days. All samples were stored at room temperature until they were used.

2.3.4 Slide preparation with Vectabond™ reagent

Vectabond™ treated slides were used throughout this work as they allow the sections to attach and not be washed away during the immunolabelling process. The Vectabond™ Reagent instructions were followed for slide preparations. Slides were placed into the metal slide racks and washed in detergent, and then rinsed in water. Slides were placed in acetone after 5 minutes; tapped many times and they were placed immediately in the Vectabond™ reagent solution for five minutes. Slides were drained and rinsed for 30 seconds with deionised water. After removing the slide rack for drying, slides were tapped to decrease water droplets and spots. They were placed at 37 °C until fully dry. Treated slides were stored, wrapped in cling film, in a box at room temperature until use.

Table 2.1 Incubation of samples with ethanol dehydration

Percentage of ethanol dilution (%)	Duration of incubation/ min
10	30
20	30
30	30
50	30
70	60
90	60
100	60

Table 2.2 Resin embedding dilutions and incubation durations

Percentage resin (%)	Duration of incubation
10	30 min
20	30 min
30	30 min
50	30 min
70	60 min
90	60 min
100	60 min
100	overnight
100	8h
100	overnight

2.3.5 Microtome cutting and gathering sections

A microtome (Ultracut, Reichert-Jung) was used to perform sectioning with a diamond blade (G339-10, Diatome histoknife, 6.0mm S/N, Agar Scientific). At the start, 0.5 µm thick sections were collected and placed onto Vectabond^{TM} treated 8-well slides (MP Biomedicals). A water droplet was positioned into each of the wells of the microscope slides. Two of the cut serial sections were placed on the water droplet in each well of the slides. Each slide contained 16 samples. Slides were placed on the LKB Bromma hot-plate in order to evaporate the water. After evaporating the water droplets, sections were checked under the microscope (Figure 2.2).

2.3.6 Immunolabelling

Generation of monoclonal antibodies by hybridoma technique was performed in Knox Cell Wall Lab by Sue Marcus. Immunization was performed by coupling a small oligosaccharides to bovine serum albumin and this was injected into 2 male Wistar rats, and test bleeds were taken to measure antibody production before the spleen was fused with a rat myeloma cell line- IR983F using polyethylene glycol. Spleen cells were isolated and myeloma cells were prepared. After cell fusion and the screening of hybridoma supernatants, best cell lines were cloned. Among the clones of hybridoma cells (antibody-producing cells), some cells produced desired antibodies. The evaluation of antibody was performed by enzyme linked immunosorbent assay (ELISA). Lots of different techniques were used to work out the specificity of the antibody such as microarray, enzyme digestion of antigen, tissue prints, hapten inhibition ELISA and immunofluorescence (Willats et al., 1998). Monoclonal antibodies from Paul J. Knox's lab (Cell Wall Lab, University of Leeds, Faculty of Biological Sciences) were used in this study. Root sections were incubated with 5% milk powder in 1x PBS for 30 minutes with 30 µl block solution added to each of the 8 wells on the slide. The block solution was replaced with primary antibody, diluted 1:5 in 5% milk powder/PBS. One of the wells on each slide was separated as a non-antibody control. This well was incubated in blocking solution alone and was then incubated with secondary antibody at the later stages. Slides were incubated with primary antibody for two hours at room temperature. Following washing each well with 1x PBS three times, the secondary antibody (anti-rat IgG-whole molecule, FITC conjugate; Antibody developed in Rabbit- adsorbed with

human IgG, Cat no. F1763; Sigma Chemical Co., USA) was diluted (1:100 in 1x PBS) and sections were incubated with secondary antibody for 1.5 hours in dark conditions. Slides were washed three times again with 1x PBS. Calcofluor White (Fluorescent Brightener 28, Sigma) 2.5x in 1x PBS was added to the sections and they were incubated for 5 minutes in the dark. Slides were washed comprehensively with 1 x PBS to wash away unbound Calcofluor White. Two small drops of antifade solution (Citifluor AF1; Agar Scientific) were placed onto each slide as a final stage in order to prevent loss of FITC fluorescence. The slides were sealed with a cover slip and placed in the dark at 4˚C. The next day imaging was performed using a fluorescence microscope.

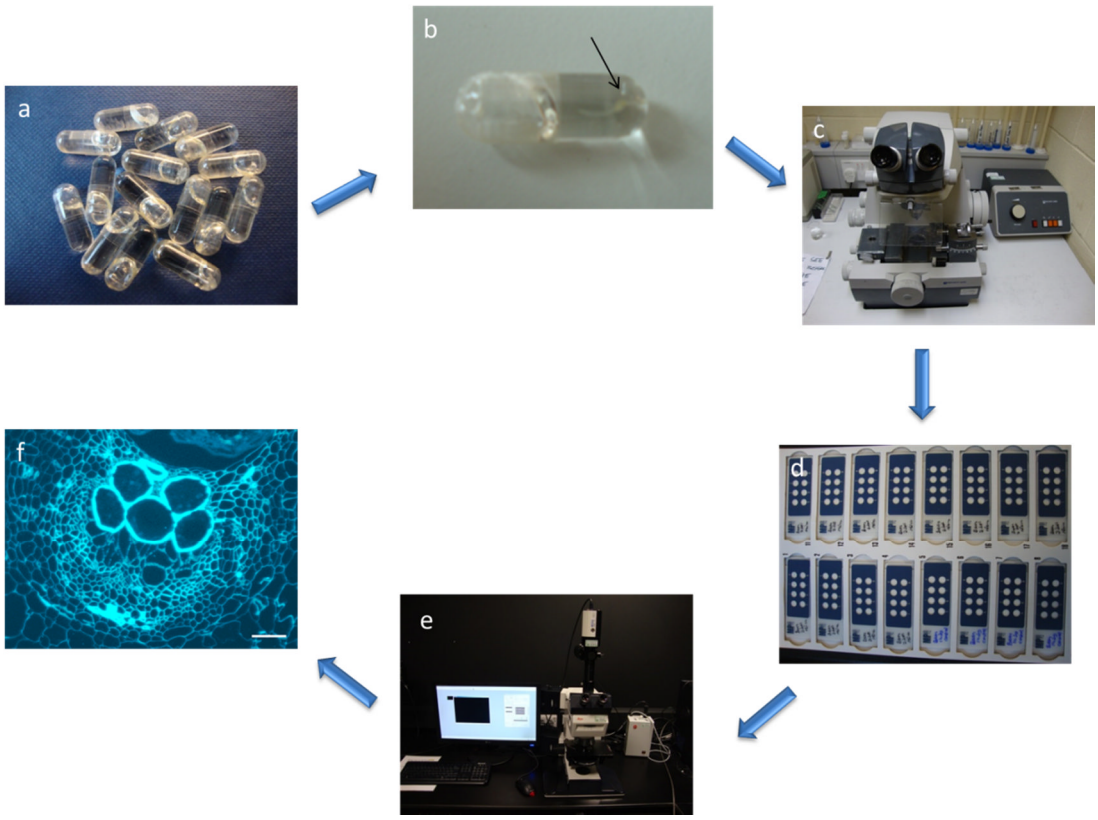

Figure 2.2 The process of resin-embedded sectioning, visualisation and immunolabelling: (a) the resin embedded root samples in gelatine capsules; (b) the resin embedded nematode infected root segment in a gelatine capsule. Arrow indicates a root gall induced by *M. incognita*; (c) a microtome cutting performed to collect sections; (d) root sections placed in Vectabond^{TM} treated slides; (e) Leica microscope with a QImaging QICAM camera for visualising sections under UV light; (f) image of transverse sections in Calcofluor–white staining of bean roots infected by *M. incognita.* Bar: 100 µm

2.3.7 Pectate lyase treatment

Pectate lyase treatment was performed before starting the antibody applications in some experiments. The large quantity of homogalacturonan can conceal the presence of other epitopes in plant cell walls. For instance, it can mask the xyloglucan and mannan epitopes and prevent binding of the LM15 and LM21 antibodies. Enzymatically degrading the homogalacturonan with pectate lyase can prevent this situation. To do this, sections that were to be incubated with LM15, LM25, LM16 and LM19 were pre-treated with 0.1 M Na_2CO_3 for 2 hours at room temperature in order to de-esterify homogalacturonan. Then, pectate lyase (Recombinant, from *Cellvibrio japonicus*; 500 U/ml, 661 U/mg in 3.2 M ammonium sulphate; Megazyme) was used to remove pectin prior to incubation with LM15, LM25 and LM16 antibodies. Pectate lyase was prepared as a 10 µg/ml solution using CAPS buffer and stock enzyme (13.2 µl per ml of 500 U/ml with 661 U/mg). The LM19 incubated sections were not treated with pectate lyase in that LM19 was pre-treated only with 0.1 M Na_2CO_3. The pre-treating of LM19 with Na_2CO_3 results in removing of methylation. Following the pre-treating with Na_2CO_3, the LM19 binds the homogalacturonan. The slides were incubated for 2 hours at room temperature. After completing the treatment, the slides were washed 3 times with ELGA water and the antibody incubation process was promptly started as the next step.

2.3.8 Fluorescence imaging

Fluorescence imaging was carried out in the dark. The Calcofluor-white and antibody labelling were visualised under ultraviolet (UV) light by using Leitz UV source. The excitation and emission wavelengths were set as 350 and 450, respectively. The microscope (Leitz DMRB) and QImaging-QIcam camera (01-QIC-F-CLR-12C cooled colour 12 BIT, Canada) were used in this process (Figure 2.2 e, f).

2.3.9 Image analysis

The Q-capture Pro 6.0 version programme was used to capture images from the microscope. Capture settings were 8 bit mono Q-imaging, 7005 drive with mono binned. The captured images were snapped to keep light intensity so that fluorescence in control samples could compared accurately. Images were analysed by using Image-pro Analyser 7.0 Windows (Media Cybernetics).

Chapter 3

Cell wall molecular architecture of giant cells in the root-knot nematode feeding site

3 Cell wall molecular architecture of giant cells in the root-knot nematode feeding site

3.1 Introduction

The primary cell wall consists of cellulose, hemicellulose, glycoproteins and pectic polysaccharides (Albersheim et al., 2011). The general structure of cell walls was discussed in Chapter 1. The characterisation of plant cell wall polysaccharides will be considered in this chapter. Specifically, techniques for the characterisation of pectin, hemicellulose and glycoproteins using monoclonal antibodies are described.

3.1.1 Characterisation methods of polysaccharide in the plant cell wall

The characterisation of primary plant cell wall polysaccharides is achieved by the combination of several techniques. Ion exchange and gel permeation chromatography can separate rhamnogalacturonan-I, rhamnogalacturonan-II, xyloglucan and glucuronoarabinoxylan (Albersheim et al., 2011). Enzymatic and chemical cleavage, glycosyl composition analysis (using alditiol acetates and trimethylsilyl methyl glycosides), glycosyl linkage composition (methylation analysis), glycosyl sequencing, nuclear magnetic resonance spectroscopy and mass spectrometry (determining polysaccharide structures), x-ray diffraction techniques (determining cellulose structure) are all used to determine the structures of plant cell wall polysaccharides (Albersheim et al., 2011). The cellulose polymers can be characterised by Attenuated Total Reflectance Fourier-Transform Infrared (ATR FT-IR) and X-ray Diffraction (Kljun et al., 2011).

In addition to the above techniques, monoclonal antibodies (molecular probes) are used to determine the cell wall molecular architectures (Moller et al., 2008, Knox, 2008, 2012, Herve et al., 2011, Knox, 2012, Lee et al., 2011, Meikle et al., 1994b, Verhertbruggen et al., 2009a).

3.1.2 *In situ* characterisation of cell wall molecular architectures by using monoclonal antibodies

Monoclonal antibodies are used against epitopes which are parts of antigens in the cell walls of vascular plants (Pattathil et al., 2010, Willats et al., 2000). They are specific components to recognise the primary cell wall structures and associations, and are significant tools to detect the plant cell wall polysaccharides using

immunofluorescence microscopy (Willats et al., 2000). Monoclonal antibodies have been used in numerous studies to detect the plant cell type, changes in the cell wall structure and cell wall architecture (Knox, 1992, 1997, Knox et al., 1991, Moller et al., 2008, Puhlmann et al., 1994).

The characterisation of hemicellulose, pectin and glycoproteins using monoclonal antibodies is the focus here.

3.1.2.1 Hemicellulose

Hemicelluloses include xylan, feruloylated xylan, mixed linkage glucan, xyloglucan and mannan (Scheller and Ulvskov, 2010). Xylan is a major hemicellulose in grasses with a backbone of β(1→4) linked xylosyl residues (Albersheim et al., 2011). Antibodies LM10 (McCartney et al., 2005) and LM11 (McCartney et al., 2005) bind to (1→4)-β-D-xylan, and LM12 (Pedersen et al., 2012) binds to feruloylated xylan in the plant cell wall. Mixed linkage-glucan, recognised by the MLG antibody (Meikle et al., 1994a) is abundant in cell walls of grass cells but it is not found in the cell walls of dicots (Vogel, 2008). Xyloglucan is a major hemicellulose (approximately 35%) in dicots, non-graminaceous plants and gymnosperms (Albersheim et al., 2011). The LM24 (Pedersen et al., 2012), LM15 (Marcus et al., 2008), and LM25 (Pedersen et al., 2012) antibodies recognise different motifs of xyloglucans, galactosylated xyloglucan, and XXXG (three-xylosyl-residues per glucosyl-residue), XXXG /galactosylated anti-xyloglucan antibodies, respectively. Mannan is a complex hemicellulosic sugar, common in land plants, that consists of β(1→4) linked mannosyl residues (Scheller and Ulvskov, 2010). The LM21 (Marcus et al., 2010) and LM22 (Marcus et al., 2010) antibodies can detect heteromannan in plant cell walls. Heteromannan is masked by the presence of pectic homogalacturonan (Marcus et al., 2010) but the epitope can also be unmasked in cell wall sections by the application of pectate lyase treatment.

3.1.2.2 Pectin

Homogalacturonan, rhamnogalacturonan-I, rhamnogalacturonan-II and xylogalacturonan are sub-groups of pectic polysaccharides (Caffall and Mohnen, 2009). Homogalacturonan is a major group of pectic polysaccharides and structural components in the cell wall matrix make connections with cellulose and

hemicellulose network (Caffall and Mohnen, 2009). Homogalacturonan interacts with other pectic polysaccharides: arabinan, galactan, xylogalacturonan, rhamnogalacturonan-I and rhamnogalacturonan-II (Lee et al., 2011). Rhamnogalacturonan-I consists of the repeated disaccharide units with predominantly arabinosyl and galactosyl containing side chains, but rhamnogalacturonan-II is a complex polysaccharide with distinct side-chain structures (Albersheim et al., 2011).

Several monoclonal antibodies bind pectic polysaccharides in the walls of plant cells: some monoclonal antibodies are used to detect homogalacturonan (Verhertbruggen et al., 2009a, Willats et al., 1999, 2001a, Clausen et al., 2003, Manfield et al., 2005), xylogalacturonan (Willats et al., 2004) and rhamnogalacturonan-I (Moller et al., 2008, Verhertbruggen et al., 2009b, Clausen et al., 2004, Jones et al., 1997, Willats et al., 1998). Some of the epitopes can be masked by other polysaccharides; for instance, xyloglucan and galactan are masked by heteroxylan in *Miscanthus* cell walls (Xue et al., 2013).

3.1.2.3 Glycoproteins

Arabinogalactan proteins (AGPs) and extensin are plant cell wall glycoproteins (Jose-Estanyol and Puigdomenech, 2000). AGPs are a subfamily of hydroxyproline rich glycoproteins (HRGP) that are found on the cell wall surface. In addition, they may have functions that include a role in growth, programmed cell death, cell proliferation, cell elongation and plant defence (Knox et al., 1991, Albersheim et al., 2011, Gao and Showalter, 1999). AGPs can be detected in the cell wall by a panel of monoclonal antibodies (Smallwood et al., 1996, Yates et al., 1996, Moller et al., 2008, Knox et al., 1989, 1991, Stacey et al., 1990, Pennell et al., 1989) which include LM2 (β-linked GlcA) (Smallwood et al., 1996, Yates et al., 1996) and JIM13 (Yates et al., 1996, Knox et al., 1991) used in this study.

Extensin (a hydroxyproline-rich glycoprotein) is involved in disease and wound responses in which the accumulation of extensin increases (Lamport et al., 2011). The antibodies LM1, JIM11, JIM12, JIM19 and JIM20 bind the extensin in cell walls (Smallwood et al., 1994, Smallwood et al., 1995, Knox et al., 1995, Wang et al., 1995).

In this study, a panel of specific monoclonal antibodies was used to reveal the molecular architecture of the giant cell walls induced by *M. incognita* in three different plant species that encompass families of *Brassicaceae* (*Arabidopsis thaliana*), *Fabaceae* (*Vigna angularis*) and *Poaceae* (*Zea mays*). The cell wall compositions in the *M. incognita* feeding site were observed by comparison with uninfected root tissues of *Arabidopsis thaliana*, *Zea mays* (maize), *Vigna angularis* (aduki bean).

3.2 Aims

The molecular architectures of giant cell walls have not been fully understood. Therefore, *in situ* analyses of transverse sections through uninfected and infected roots were performed.

- Characterising the comparative cell wall molecular architecture of *M. incognita* induced giant cell walls in three hosts: aduki bean, Arabidopsis and maize at 21 dpi.
- Using several monoclonal antibodies to determine cell wall polysaccharides in giant cell walls, surrounding gall cells and cell walls of uninfected root sections:
    - Hemicellulose
        - Mixed linkage glucan, xylan, feruloylated xylan, mannan, xyloglucan
    - Pectin
        - Homogalacturonan (Methyl esterified pectic homogalacturonan, de-esterified pectic homogalacturonan)
        - Rhamnogalacturonan-I (Galactan, Arabinan, Processed arabinan)
    - Glycoproteins
        - Arabinogalactan proteins
        - Extensin
- Determining the comparative cell wall thickness of nematode-induced giant cells in the three host species

3.3 Materials and Methods

Detailed methods are described in Chapter 2. Those methods specific to this chapter are given below.

3.3.1 Monoclonal antibodies

Fifteen monoclonal antibodies were used to detect the cell wall epitopes in nematode infected and uninfected root samples (Table 3.1). Antibodies generated from rat spleen cells were obtained from the Cell Wall Biology group (Prof. Paul J. Knox) at the University of Leeds with the exception of anti-MLG that was obtained from Biosupplies, Australia. Monoclonal antibodies LM11, LM12, LM21, LM25, LM15 and MLG bind cell wall epitopes of hemicellulosic polysaccharides: (1→4)-ß-D-xylan/arabinoxylan, feruloylated xylan, heteromannan, XXXG/ galactosylated xyloglucan, XXXG motif of xyloglucans and mixed linkage glucan, respectively (McCartney et al., 2005, Pedersen et al., 2012, Marcus et al., 2008, 2010, Meikle et al., 1994a). Pectin related antibodies: LM5, LM6, LM16, LM19, and LM20 bind to pectin related cell wall epitopes: (1→4)-ß-D-galactan, (1→5)-α-L-arabinan, processed arabinan, de-esterified homogalacturonan and partially methyl-esterified homogalacturonan, respectively (Jones et al., 1997, Willats et al., 1998, Verhertbruggen et al., 2009a,b). Antibodies LM2 and JIM13 detect arabinogalactan protein glycan epitopes in the cell wall. Antibodies JIM19 and JIM20 detect extensin epitopes in cell walls (Knox et al., 1991, Yates et al., 1996, Smallwood et al., 1996, Knox et al., 1995, Smallwood et al., 1994, Wang et al., 1995).

3.3.2 Cell wall thickness measurement

Determining cell wall thickness of giant cells was performed in three hosts: Calcofluor White (Fluorescent Brightener 28, Sigma) was applied to root sections of aduki bean, maize and Arabidopsis to reveal all of the cells walls - giant cell walls and neighbouring cell walls - of a section. Images were taken with Q-capture Pro 6.0 programme. Image pro analyser 7.0 (2009 Media Cybernetics) was used to measure cell wall thickness from captured images. Ninety measurements from 20 giant cells were performed. The statistical analysis was performed using “Microsoft Excel t-test” to analyse the differences between the giant cell wall and neighbouring cell walls in the vascular cylinder.

Table 3.1 List of monoclonal antibodies used to analyse the nematode infected and uninfected plant cell wall molecular architectures.

Plant cell wall component		Antibody	References
Hemicellulose	Xylan	LM11	(McCartney et al., 2005)
	Feruloylated xylan	LM12	(Pedersen et al., 2012)
	Heteromannan	LM21	(Marcus et al., 2010)
	Xyloglucan	LM25	(Pedersen et al., 2012)
	Xyloglucan	LM15	(Marcus et al., 2008)
	Mixed Linkage Glucan	MLG	(Meikle et al., 1994a)
Pectin	Galactan	LM5	(Jones et al., 1997)
	Arabinan	LM6	(Willats et al., 1998)
	Processed arabinan	LM16	(Verhertbruggen et al., 2009b)
	DeSPHG	LM19	(Verhertbruggen et al., 2009a)
	MPHG	LM20	(Verhertbruggen et al., 2009a)
Glycoprotein	AGPs	JIM13	(Knox et al., 1991, Yates et al., 1996)
	AGPs	LM2	(Smallwood et al., 1996, Yates et al., 1996)
	Extensin	JIM20	(Knox et al., 1995, Smallwood et al., 1994)
	Extensin	JIM19	(Smallwood et al., 1994, Wang et al., 1995)

MLG, Mixed linkage glucan; MPHG, Methyl esterified pectic homogalacturonan; DeSPHG, De-esterified pectic homogalacturonan; AGPs, Arabinogalactan proteins; LM, Leeds Monoclonal; JIM, John Innes Monoclonal.

3.4 Results

Thin sections are required for *in situ* analysis of inner cell walls of plant roots to define the cell wall molecular components. Transverse sections of the root knot nematode (*M. incognita*) feeding site were prepared at 21 days post infection (dpi) in addition to those from uninfected root sections of Arabidopsis, bean and maize. Transverse sections were stained by Calcofluor-white to provide easy visualisation of all cell walls and allow the giant cells to be identified. Cell walls of phloem, xylem vessels, endodermis and pericycle cells in uninfected cells and the thickened cell walls of the enlarged giant cell walls in nematode infected roots were strongly stained (Figure 3.1a, b). The enlargement of the vascular cylinder is apparent within sections of nematode feeding sites in contrast to uninfected (control) sections. The modification of the *M. incognita* induced giant cell wall molecular architecture takes place in the vascular cylinder; hence, this study was focused on the vascular cylinder within root sections.

3.4.1 Immunolabelling of giant cell walls induced by *Meloidogyne incognita* in the roots of aduki bean, maize and Arabidopsis at 21 dpi

3.4.1.1 Hemicellulose

Antibodies were used to detect the presence and abundance of five members of the hemicellulose group of plant cell wall polysaccharides: xylan, feruloylated xylan, mannan, xyloglucan and mixed linkage glucan (MLG).

Xylan detection and proliferation of xylem vessels

Xylem vessels are responsible for water transport from roots to higher part of the plant. The LM11 antibody detects the xylan in secondary cell walls of dicot plants. Binding of this antibody serves to distinguish between the giant cells and xylem vessels and allows orientation of sections in Arabidopsis and aduki bean. Xylem vessel proliferation was observed at increased levels at 21 dpi (Figure 3.2) in the nematode infected root sections of aduki bean and Arabidopsis (Figure 3.2 d, e), but could not be observed in the infected root sections of maize (Figure 3.2 f). Binding of LM11 was not observed in giant cell walls of aduki bean and Arabidopsis (Figure 3.2 d, e). The absence of xylan suggested that the cell wall thickening that occurs in

giant cell walls formed by *M. incognita* does not result from the presence of a secondary cell wall. Xylan was detected in giant cell walls and faint binding was also observed in phloem and xylem cells of the vascular cylinder in the nematode infected maize root sections (Figure 3.2 f). No xylan binding was detected in any other cells except xylem vessels in sections of uninfected aduki bean and Arabidopsis roots (Figure 3.2 g, h). However, xylan was detected in both xylem vessels and faintly in other cell walls in uninfected root sections of maize (Figure 3.2 i).

Feruloylated xylan is abundant in maize root sections

Feruloylated xylan was detected by the monoclonal antibody LM12 that recognises the feruloyl residues attached to a range of sugars (Pedersen et al., 2012). Binding of LM12 was observed in neither giant cell walls nor the cell walls of xylem vessels in the vascular cylinder of aduki bean and Arabidopsis root sections (Figure 3.3 d, e). The absence of feruloylated xylan suggested that feruloyl residues do not occur in dicot plants. Feruloylated xylan was abundant in giant cell walls and the xylem vessels, endodermis, cortex, phloem and periderms cells in the vascular cylinder of nematode infected root sections of maize (Figure 3.3 f). Low levels of LM12 binding were observed in uninfected root sections of maize (Figure 3.3 i) but not in Arabidopsis and aduki bean (Figure 3.3 g, h).

Heteromannan epitopes are a component part of giant cell walls in Arabidopsis and maize but not aduki bean

Mannan is one of the major cross-linking glycans in cell walls. The antibody LM21 revealed that heteromannan was partially masked by pectic homogalacturonan, hence, sections were pre-treated by pectate lyase to reveal the epitope. The localization of LM21 in giant cell walls was not detected in aduki bean but binding was detected in the xylem cell walls of the vascular cylinder (Figure 3.4 d). Heteromannan was localised in both giant cell walls and vascular cell walls of Arabidopsis and maize after infection of *M. incognita* at 21 dpi (Figure 3.4 e, f). The binding of LM21 was observed in the xylem vessels and phloem cell walls of uninfected aduki bean (Figure 3.4 g), Arabidopsis (Figure 3.4 h) and maize (Figure 3.4 i) roots. It was then evident that LM21 bound to epidermis, cortex and phloem cell walls and the giant cell walls formed by *M. incognita* in Arabidopsis and maize

but not aduki bean. Mannan was, however, observed in the xylem and phloem cells in the vascular cylinder of uninfected root sections for all three host plants. This suggests that infection of aduki bean by *M. incognita* suppresses the presence of mannan in the cell walls, with this being particularly evident for the giant cell walls (Figure 3.4 d, g).

The xyloglucan epitope is abundant in giant cell walls

The LM15 and LM25 xyloglucan epitopes are masked by pectic HG in both infected and uninfected *A. thaliana* root sections. Both antibodies were detected after elimination of pectic HG. It can be concluded that the binding of the antibody was prevented by pectic HG in cell walls. LM15 binds the XXXG motif of xyloglucans (Marcus et al., 2008) and LM25 binds to the XXXG motif of xyloglucans and galactosylated xyloglucan (Pedersen et al., 2012). Both antibodies detected xyloglucan only after removal of pectic HG from the sections. Binding of LM25 and LM15 revealed that xyloglucan was abundant in giant cell walls, in addition to xylem vessels, endodermis and phloem cell walls in the vascular cylinder at 21 days post infection (dpi) in all three host plants (Figure 3.5 d, e, f and Figure 3.6). Binding of LM25 and LM15 to the xyloglucan appears stronger in all cell types, including giant cells, formed in Arabidopsis in comparison to aduki bean and maize host plants (Figure 3.5 d, e, f and Figure 3.6). LM15 and LM25 bound to xyloglucan epitopes in uninfected root sections of the three host-plant species with the exception of LM15 in maize uninfected root sections (Figure 3.5 g, h, i and Figure 3.6).

The presence of mixed linkage glucan in giant cell walls in maize infected with *M. incognita*

Mixed linkage glucan (MLG) is not found in the cell walls of dicotyledonous plants (Vogel, 2008). The MLG antibody directed against mixed linkage glucan revealed that this is highly abundant in giant cell walls of maize. Strong binding was observed in all cell walls of both infected and uninfected root sections, including those of the giant cells (Figure 3.7 b, d).

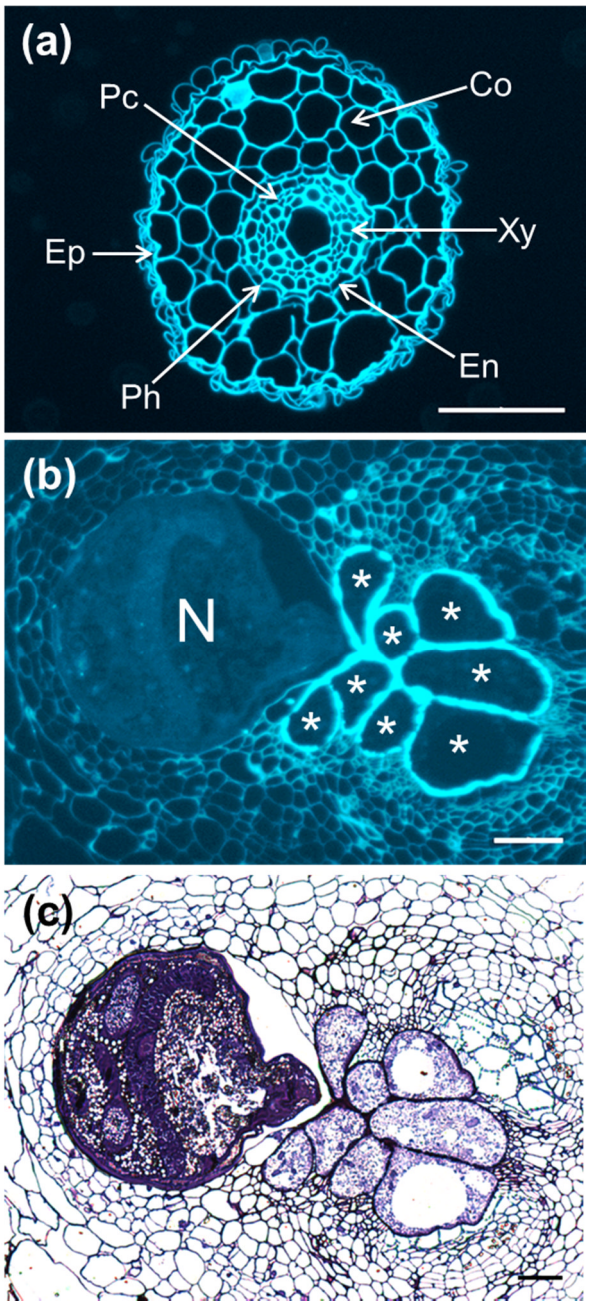

Figure 3.1 ***Meloidogyne incognita*** **infected and uninfected root sections at 21 days post infection (dpi) with Calcofluor white and toluidine blue staining.** The Calcofluor White binds strongly to structures containing cellulose and the toluidine blue stains the plant and animal tissues. The staining of Calcofluor white in uninfected root section of maize (a) and nematode-infected aduki bean root section (b). The same infected root section stained with toluidine blue is presented in (c). Asterisks indicate giant cells; N, represents the nematode; Co, cortex; Xy, xylem; En, endodermis, Ph, phloem; Ep, epidermis; Pc, pericycle. Bars: (a) 100 µm (b) 100 µm (c) 70 µm.

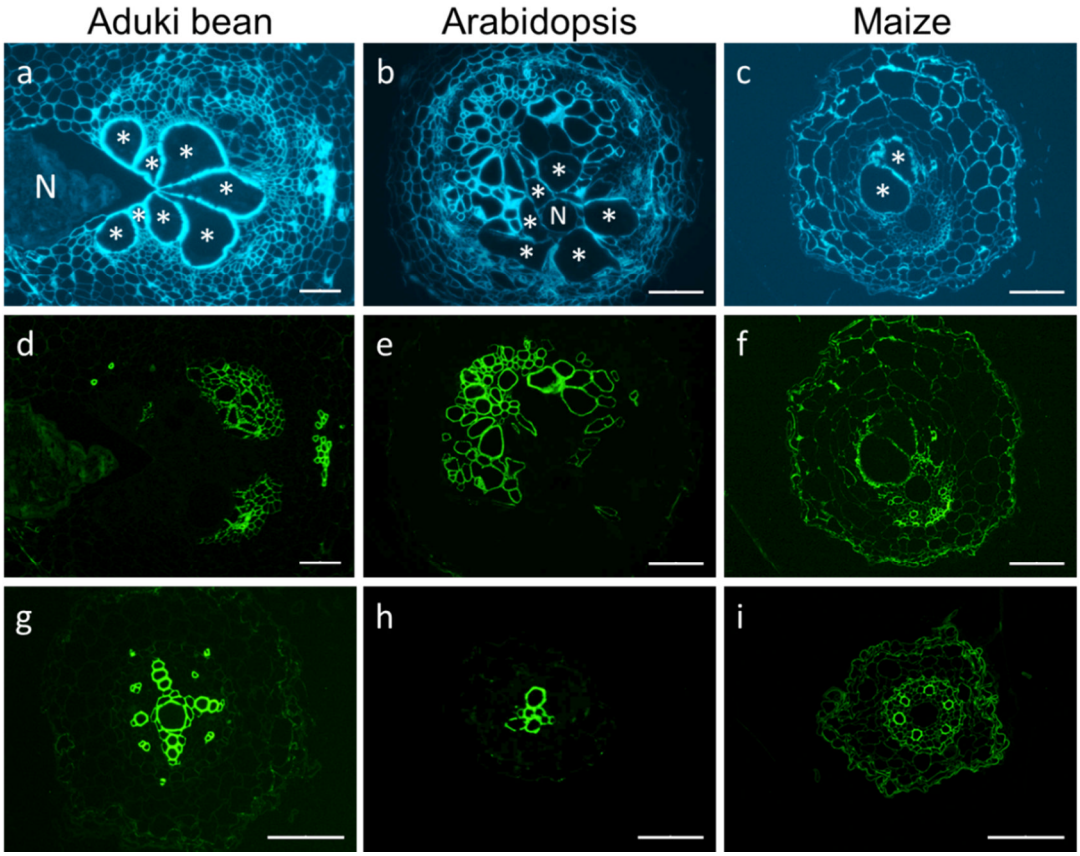

Figure 3.2 Immunolabelling of xylan in nematode-infected and uninfected aduki bean, Arabidopsis and maize root sections at 21 days post infection (dpi). LM11 antibody localised xylan in nematode-infected and uninfected root sections of host plants. The localization of xylan in infected root sections of aduki bean (d), Arabidopsis (e) and maize (f) and uninfected root sections of aduki bean (g), Arabidopsis (h) and maize (i) are presented. The corresponding Calcofluor white stained infected root sections are presented for aduki bean (a), Arabidopsis (b), and maize (c). Asterisks indicate giant cells; N, represents the nematode. Bars: (a-f) 100 µm; (h) 50 µm and (g & i) 70 µm

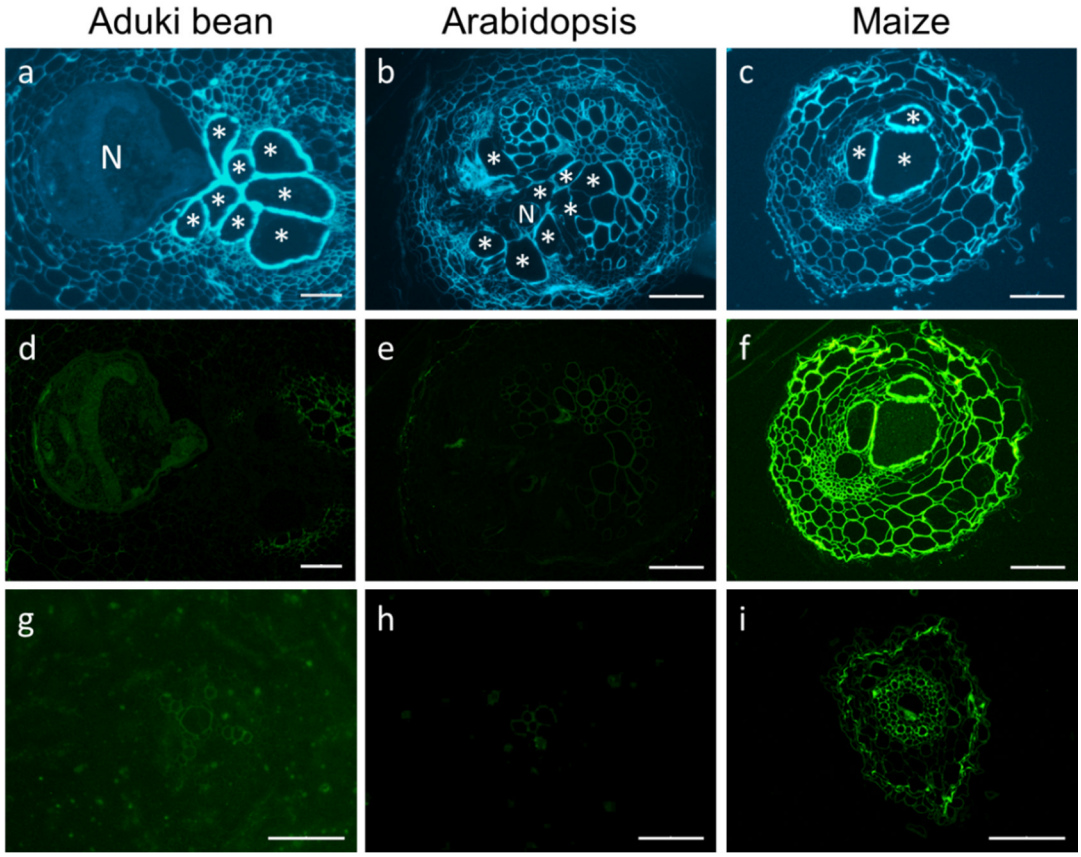

Figure 3.3 Immunolabelling of feruloylated xylan in nematode infected and uninfected aduki bean, maize and Arabidopsis root sections at 21 days post infection (dpi). LM12 localised feruloylated xylan in nematode-infected and uninfected root sections of maize plants. The localization of LM12 in infected root sections of aduki bean (d), Arabidopsis (e) and maize (f) and uninfected root sections of aduki bean (g), Arabidopsis (h) and maize (i) are presented. Corresponding Calcofluor white stained infected root sections are presented for aduki bean (a), Arabidopsis (b) and maize (c). Asterisks indicate giant cells; N, represents the nematode. Bars: (a-f) 100 µm (h) 30 µm and (g & i) 70 µm.

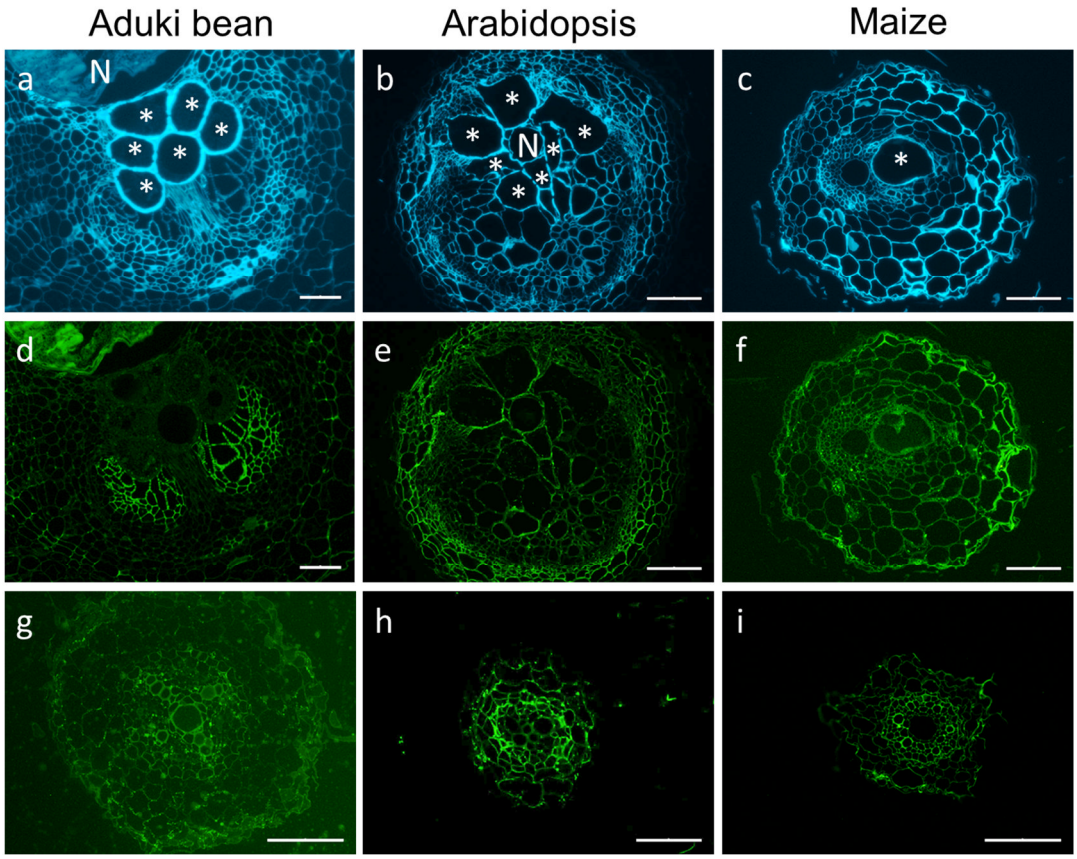

Figure 3.4 Immunolabelling of mannan in nematode-infected and uninfected aduki bean, Arabidopsis and maize root sections at 21 days post infection (dpi). LM21 antibody localised mannan in nematode-infected and uninfected root sections of host plants. The localization of mannan in infected root sections of aduki bean (d), Arabidopsis (e) and maize (f) and uninfected root sections of aduki bean (g), Arabidopsis (h) and maize (i) are presented. The corresponding Calcofluor white stained infected root sections are presented for aduki bean (a), Arabidopsis (b), and maize (c). Asterisks indicate giant cells; N, represents the nematode. Bars: (a-f) 100 µm; (h) 30 µm and (g & i) 70 µm

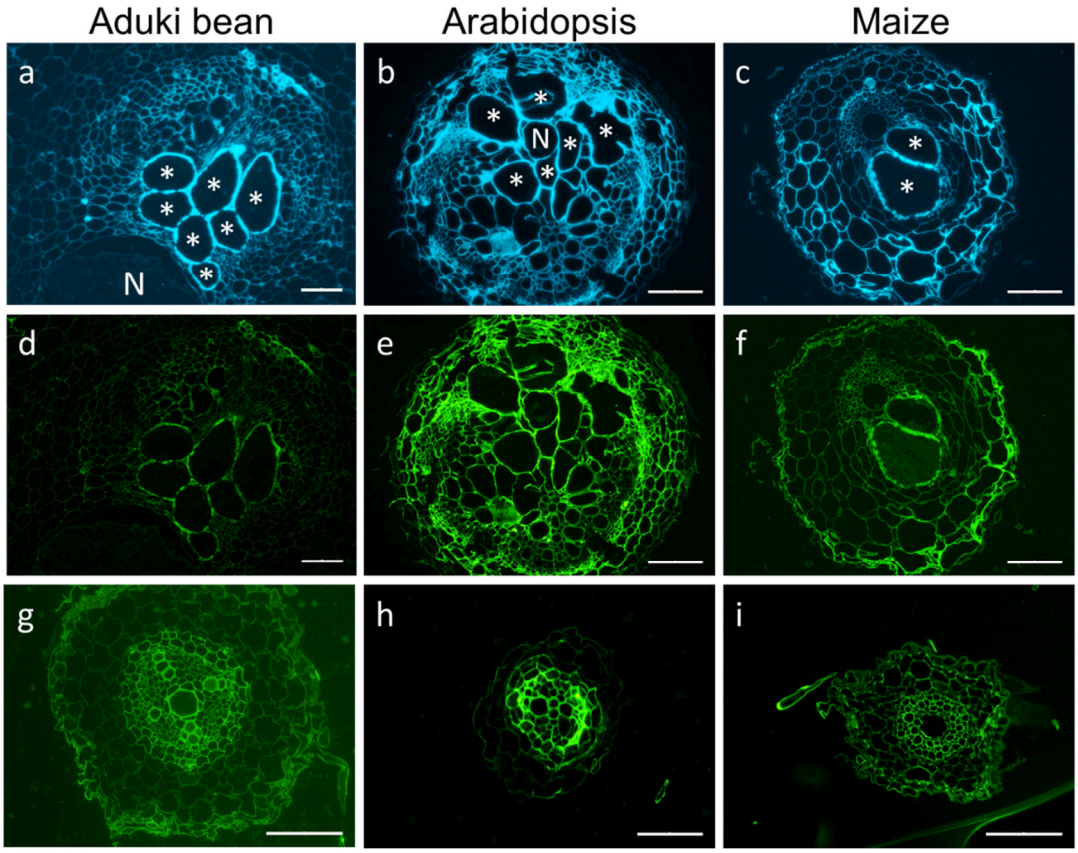

Figure 3.5 Immunolabelling of xyloglucan (LM25) in nematode-infected and uninfected aduki bean, Arabidopsis and maize root sections at 21 days post infection (dpi). The LM25 antibody localised xyloglucan in nematode-infected and uninfected root sections of host plants. The localization of xyloglucan in infected root sections of aduki bean (d), Arabidopsis (e) and maize (f) and uninfected root sections of aduki bean (g), Arabidopsis (h) and maize (i) are presented. The corresponding Calcofluor white stained infected root sections are presented for aduki bean (a), Arabidopsis (b), and maize (c). Asterisks indicate giant cells; N, represents the nematode. Bars: (a-f) 100 µm; (h) 30 µm and (g & i) 70 µm

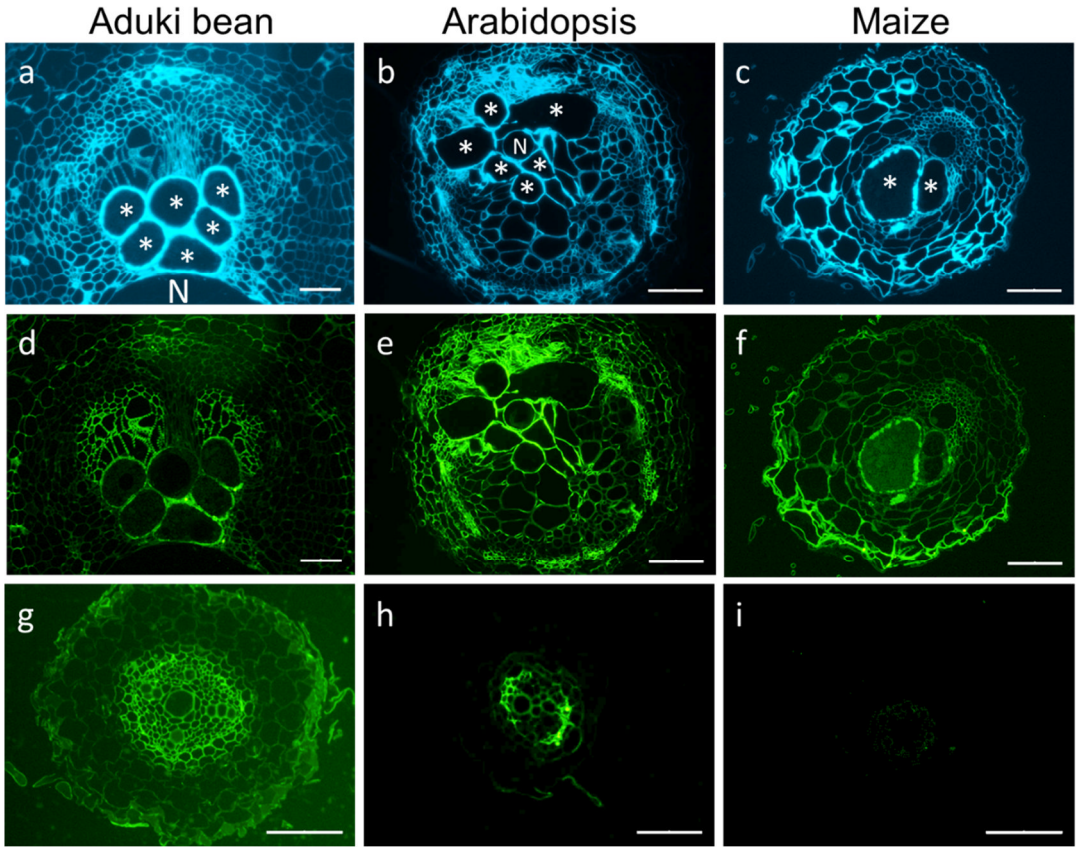

Figure 3.6 Immunolabelling of xyloglucan (LM15) in nematode-infected and uninfected aduki bean, Arabidopsis and maize root sections at 21 days post infection (dpi). The LM15 antibody localised xyloglucan in nematode-infected and uninfected root sections of host plants. The localization of xyloglucan in infected root sections of aduki bean (d), Arabidopsis (e) and maize (f) and uninfected root sections of aduki bean (g), Arabidopsis (h) and maize (i) are presented. The corresponding Calcofluor white stained infected root sections are presented for aduki bean (a), Arabidopsis (b), and maize (c). Asterisks indicate giant cells; N, represents the nematode. Bars: (a-f) 100 µm; (h) 30 µm and (g & i) 70 µm

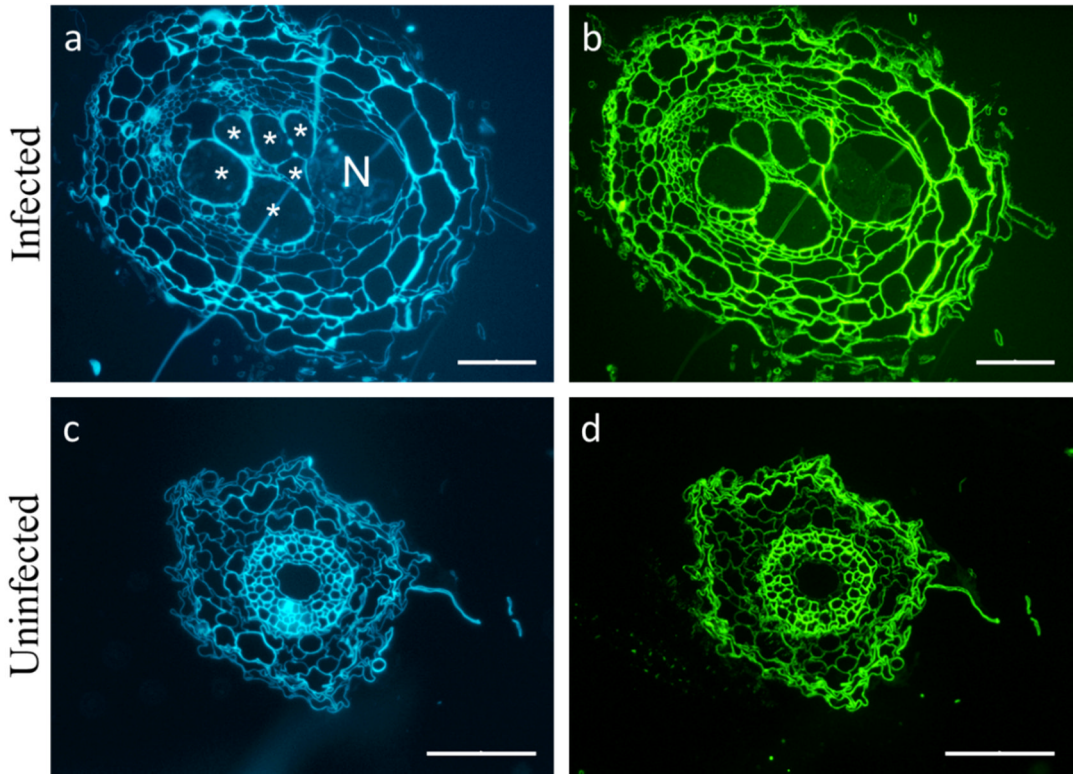

Figure 3.7 Immunolabelling of mixed-linkage glucan (MLG) in nematode-infected and uninfected maize root sections at 21 days post infection (dpi). The MLG antibody localised the mixed-linkage glucan in nematode-infected and uninfected root sections of maize plants. The localization of MLG in infected root sections of maize (b) and uninfected root sections of maize (d) are presented. The corresponding Calcofluor white stained root sections are presented (a & c). Asterisks indicate giant cells; N, represents the nematode. Bars: (a & b) 100 µm; (c & d) 70 µm.

3.4.1.2 Pectin

Homogalacturonan and rhamnogalacturonan-I are important and major components of the pectic polysaccharides.

Homogalacturonan (HG)

The LM19 antibody detects de-esterified pectic HG. In giant cell walls the LM19 epitope of pectic HG was masked by methyl esters that required removal by sodium carbonate (Na_2CO_3) treatment. Although some cell walls bound the LM19 antibody before pre-treatment with sodium carbonate, no giant cell walls bound LM19 prior to sodium carbonate treatment in any of the host plants (Figure 3.8). Low and inconsistent levels of binding were detected in giant cell walls infected Arabidopsis root sections (Figure 3.8 e). Generally, a relatively high level of binding of LM19 was observed in the cell walls of uninfected root sections in all hosts compare to infected sections (Figure 3.8). This indicates that the pectic HG in giant cell walls is heavily methyl esterified. The LM19 epitope was detected strongly after pre-treatment by Na_2CO_3 in giant cell walls at 21 dpi in all plant hosts and its abundance was comparable across each of the three host plant species (Supplementary data in CD). Following de-esterification LM19 also bound to the cell walls of all the cells in the vascular cylinder in uninfected sections (Supplementary data S1 in CD).

LM20 also detects pectic HG but in contrast to LM19 it specifically binds to the methylesterified form and revealed the abundant presence of this epitope in the giant cell walls in all three host-plant species (Figure 3.9 d-f). The pectic HG epitope recognised by LM20 is also far more evident in the cell walls, including the giant cell walls of Arabidopsis than in aduki bean and maize (Figure 9 d-f). The phloem and endodermis cell walls within the uninfected vascular cylinder equivalent to 21 dpi also revealed binding of LM20 in aduki bean and Arabidopsis root sections but not maize (Figure 3.9 g-i).

Rhamnogalacturonan-I

Galactan, arabinan and processed arabinan are types of pectic rhamnogalacturonan-I. These related epitopes are differentially detected in giant cell walls. Induction of galactan in Arabidopsis and maize infected with *M. incognita* contrasts with suppression of galactan in infected aduki bean. Galactan was detected with the

antibody LM5. Binding was apparent in the cambial zone and associated with thickening of cell walls of all three host plant species. Galactan was also detected in walls of giant cells formed in Arabidopsis and maize but was absent from the giant cells formed in aduki bean (Figure 3.10 e, f). This difference is even more interesting when it is noted that binding of LM5 was extremely low in uninfected root cells of Arabidopsis and maize, but was clearly evident in uninfected aduki bean root sections (Figure 3.10 h, i). This suggests that the galactan is induced in the cell walls of Arabidopsis and maize infected with *M. incognita* but conversely, in aduki bean the presence of the galactan epitope is suppressed upon infection.

Among the arabinan antibodies; LM6 binds to 1,5-α-linked L-arabinan epitopes, possibly short side chains; however, LM16 which is also termed as processed arabinan binds to linear arabinan and it prefers strong binding to the de-branched arabinan (Verhertbruggen et al., 2009b). The antibody LM6 bound to the giant cell walls of Arabidopsis, aduki bean and maize and in uninfected root sections (Figure 3.11 d-i). Processed arabinan is detected by the LM16 antibody in cell walls that was not present in any giant cell walls of infected, Arabidopsis, aduki bean and maize roots (Figure 3.12 d, e, f) but processed arabinan was detected in uninfected sections of all three host plant species (Figure 3.12 g-i). These observations suggest that infection of Arabidopsis, aduki bean and maize with *M. incognita* leads to a reduction of processed arabinan in giant cell walls.

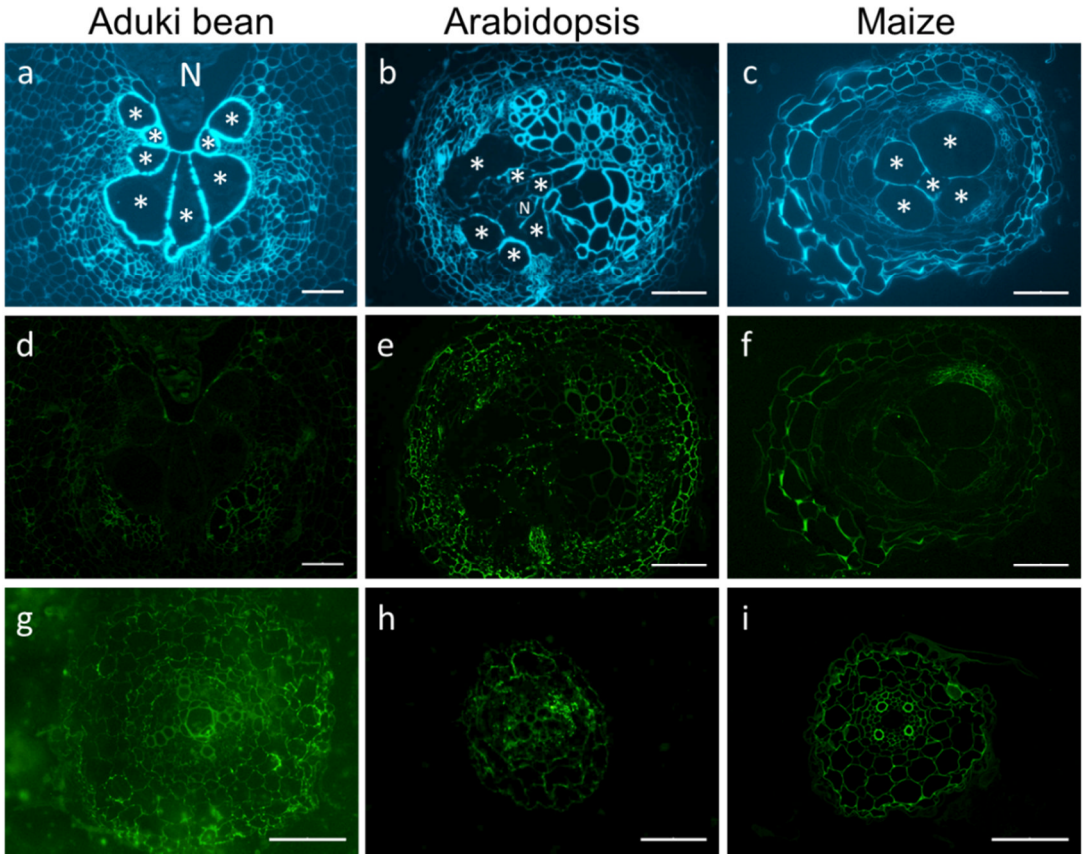

Figure 3.8 Immunolabelling of de-esterified pectic homogalacturonan in nematode infected and uninfected aduki bean, Arabidopsis and maize root sections at 21 days post infection (dpi). The LM19 antibody localised de-esterified pectic homogalacturonan in nematode-infected and uninfected root sections of host plants. The localization of de-esterified pectic homogalacturonan in infected root sections of aduki bean (d), Arabidopsis (e) and maize (f) and uninfected root sections of aduki bean (g), Arabidopsis (h) and maize (i) are presented. The corresponding Calcofluor white stained infected root sections are presented for aduki bean (a), Arabidopsis (b), and maize (c). Asterisks indicate giant cells; N, represents the nematode. Bars: (a-f) 100 µm; (h) 30 µm and (g & i) 70 µm.

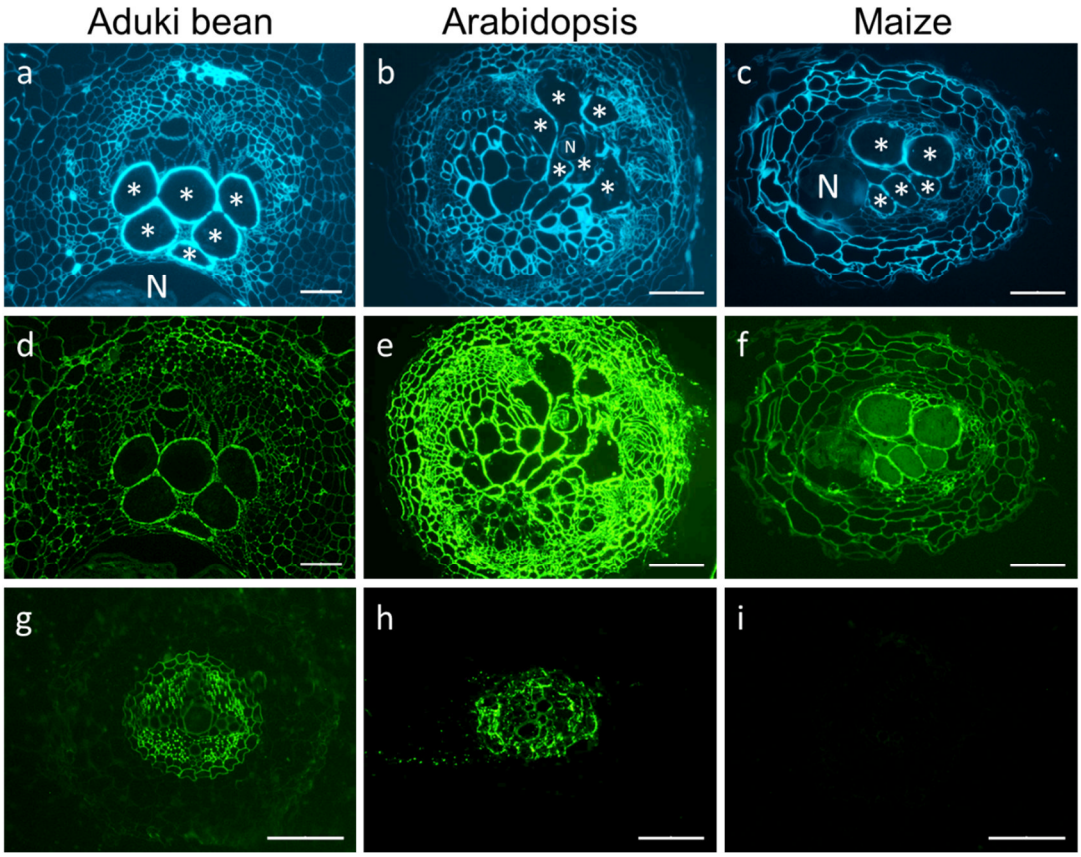

Figure 3.9 Immunolabelling of methyl esterified pectic homogalacturonan in nematode infected and uninfected aduki bean, Arabidopsis and maize root sections at 21 days post infection (dpi). LM20 antibody localised methyl esterified pectic homogalacturonan in nematode-infected and uninfected root sections of host plants. The localization of methyl esterified pectic homogalacturonan in infected root sections of aduki bean (d), Arabidopsis (e) and maize (f) and uninfected root sections of aduki bean (g), Arabidopsis (h) and maize (i) are presented. The corresponding Calcofluor white stained infected root sections are presented for aduki bean (a), Arabidopsis (b), and maize (c). Asterisks indicate giant cells; N, represents the nematode. Bars: (a-f) 100 µm; (h) 30 µm and (g & i) 70 µm

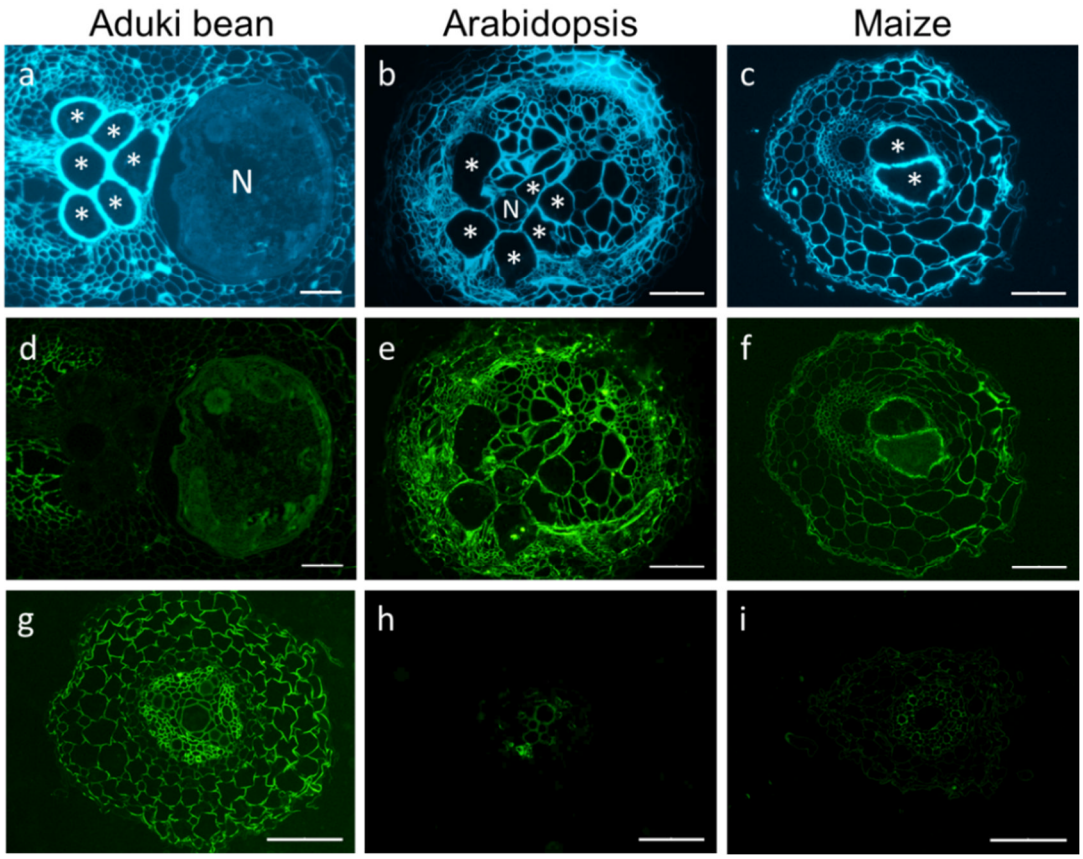

Figure 3.10 Immunolabelling of galactan in nematode infected and uninfected aduki bean, maize and Arabidopsis root sections at 21 days post infection (dpi). LM5 localised galactan in nematode-infected and uninfected root sections of host plants. The localization of LM5 in infected root sections of aduki bean (d), Arabidopsis (e) and maize (f) and uninfected root sections of aduki bean (g), Arabidopsis (h) and maize (i) are presented. The corresponding Calcofluor white stained infected root sections are presented for aduki bean (a), Arabidopsis (b), and maize (c). Asterisks indicate giant cells; N, represents the nematode. Bars: (a-f) 100 µm; (h) 30 µm and (g & i) 70 µm.

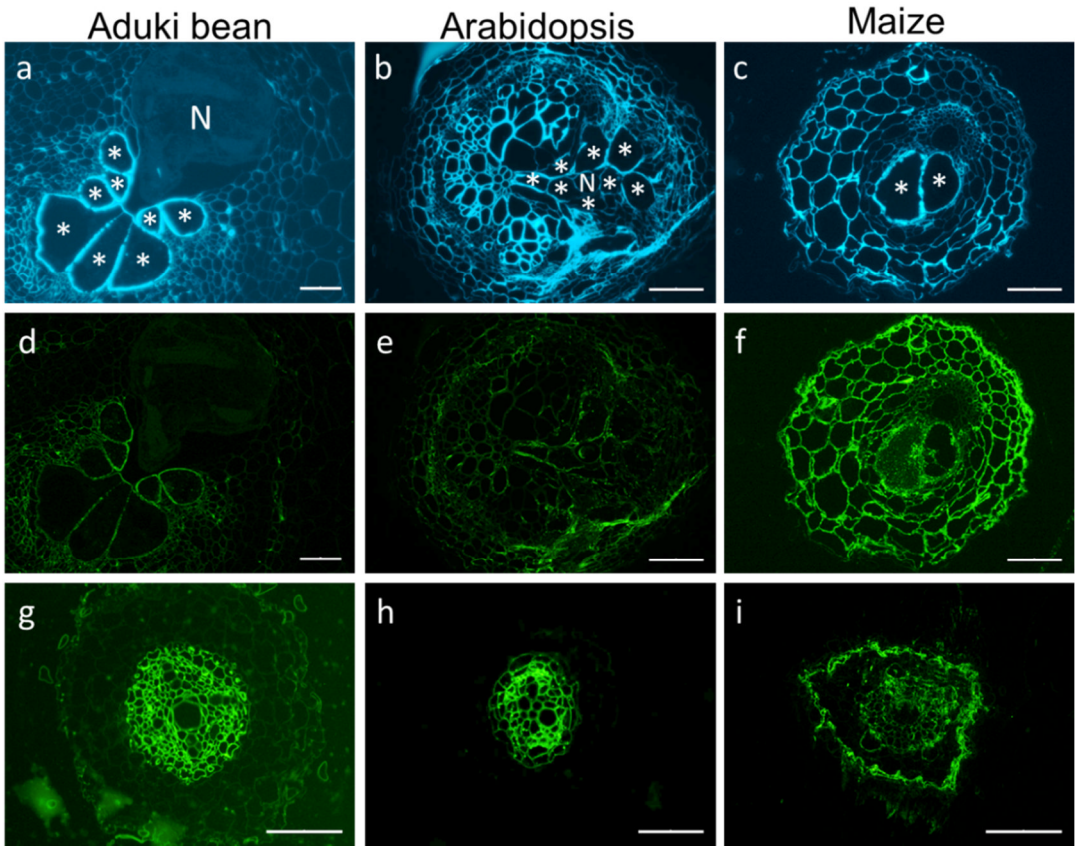

Figure 3.11 Immunolabelling of arabinan in nematode infected and uninfected aduki bean, Arabidopsis and maize root sections at 21 days post infection (dpi). LM6 antibody localised arabinan in nematode-infected and uninfected root sections of host plants. The localization of arabinan in infected root sections of aduki bean (d), Arabidopsis (e) and maize (f) and uninfected root sections of aduki bean (g), Arabidopsis (h) and maize (i) are presented. The corresponding Calcofluor white stained infected root sections are presented for aduki bean (a), Arabidopsis (b), and maize (c). Asterisks indicate giant cells; N, represents the nematode. Bars: (a-f) 100 µm; (h) 30 µm and (g & i) 70 µm

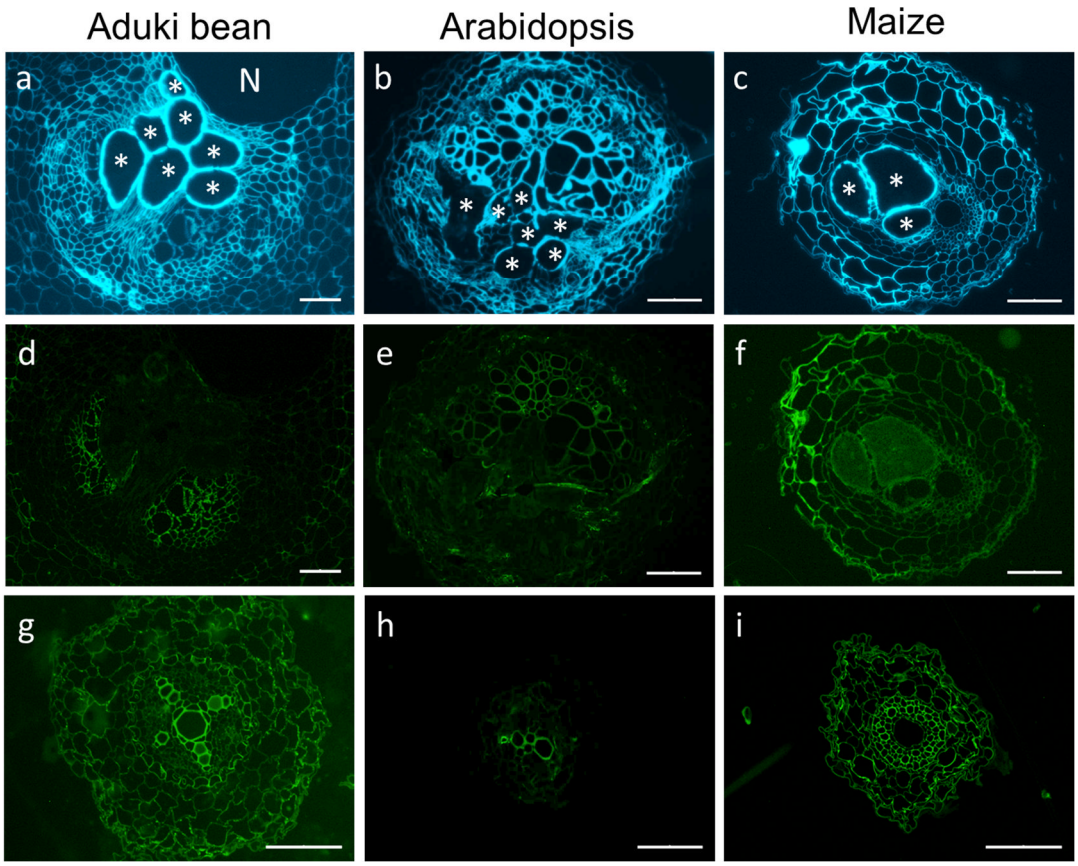

Figure 3.12 Immunolabelling of processed arabinan in nematode infected and uninfected aduki bean, Arabidopsis and maize root sections at 21 days post infections (dpi). LM16 antibody localised the processed arabinan in nematode infected and uninfected root sections of host plants. The Calcofluor white staining root sections are presented with aduki bean (a), Arabidopsis (b), and maize (c). The localization of processed arabinan in infected root sections of aduki bean (d), Arabidopsis (e) and maize (f) and uninfected root sections of aduki bean (g), Arabidopsis (h) and maize (i) are presented. Asterisks indicate giant cells; N, represents the nematode. Bars: (a, b, c, d, e, f) 100 µm; (h) 30 µm and (g & i) 70 µm

3.4.1.3 Glycoproteins

Arabinogalactan proteins (AGPs) and extensin are glycoproteins recognised by antibodies LM2 and JIM13. Induction of Arabinogalactan protein (AGPs) in maize infected with *M. incognita* contrasts with suppressed AGP patterns in infected Arabidopsis and aduki bean. The antibody LM2 recognises glycan epitopes (β-linked GlcA) of AGPs. LM2 bound to the walls of giant cells and all other cell types within the vascular cylinder of infected maize root sections (Figure 3.13 f) but binding of LM2 was very low in cell walls of the uninfected maize root (Figure 3.13 i). This suggests that the presence of the LM2 AGP epitope is induced in the root by nematode infection. Conversely LM2 binding was observed in uninfected aduki bean (Figure 3.13 g) and a low level of binding in Arabidopsis (Figure 3.13 h) but that binding was not or barely evident in infected root sections (Figure 3.13 d, e). This suggests that nematode infection acts to suppress the presence of AGPs in cell walls of these hosts. Another anti-AGP glycan antibody JIM13 showed similar binding patterns to LM2 in uninfected of Arabidopsis and bean root sections (Figure 3.14 g, h). However, no binding was detected in uninfected and infected root sections in vascular cylinder of maize and infected root sections of aduki bean (Figure 3.14 f, i, d).

The JIM19 and JIM20 antibodies detect extensin epitopes on the cell wall. In this study, JIM20 bound inconsistently in the vascular cylinder of uninfected root sections of aduki bean and maize but no binding was detected in Arabidopsis root sections (Figure 3.15). Another anti-extensin monoclonal antibody JIM19 did not bind any of the cell wall walls of the nematode feeding site, but weak and inconsistent binding was observed in root sections of maize and infected section of aduki bean (Figure 3.16).

3.4.2 Cell wall thickness

In comparison to the thickness of neighbouring cell wall in the vascular cylinder, in the cell wall thickness of giant cells, induced by *M. incognita* was much greater. Walls of giant cells induced in aduki bean were thicker (6.6 ± 0.3 µm) than those in the other two hosts whilst the thickness of neighbouring cell walls of aduki bean was only 1.4 ± 0.05 µm. The giant cell walls of Arabidopsis and maize were 4.3 ± 0.2 µm and 4.5 ± 0.2 µm thick respectively (Figure 3.17). This result suggests that giant cells

have walls at least 2.5 times thicker than those of other root cells, possibly helping to strengthen the giant cell wall.

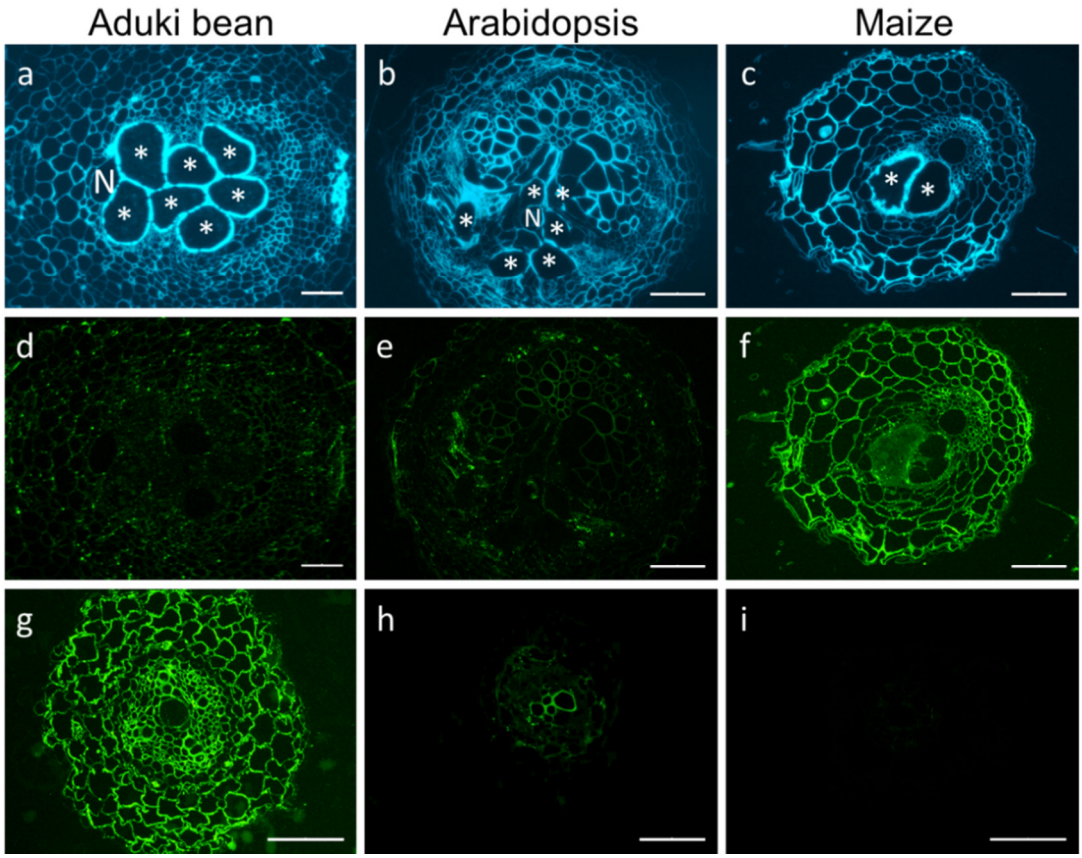

Figure 3.13 Immunolabelling of arabinogalactan proteins (AGPs) in nematode infected and uninfected aduki bean, Arabidopsis and maize root sections at 21 days post infections (dpi). LM2 antibody localised the AGPs in nematode infected and uninfected root sections of host plants. The localization of AGPs in infected root sections of aduki bean (d), Arabidopsis (e) and maize (f) and uninfected root sections of aduki bean (g), Arabidopsis (h) and maize (i) are presented. The Calcofluor white staining root sections are presented with aduki bean (a), Arabidopsis (b), and maize (c). Asterisks indicate giant cells; N, represents the nematode. Bars: (a-f) 100 µm; (h) 30 µm and (g & i) 70 µm.

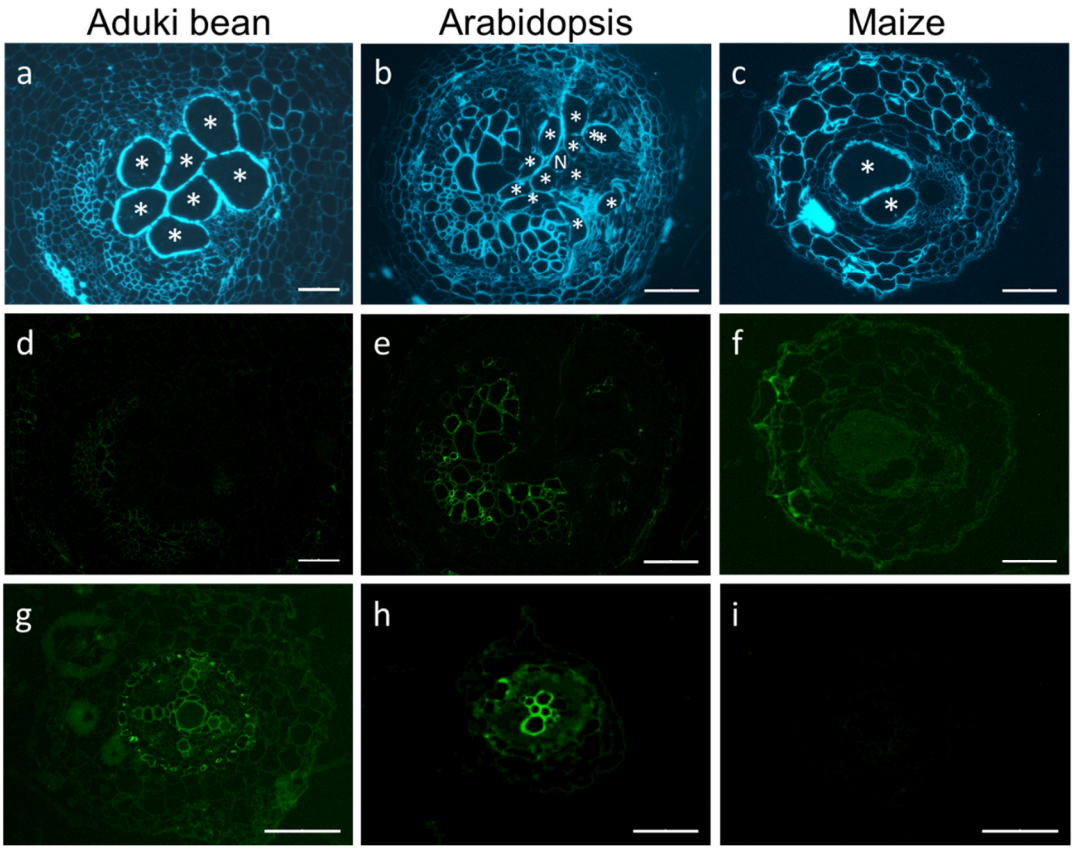

Figure 3.14 Immunolabelling of arabinogalactan proteins (AGPs) in nematode infected and uninfected aduki bean, Arabidopsis and maize root sections at 21 days post infections (dpi). JIM13 antibody localised the AGPs in nematode infected and uninfected root sections of host plants. The localization of AGPs in infected root sections of aduki bean (d), Arabidopsis (e) and maize (f) and uninfected root sections of aduki bean (g), Arabidopsis (h) and maize (i) are presented. The Calcofluor white staining root sections are presented with aduki bean (a), Arabidopsis (b), and maize (c). Asterisks indicate giant cells; N, represents the nematode. Bars: (a-f) 100 µm; (h) 30 µm and (g & i) 70 µm.

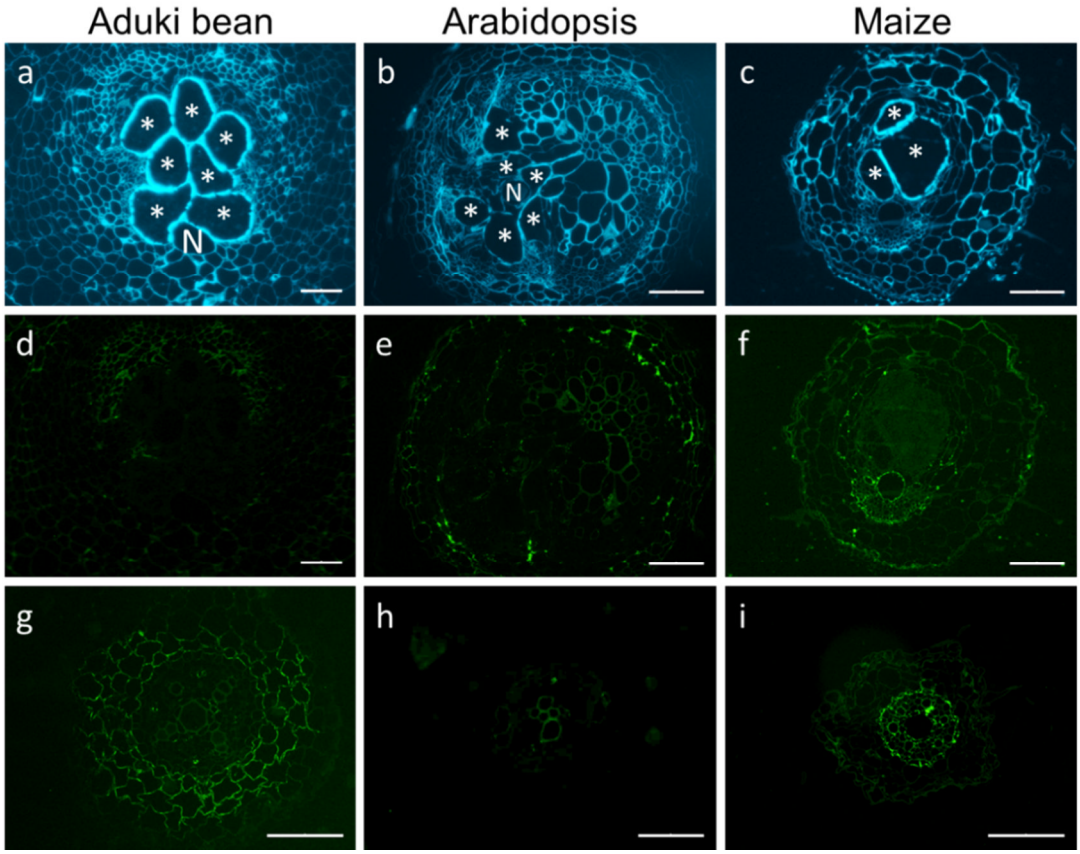

Figure 3.15 Immunolabelling of extensin in nematode infected and uninfected aduki bean, maize and Arabidopsis root sections at 21 days post infection (dpi). The JIM20 antibody localised extensin in nematode-infected and uninfected root sections of host plants. The localization of JIM20 in infected root sections of aduki bean (d), Arabidopsis (e) and maize (f) and uninfected root sections of aduki bean (g), Arabidopsis (h) and maize (i) are presented. The corresponding Calcofluor white stained infected root sections are presented for aduki bean (a), Arabidopsis (b), and maize (c). Asterisks indicate giant cells; N, represents the nematode. Bars: (a-f) 100 µm; (h) 30 µm and (g & i) 70 µm.

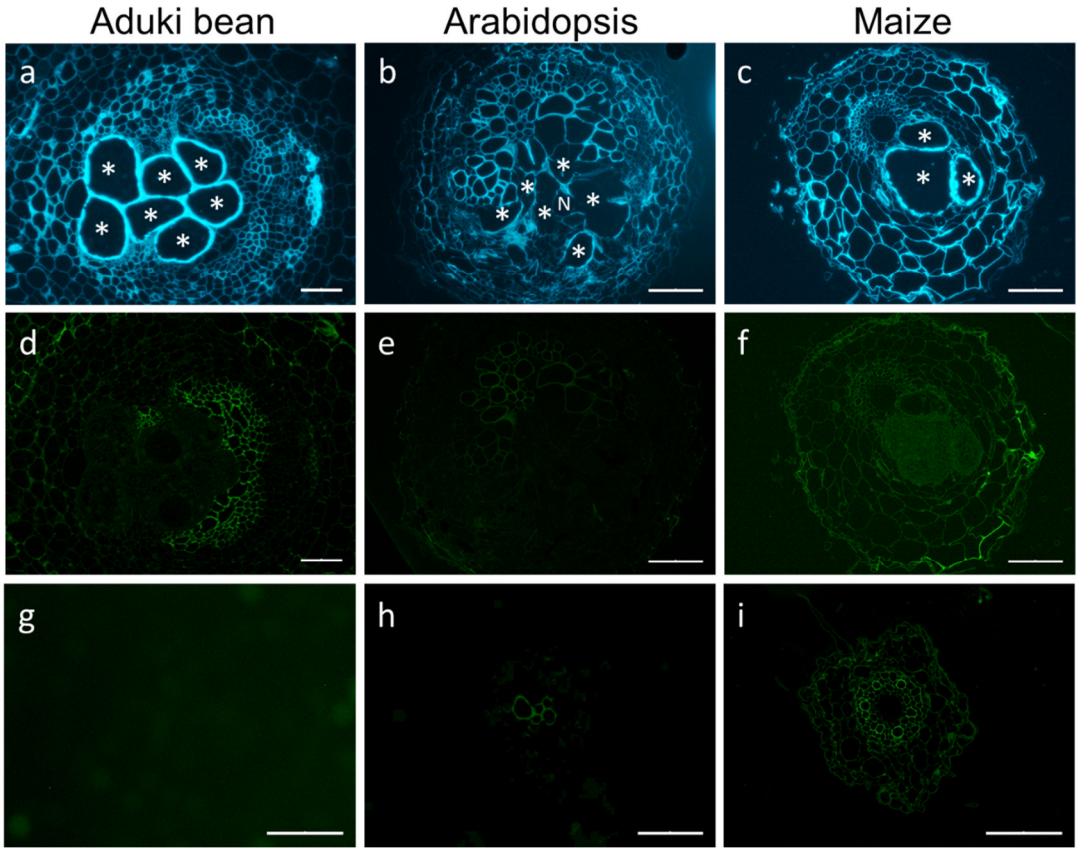

Figure 3.16 Immunolabelling of extensin in nematode infected and uninfected aduki bean, maize and Arabidopsis root sections at 21 days post infection (dpi). The JIM19 antibody localised extensin in nematode-infected and uninfected root sections of host plants. The localization of JIM19 in infected root sections of aduki bean (d), Arabidopsis (e) and maize (f) and uninfected root sections of aduki bean (g), Arabidopsis (h) and maize (i) are presented. The corresponding Calcofluor white stained infected root sections are presented for aduki bean (a), Arabidopsis (b), and maize (c). Asterisks indicate giant cells; N, represents the nematode. Bars: (a-f) 100 µm; (h) 30 µm and (g & i) 70 µm.

Table 3.2 Immunolocalization of antibodies in *Meloidogyne incognita* infected and uninfected cell walls of aduki bean, Arabidopsis and maize roots at 21 days post infection*

Cell Wall Component		Primary Antibody	Host species								
			A.bean			Arabidopsis			Maize		
			Infected		Uni	Infected		Uni	Infected		Uni
			VC	GC	VC	VC	GC	VC	VC	GC	VC
Hemicellulose	Xylan	LM11	++	-	++	++	-	++	++	++	++
	Fer. xylan	LM12	-	-	-	-	-	-	++	++	+
	Mannan	LM21	+/-	-	+	+	++	++	+	+/-	+
	MLG	MLG	na	na	na	na	na	na	++	++	++
	Xyloglucan	LM25	+/-	+	++	++	++	++	+/-	++	++
	Xyloglucan	LM15	+/-	+	++	++	++	+	++	++	-
Pectin	MePHG	LM20	+	++	++	++	++	++	+	++	-
	DeSPHG	LM19	+/-	-	+/-	+/-	-	+/-	+/-	-	+
	Galactan	LM5	+/-	-	++	++	++	-	+/-	++	-
	Arabinan	LM6	+/-	+	++	+/-	+/-	++	+	+	+
	P. arabinan	LM16	+/-	-	+	+/-	-	+/-	+/-	-	+
Glycoprotein	AGPs	JIM13	-	-	+/-	+/-	-	+	-	-	-
	AGPs	LM2	+/-	-	++	+/-	-	+/-	+	+	-
	Extensin	JIM20	-	-	+/-	+/-	-	-	+/-	-	+
	Extensin	JIM19	+/-	-	-	-	-	-	+/-	-	+/-
No antibody			-	-	-	-	-	-	-	-	-

* Table was prepared based on images from figures 3.2-3.16 and Supplementary Data S1 on the digital optical disc data storage (Supplementary data S1 in CD). Antibody detection is shown in vascular cylinder and giant cell walls: VC, cells walls of whole vascular cylinder apart from giant cells; GC, Giant cells walls; Uni, uninfected; MLG, Mixed linkage glucan; Fer. xylan, Feruloylated xylan; MePHG, Methyl esterified pectic homogalacturonan; DeSPHG, De esterified pectic homogalacturonan; P arabinan, Processed arabinan; AGPs, Arabinogalactan proteins; antibody binding:(-) antibody not detected; (+/-) inconsistent binding; (+) binding; (++) strongly binding.

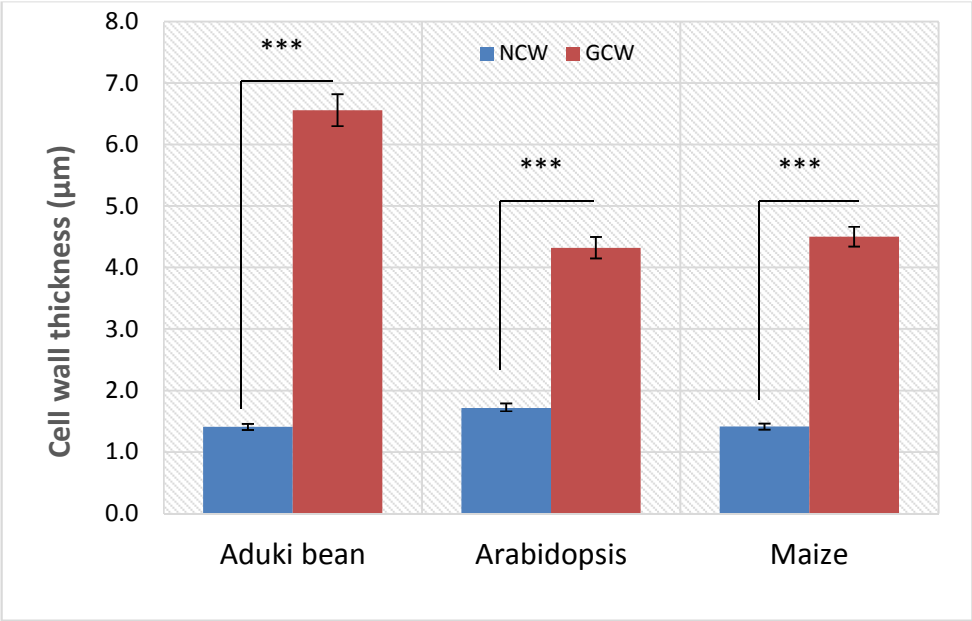

Figure 3.17 Thickness of giant cell wall and neighbouring cell walls in nematode infected root sections of aduki bean, Arabidopsis and maize at 21 days post infection (dpi). Ninety measurements from 20 cells were performed. Asterisks indicate significance level ***P ≤ 0.001 (Microsoft Excel t-test). NCW, Neighbouring cell walls around giant cells; GCW, giant cell walls in nematode infected root sections.

3.5 Discussion

3.5.1 Cell wall molecular architectures in nematode feeding sites

Root-knot nematodes cause robust changes during the formation of their feeding sites in host plant roots, not only at the physiological and molecular level, but also at the morphological level of cell development. This leads to the formation of a feeding site together with cell wall modifications within host plant roots (Table 3.2 and Figure 3.1). The root knot nematodes also effect alterations in the vascular cylinder in addition to the induction of giant cells (Figure 3.1). Elucidating the molecular architecture of giant cell walls is crucially important to understanding the functions and structural mechanisms of this specialized cell form.

The result of *in situ* analyses showed that the glycan components of giant cell walls, vascular cylinder cells and xylem elements varied based on plant hosts (Table 3.2). Xyloglucan, methyl esterified pectic homogalacturonan and arabinan were present in the giant cell wall of all three hosts. Extensin was lacking in the giant cell walls of all hosts and the rest of the cell wall components analyzed: mixed linkage glucan, feruloylated xylan, xylan, arabinogalactan proteins, mannan, processed arabinan and galactan varied depending on the aduki bean, maize and Arabidopsis hosts.

3.5.1.1 Hemicellulose

Hemicellulose, together with the network of cellulose microfibrils, is responsible for the structural integrity of the cell wall, providing strength and rigidity. Xylan is a major hemicellulose in secondary cell walls in dicots (Rennie and Scheller, 2014). Xylan synthesis occurs during the development of xylem vessels, which in dicots are the main site of secondary cell walls and hence the location of most xylan. However, xylan is distinct from xyloglucan (Northcote et al., 1989). Xylan is arranged into large units before integration into the cell wall (Bowles and Northcote, 1976). Xylan is not present in cyst nematode-induced syncytium cell walls in Arabidopsis roots (Davies et al., 2012). Likewise, in our study, xylan was not detected in the giant cell walls of Arabidopsis and aduki bean, indicating that neither type of feeding cell has a secondary cell wall. Xylan was detected in giant cell walls of maize, where its presence likely just reflects the fact that xylan is a common component of all cell walls in grasses, including maize. Some parasitic nematode species break down xylan for successful parasitism. For instance, a secreted endoxylanase is thought to disrupt

xylan during the parasitism of *Radopholus similis* (a migratory endoparasitic nematode) so facilitating the migration of the nematode through roots (Haegeman et al., 2012). The root-knot nematode used in this work, *M. incognita,* also has a xylanase gene *Mi-xyl1,* which encodes a glycosyl hydrolase family 5 enzyme (Mitreva-Dautova et al., 2006). This secreted enzyme may be important during the intial migratory phase of the J2s, or it may be involved during the formation of giant cells. In contrast, xylanase genes have not been identified in the cyst nematodes *H. schachtii, H. glycines* (Fosu-Nyarko et al., 2016) and *G. pallida* (Cotton et al., 2014). Mannan is detected in syncytial cell walls at 14 dpi after removing the pectic homogalacturonan in the root sections of Arabidopsis (Davies et al., 2012). Mannan was detected at 21 dpi in the giant cell walls of Arabidopsis and maize but not aduki bean in this study. The mannan backbone is involved in remodeling and loosening the plant cell wall (Rodriguez-Gacio et al., 2012). The abundance of mannan in giant cell walls may suggest that the walls are loosened to allow the rapid expansion of these multinuclear cells that occurs during feeding site development.

LM15 and LM25 were used to detect xyloglucan in the roots of Arabidopsis, aduki bean and maize in this study. Several enzymes are involved during xyloglucan synthesis with different combinations of xylosyltransferases promoting the diversity of side chains found decorating the glucan backbone (Zabotina et al., 2012). Xyloglucan plays a key role in cell expansion and probably controls the size of the microfibrils during cellulose biogenesis and the enlargement of cells during growth (Hayashi, 1989). The glucan backbone of xyloglucan forms cross-links between adjacent cellulose microfibrils. A high level of cross-linking contributes to increased rigidity of the cell wall while degradation of the cellulose-xyloglucan links causes the walls to loosen (Pauly et al., 2013). The presence of xyloglucan in giant cell walls may reflect the need for strength combined with the flexibility that could be achieved through dynamic modulation of the cross-links. Similarly, both the external and internal cell walls of syncytia induced by *H. schactii* in Arabidopsis roots contain abundant xyloglucan (Davies et al., 2012).

3.5.1.2 Pectin

Homogalacturonan

The LM20 (methyl-esterified pectic homogalacturonan (HG)) and LM19 (de-esterified pectic HG) antibodies were used to define the pectic homogalacturonan content of the giant cell walls in this study. Both the methyl-esterified and de-esterified forms of HG were observed in cell walls in roots of all three hosts, although binding of LM20 was generally stronger. However the LM19 epitope was almost completely absent from the walls of giant cells, in contrast to the strong binding of LM20, suggesting that the HG in these walls is highly methyl-esterified. The highly methyl-esterified form of HG is predominant during embryonic maturation and low ester HG is most abundant at the beginning of the embryo formation in the somatic embryogenesis of *Trifolium nigrescens* (Pilarska et al., 2013). *AtPM3* (Arabidopsis *PECTIN METHYLESTERASE 3*) is up-regulated after infection of a cyst nematode (*H. schachtii*) at 8 dpi. To make it more clear, higher (over-expression) and knock-out expression of *AtPM3* lines indicated the increased susceptibility and lower susceptibility to the nematode, respectively (Hewezi et al., 2008).

The methyl-esterification affects the cell wall strength (Willats et al., 2001b). When pectic HG is first secreted into the wall it is highly methyl-esterified and then subsequently de-esterified. Strengthening of the cell wall is associated with de-esterified HG, which forms cross-linkages with cations, mostly Ca^{2+}, resulting in the formation of pectic gels (Wolf et al., 2009). Similar to the present result, the cyst nematode formed syncytia cell walls contain abundant methyl-esterified pectic HG in Arabidopsis roots (Davies et al., 2012). Methyl-esterified residues are abundant and harmoniously distributed in all cells of sugar beet but un-esterified residues are found in some cell junctions and the lining of intercellular spaces (Guillemin et al., 2005). The LM19 (de-esterified HG) epitope is sensitive to acetylation (the process of introducing an acetyl group (CH_3CO)) (Yu et al., 2011). Ca^{2+} cross-linked pectin is found in cell walls lining intercellular spaces that it shows its role in cell-cell adhesion (Christiaens et al., 2011). The abundant methyl-esterified HG present in giant cell walls suggests that the walls retain flexibility that may be important for their function.

Rhamnogalacturonan-I

Rhamnogalacturonan-I comprises the large polysaccharides with a backbone of disaccharide units (Harholt et al., 2010). The pectic polysaccharides constitute approximately one third of the primary cell walls of dicotyledonous plants (Zhu et al., 2005). The pectic rhamnogalacturonan-I-associated LM5 β-1,4-D-galactan epitope occurs in a limited manner on epidermal, cortical and endodermal cell walls of Arabidopsis roots (McCartney et al., 2003).

The pectic polysaccharides have a possible important role in plant cell development as β(1→4)-D-galactan is seen in the root cap cell differentiation and in cell walls of differentiating stele (central part of root) and cortical cells but it is absent from the cell walls of the central meristematic cells (Willats et al., 1999). Galactan is mainly located in the Golgi apparatus and incorporated with the membrane of the potato plant cell (Geshi et al., 2004). The LM5 (galactan) epitope is mainly found in the cambial zone and is associated with stiffening of cell walls (Guillemin et al., 2005, McCartney et al., 2003), but the LM6 (arabinan) epitope is widely distributed throughout primary walls and is abundant in sugar beet roots (Guillemin et al., 2005). I can conclude from my results that the giant cell wall thickening was increased at 21 dpi based on binding of galactan and arabinan.

Arabinan (in some walls) and galactan (in the xylem parenchyma) are increased during the infection of *Ralstonia solanacearum* (a harmful bacterium species) in tomato roots (Diogo and Wydra, 2007). Galactan is not visualized in the cyst nematode (*H. schachtii*) induced syncytia cell walls; however, arabinan is observed. The processed arabinan detecting antibody, LM16, binds to the inner cell wall fragments within the syncytia (Davies et al., 2012). Binding of LM16 was not detected in the giant cell wall of bean and maize in this study. Arabinan detection varies depending on the presence of arabinan structures, and arabinan binding can also be changed depending on plant tissues and antibodies complex patterns (Willats et al., 1998, Verhertbruggen et al., 2009b). LM16 is also sensitive to the action of beta-galactosidase and it binds the de-branched arabinan (Verhertbruggen et al., 2009b).

In this study, the specific antibodies were used to detect galactan (LM5), processed arabinan (LM16) and arabinan (LM6) within the rhamnogalacturonan-I. Galactan was not observed in the giant cell walls of aduki bean but was present in the giant cell

Table 3.3 Comparison of the cell wall molecular architectures in the feeding site of a cyst nematode *Heterodera schachtii and root knot nematode *Meloidogyne incognita*[#] induced feeding site (giant cell) cell walls in *Arabidopsis thaliana*.**

Primary Antibody	Cell wall components	Syncytium cell walls*	Giant cell walls[#]
LM11	Xylan	**-**	**-**
LM12	Feruloylated xylan	**n/a**	**-**
LM21	Mannan	**+**	**+**
LM15	Xyloglucan	**+**	**+**
LM25	Xyloglucan	**n/a**	**+**
LM19	De-esterified HG	**-**	**-**
LM20	Methyl esterified HG	**+**	**+**
LM5	Galactan	**-**	**+**
LM6	Arabinan	**+**	**+/-**
LM16	Processed arabinan	**+/-**	**+/-**
LM2	Arabinogalactan protein (AGP)	**-**	**-**
JIM13	Arabinogalactan protein (AGP)	**+**	**-**
JIM19	Extensin	**-**	**-**
JIM20	Extensin	**n/a**	**-**

*****The data of syncytium cell wall composition was taken from (Davies et al., 2012) at 14 dpi. [#]Root knot nematode infected giant cell wall molecular architectures in Arabidopsis root sections at 21 dpi (present study). (+), represents the antibody binding; (+/-), inconsistent binding; (-), no binding; (n/a), no study has been done.

walls of maize and Arabidopsis. Although arabinan was detected in the giant cell walls of all hosts, processed arabinan was only detected in the giant cell walls of Arabidopsis at 21 dpi.

In general, pectin plays a role in cell wall flexibility and stiffness and the particular distribution of RGI and HG in giant cell walls, particularly the high methyl-esterification of HG and the presence of arabinan may suggest that the giant cell wall is highly flexible. The flexibility of giant cells may be important to resist high turgor pressure during the nematode feeding. The cell wall flexibility may also be closely related to nutrient flow in giant cells.

3.5.2 Glycoproteins in the nematode feeding site

Neither arabinogalactan proteins nor extensin were readily detected in giant cell walls.

3.5.2.1 Arabinogalactan proteins (AGPs)

Arabinogalactan proteins (AGPs) are heavily glycosylated cell wall proteins that contain abundant arabinose, galactose and hydroxyproline residues. They are found in almost all organs of plants and they play important roles in plant survival and development; however, the presence of AGPs varies in diverse plant species (Nguema-Ona et al., 2012, Nobre and Evans, 1998). Accordingly, AGPs were not detected in Arabidopsis or aduki bean but they were detected in the giant cell walls of maize in this present study. Antibody JIM15 (AGP binding) recognizes plasma membrane glycoproteins and JIM13 binds to the surface of the epidermis (Knox et al., 1991). In this study, the AGP detecting antibody JIM13, did not bind to any giant cell walls of any plant host. Similarly, Knox *et al.* (1991) indicated that JIM13 gave a weak reaction during the reactivity of anti-AGP probes with molecules at the rice (*Poaceae* family) cell surface. However, LM2 binding was observed in maize root sections in this study. The JIM13 antibody localizes in all syncytial cell surfaces in Arabidopsis roots after infection with *H. schachtii*. The LM2 epitope was not visualized in syncytial cell walls (Table 3.3) (Davies et al., 2012). Although AGP epitopes are seen on the plasma membrane of giant cells during the early nematode infection, after maturation of giant cells AGP epitopes are invisible (Nobre and Evans, 1998). In general anti-AGP monoclonal antibodies including JIM13 are used

to recognize carbohydrate epitopes but LM2 recognizes a glucuronic acid-containing epitope and the plasma membrane of all cells at the root apices is recognized by LM2 (Smallwood et al., 1996). I can conclude from my study results that the giant cell walls of dicots (aduki bean and Arabidopsis) do not contain either carbohydrate or glucuronic acid-containing epitopes but the giant cell walls of maize (*Poaceae* family) contain the glucuronic acid-containing epitope.

3.5.2.2 Extensin

Extensin is a structural protein found in plant primary cell walls. It is involved in disease and wound responses in plants: pathogen induced extensin accumulation correlated with disease resistance and biosynthesis of extensin is seen during physical wounding (Lamport et al., 2011). Accumulation of extensin leads to an increase in Arabidopsis stem thickness (Roberts and Shirsat, 2006). The expression of extensin is induced after pathogen attack (Keller, 1993) and during the wounding of leaves but it is not increased by viral infection (Hirsinger et al., 1997). Moreover, the infection of anthracnose fungus causes the hydroxyproline (Hyp)-rich glycoprotein (HRGP), arabinose and hydroxyproline contents to increase in melon plants (Esquerretugaye et al., 1979). Although high extensin expression is found in tobacco plants after inoculation with *M. incognita*, there is virtually no extensin found in giant cells (Nobre and Evans, 1998). In this study, extensin was not observed in the giant cell wall of maize, Arabidopsis or aduki bean. The extensin was determined in the root section of uninfected maize roots but no antibody detection was seen in the giant cell walls of any host plants (Figure 3.15, 3.16). It can be concluded from these results that nematodes may suppress the extensin accumulation in giant cell walls.

The rapid protein insolubilization leads to a strengthened cell wall of soybean during attack by the pathogen *Pseudomonas syringae* in incompatible interactions but not compatible interactions (Brisson et al., 1994). The pathogen attack causes the insolubilization of extensin within minutes (Lamport et al., 2011, Bradley et al., 1992). For successful parasitism, *Meloidogyne* species manipulate the fundamental elements of the host plant cell during the compatible interaction. During the nematode infection, the extensin may be solubilized in the feeding site cell walls in this study as it was observed in some cortical cells but not in giant cells. Solubilised extensin could not be detected by JIM19 and JIM20. Extensin also plays a role in the innate

immunity response during the pathogen interactions (Plancot et al., 2013). The result of our study indicated that innate immunity may not be present during the successful nematode parasitism.

3.6 Overview

- ✓ The host plant species manipulated the giant cell wall molecular architectures after infection with *M. incognita* at 21 dpi.
- ✓ Host plants influenced the availability of mixed linkage glucan, feruloylated xylan, xylan, mannan, processed arabinan, galactan and arabinogalactan proteins in the giant cell wall.
- ✓ Homogalacturonan, xyloglucan and arabinan were common amongst host plants in the giant cell wall of feeding site.
- ✓ The arabinogalactan proteins epitope recognised by JIM13 was not present in any host plant species but the LM2 AGP epitope was observed in maize giant cell walls.
- ✓ Extensin was not detected in giant cell walls in any hosts.
- ✓ Giant cell walls were thicker than surrounding cell walls.

Chapter 4

Gall structure and cell wall composition

4 Gall structure and cell wall composition

4.1 Introduction

Root knot nematodes cause dramatic changes in host plant roots, including swollen structures termed galls that surround the nematode feeding sites. The proliferated vascular and cortical cells of the gall are distinct from the giant cells that they surround. The focus of the previous chapter was on the cell wall architecture of the giant cells and the immediately adjacent cells of the root vascular cylinder. In this chapter, analysis is extended to encompass the whole gall region of *Meloidogyne*-infected roots of Arabidopsis, aduki bean, maize and potato plant species. The presence/absence and relative levels of different cell wall components in galls was determined by Enzyme-Linked Immunosorbent Assay (ELISA).

4.1.1 Galls

Galls are abnormal growths of the plant tissue that some pests, including insects (Maia and Silva, 2016, Giron et al., 2016) and pathogens such as bacteria and fungi (Le Fevre et al., 2015), may cause in their host plants. Among the plant parasitic nematodes, the root knot nematodes (*Meloidogyne* spp.) also cause the formation of galls, termed "root-knots," within the host plant roots. A combination of hyperplasia (the enlargement of a tissue increased by the division and differentiation of cells) and hypertrophy (enlargement of a tissue due to the increasing size of its cells) leads to the formation of root galls around the giant cells following the establishment of RKN feeding sites within the host (Favery et al., 2016b, Caillaud et al., 2008). Higher levels of endoreduplication occur within the galls for the duration of gall development; however, the endoreduplication is reduced during the gall maturation (de Almeida Engler and Gheysen, 2013).

Plant hormones play an important role in regulation of plant growth and development (Santner and Estelle, 2009). Gall formation is related to the induction of plant hormones (Glickmann et al., 1998, Goethals et al., 2001, Hutangura et al., 1999). Manipulation of these hormones by nematodes causes abnormal growth of the root tissue (Hutangura et al., 1999). Ethylene, a plant hormone, plays a role in RKNs induced-gall formation in tomato plants (Glazer et al., 1983). Auxin has a role in the development of plant roots and cell division (De Smet et al., 2010). The nematode feeding site initiation and development (including gall number and expansion) are

affected by the modification of auxin transport in *M. incognita* infected *A. thaliana* roots (Kyndt et al., 2016). *M. javanica*, controls the auxin distribution and accumulation in plant root (Hutangura et al., 1999). The secretions of *M. incognita* result in increased auxin and cytokinin levels in host cells (Viglierchio, 1971). Particular gene expression patterns occur in nematode induced galls (Hammes et al., 2005).

Therefore, galls are a sustainable living space for the nematode, in which living necessities are provided by the host plant. The glycan structure of galls (hemicellulose, pectin and glycoprotein) have not been fully understood. Hence, Enzyme-Linked Immunosorbent Assay (ELISA) using monoclonal antibodies was used to reveal the gall molecular architectures in nematode feeding site.

4.1.2 Enzyme Linked Immunosorbent Assay (ELISA)

ELISA is a sensitive and effective method to determine the levels of antigens using antibodies which are highly specific and was firstly developed in the early 1970's (Engvall and Perlmann, 1972). It can be employed as a diagnostic tool in plant pathology when specific antibodies are used to detect levels of antigens, which are biomarkers for viruses and pathogenic microbes (Kumada, 2014). Antibodies are obtained from animal serum (polyclonal antibodies) or hybridoma (producing hybrid cell line) cells (monoclonal antibodies) that are used in a variety of areas including molecular biology (Kumada, 2014). Monoclonal antibodies generated from rat spleen cells are important molecular probes that can detect the epitopes or specific binding sides of cell wall structures in plant cell walls (Hervé et al., 2011).

The ELISA technique employed in these experiments uses antibodies to detect the concentration of particular molecules in cell wall extracts of nematode induced galls of host plants. A horseradish-peroxidase-conjugated secondary antibody that recognises the primary antibody is used in conjunction with a colorimetric substrate, allowing detection and quantification of the target molecules. However, root knot nematodes induced gall molecular architectures have not been fully understood. For this aim, ELISA using monoclonal antibodies was performed as a method to analyse the gall molecular architecture in galls of host plant roots in this chapter.

4.2 Aims

The main aim of this chapter was to use enzyme-linked immunosorbent assay to comparatively quantify the cell wall molecular constituents of *M. incognita*-induced galls in maize, Arabidopsis, aduki bean, and potato hosts.

- Analysis of polysaccharides in nematode-induced galls and uninfected roots of host plants.
    - Hemicellulose related polysaccharides
        - Xyloglucan
        - Mannan
    - Pectin
        - Arabinan
        - Processed arabinan
        - Galactan
    - Glycoprotein
        - Arabinogalactan proteins (AGPs)
- Comparison of nematode-induced gall size between different host species

4.3 Material and Methods

Collection of root samples, tissue sample fixation, ethanol dehydration and resin embedding of root samples, slide preparation with Vectabond™ reagent, and microtome cutting and gathering of sections are discussed in Chapter 2.

4.3.1 Plant and nematode culture

Potato (*Solanum tuberosum*, 'Desiree'), aduki bean (*Vigna angularis*) and maize (*Zea mays*) hosts were grown in pouches as described in section 2.1.1. *Arabidopsis thaliana* was grown in sterile culture on solidified Gamborg's B5 medium including vitamins (Duchefa Biochemie, Haarlem, The Netherlands). The newly emerged chits of potato tubers were gently removed and seeds of aduki bean and maize placed into the upper fold of growth pouches (Mega International) and they were grown in pouches. Second-stage juveniles (infective stage of nematode) of *Meloidogyne incognita* VW6 (University of California, Davis), collected as described in section 2.2, were used to infect plants: the nematode infective juveniles were sterilised prior to infection of Arabidopsis roots. Sterilised nematodes were inoculated to Arabidopsis plants, which were grown in sterile conditions as described in section 2.1.2. All nematode infected plants were grown at 25 °C with 16h light/8h dark conditions. Uninfected plants were also grown in the same conditions as control plants. Detailed information about plant and nematode culture was given in Chapter 2. Two plants were grown in each pouch and around 30 plants (15 pouches) of each species were infected with *M. incognita,* with five root tips infected per plant. The same number of uninfected control plants was also grown in identical conditions for each experiment.

Following the nematode infection, galls and equivalent length pieces of uninfected roots which were located at similar positions relative to the root tip, were collected at 21 days post infection (dpi).

4.3.2 Preparation of samples for Enzyme Linked Immunosorbent Assay

The nematode-induced galls and uninfected root segments were collected using scalpels into 1.5 ml Eppendorf tubes (Sarstedt, Germany) and immediately flash frozen in liquid nitrogen. Following the collection of root samples, the frozen tubes were stored at -80 °C until use.

Samples were taken from -80 °C and placed within dry ice while carrying to the freeze dryer (LyoPro 6000). Samples were placed in the freeze dryer to dry the sample overnight. The next day, samples were taken out from the freeze dryer and 1 mg of sample was weighed into a 2 mL sample tube (Qiagen, Hilden).

4.3.3 Cell wall extraction

The extraction of cell wall components was carried out as follows. Two stainless steel beads were placed within dried sample tubes in liquid nitrogen. The cold rack and tubes were placed in the tissue lyser (TissueLyser LT, Qiagen), which was set to 50 Hz for 3 minutes. Samples were ground for a second time after centrifuging the tubes at 13,000 *g* for 1 minute. Aliquots 100 µl of 4M KOH and 1% sodium borohydride (Fisher Scientific, UK) per 100 µg samples were added. The tubes were again placed in the tissue lyser for 20 min at 50 Hz. Samples were placed on ice for 3 h, then they were microcentrifuged at 13,000 *g* for 5 min. Supernatants were transferred into new tubes with acetic acid to neutralise the KOH (240ul 80% Acetic acid to neutralise 1ml of 4M KOH). 100 µl of each sample was diluted to 3 ml with phosphate buffered saline (1X PBS).

The diluted solutions were used to coat the wells of ELISA plates (Thermo Fisher Scientific, Denmark). 125 µl were added into well up row A, and was titrated 1 in 5 down the plate with 1X PBS. Plates were incubated at 4 °C overnight.

4.3.4 Enzyme Linked Immunosorbent Assay (ELISA)

The sample coated ELISA plates were taken from the cold room, and washed three times with tap water using plate (zoom) washer (Titertek-Berthold, Huntsville, USA). PBS solution containing 5% milk powder (Marvel, London, UK) was added (300 µl) into each well for 2 h. Then, ELISA plates were washed vigorously 9 times. A panel of monoclonal antibodies were used to detect cell wall components of galls and uninfected roots of maize, Arabidopsis, aduki bean and potato (Table 4.1) in this experiment. Antibodies were chosen to represent the same polysaccharide targets as those investigated in the gall sections described in Chapter 3. The monoclonal antibodies were diluted 1:10 in 5% milk powder/PBS before use. 100 µl of antibody dilutions were put into the each well and plates were incubated for 1 h at room temperature. Plates were washed again nine times using a plate washer. The

secondary antibody, Anti Rat IgG-HRP (Sigma Aldrich, USA) was diluted 1/1000 in 5 % milk/PBS solution with 100 µl added to each well for 1 h. Following washing of plates, 100 µl of substrate was added into each well. The substrate comprised of 2 ml 1M sodium acetate buffer, 200µl Tetramethyl Benzidine 10 mg/ml in DMSO: (3,3,5'5'Sigma T-2885) and 20µl 6% (v/v) hydrogen peroxide. The blue colour was developed within seconds. The reaction was stopped by adding of 50 µl per well of 2.5 M sulphuric acid: the blue colour turned into yellow. ELISA plates were read using a Multiskan FC microplate photometer (Thermo Scientific, USA) at 450 nm wavelength. The ELISA experiment was carried out using three biological and three technical repeats. Statistical analysis was performed (t-test).

4.3.5 Transverse sectioning of galls and toluidine blue application

Galls induced on the four different host plants were collected at 21 dpi and the resin embedding protocol was performed before microtome cutting (Chapter 2). The samples were cut to a thickness of 0.5 µm in the microtome and placed on to Vectabond™ slides (detailed procedures were given in Chapter 2). Toluidine blue staining was carried out to allow easy observation of the nematode feeding site within the galls. Toluidine blue O (BDH chemicals, England) and sodium borate ($B_4Na_2O_{7.10}H_2O$, Sigma chemical) was diluted in distilled water (1 toluidine blue and 1 sodium borate were dissolved in 100 mL distilled water) and the solution was applied to the sections on the Vectabond™ treated slides for 5 min at room temperature. Following the application of toluidine blue O, the sections were rinsed with distilled water to remove the excessive dye. Images were captured in Leica microscope with a QImaging-QIcam camera (Canada) camera.

4.3.6 Determining the gall thickness

The *M. incognita* induced single galls were selected, and images were taken using QImaging-QIcam camera (Canada) combined with GX microscope (Leica). Image pro analyser 7.0 (2009 Media Cybernetics) was used to measure the gall size of these samples. The maximum diameter of each gall was measured, together with the root width of an equivalent position on a non-galled root. For each plant species 22-32 single galls and corresponding non-galled roots were measured. Statistical analysis

was performed using “Microsoft excel t -test” to analyse the differences between the gall thickness and ungalled root thickness.

Table 4.1 List of monoclonal antibodies used for ELISA analysis of gall and uninfected root cell wall components.

Plant cell wall component		Antibody	References
Hemicel.	Xyloglucan	LM25	(Pedersen et al., 2012)
	Heteromannan	LM21	(Marcus et al., 2010)
Pectin	De-PHG	LM19	(Verhertbruggen et al., 2009a)
	Arabinan	LM6	(Willats et al., 1998)
	Processed arabinan	LM16	(Verhertbruggen et al., 2009b)
	Arabinan	BR12	(-) *
	Galactan	LM5	(Jones et al., 1997)
Glyp	AGPs	LM2	(Smallwood et al., 1996, Yates et al., 1996)

* BR12 antibody unpublished. Hemicel., hemicellulose; De-PHG, De-esterified pectic homogalacturonan; AGPs, Arabinogalactan proteins; Glyp., glycoproteins; LM, Leeds Monoclonal.

4.4 Results

4.4.1 Quantification of gall cell wall components

A five-fold serial dilution of neat cell wall extract, 1/5, 1/25, 1/125, 1/625, 1/3125 and 1/15625 was first tested in ELISA assay with each antibody (Table 4.1) to determine the optimum concentration of extract to use in subsequent experiments. The selected antibodies detected hemicellulose (xyloglucan and mannan), pectin (homogalacturonan, arabinan, processed arabinan and galactan) and arabinogalactan protein epitopes. Based on these results, the 1/5 antigen dilution was chosen to determine the relative quantities of the different cell wall components in nematode galls and uninfected roots of host plants at 21 days post infection.

4.4.1.1 Hemicellulose (xyloglucan and heteromannan) were differently regulated in the *Meloidogyne incognita*-induced galls of hosts

This general difference in the abundance of xyloglucan and mannan was reflected in the ELISA results. Much higher absorbance readings were obtained for the same samples using the LM25 antibody that detects xyloglucan, than with the LM21 antibody (Figure 4.1). The relative difference in absorbance values between the two was similar to the previously reported differences in abundance of xyloglucan and mannan mentioned above. The heteromannan epitope recognised by LM21, although generally low, was significantly more abundant in the galls of maize and aduki bean than in equivalent non-galled root segments; however, there was no significant difference for galls of Arabidopsis and potato (Figure 4.1). Although xyloglucan was more abundant in all gall samples than in uninfected roots of the same host plant species, none of these differences were statistically significant ($P>0.05$; Students T-test), due to the greater variability observed between replicate samples.

4.4.1.2 Pectic polysaccharides were upregulated in the *Meloidogyne incognita*-induced galls of all hosts

Pectin is a very complex polysaccharide, which forms ~35% of the primary cell wall of dicotyledonous and non-graminaceous monocots, whereas pectin is a minor component (2-10 %) in grasses (Mohnen, 2008). The relative quantification of four different pectic epitopes: de-esterified pectic homogalacturonan, arabinan, processed arabinan and galactan was examined in galls compared to non-galled roots.

Homogalacturonan is the major component (~65% of pectin) in pectic polysaccharides (Mohnen, 2008). The LM19 antibody detects the de-esterified form of pectic homogalacturonan (De-PHG) in plant cell walls (Verhertbruggen et al., 2009a). The method for extraction of the cell wall components involved treatment with an alkaline solution, which would effectively remove all methyl-esterification from pectic homogalacturonan. For this reason, the LM20 antibody was not used in the ELISA assays. The homogalacturonan detected by LM19 therefore represents the total amount present in the samples, regardless of its esterification status. Rhamnogalacturonan-I consists of a galacturonic acid backbone that may be substituted with β(1→4)-galactan, branched arabinan and arabinogalactan (Harholt et al., 2010).

In general, *M. incognita*-induced galls contained more pectic polysaccharides than uninfected roots of the same plant species. The homogalacturonan epitope detected by LM19 was significantly higher in the galls of Arabidopsis, aduki bean and potato although there was no significant difference between galled and non-galled roots of maize (Figure 4.2). Similarly, galactan was significantly enriched in the galls of maize, Arabidopsis and aduki bean whilst it was higher, but not significantly so, in the galls of potato ($P = 0.08$) (Figure 4.2). Arabinan related epitopes (both arabinan and processed arabinan) were enriched in *M. incognita* induced galls compared to uninfected roots of all host plants (Figure 4.3). The significant increase of the LM6 arabinan epitope was detected in the galls of maize, aduki bean and potato, whilst that of the BR12 antibody was significantly increased in the galls of maize, Arabidopsis and aduki bean. Although both antibodies (LM6 and BR12) bind the arabinan epitope, BR12 has higher affinity than LM6 (Personal communication from Dr Valérie Cornuault and Prof J. Paul Knox). Processed arabinan followed a similar trend, but was detected at relatively low levels in aduki bean and the increased epitope abundance in galls was not significant ($P = 0.08$) in this host (Figure 4.3).

4.4.1.3 *M. incognita* does not affect the presence of arabinogalactan proteins in the galls in all host species

Arabinogalactan proteins are cell wall proteoglycans that consist of 1-10% protein and 90-99% carbohydrates (Albersheim et al., 2011). The antibody LM2 binds to AGPs (Smallwood et al., 1996, Yates et al., 1996). The LM2 antibody binds to

arabinogalactan proteins in the plant cell wall of maize, Arabidopsis, aduki bean and potato samples at 21 dpi. There were no significant differences detected in *M. incognita* induced galls of all hosts (Figure 4.4).

The comparative heat map of glycan antigen concentration in nematode induced galls and uninfected root tissues revealed that the differential antigen concentrations were observed. The heat map revealed that xyloglucan epitopes were detected as the highest level, but mannan and arabinogalactan proteins were detected as the lowest concentration in all hosts of both galls and uninfected roots (Figure 4.4).

In general, ELISA uncovered polysaccharide composition of cell walls in the galls of *M. incognita* that differed to that of unaffected tissue. Different epitopes are upregulated and downregulated in different hosts.

4.4.2 Comparison of gall size between different host species

The transverse sections of root galls after applying with toluidine blue allowed the visualising of nematode feeding site and giant cell positions. *M. incognita* caused morphologically different shape and structure of galls and feeding site in maize (Figure 4.5 a, c), Arabidopsis (Figure 4.5 b, d), aduki bean (Figure 4.5 e, g) and potato (Figure 4.5 f, h) at 21 dpi.

The diameter of *M. incognita* induced galls was measured at the thickest part and compared with the diameter of adjacent non-galled roots of maize, Arabidopsis, aduki bean and potato hosts. The nematode induced galls were thicker by 317 % (maize), 244 % (Arabidopsis), 679 % (aduki bean), and 289 % (potato) (Figure 4.6). The thickest galls were on the aduki bean (1215.6 µm) following the potato (991 µm), maize (940.6 µm) and Arabidopsis (332.4 µm) hosts at 21 dpi.

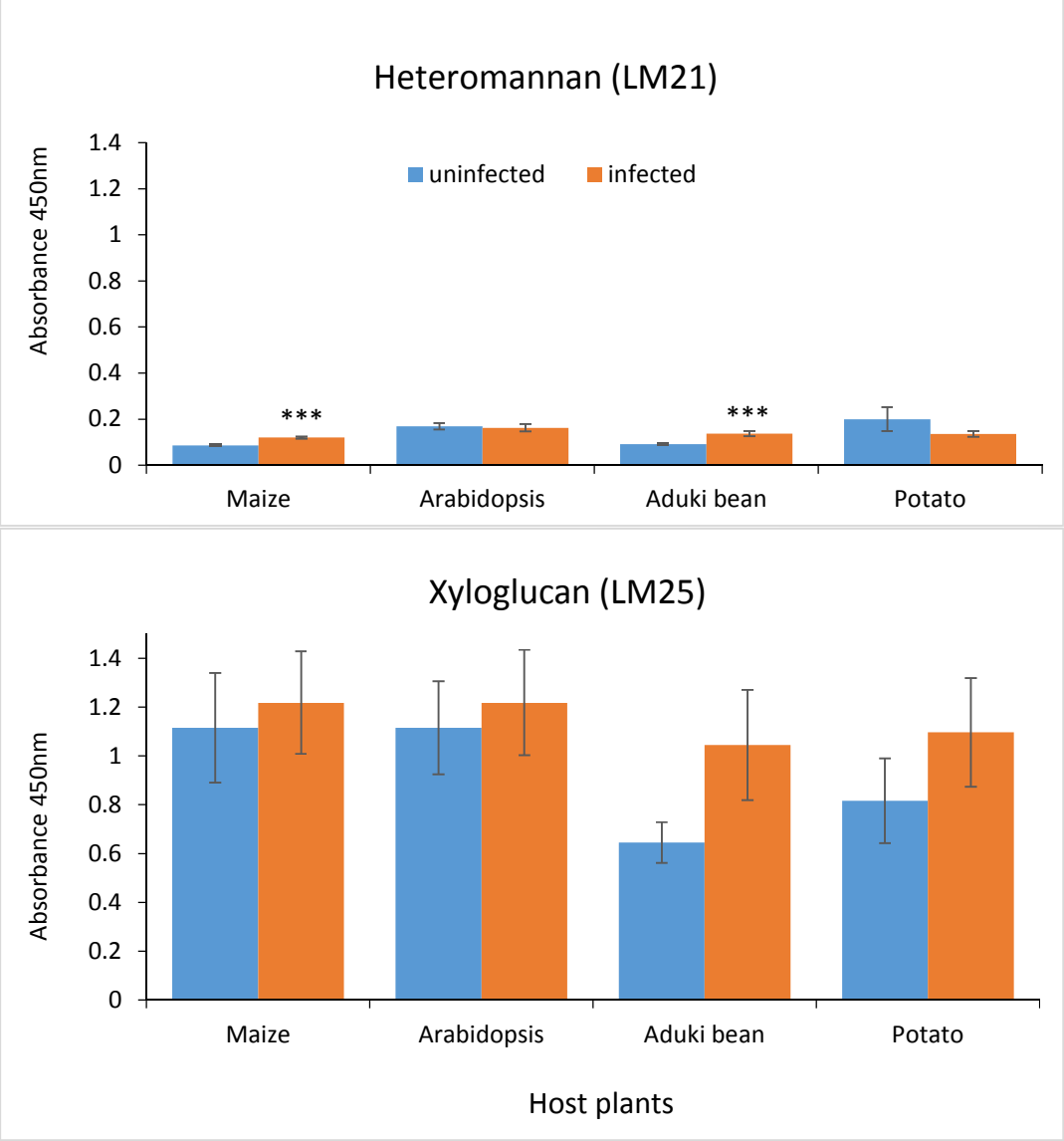

Figure 4.1 Relative quantification of hemicellulose epitopes (heteromannan and xyloglucan) in *Meloidogyne incognita* induced galls and uninfected roots of host plants. The LM21 and LM25 antibodies bind to mannan and xyloglucan epitopes in the plant cell wall, respectively. Maize, Arabidopsis, aduki bean and potato samples were collected at 21 days post infection or from equivalent non-infected control plants. The x-axis represents the host plants, y axis specifies the absorbance at 450 nm wavelength to provide a measure of epitope abundance. Error bars represent standard error (n=9 replicates). *** = P value < 0.001 for comparison between uninfected and infected root samples from the same host species.

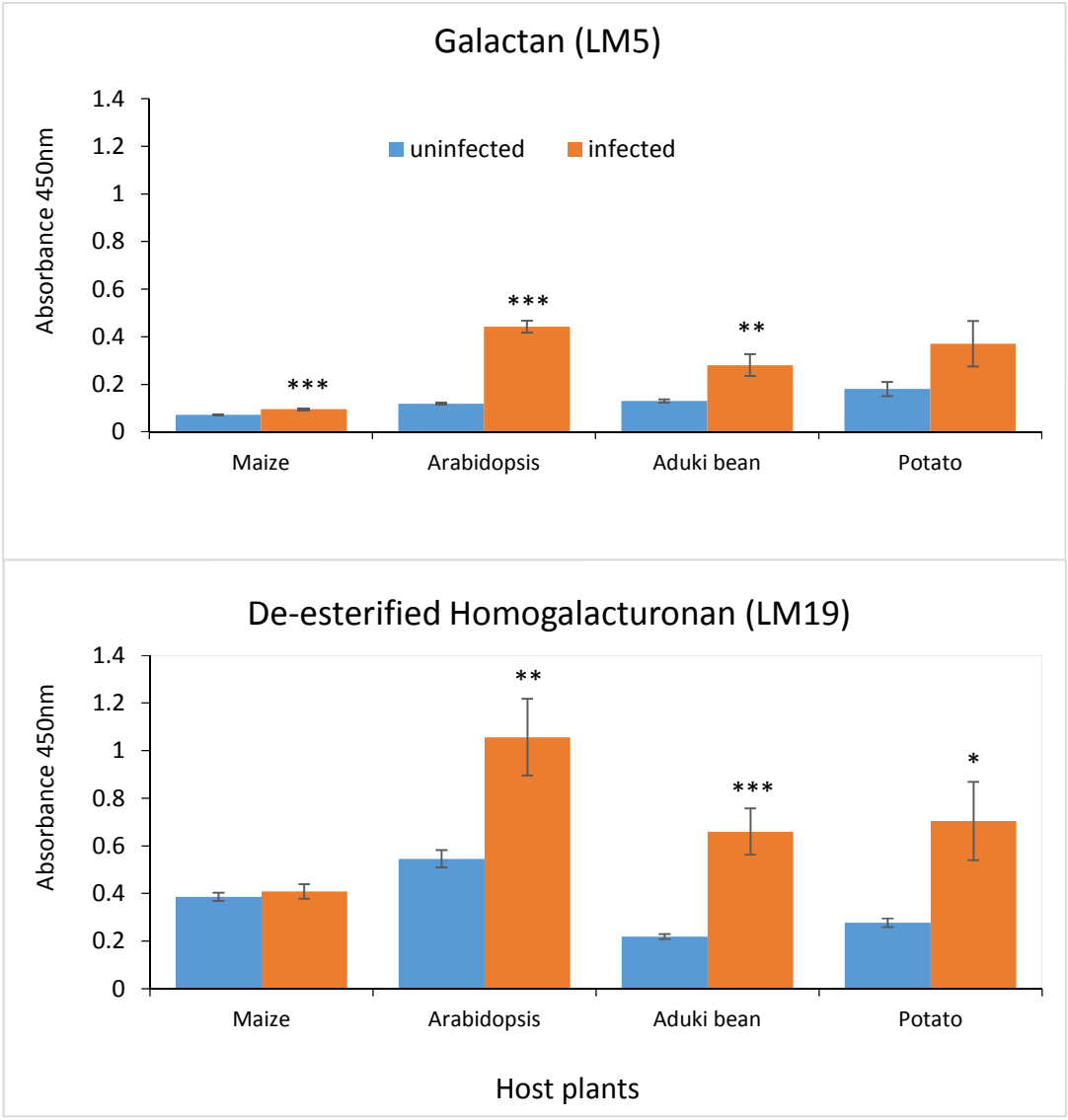

Figure 4.2 Presence of pectic epitopes (galactan and homogalacturonan) in *Meloidogyne incognita* induced gall, and uninfected roots of host plants following the 1/5 antigen dilution. The LM5 and LM19 antibodies bind to galactan and de-esterified pectic homogalacturonan in the plant cell wall, respectively. Maize, Arabidopsis, aduki bean and potato samples were collected after 21 days post infection. The X axis represent the host plants, y axis specifies the absorbance at 450 nm wavelength. Error bars represent standard error (n=9 replicates). * = P value < 0.05, ** = P value < 0.01, *** = P value < 0.001 for comparison between uninfected and infected root samples from the same host species.

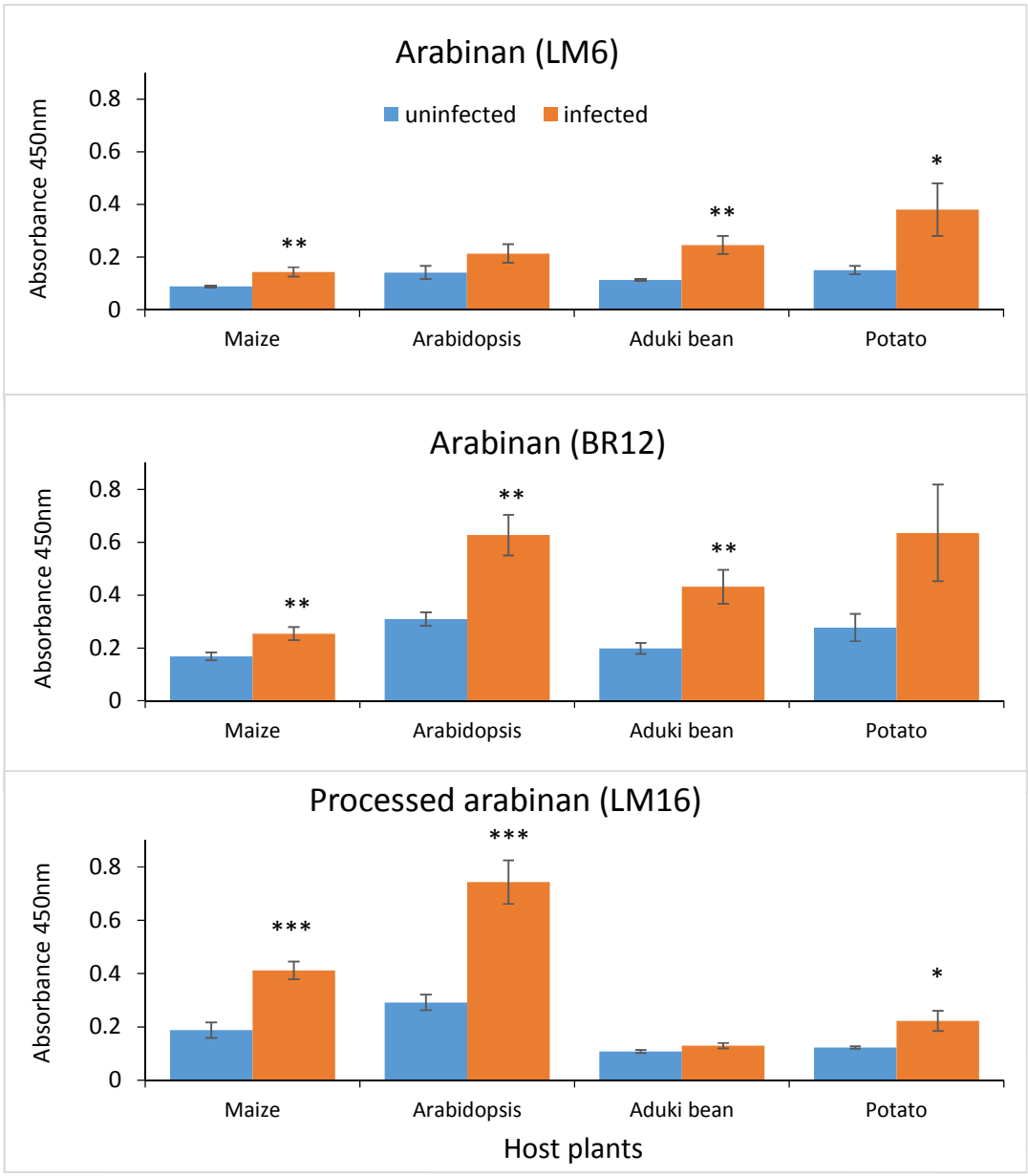

Figure 4.3 Detection of arabinan epitopes (arabinan; BR12, arabinan; LM6 and processed arabinan) in *Meloidogyne incognita* induced gall, and uninfected roots of host plants following the 1/5 antigen dilution. The LM12, LM6 and LM16 antibodies bind to arabinan, arabinan and processed arabinan epitopes in the plant cell wall, respectively. Maize, Arabidopsis, aduki bean and potato samples were collected after 21 days post infection. The X axis represent the host plants, y axis specifies the absorbance at 450 nm wavelength. Error bars represent standard error (n=9 replicates). * = P value < 0.05, ** = P value < 0.01, *** = P value < 0.001 for comparison between uninfected and infected root samples from the same host species.

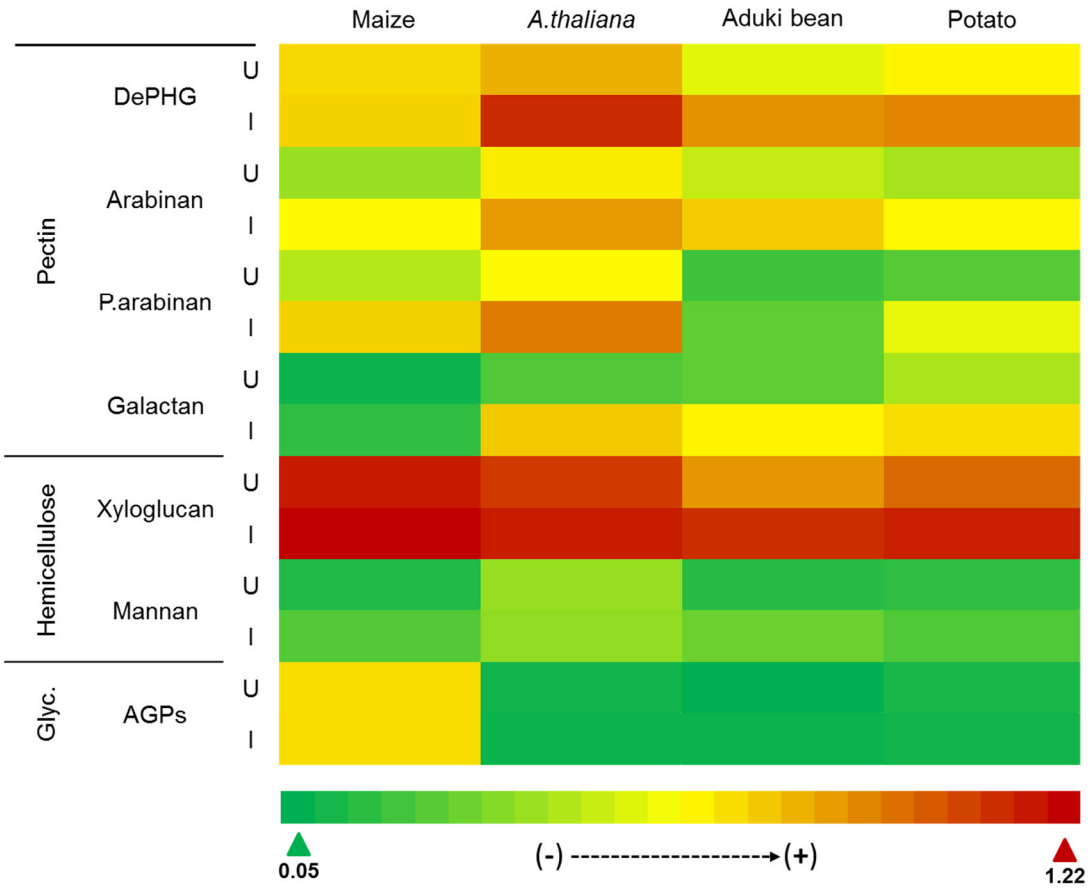

Figure 4.4 The comparative heat map of glycan antigen concentration in nematode induced galls and uninfected root tissues. The antigen concentration was measured in ELISA plate reader measuring the absorbance at 450 nm wavelength. Nematode induced galls and uninfected root tissues of maize, Arabidopsis, aduki bean and potato are displayed, samples were taken at 21 days post infection using the three technical and three biological replicates. Antibodies LM19 (de-esterified pectic homogalacturonan), BR12 (arabinan), LM16 (processed arabinan), LM5 (galactan), LM25 (xyloglucan), LM21 (heteromannan), and LM2 (arabinogalactan proteins) were applied to detect DePHG, arabinan, p. arabinan, galactan, xyloglucan, and mannan antigens, respectively. Colour differences between uninfected (U) and infected (I) root tissues shows the altered level of antigen concentration. The higher level of xyloglucan antigen concentration (red colour) was detected in all hosts of both root and galls. The lower level of antigen concentration of AGPs (all hosts), mannan (all hosts), galactan (maize), processed arabinan (aduki bean and potato) were detected (green and yellow colour). Differences were detected among antigen concentrations in gall and ungalled roots of *A. thaliana* (DePHG, arabinan, processed arabinan and galactan), maize (arabinan and processed arabinan), aduki bean (DePHG, arabinan, processed arabinan and galactan) and potato (DePHG, arabinan, processed arabinan and galactan). DePGH, de-esterified pectic homogalacturonan; P. arabinan, processed arabinan; Glyc, glycoproteins; AGPs, arabinogalactan proteins; U, uninfected plant roots; I, *Meloidogyne incognita* infected (gall) root samples.

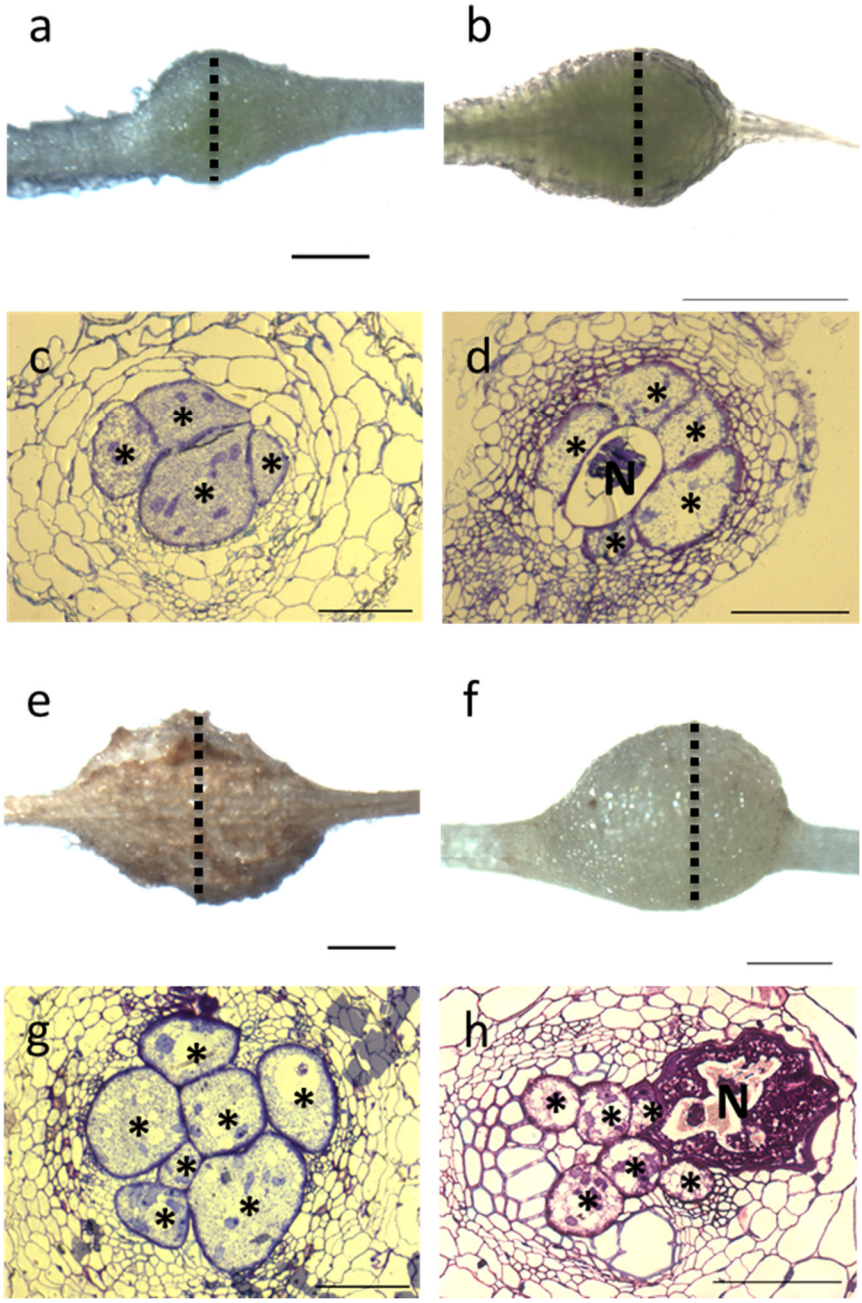

Figure 4.5 Nematode induced galls and transverse sections of galls in aduki bean, potato, maize and Arabidopsis hosts at 21 days post infection (dpi). The root galls and toluidine blue stained transverse root sections of maize (a, c), Arabidopsis (b, d), aduki bean (e, g) and potato (f, h). Dashed lines represent transverse section cutting position. Asterisks indicate giant cells; N, represents the nematode. Bars: (a, b, e, f) 500 µm; (c, d, g, h) 100 µm.

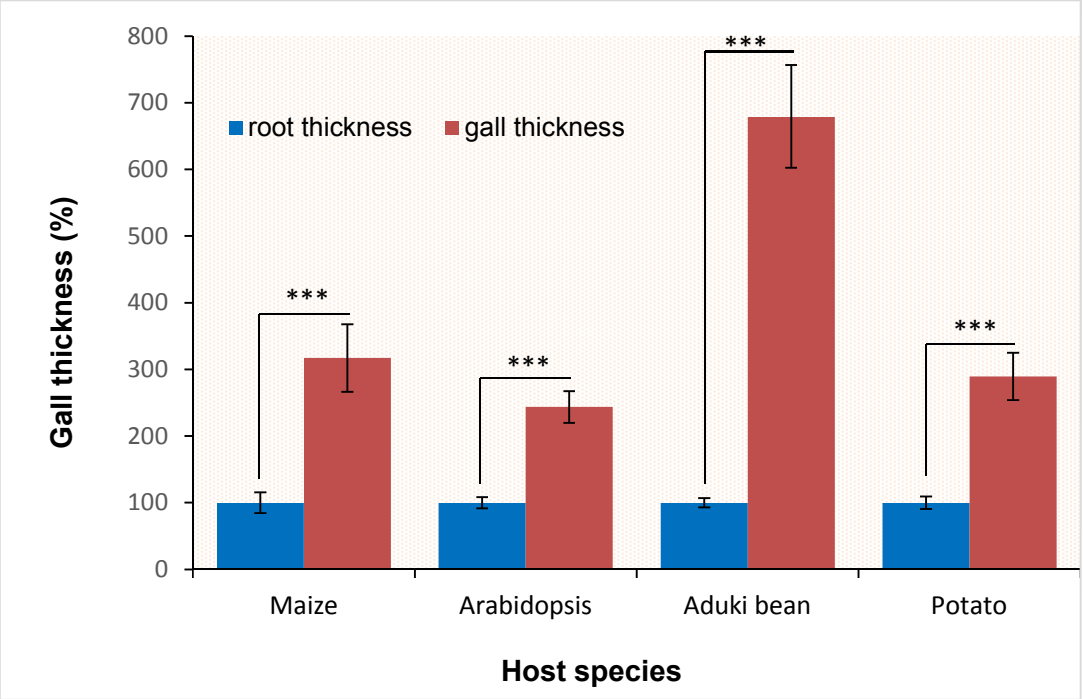

Figure 4.6 The relative thickness of *Meloidogyne incognita* induced galls and their host roots. The thickest part of the gall was measured following images taken using Image Pro-Analyser (Media Cybernetics) and compared with the diameter of non-galled root size next to gall. The x-axis indicates host plants and the y-axis represents the gall thickness as a percentage of adjacent root thickness, which is set to 100% for each host species. The experiment was performed using nematode-induced galls and ungalled roots of maize, Arabidopsis, aduki bean and potato at 21 days post infection with 22-32 biological replicates per host species. Error bars represent standard error.

4.5 Discussion

Root knot nematodes modify host cells to build a feeding site and as a result cause extensive changes in root vascular tissues. *M. incognita* infection of most hosts causes hypertrophy and hyperplasia of root cortical cells around the head and body of the nematode so forming the enlarged gall or root-knot. The gall shelters the developing nematode and the giant cells that supply the nutrient to the nematode and other type of cells. The comparative analysis of the gall cell wall components may help to understand the broad range of gall morphologies observed amongst different host plants. The work could be extended to similar studies comparing the galls formed by different root-knot nematode species on the same host plant.

Abnormal arrangement in xylem and phloem around the giant cell can be visible within galls (Azam et al., 2011). Abnormal reorganisation of these vascular elements was observed in sections through the galls of all hosts studied (Figure 4.5). The nematode-induced root galls can be varied not only according to the root-knot nematode species (Vovlas et al., 2005) but also host plant species (Yousif, 1979). In this study, gall size and thickness showed variability across four very diverse host species. This did not just reflect the diameter of uninfected roots of the different plant species – galls of aduki bean were the largest of the four hosts, but uninfected aduki bean roots were thinner than those of both maize and potato. This led to aduki bean also having the highest infected: uninfected root diameter ratio. Galls on aduki bean were found to be around seven times thicker than ungalled (control) roots (Figure 4.6).

Galactan and arabinan are major polysaccharides of pectic rhamnogalacturonan-I that are neutral pectic side chain in the cell wall of dicotyledon plants (Wefers et al., 2014). The galactan is found in the gelatinous layer and in the secondary cell wall. It strengthens the cell wall in mechanically stressed plants (Arend, 2008) and is involved in the cell-wall modification during the tissue differentiation and development (Martin et al., 2013). In contrast to our result, the galactan is not detected in the cyst nematode, *H. schachtii*, induced syncytia cell walls in *Arabidopsis thaliana* (Davies et al., 2012). It is suggested from results that galactan increases the strength of galls during nematode infection as the nematode feeding site (gall) needs to resist strong turgor pressures. Arabinan sustains the flexibility of cell wall by preventing the biosynthesis of homogalacturonan polymers (Jones et al.,

2003). Also arabinan maintains the flexibility of cell wall during the water stress (Moore et al., 2008).

The de-esterified pectic homogalacturonan was abundant in the nematode induced galls of dicot plants: Arabidopsis, aduki bean and maize (Figure 4.2). In general, pectin rhamnogalacturonan-I (Figure 4.3) and homogalacturonan (Figure 4.2) were significantly increased during the nematode infection in plant hosts in this experiment.

The presence of heteromannan was one of the most distinctive polysaccharides among the plant species. The nematode induced galls on aduki bean and maize had increased levels of heteromannan but detection was low in the galls of Arabidopsis and potato (not significant level) (Figure 4.1). The epitopes of heteromannan involve the development of mechanical tissues in ferns (Leroux et al., 2015) and is mainly localised in the primary cell wall and found during the fibre elongation phase in cotton (Hernandez-Gomez et al., 2015). Additionally, the heteromannan is found in the cyst nematode (*H. schachtii*) induced-syncytia cell walls in Arabidopsis (Davies et al., 2012). In this experiment, the nematode effected increase of heteromannan levels in the galls of aduki bean, maize but not in Arabidopsis and potato. Heteromannan may be involved in the mechanical strength, tissue and cell expansion and biotic stress in the plant (Figure 4.1).

Homogalacturonan plays a role the absence of xyloglucan, maintains in the network of other cell wall polysaccharides (Zabotina et al., 2012). The galls induced following nematode infection do not have increased levels of xyloglucan in galls of all hosts (maize, Arabidopsis, aduki bean and potato) (Figure 4.1). Other cell wall polysaccharides may have covered the xyloglucan absence in this study. In contrast to this result, the xyloglucan was abundant within the cyst nematode, *H. schachtii*, induced syncytia cell walls in *A. thaliana* (Davies et al., 2012). Nematode species and feeding sites are different as root knot nematodes cause gals but cyst nematode do not cause gall like structures. Also, the high presence of xyloglucan in cell walls differs from that in whole galls; the result of the ELISA method represents all cells within galls including giant cell walls, but *in situ* analysis focussed on nematode feeding cell walls.

Arabinogalactan protein (AGPs) is a diverse class of glycoproteins that is involved in cell division and programmed cell death, formation, growth, cell proliferation and

plant-microbe interactions (Seifert and Roberts, 2007). AGP gene expression is down-regulated during the wounding in internodes of the tomato plant (Li and Showalter, 1996). The overexpression of AGPs in tomato plant prevents the plant development and growth. In this study, the nematode did not affect the presence of AGPs in the galls (Figure 4.4). Likewise, AGPs (binding of LM2 antibody) was not detected in the cyst nematode, *H. schachtii*-induced syncytia cell walls of *A. thaliana* (Davies et al., 2012).

4.6 Overview

- ✓ Enzyme Linked Immunosorbent Assay revealed the cell wall composition of galls on maize, aduki bean, Arabidopsis and potato hosts after infection with *M. incognita* at 21 dpi.
- ✓ Hemicellulose (xyloglucan and heteromannan) were differently regulated in the *M. incognita*-induced galls of hosts.
- ✓ Pectic polysaccharides were upregulated in the *M. incognita*-induced galls of all hosts.
- ✓ *M. incognita* does not affect the presence of arabinogalactan proteins in the galls in all host species.

Chapter 5

Functional analysis of cell wall genes

5 Functional analysis of cell wall genes

5.1 Introduction

Analysis of gene expression in the *M. incognita* feeding site reveals that 701 genes are down-regulated and 258 genes are up-regulated in galls induced by the nematode (Fuller et al., 2007). The formation of the feeding cell is closely related to down-regulation of genes (Gheysen and Mitchum, 2009). Many of the changes in plant gene expression that accompany root-knot nematode parasitism are associated with cell wall components. In one study, 90 cell wall genes were up-regulated and 26 cell wall genes were down-regulated in *M. incognita* infected roots (Li et al., 2009), displaying an opposite trend of fewer down-regulated genes. This would suggest that knocking out the function of these genes may have an impact on nematode success.

5.1.1 Arabidopsis cell wall genes

The functions of many genes within the genomes of multicellular organisms remain unknown (Kaul et al., 2000). Arabidopsis is one of the most well-characterised plants, with many genomic resources available, therefore it is a good model for cell wall studies (Liepman et al., 2010). There are more than 420 genes involved in the synthesis of the cell wall (Kaul et al., 2000) and probably more than 1000 genes encoding cell-wall-related proteins (Carpita et al., 2001). Creating mutations is an essential tool with which to understand the function of genes. A great number of *Agrobacterium* transferred-DNA (T-DNA) insertion lines of Arabidopsis have been generated that produce knock-out mutants for the majority of genes in the genome. For example, the SALK SIGnAL (Salk Institute Genomic Analysis Laboratory) collection alone contains characterised insertion lines for almost 22,000 of the annotated Arabidopsis genes (Alonso et al., 2003). Amongst these collections there are obviously many mutants for cell wall-related genes. These mutants can be grouped into a number of functional categories, each of which is expected to have a different spectrum of phenotypic effects on the plant (Yong et al., 2005). For instance, mutation of genes involved in monosaccharide synthesis is likely to produce more complex effects as it will impact on all polysaccharides which contain that sugar. Other groups of mutations that affect the cell wall include those involved in polysaccharide synthesis, secretion of cell wall components, wall assembly and structural rearrangements and signalling and response in the cell wall. Essentially, the

vast resource of available Arabidopsis mutants gives an opportunity to study the functions of cell wall related genes, cell wall polysaccharides and cell wall biosynthesis (Reiter et al., 1997).

From the many cell wall-related Arabidopsis mutants, a number were selected for analysis in this project based on their connection with the cell wall components found to be relevant to the walls of giant cells through the immunohistochemical and ELISA studies. The associated genes are introduced below.

5.1.1.1 Hemicellulose-related cell wall genes

The xylan-related *GLZ1 (Galacturonosyltransferase-like 1)* gene is predicted to be a galacturonosyltransferase involved in xylan biosynthesis with a subsequent impact on secondary cell wall thickening, plant development and carbohydrate metabolism (Shao et al., 2004, Lee et al., 2007a). This gene is expressed in many organs of plants including the siliques, stem, root, flower and leaf (The Arabidopsis Information, 2011, Lee et al., 2007a), particularly in cells undergoing secondary cell wall thickening. Mutant *glz1* plants have a comparatively dwarf phenotype (Lao et al., 2003).

The mannan-related gene *MSR1* (*MANNAN SYNTHESIS RELATED 1*) is involved in transferring glycosyl groups that *msr1* is expressed in the root, hypocotyl, leaf, cotyledon and stems and the mannosyl amount is decreased by 40% in the *msr1* mutant of Arabidopsis (Wang et al., 2013).

The xyloglucan-related *mur3 (xyloglucan galactosyltransferase)* gene is involved in the biosynthetic processes of xyloglucan, reduction of fucose (90%) and cell growth (Madson et al., 2003). The *MUR3* is expressed in many plant organs including: root, stem, shoot and leaves, however the *mur3* shows no visible differences in phenotype compared to the wild type (Madson et al., 2003). MUR3 encodes a xyloglucan galactosyltransferase that belongs to the membrane protein family (Madson et al., 2003).

5.1.1.2 Pectin-related cell wall genes

Pectin methylesterase enzymes (PMEs) remove methyl ester groups from homogalacturonan thus affecting various cell wall properties, particularly cell wall rigidity (Micheli, 2001). The pectic homogalacturonan-related gene *PME31* is

expressed in different plant organs including silique, root and the leaf (Louvet et al., 2006). Arabidopsis *PME* genes may play a role in pathogen resistance as *pme31* mutant plants have significantly increased susceptibility to infection with *Pseudomonas syringae* pv. maculicola (Bethke et al., 2014). The *QUASIMODO2LIKE1* (*QUL1*) gene encodes a pectin methyltransferase that is a paralogue of *QUASIMODO2* (*QUA2*), and is probably involved in synthesis of homogalacturonic acid (Fuentes et al., 2010). No developmental defects were apparent in the single *qul1* mutant compared to wild type plants, however use of *qua2qul1qul2* triple mutants revealed a likely role in temperature-sensitive vascular development. The alteration of cell wall structure may closely be related to an adaptation strategy during the changing conditions of environment (Fuentes et al., 2010).

Plant β-galactosidases belong to the glycoside hydrolase (GH) family 35, which has been implicated in both mobilisation of carbohydrate reserves and in cell wall biogenesis and modification. There are 17 β-galactosidase genes in Arabidopsis that can be divided into two groups. *BETA-GALACTOSIDASE 5* (*BGAL5*) belongs to the largest subfamily, a1, and its encoded protein localises in the cell wall where it is involved in cell wall modification (The Arabidopsis Information, 2011, Gantulga et al., 2008). *BGAL5* is expressed in many parts of the plant including trichomes and roots, where its expression correlates particularly with regions of elongation (Albornos et al., 2012, Hruba et al., 2005).

RHAMNOGALACTURONAN XYLOSYLTRANSFERASE 1 (*RGXT1*) encodes a (1,3)-α-D-xylosyltransferase that is localised in the Golgi apparatus and may be involved in the biosynthetic process of rhamnogalacturonan II. *RGXT1* is expressed in roots and the rosette leaves of *Arabidopsis* (Egelund et al., 2006, The Arabidopsis Information, 2011).

The arabinan-related *ARAD1* (*ARABINAN DEFICIENT 1*) gene encodes an arabinosyltransferase involved in biosynthesis of pectic arabinan in Arabidopsis. It is expressed in many plant organs including roots, leaves and shoots (Harholt et al., 2006). Arabinose content in *arad1* mutant plants is reduced by 75% and 46% in leaves and stems respectively (Harholt et al., 2006). Another arabinan deficient mutant, *arad2* (*arabinan deficient 2*), is also related to arabinan biosynthesis (Harholt et al., 2012). The *ARAD2* gene is the closest homolog to *ARAD1* and both are involved

in the biosynthetic process of arabinan. However, different labelling in *arad1* and *arad2* mutants after applying antibody LM13 which binds to the epitopes of linearized arabinan is visible (Harholt et al., 2010). *ARAD2* is expressed in roots, seeds, vascular tissue of leaves and other plant organs (The Arabidopsis Information, 2011). There is no visible difference between *arad2* plants compared to the wild type (Scheller et al., 2007).

5.1.1.3 Glycoprotein-related cell wall genes

A*RABINOGALACTAN PROTEIN 8*, (*AGP8*)*, PROLINE-RICH EXTENSIN-LIKE RECEPTOR KINASE 10* (*PERK10*) and *LEUCINE-RICH REPEAT/EXTENSIN 3* (*LRX3*) are all glycoprotein-related cell wall genes that were investigated in this work. *AGP8* is expressed in roots (Johnson et al., 2003), leaves and flowers (Schultz et al., 2000, Ito et al., 2005). AGPs are highly glycosylated hydroxyproline-rich glycoproteins that are abundant in the plant cell wall (Showalter, 2001). AGPs occur in almost all cells of root tissues and are involved in root–microbe interactions (Nguema-Ona et al., 2013).

Extensin-related *PERK10* encodes a proline-rich extensin-like receptor kinase that belongs to the *PERK* family (Nakhamchik et al., 2004). *PERK10* is expressed in different plant tissues such as the root, leaf, seedling, bud, silique (Nakhamchik et al., 2004). *PERK* genes are negatively regulated during root growth in Arabidopsis (Humphrey et al., 2015).

Another extensin-related gene *LRX3* is involved in cell wall extension and is expressed in plant developmental stages (Irshad et al., 2008). LRX3 is an N-terminal leucine-rich repeat domain protein and is important for cell wall development. There is less available rhamnose and galactose in cell walls of rosette leaves in *lrx3* mutant plants of Arabidopsis (Draeger et al., 2015).

In this chapter, the roles of the described cell wall genes in nematode development were investigated.

5.1.2 Quantification of gene expressions

Quantitative PCR (qPCR) is a real-time PCR technology that quantifies the amount of nucleic acids, and is used in many disciplines including: molecular diagnostics, clinical microbiology, clinical oncology and gene expression studies (Klein, 2002).

Quantitative reverse transcriptase PCR (qRT-PCR) is a very important method for quantifying the mRNA transcription levels because of its sensitivity, accuracy and broad dynamic range, fast efficiency, ease of use and high reproducibility (Ginzinger, 2002, Radonic et al., 2004). Relative quantification is a method of comparative quantification ($\Delta\Delta C_T$) that uses the differences in threshold cycles between a house keeping gene and a gene of interest (Klein, 2002). A fluorescent reporter, such as SYBR Green which fluoresces when bound to double-stranded DNA, is required to reveal the amounts of the product within qRT-PCR (Kubista et al., 2006). A reference gene that is assumed to maintain constant expression across the analysed samples allows the standardisation (normalisation) of different amounts of amplifiable cDNA in the different samples (Radonic et al., 2004).

Whilst qRT-PCR is a useful technique for measuring expression of a small number of genes, DNA microarrays allow expression analysis of potentially all genes in an organism (Alter, 2006). Total messenger RNA from samples is used to prepare fluorescently labelled cDNA, and samples are labelled with different fluors to compare genes (Brown and Botstein, 1999). cDNAs are mixed and hybridised with a DNA microarray containing sequences or oligonucleotide probes representing many thousands of genes, and the measurement of the relative abundance of fluorescence of cDNAs is reflected by red and green signals (Brown and Botstein, 1999). DNA microarray is used in different disciplines from diagnostics of pathogens (Yoo and Lee, 2008) including food pathogens (Rasooly and Herold, 2008, Severgnini et al., 2011) to systems biology, functional genomics and pharmacogenomics (Teng and Xiao, 2009).

In this project, existing microarray data for cell wall-related genes of Arabidopsis were collated from “Genevestigator” (https://genevestigator.com) and analysed with respect to their expression in roots infected with root-knot nematode.

5.2 Aims

Wild type Arabidopsis and 12 cell wall-related mutants were analysed and compared to define the effect of cell wall genes on *Meloidogyne incognita* development and function. The following mutants were used:

- Hemicellulose (*glz1, msr1* and *mur3*),
- Pectin (*qul1*, *pme31*, *bgal5*, *rgxt1 arad1* and *arad2*)
- Glycoprotein (*agp8*, *perk10* and *lrx3*)

- Gene expression of cell wall-related genes in *Arabidopsis thaliana* in nematode infected tissues:
  - Quantification of gene expression in nematode infected plant roots by qRT-PCR at 14 dpi
  - Analysis of existing microarray data for Arabidopsis cell wall-related gene expression in response to *M. incognita* infection at 7, 14, 21 and 28 dpi (Genevestigator)
- *In situ* analysis of Arabidopsis cell wall mutants with 17 different monoclonal antibodies
- Use Arabidopsis cell wall mutants to determine the role of cell wall genes in nematode and gall development

5.3 Material and Methods

5.3.1 Plant material

Arabidopsis thaliana, ecotype Columbia-0 (Col-0) and Arabidopsis cell wall mutants (Table 5.1) were grown in tissue culture for *in situ* immunochemical analysis (details were discussed in Chapter 2) and in the glasshouse for functional analysis. The particular mutant line for each selected cell wall-related gene was chosen based on information available from the database of *Arabidopsis thaliana*, The Arabidopsis Information Resource (TAIR). Mutants in which the T-DNA insertion was located within an exon towards the 5' end of the gene were preferred and homozygous lines were chosen where possible. The selected cell wall-related mutant seeds were ordered from The European Arabidopsis Stock Centre (NASC).

5.3.2 Cultivation of *Arabidopsis thaliana* mutants and homozygosity test for T-DNA mutants

A small number of seeds for each Arabidopsis mutant line were sown in compost and grown at 20 °C with 16 h light conditions in a glasshouse. At the beginning of the flowering period, Aracons™ were placed on pots to prevent cross-pollination with other plants. A single leaf of each plant was collected and placed at -80 °C until samples were used for DNA extraction. The SALK or SAIL code, depending on the collection from which each mutant was derived, was obtained for each mutant from TAIR. Primers that could be used to determine the presence of wildtype and mutant alleles in each plant were designed using the T-DNA primer design tool (http://signal.salk.edu/tdnaprimers.2.html) to perform the homozygosity test. Three primers (Left border primer + Left gene-specific primer + Right gene-specific primer) were used for each SALK or SAIL line (Table 5.2). Wild type (no T-DNA insertion) PCR products were 900-1000 base pairs (bp) (from Left primer to Right primer). Mutant allele PCR products (left border primer to right primer) were around 400-500 bp. Designed primers (Table 5.2) were ordered from Sigma-Aldrich, and the homozygosity test was performed after extraction of DNA.

5.3.2.1 DNA extraction from Arabidopsis mutants

Frozen leaf samples were ground with micro-pestles in liquid nitrogen, and ground tissue powder was suspended in 700 µl DNA extraction buffer (2% Sodium

Lauroylsarcosine, 0.1 M Tris-HCl, 10 mM EDTA (pH 8.0). Then, 500 µl Phenol:Chloroform:Isoamyl Alcohol (25:24:1, v/v) was added. The tube was vortexed to mix the sample, the samples were then placed on ice for 20 min and centrifuged for 5 min at 12000 *g* at 4 °C. The aqueous phase (top layer) was transferred (without disturbing the debris) to a new, labelled tube. Four µL RNase (10mg/ml) was added and the sample incubated at 37 °C for 1 h. Then 250 µl of aqueous phase, 175 µl of isopropanol, 25 µl of 3M NaAc (pH 5.2) were combined, mixed well and incubated for 15 min at room temperature. The solution was centrifuged at 12000 *g* for 5 min and the supernatant removed. The DNA pellet was washed using 75% EtOH and centrifuged at 12000 *g* for 1 min. The supernatant was then discarded with the pellet finally being washed using 100% EtOH and re-centrifuged for 1 min. DNA pellets were dried at room temperature for 20 min then dissolved in 50 µl volume of sterile deionised water. Samples were stored at -20 °C until they were used.

5.3.2.2 Polymerase Chain Reaction (PCR) and agarose gel electrophoresis

Polymerase chain reaction was conducted to determine the presence of wildtype/mutant alleles in Arabidopsis DNA samples using MyTaq™ Red Mix (Bioline) based on manufacturer's guidelines. This mix consists of 2x PCR mix containing DNA polymerase, buffer, dNTPs, $MgCl_2$, enhancers and stabilizers. DNA templates (2 µl) were transferred to 8-well, 0.2 ml strip tubes The left border primer and appropriate gene specific left and right primers were added to the PCR mix, with water to make the final volume 20 µl, then the mix was added to the template. DNA from a known wild-type Arabidopsis plant was included as a control for each set of PCR primers. PCR cycling conditions were set up as: initial denaturation 95 °C for 3 mins, followed by 35 cycles of 95 °C for 30 s, 57 ^{o}C for 30 s and 72 °C for 1 min and 5 min extension at 72 °C as a final stage. The PCR mix and program are summarised below:

PCR mix in each tube	Step	Temperature	Duration
10 µl 2x PCR mix (MyTaq™)	1	95 °C	3 min
2 µl DNA sample	2	95 °C	30 s
1 µl RP (10 µM)	3	57 °C	30 s
1 µl LP (10 µM)	4	72 °C	1 min
1 µl LBb1.3/LB1 (10 µM)	5	Go to step 2,	34X
5 µl H_2O	6	72 °C	5 min
Total: 20 µl	7	12 °C	End

Agarose gel electrophoresis was conducted on to separate amplified DNA fragments and determine their size. A 1% w/v agarose gel (Sigma Aldrich Co. St Louis USA) was prepared with TAE buffer (40 mM Tris, 20 mM acetic acid, 1mM EDTA). The agarose was dissolved by microwaving for 2 min until boiling. A 1:20,000 dilution of Gel Red nucleic acid gel stain (Cambridge Bioscience, Cambridge, UK) was added to the molten agarose to aid visualisation of DNA. The gel was placed in a Wide Mini-sub Cell GT tank (BioRad) filled with TAE buffer. Aliquots (4 µl) of PCR product for each sample along with 2 µl of hyper ladder 1 kb DNA ladder (Bioline) were loaded into wells on the gel and separated at 90 v for 1 h using a Power Pac 300 (Bio-Rad). The gel was photographed under UV light (Syngene, Genius).

Table 5.1 List of *Arabidopsis thaliana* cell wall mutants and relations with cell wall components

Plant cell wall components		**Mutant**	**Gene accession**
Hemicellulose	Xylan	*galacturonosyltransferase-like 1* (*glz1*)	At1g19300
	Heteromannan	*mannan synthesis related 1* (*msr1*)	At3g21190
	Xyloglucan	*xyloglucan galactosyltransferase* (*mur3*)	At2g20370
Pectic polysaccharides	Homogalacturonan	*quasimodo2 like 1* (*qul1*)	At1g13860
		pectin methylesterase 31 (*pme31*)	At3g29090
	Rhamnogalacturonan	*beta-galactosidase 5 (bgal5)*	At1g45130
		rhamnogalacturonan xylosyltransferase 1 (*rgxt1*)	At4g01770
		arabinan deficient 1 (*arad1*)	At2g35100
		arabinan deficient 2 (*arad2*)	At5g44930
Glycoproteins	Arabinogalactan proteins	*arabinogalactan protein 8* (*agp8*)	At2g45470
	Extensin	*proline-rich extensin-like receptor kinase 10* (*perk10*)	At1g26150
		leucine-rich repeat/extensin 3 (*lrx3*)	At4g13340

Table 5.2 Designed primers for homozygosity test of cell wall-related genes in *Arabidopsis thaliana* mutants

Gene accession	Gene name	Salk code and References	LP primer	RP primer
At2g45470	*AGP8*	SALK_141852	ATGTAGAACATGAACGTCGGC	CTTTGCCTCCTTTAAGATCGG
At1g45130	*BGAL5*	SALK_139681	TGCTCCTATCGATGAATACGG	CTTAGAACTAACCGGCAACCC
At3g29090	*PME31*	SALK_074820	TCAAATTTCACCTAGGTGATTTG	CACAACCAAACGTACCAGTCC
At1g13860	*QUL1*	SALK_094635	CATTTGACATGGTCCACTGTG	TCATCACCCAAACTGATTTCC
At2g20370	*MUR3*	SALK_021282	TTGGAGCATTTTTGGTCTTTG	AGCAACCAACAAACAGATTCG
At1g19300	*GLZ1*	SALK_045368	GTTGAAGTAGCATGCTTTCCG	TATGCACAGACAAACATAGCG
At3g21190	*MSR1*	SALK_075245	CAAGACCTTCCATTTTTGGATC	TACAGGATCAGTTTCGCCATC
At2g35100	*ARAD1*	(Harholt *et al*., 2006)	TATGTGTTCAGGGTGGAAAAGT	GGGAGACTTGACGCCAGATT
At5g44930	*ARAD2*	(Harholt *et al*., 2012)	GTAGTTGTGTATACCCTAGACT	CGCCTCAGCCGGGTCAAAA
At4g01770	*RGXT1*	SALK_123513	TTGGTCAACTCCGGGTTTAAC	CTCATGATTTACCACATCCGG
At1g26150	*PERK10*	SALK_022872	TTACCCACAGATTCGGACAAG	CTTCTGAATTTGCAAAGCTGC
At4g13340	*LRX3*	SALK_037606	CGAAGAATGTCACATAAATCCG	ATGTGACGGACTTCGTTATCG

The primers LBb1.3 “ATTTTGCCGATTTCGGAAC” for SALK lines and LB1 “GCCTTTTCAGAAATGGATAAATAGCCTTGCTTCC” for SAIL lines (*arad1* and *arad2*) were used as left border (LB) primers.

5.3.3 Gene expression of cell wall-related genes in *Arabidopsis thaliana* wild type nematode infected tissues

Arabidopsis plants (Col-0) were grown in tissue culture Gamborgs B5 growth media. Two week old Arabidopsis roots were infected with sterilised nematodes (J2s). After 14 days of nematode infection, root samples were collected in RNase free Eppendorf tube in liquid nitrogen and placed in the -80 °C until they were used. Similarly, non-infected samples were also simultaneously collected (details were discussed in Chapter 2).

Ten cell wall-related genes, *MUR3, MSR1, GLZ1, PME31, BGAL5, ARAD1, ARAD2, AGP8, PERK10, LRX3* were selected for analysis. qPCR primers (Table 5.4) were designed at Universal Probe Library Assay Design Center (https://lifescience.roche.com/ products/ universal-probe-library) and ordered from the primer company (Integrated DNA Technologies). Primers were diluted with sterile distilled H_2O, and placed at -20 °C until use. Housekeeping gene (Elongation Factor 1-α) was used as the normaliser for qPCR.

5.3.3.1 mRNA isolation, DNase treatment and cDNA synthesis

Total RNA was isolated from roots of Arabidopsis plants (10 root segments per biological replicate) with two biological replicates. The E.Z.N.A.™ Plant RNA Protocol I (Standard Protocol) from E.Z.N.A.® Plant RNA Kit (Omega, Biotek) was used to isolate the total RNA. The following protocol was used: 20 µl of 2-mercaptoethanol (β-mercaptoethanol) per 1 mL of Buffer RB was added at room temperature. Root samples in 1.5 mL microcentrifuge tubes were placed in liquid nitrogen and ground in situ with a micropestle. The liquid nitrogen was allowed to evaporate and 500 µL of RB buffer/2-mercaptoethanol was added to the frozen ground powder. Samples were vortexed vigorously to disperse all of the clumps. The lysates were transferred into Homogenizer Columns that were placed in 2 mL collection tubes. They were centrifuged at 14000 rpm for 5 min. The cleared lysates were transferred to new 1.5 mL microcentrifuge tubes without disturbing the debris pellets. One volume of 70% ethanol was added and vortexed for 20 s. Samples were applied to HiBind® RNA columns centrifuged at 13400rpm for 1 min. The filtrate was discarded and an on-column DNase I digestion was performed to remove genomic DNA. The DNase I stock solution was prepared (E.Z.N.A.® DNase I

digestion buffer (73.5 µL) and RNase-free DNase I (20 kunitz U/µL) (1.5 µL)/for each HiBind® RNA mini column). 250 µL RNA wash buffer I was added to the HiBind® RNA mini column and centrifuged at 10000 rpm for 1 min. 75µL of DNase I digestion mixture was added on the surface of HiBind® RNA mini column and incubated at room temperature for 15 mins. RNA Wash Buffer I (250 µL) was added, and incubated for 2 mins at room temperature. Following the incubation, samples were centrifuged at 10000 rpm for 1 min. Filtrate was discarded and 600 µL of the RNA Wash Buffer II was added. Centrifugation (10000 rpm for 1 min) was performed with the flow-through discarded. Following the second time of the RNA Wash Buffer II step, centrifugation was performed at 13400 rpm for 2 min to dry the HiBind® RNA mini column matrix. The column was placed onto the clean 1.5 mL microcentrifuge tube. DEPC water (100 µL) was added onto HiBind® RNA mini column matrix and centrifuged at maximum speed for 2 min. The concentration and purity of each RNA sample was assessed using a Nanodrop spectrophotometer then RNA was stored at -80 °C until use.

cDNA synthesis was performed using SuperScript II reverse transcriptase (Life Technologies) with 1 µg total RNA used as template for each reaction. This was combined in a PCR tube with 1 µl of oligo(dT) primer (10 µM), 1 µl of 10 mM dNTP mix, and RNase-free H_2O to a volume of 13 µl. The PCR tube was heated at 65 °C in the PCR block for 5 minutes and then placed on ice. After a short centrifugation, 4 µl of 5x first-strand buffer and 2 µl of 0.1M DTT were added and incubated at 42 °C for two mins. One microlitre of Superscript II reverse transcriptase was added and mixed gently with a pipette. After incubating for 50 mins at 42 °C, the reaction was inactivated by heating at 70 °C for 15 minutes. Then 20 µl of sterile water was added and the cDNA was stored at -20 °C until use. For testing the efficiency of qPCR primer pairs a dilution series (1x, 10x, 100x, 1000x and 10,000x) was prepared to generate a standard curve. The dilution of 1:100 (100x) was used for subsequent qRT-PCR reactions to determine relative gene expression.

5.3.3.2 Quantitative reverse transcriptase polymerase chain reaction (qRT-PCR)

Cell wall-related gene expression in plant roots at 14 days after infection with *M. incognita* was analysed by qRT-PCR using a CFX Connect™ Real Time System (Bio-Rad). SsoAdvanced™ Universal SYBR® Green Supermix (Bio-Rad) was used for quantitative measurement of PCR products. This mix contains polymerase enzyme, buffer, dNTPs, and the double-stranded DNA binding dye SYBR Green. The gene-specific primer pairs used (detailed in Table 5.4) were diluted to provide a solution containing 7.5 µM of each. The housekeeping gene Elongation Factor 1-α (Table 5.3) was used to normalise expression of the genes of interest.

The PCR was carried out in 96-well plates (Bio-Rad), the plates were sealed with optical sealing film and each well contained the reagents below. Each reaction was set up for three technical triplicate wells and three negative control reactions for each primer pair contained additional water in place of the cDNA template. The cycling conditions used are shown below. Fluorescence data were collected at the end of step 3 for each cycle. After 40 cycles, the temperature was gradually increased from 60 °C to 95 °C with fluorescence data collected continually to provide a dissociation curve to test for the specificity of the amplification products.

PCR mix in each well	Step	Temperature	Duration
10 µl SYBR green mix	1	95 °C	30 seconds
4 µl cDNA	2	95 °C	5 seconds
0.8 µl LP + RP mix (7.5 µM each)	3	60 °C	10 seconds
5.2 µl H_2O	4	Go to step 2,	39X
Total: 20 µl	5	60 °C	5 seconds
	6	Ramp to 95 °C	

Microsoft Excel was used for analysis after exporting the Ct values (cycle number at which the defined fluorescence threshold was crossed) from the CFX Manager Software (BioRad). The change in relative abundance of mRNA for each target gene upon nematode infection was calculated (fold change) using the $2^{\Delta\Delta Ct}$ method. The Ct value of the normaliser gene was subtracted from the Ct value of the target gene for each reaction (ΔCt), then the control (uninfected) mean ΔCt value for the technical replicates was subtracted from the infected sample mean ΔCt value for each gene of interest (ΔΔCt). The log2 fold change was then determined.

5.3 Primers of cell wall-related genes and housekeeping gene for qRT-PCR experiment

Gene accession	Gene name	Left primer	Right primer
At1g19300	*GLZ1*	CGACGCTTCTTCCTTACGAG	ACGTAGACGGTGAAATCAAGG
At3g21190	*MSR1*	TGCTTGGACAGATGCTTCATA	AATATCTTGTGCATCTCCCTGAG
At2g20370	*MUR3*	GGCCGAACCGAGTATGACTA	CTCCAGCAACGCATACTTCC
At3g29090	*PME31*	ACTTTTGAGAACTCTGCTCCTGA	ACGGTCTGCAGTGACTCGTAT
At1g45130	*BGAL5*	TATGTGGACAGAGGCATGGA	ATCCTCTACAGGTCGTTTAGGAAC
At2g35100	*ARAD1*	AAATCGATATCGCAAAGATGGT	TTGTTACATCATCTTCCTTTTCAAGT
At5g44930	*ARAD2*	AATCGATATCGCAAAGATGGA	ACTGTGTTCCGCGTTTGAT
At2g45470	*AGP8*	CCGGAAAATTCGATCTAACG	CGCCGGTGTGGAGAATAA
At1g26150	*PERK10*	GAGACCCCGAATGAGTCAAA	AGTCTCATTCCATTGGTGAGG
At4g13340	*LRX3*	ACCATCAGCTCCATGTGAAGA	GGTGGACTGTGGTGAACTACC

*Housekeeping gene: Elongation Factor 1-α, At5g60390, (Forward primer 5′-GACAGGCGTTCTGGTAAGGA-3’; Reverse primer 5′-GCTTGGTTGGGGTCATCTTA-3′)

5.3.4 Arabidopsis cell wall-related gene expression in *Arabidopsis thaliana* of *M. incognita* infection at 7, 14, 21 and 28 days post infection (Microarray data)

Existing microarray data of Arabidopsis roots after infection with *M. incognita* at 7, 14, 21 and 28 dpi were taken from "Genevestigator". The expression data of 12 cell wall-related genes, *MUR3*, *MSR1*, *GLZ1, QUL1*, *PME31*, *BGAL5*, *RGXT1*, *ARAD1*, *ARAD2*, *AGP8*, *PERK10* and *LRX3* in infected and uninfected roots was compared. Statistical analysis (Microsoft Excel, t-test) was applied to find the significant differences in gene expression in infected roots compared to uninfected root sections ($P<0.05$).

5.3.5 *In situ* cell wall analysis of Arabidopsis mutants

Arabidopsis seedlings (either wild type or mutants) growing in sterile tissue culture (section 2.1.2) were infected at day 15 with J2s of *M. incognita*, population VW6, which had been surface sterilised as described in section 2.2.4. Five *Arabidopsis* root tips per plant were infected (20 nematodes/ root tip) and covered with Glass Microfiber Filter (GF/A – Whatman) paper to ensure synchronous infection. GF/A papers were removed after 48 hours. Root samples were collected on day 21 post infection (dpi) to conduct the sectioning and immunolabelling. Galled root segments from infected plants and similar sized segments from the corresponding age and relative location of roots in non-infected plants were collected.

Monoclonal antibodies were used to reveal the molecular architecture of the giant cell walls induced by *M. incognita* in 12 different cell wall mutants (Table 5.1). The cell wall compositions in the *M. incognita* feeding site were observed by comparison with nematode infected root tissues of wild type (Col-0). Tissue sample fixation, ethanol dehydration and resin embedding, Vectabond^{TM} slide preparation, microtome cutting, gathering sections, immunolabelling, application of monoclonal antibodies, a secondary antibody, Calcofluor-white staining, pectate lyase treatment, florescence imaging and image analysing were carried out as described in section 2.3.

Seventeen monoclonal antibodies were used to detect the cell wall epitopes in nematode infected and uninfected root samples (Table 5.3). Monoclonal antibodies LM15 and LM25 were applied to the root sections of the *xyloglucan galactosyltransferase (mur3)* mutant to reveal any alteration in xyloglucan. LM21

and LM22 antibodies were applied to the root sections of *mannan synthesis related 1* (*msr1*) mutant to detect the heteromannan epitopes in the cell walls. Xylan binding antibodies, LM10 (xylan), LM11 (arabinoxylan) and LM28 (glucoronoxylan) were applied to the *galacturonosyltransferase-like 1 (glz1*) mutant. Homogalacturonan binding antibodies LM19 (de-esterified pectic homogalacturonan) and LM20 (methyl esterified pectic homogalacturonan) were applied to the homogalacturonan-related *quasimodo2 like 1 (qul1)* and *pectin methylesterase 31 (pme31)* mutants. LM5 antibody was applied to *beta-galactosidase 5 (bgal5)* mutant to detect galactan in the cell walls. Arabinan, processed arabinan and linearised arabinan binding antibodies: LM6, LM16 and LM13 were applied to *arabinan deficient 1 (arad1)* and *arabinan deficient 2 (arad2)* mutants to detect the epitopes of arabinan in the cell walls. AGP-binding antibodies, LM2 and JIM14 were applied to the *arabinogalactan protein 8 (agp8)* mutant to detect the AGP glycan in the cell walls. Extensin binding antibodies, JIM19 and JIM20 were applied to extensin-related mutants (*rhamnogalacturonan xylosyltransferase 1 (rgxt1), proline-rich extensin-like receptor kinase 10 (perk10)* and *leucine-rich repeat/extensin 3 (lrx3*)) to detect the extensin in the cell walls.

Table 5.4 Plant cell wall monoclonal antibodies used for the *in situ* analysis of Arabidopsis cell wall mutants

Plant cell wall components			Antibody	Cell wall related mutant
Hemicellulose	Xyloglucan	XXXG Xyloglucan	LM15	*xyloglucan galactosyltransferase (mur3)*
		Galactosylated xyloglucan	LM25	*xyloglucan galactosyltransferase (mur3)*
	Mannan	Heteromannan	LM21	*mannan synthesis related 1* (*msr1*)
		Heteromannan	LM22	*mannan synthesis related 1* (*msr1*)
	Heteroxylan	Xylan	LM10	*galacturonosyltransferase-like 1 (glz1)*
		Arabinoxylan	LM11	*galacturonosyltransferase-like 1 (glz1)*
		Glucuronoxylan	LM28	*galacturonosyltransferase-like 1 (glz1)*
Pectic polysaccharides	HG	DePHG	LM19	*related quasimodo2 like 1 (qul1), pectin methylesterase 31 (pme31)*
		MePHG	LM20	*related quasimodo2 like 1 (qul1), pectin methylesterase 31 (pme31)*
	RG-I	Galactan	LM5	*beta-galactosidase 5 (bgal5), rhamnogalacturonan xylosyltransferase 1 (rgxt1)*
		Arabinan	LM6	*arabinan deficient 1 (arad1), arabinan deficient 2 (arad2), rhamnogalacturonan xylosyltransferase 1 (rgxt1)*
		Processed arabinan	LM16	*arabinan deficient 1 (arad1), arabinan deficient 2 (arad2), rhamnogalacturonan xylosyltransferase 1 (rgxt1)*
		Linearized arabinan	LM13	*arabinan deficient 1 (arad1), arabinan deficient 2 (arad2), rhamnogalacturonan xylosyltransferase 1 (rgxt1)*
Glycoproteins	AGPs	AGP glycan	LM2	*arabinogalactan protein 8 (agp8)*
		AGP glycan	JIM14	*arabinogalactan protein 8 (agp8)*
	Extensin	Extensin	JIM19	*proline-rich extensin-like receptor kinase 10 (perk10), leucine-rich repeat/extensin 3 (lrx3*)
		Extensin	JIM20	*proline-rich extensin-like receptor kinase 10 (perk10), leucine-rich repeat/extensin 3 (lrx3*)

HG; Homogalacturonan, RG-I; Rhamnogalacturonanan-I DePHG; de-esterified pectic homogalacturonan, MePHG; methyl esterified pectic homogalacturonan, AGPs; arabinogalactan proteins.

5.3.6 Role of cell wall genes in nematode development and function in Arabidopsis mutants

M. incognita infective second stage juveniles (J2s) were used to infect Arabidopsis cell wall mutants (Table 5.1) in the glasshouse. Following preparation of the soil mix (40% loam, 40% sand, 20% compost), Arabidopsis seeds were sown in 9 cm diameter pots and 5 plants were grown in each pot. When the primary roots reached the bottom of the pots, 100 second stage juveniles of *M. incognita* were inoculated into the soil around the root system of each plant (total of 500 J2s per pot). For each experiment 30 wild-type and 30 mutant plants were infected with *M. incognita* and each complete experiment was replicated on two separate occasions at 25 °C with 16 hours light and 8 h dark conditions in the glasshouse. Roots were removed from the soil at 28 dpi, washed and stained with acid fuchsin to determine nematode number, nematode size, gall number and gall size.

5.3.6.1 Acid fuchsin staining

The roots were gently washed of any soil particles with tap water and acid fuchsin staining was performed to improve visibility of nematodes in the root sections. Stock 10X acid fuchsin was prepared; 750 ml Elga H_2O, 250 ml acetic acid, 3.5 g acid fuchsin. Collected roots were washed with tap water and were placed in sodium hypochlorite (1% available chlorine) for 2 mins. Roots were boiled in 1x acid fuchsin for 3 mins in a beaker then rinsed with tap water. The roots of each plant were individually boiled and were then placed into 90 mm Petri dishes filled with acidified glycerol.

5.3.6.2 Determining nematode number, gall number, nematode size and gall size

Numbers of nematodes (fusiform, adult female and total nematode number), and galls were counted under the microscope (Olympus SZX, Japan). For nematode size, the images of 32 randomly selected nematodes were captured with a QImaging camera (Canada) under the microscope (Leica, M165C) connected to a computer. The nematode images were measured using Image ProAnalyser 7.0 software (2009 Media Cybernetics).

Each plant was treated as a biological replicate and data from the two separate experiments carried out for each mutant line were combined. The nematode and gall numbers were counted for 35 to 50 plants for each mutant and wild type group. Nematodes were assigned as either fusiform (parasitic juvenile stages) or females based on their size and morphology. The gall diameter was measured on the thickest part of each gall from 30 randomly selected galls of infected mutant and wild type Arabidopsis roots for each experiment. The nematode size (area) was measured from 32 randomly selected nematodes. Statistical significance between mean values of wild type and mutant plants in each experiment was determined with the t-test and differences with P value of <0.05 were classed as significant.

5.4 Results

Cell wall-related genes for analysis in this Chapter were chosen based on their genetic characteristics which were taken from the database of *Arabidopsis thaliana*, The Arabidopsis Information Resource (TAIR). The expression of genes in roots, mutant availability, quantification of gene expression at 14 dpi (qRT-PCR), differential gene expression (microarray data) during the nematode infection were all considered when making the selections. *M. incognita* infects the roots of plants, therefore genes were selected which are expressed in the roots of Arabidopsis.

In this study hemicellulose related genes (xylan: *GLZ1*; heteromannan: *MSR1*; xyloglucan: *MUR3*), pectin related genes (homogalacturonan: *PME31* and *QUL1*; Rhamnogalacturonan: *BGAL5*, *RGXT1*, *ARAD1*, *ARAD2*) and glycoprotein related genes (Arabinogalactan proteins: *AGP8*; extensin: *PERK10* and *LRX3*) were selected for expression and mutant analysis (Table 5.1).

Arabinan-deficient mutants were provided by the Cell Wall Lab at the University of Leeds, and other cell wall-related mutants (Table 5.1) were obtained from Nottingham Arabidopsis Stock Centre (NASC). Following the cultivation of Arabidopsis seeds which were ordered from NASC, the homozygosity test was performed to ensure that all plants used for subsequent experimentation were homozygous insertion mutants for the expected gene. The result of the homozygosity tests revealed that *mur3*, *msr1*, *glz1*, *qul1*, *pme31*, *bgal5*, *rgxt1*, *arad1*, *arad2*, *agp8, perk10* and *lrx3* were all homozygous mutants (Figure 5.1). Homozygous mutants gave single amplified bands following PCR of 400-500 bp: *mur3* (~400 bp), *msr1* (~400 bp), *glz1* (~500 bp), *qul1* (~400 bp), *pme31* (~500 bp), *bgal5* (~500 bp), *rgxt1* (~400 bp), *agp8* (~500 bp), *perk10* (~400 bp) and *lrx3* (~400 bp). Arabinan deficient mutants gave bands around 100-150bp (Figure 5.1).

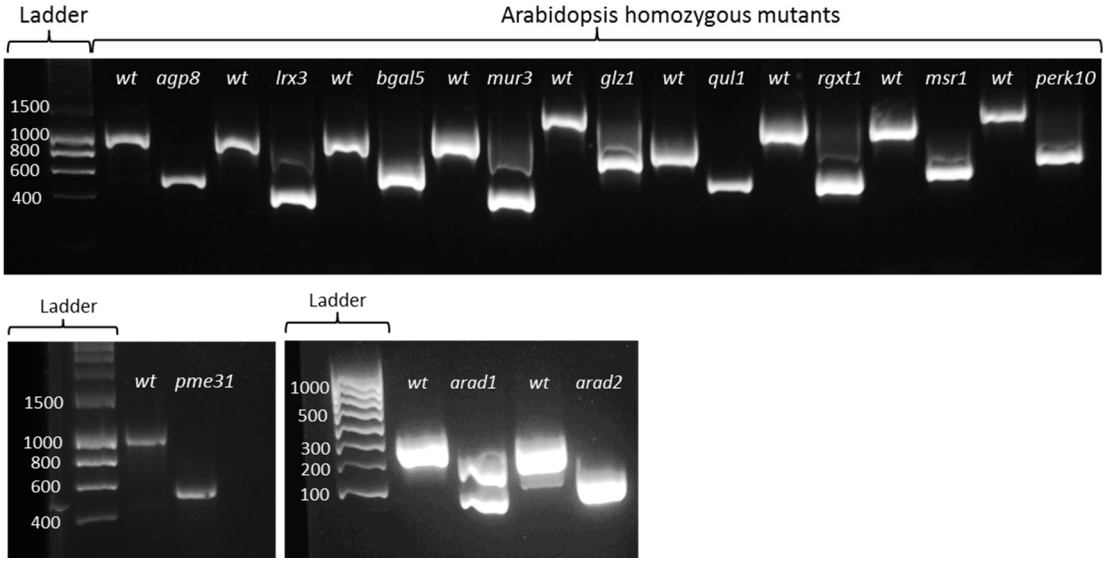

Figure 5.1 Homozygosity test of Arabidopsis mutants. Arabidopsis homozygous mutants which carry only mutant alleles of the gene of interest gave a single band around 400-500 base pairs (bp) and the wild type gene gave bands around 900-1000 bp for Salk lines. Arabinan deficient homozygous mutants (*arad1* and *arad2*) gave bands around 100-150 bp (Sail lines). *agp8, arabinogalactan protein 8; lrx3, leucine-rich repeat/extensin; bgal5, beta-galactosidase 5; mur3, xyloglucan galactosyltransferase; glz1, galacturonosyltransferase-like 1; qul1, quasimodo2 like 1; rgxt1, rhamnogalacturonan xylosyltransferase 1; msr1, mannan synthesis related 1; perk10, proline-rich extensin-like receptor kinase 10; pme31, pectin methylesterase 31; arad1, arabinan deficient 1; arad2, arabinan deficient 2* and wt, indicates Arabidopsis wild type (Col-0).

qRT-PCR was used to quantify the gene expression of cell wall-related genes: *GLZ1*, *MSR1*, *MUR3*, *PME31*, *BGAL5*, *ARAD1*, *ARAD2*, *AGP8*, *PERK10* and *LRX3* in nematode infected and uninfected root samples of Arabidopsis. The level of gene expression did not differ significantly from the uninfected roots at 14 dpi.

The gene expression data was then taken from Genevestigator, which is a high performance search engine that provides access to public microarray data. This allowed gene expression data to be interrogated for a wider range of time-points in the interaction between Arabidopsis and *M. incognita*. The expression of cell wall-related genes is likely to vary over the course of giant cell development and the qRT-PCR provided only a snap-shot of expression at a single time point. The statistical analysis was performed of the microarray expression data of *MSR1, MUR3, GLZ1, BGAL5, RGXT1, QUL1, PME31, ARAD1*, *ARAD2, AGP8, LRX3, PERK10* after infection of *M. incognita* at 7, 14, 21 and 28 dpi in comparison with non-infected roots (Table 5.5). Hemicellulose-related genes: mannan-related *MSR1* was down-regulated at 21 dpi and xyloglucan-related *MUR3* was up-regulated at both 7 and 14 dpi. For the pectin related genes, *BGAL5* was down-regulated 21 dpi and *RGXT1* was down-regulated at 7 dpi, but *ARAD1* at 21 dpi and *ARAD2* at 14 dpi were up-regulated. The glycoprotein related genes were either upregulated (*PERK10* at 14 and 21 dpi) or down-regulated (*AGP8* and *LRX3* at 21 dpi) following the infection of *M. incognita* (Table 5.5). However, the *GLZ1*, *QUL1* and *PME31* genes did not significantly change in the expression at 7, 14, 21 or 28 dpi (Table 5.5).

5.4.1 *In situ* analysis of Arabidopsis cell wall-related mutants

M. incognita causes major changes and orientation of cell walls in the feeding site during the infection of *Arabidopsis thaliana* (Figure 5.2). During the nematode feeding, the gall formation in the roots was visible in both wild type and mutant plants. Transverse sections of galls revealed the structure of the nematode-induced feeding site (Figures 5.2; 5.3, 5.4, 5.5, 5.6, 5.7, 5.8 and Supplementary Data in CD).

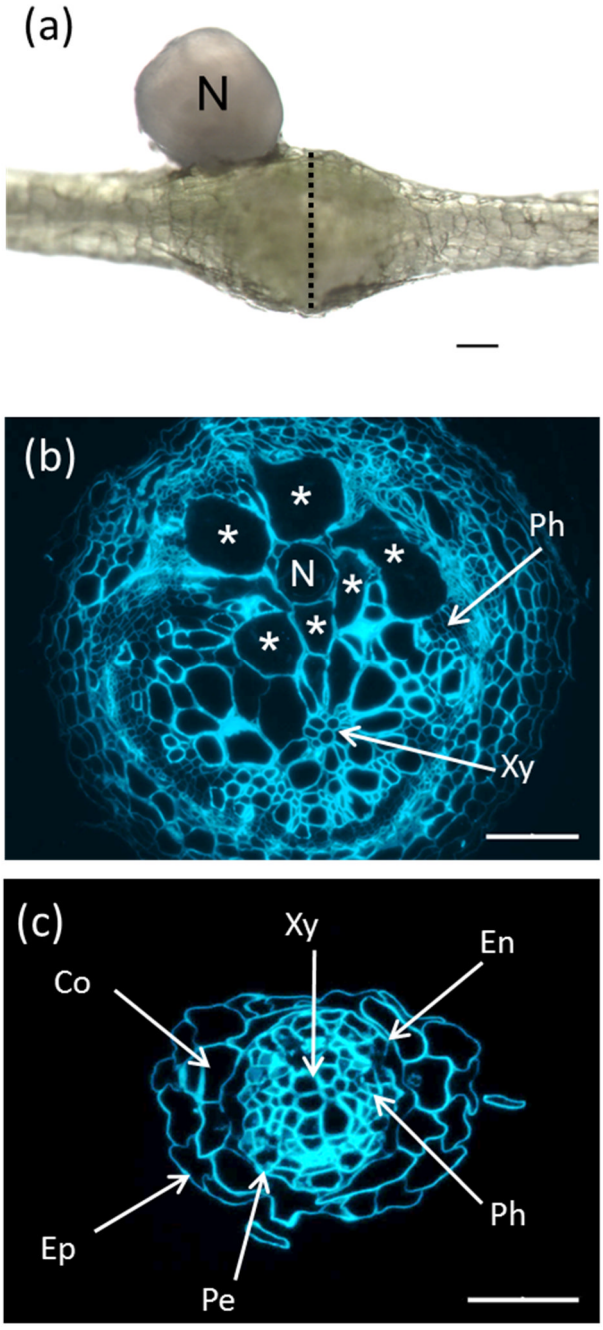

Figure 5.2 The structure of a root knot nematode feeding site (infected) and non-infected root sections of *Arabidopsis thaliana*. (a) The *Meloidogyne incognita* infected Arabidopsis root galls at 21 days post-infection (dpi); the dotted line represents the location of the characteristic transverse section; (b) Calcofluor- white staining of a 0.5 µm transverse nematode-infected root section. Asterisks indicate giant cells; N, represents the nematode *M. incognita*; Xy, xylem vessels; Ph, phloem. (c) Calcofluor-white staining of transverse uninfected (control) Arabidopsis root section; Co, cortical cells; Xy, xylem vessels; En, endodermis; Pe, pericycle; Ep, epidermis; Ph, phloem cells. Bars: (a- b) 100 µm; (c) 30 µm.

5.4.1.1 Reduced level of cell wall polysaccharides were detected in the cell wall mutants

Hemicelluloses are generally branched, short chains of matrix polysaccharides that mainly consist of xyloglucan, mannan, xylan, arabinoxylan and glucuronoxylan. Arabidopsis xyloglucan knockout mutant (*mur3*) had lower levels of xyloglucan-specific antibody binding compare to wild type Arabidopsis (Col-0). The LM25 and LM15 antibodies both bind to epitopes of xyloglucan in cell walls. Specifically, the antibody LM25 binds the XXXG/galactosylated xyloglucan and LM15 binds the XXXG motif of xyloglucans. LM25 bound xyloglucan with higher affinity than LM15 in the root sections of both mutant and wild type plants. Xyloglucan was shown to be less abundant in the roots of xyloglucan galactosyltransferase mutant (*mur3*) compared to wild type Arabidopsis at 21 dpi with both antibodies. The localisation of both antibodies was detected in the giant cell walls and other cell walls in the vascular cylinder of wild type but there was a lower level of antibody binding in *mur3* (Figure 5.3). The xylan-specific antibodies were used to determine the location of xylem vessels in the root sections to distinguish these from giant cells. Antibodies, LM11, LM10 and LM28 that bind to arabinoxylan, xylan and glucuronoxylan respectively were used. The highest level of binding was observed with the antibody LM11 in both mutant and wild type plants. The binding of all three antibodies was higher in wild type than the *parvus/glz1* mutant (Figure 5.4). The *glz1* gene is involved in xylan and secondary cell wall synthesis (Lee et al., 2007); hence the *glz1* mutant has thinner cell walls. The mannan synthesis-related mutant (*msr1*) affects mannan biosynthesis and the glucomannan level is approximately 40% less than wild type (Wang et al., 2013). The binding of mannan specific antibodies (LM21 and LM22) was correspondingly higher in the root sections of wild type than *msr1* mutant plants. The LM21 antibody was bound to the cell walls of nematode-induced giant cells in wild type Arabidopsis but not in *msr1* (Figure 5.5).

Pectic polysaccharides are essential wall components for plant growth and development. Pectin is rich in galacturonic acid and substitution of the backbone of D-galacturonic acid generates distinct groups such as homogalacturonan and rhamnogalacturonan-I within pectin. In this study, pectic homogalacturonan-related mutants (*pme31* and *qul1*) and rhamnogalacturonan-related mutants (*bgal5, rgxt1, arad1* and *arad2*) were tested alongside wild-type plants to compare the differential

binding of pectic polysaccharides by the antibodies LM19, LM20, LM5, LM6 LM16, and LM13. Galacturonic acid that is methylesterified can be revealed by the antibody LM20. The non-esterified galacturonic acid is revealed by the antibody LM19. The binding of LM20 antibody to the giant cell walls and other cell walls within the vascular cylinder was higher than LM19 in the root sections of both wild type and *pectin methyl esterase 31* (*pme31)* mutant (Figure 5.6). The binding of both antibodies was slightly lower in the root sections of *pme31* than the wild type (Figure 5.6). The *quasimodo2 like1* (*qul1*) mutant has a reduced level of homogalacturonic acid, which results in cell adhesion defects (Fuentes et al., 2010). The localisations of LM20 and LM19 antibodies in the cell walls of the root section of *qul1* mutant were similar to those observed with the *pme31* mutant. The detection of antibody binding was lower in *qul1* mutant compare to wild type (Figure 5.7). Galactan and arabinan are pectic rhamnogalacturonan-I, and are detected by LM5 and LM6 antibodies, respectively. The binding of both antibodies was lower in giant cell walls of root sections in *beta galactosidase 5* (*bgal5*) mutant than the wild type (Supplementary data). The LM5 and LM6 antibodies had reduced binding in giant cell walls in root sections of rhamnogalacturonan xylosyltransferase 1 (*rgxt1*) mutant (supplementary data). Arabinan, processed arabinan and linearized arabinan were localised by LM6, LM16 and LM13 antibodies, respectively. The lower binding of antibody LM6 in arabinan-deficient mutants (*arad1* and *arad2*) compared to wild type reflected a reduced level of arabinan in these plants. The binding of antibodies LM16 (processed arabinan) and LM13 (linearized arabinan) was not detected in either wild type or arabinan deficient mutants in infected roots (Figure 5.8).

Arabinogalactan proteins (AGPs) and extensin are glycoproteins that covalently attach to polypeptide side chains. AGPs have varied size and class of cell surface glycoproteins found in plant cell walls that play many roles from cell division to plant microbe interactions. LM2 and JIM14 are AGP-specific antibodies. Inconsistent binding of LM2 was observed in wild type and arabinogalactan protein 8 (*agp8*) mutant but no binding was detected with the JIM14 antibody in the root sections of either *agp8* or wild type (supplementary data in CD). Extensins are hydroxyproline-rich glycoproteins (HRGPs) in the plant cell wall with 20 extensin genes found specifically in Arabidopsis. The extensin-related mutants analysed in this work were proline rich extensin-like kinase (*perk*) and *leucine-rich repeat/extensin 3* (*lrx3*).

Extensin can be localised by the JIM19 and JIM20 antibodies but in this work no binding was detected in the cell wall of root sections of either wild type or extensin-related (*perk* and *lrx3*) mutants (supplementary data in CD).

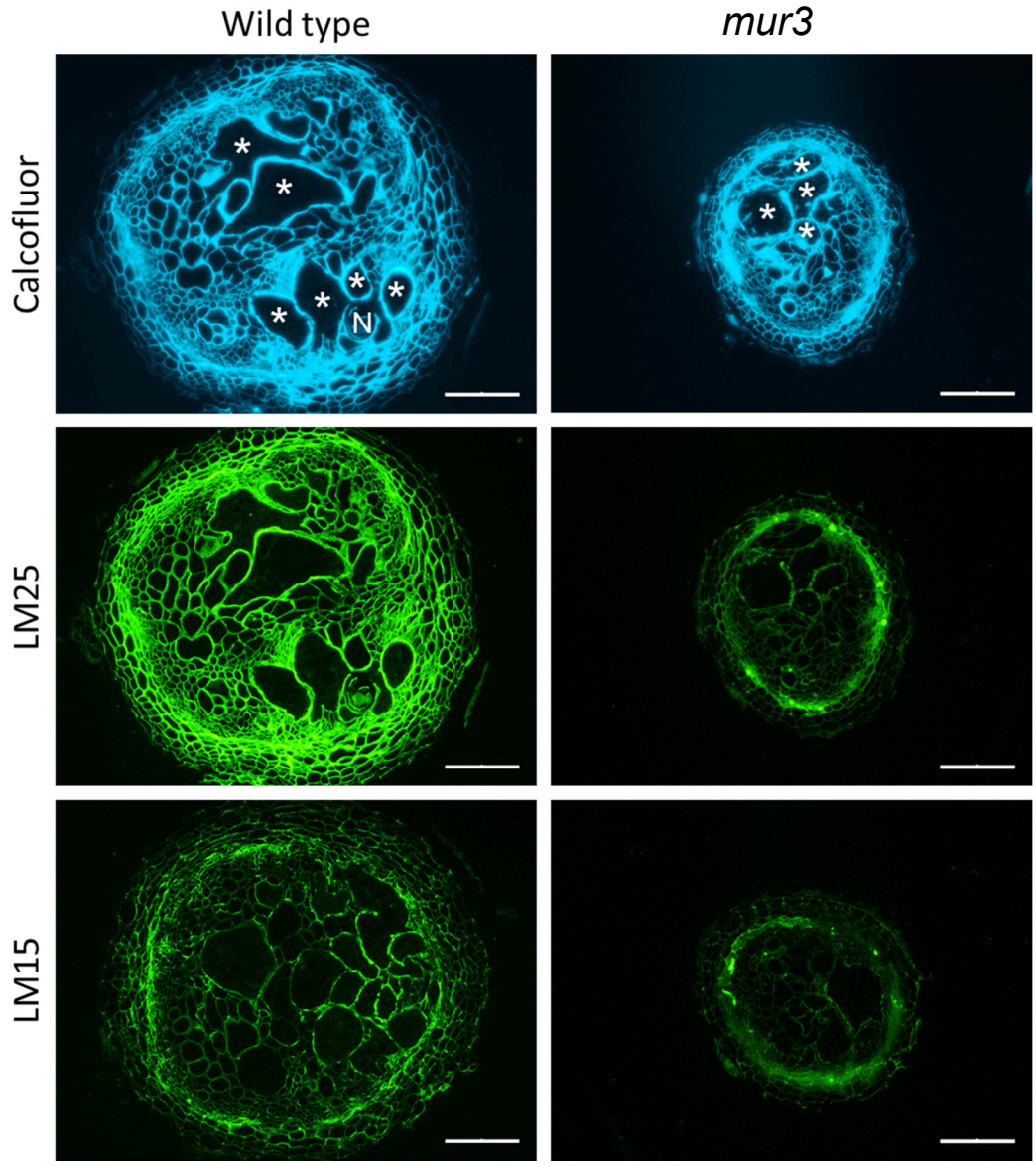

Figure 5.3 Immuno-labelling of xyloglucan in nematode infected *Arabidopsis thaliana* wild type (Col-0) and *xyloglucan galactosyltransferase* (*mur3*) mutant root sections at 21 dpi. Calcofluor white staining of root sections allows visualisation of all cell walls. LM25 and LM15 antibodies were applied to reveal the presence and abundance of xyloglucan. Asterisks represents giant cells in nematode feeding sites; N, nematode; Bars: 100 µm.

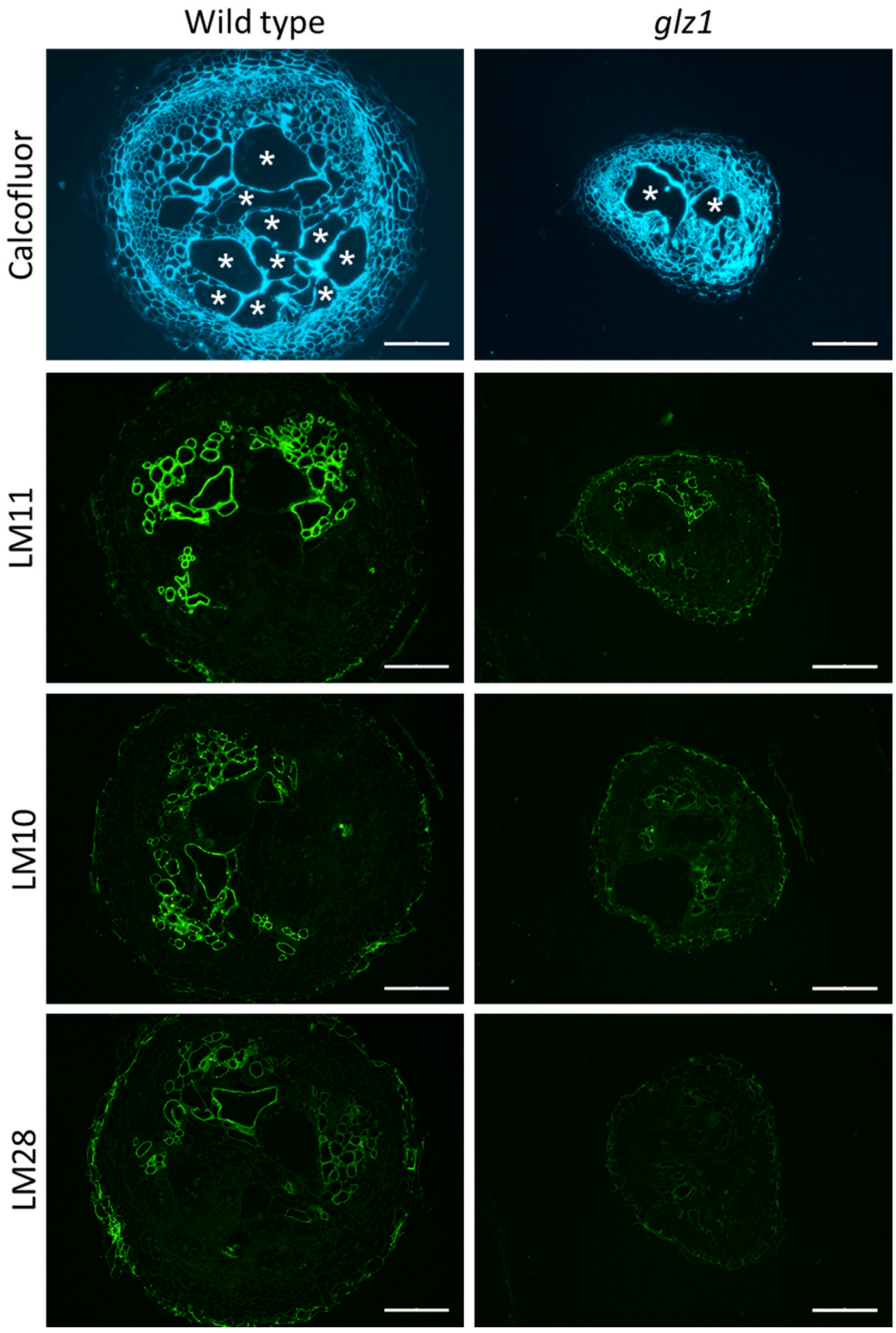

Figure 5.4 Immuno-labelling of xylan in nematode infected *Arabidopsis thaliana* wild type (Col-0) and *galacturonosyltransferase-like 1* (*glz1)* mutant root sections at 21 dpi. Calcofluor white staining of root sections allows visualisation of all cell walls. LM11, LM10 and LM28 antibodies were applied to reveal the presence and abundance of arabinoxylan, xylan and glucuronoxylan, respectively. Asterisks represent giant cells in nematode feeding site; N, nematode; Bars: 100 µm.

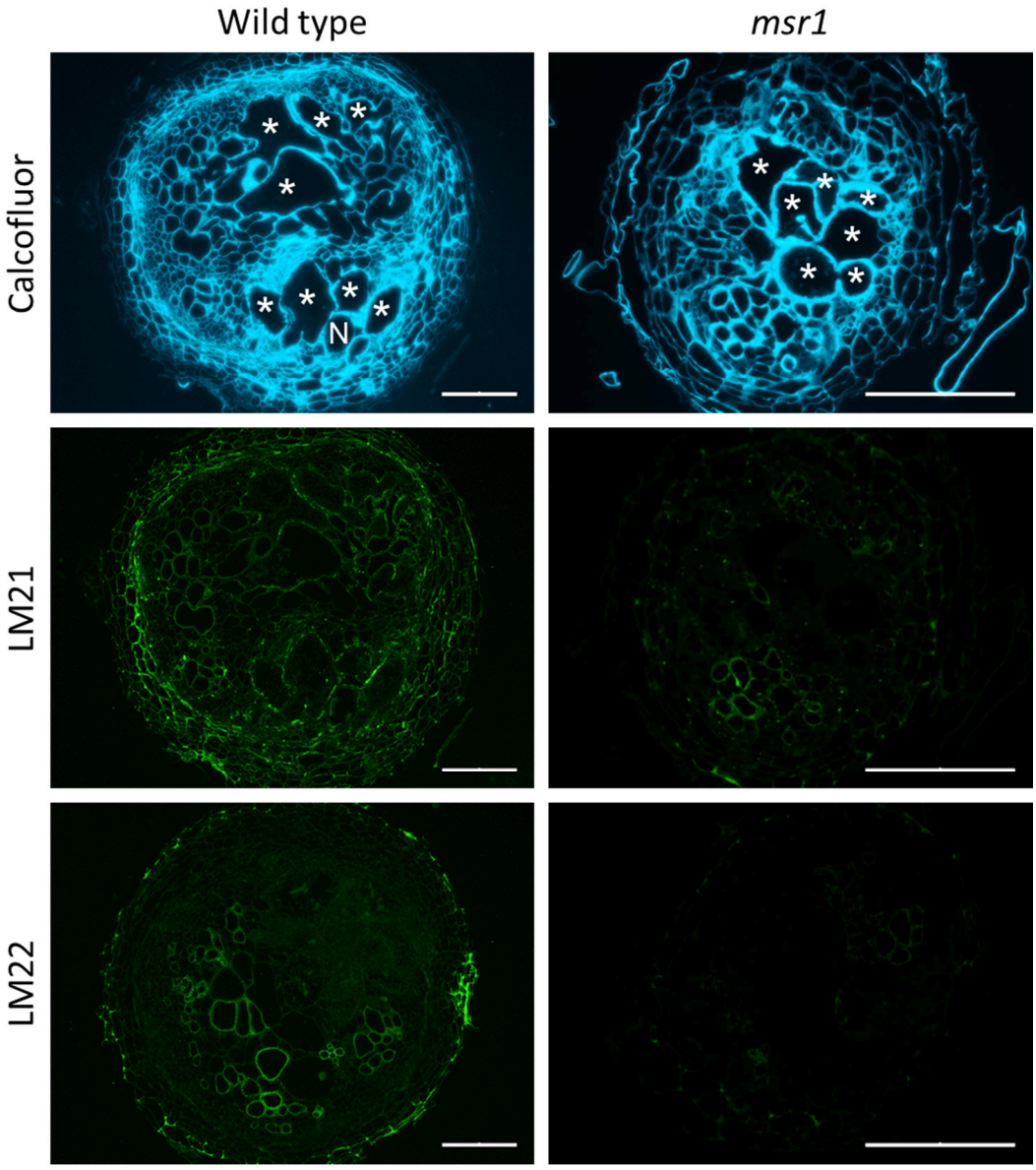

Figure 5.5 Immuno-labelling of mannan in nematode infected *Arabidopsis thaliana* wild type (Col-0) and *mannan synthesis related 1* (*msr1*) mutant root sections at 21 dpi. Calcofluor white staining of root sections allows visualisation of all cell walls. LM21 and LM22 antibodies were applied to reveal the presence and abundance of mannan. Asterisks represent giant cells in nematode feeding site; N, nematode; Bars: 100 µm.

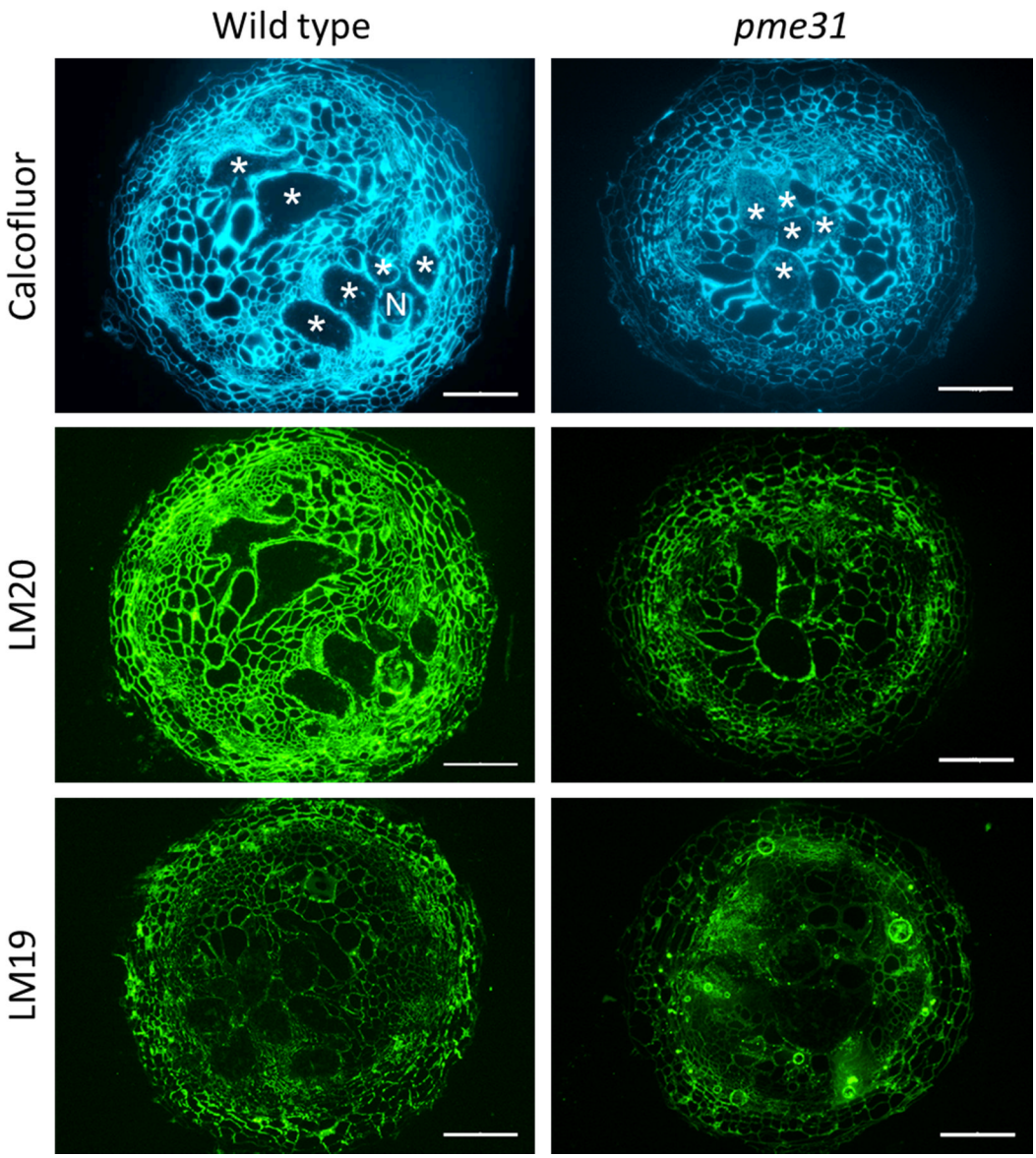

Figure 5.6 Immuno-labelling of pectic homogalacturonan in nematode infected *Arabidopsis thaliana* wild type (Col-0) and *pectin methylesterase 31* (*pme31*) mutant root sections at 21 dpi. Calcofluor white staining of root sections allows visualisation of all cell walls. LM20 and LM19 antibodies were applied to reveal the presence and abundance of methyl esterified pectic homogalacturonan and de-esterified pectic homogalacturonan, respectively. Asterisks represent giant cells in nematode feeding site; N, nematode; Bars: 100 µm.

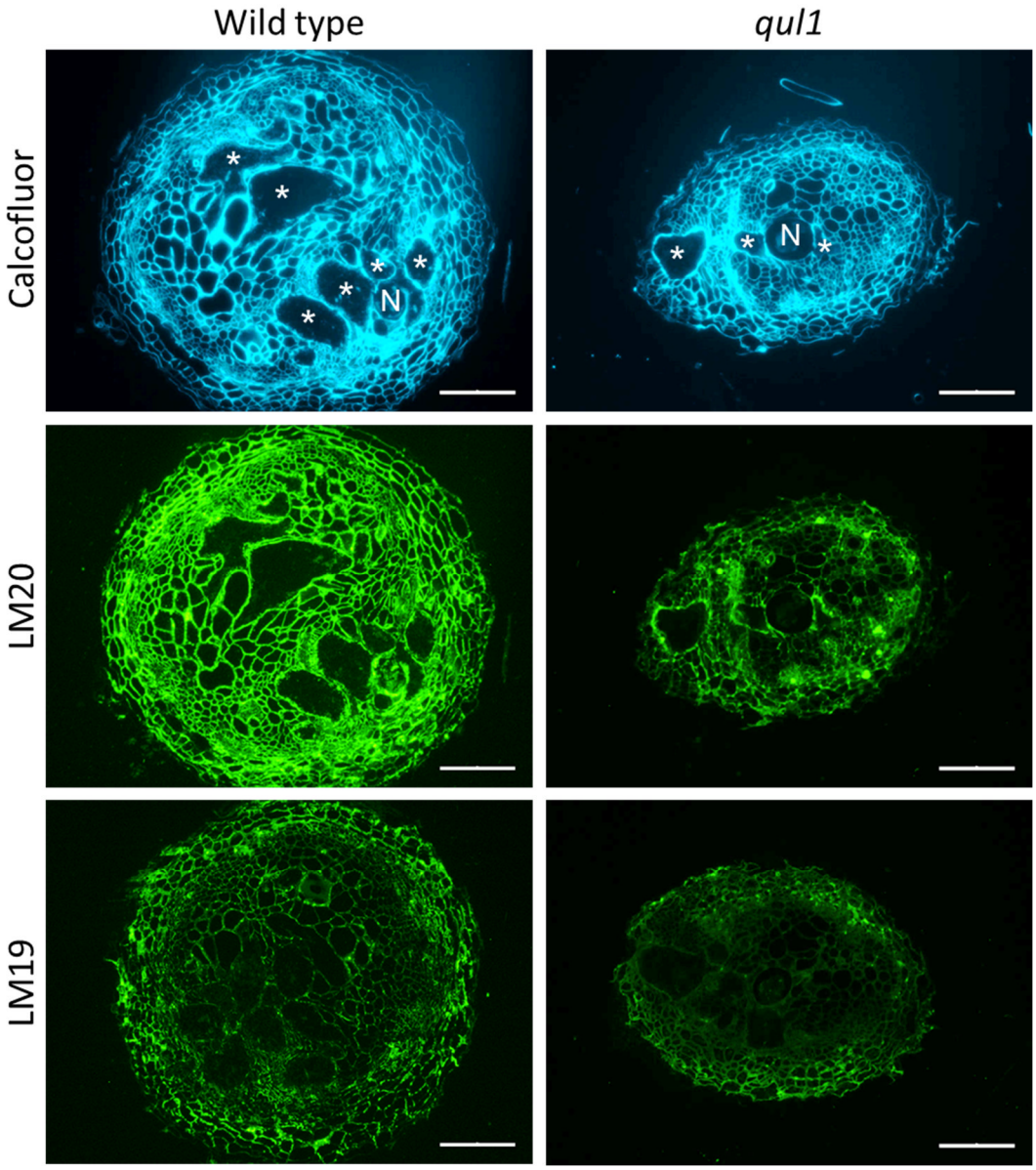

Figure 5.7 Immuno-labelling of pectin in nematode infected *Arabidopsis thaliana* wild type (Col-0) and *quasimodo2 like 1* (*qul1*) mutant root sections at 21 dpi. Calcofluor white staining of root sections allows visualisation of all cell walls. LM20 and LM19 antibodies were applied to reveal the presence and abundance of methyl esterified pectic homogalacturonan and de-esterified pectic homogalacturonan, respectively. Asterisks represent giant cells in nematode feeding site; N, nematode; Bars: 100 µm.

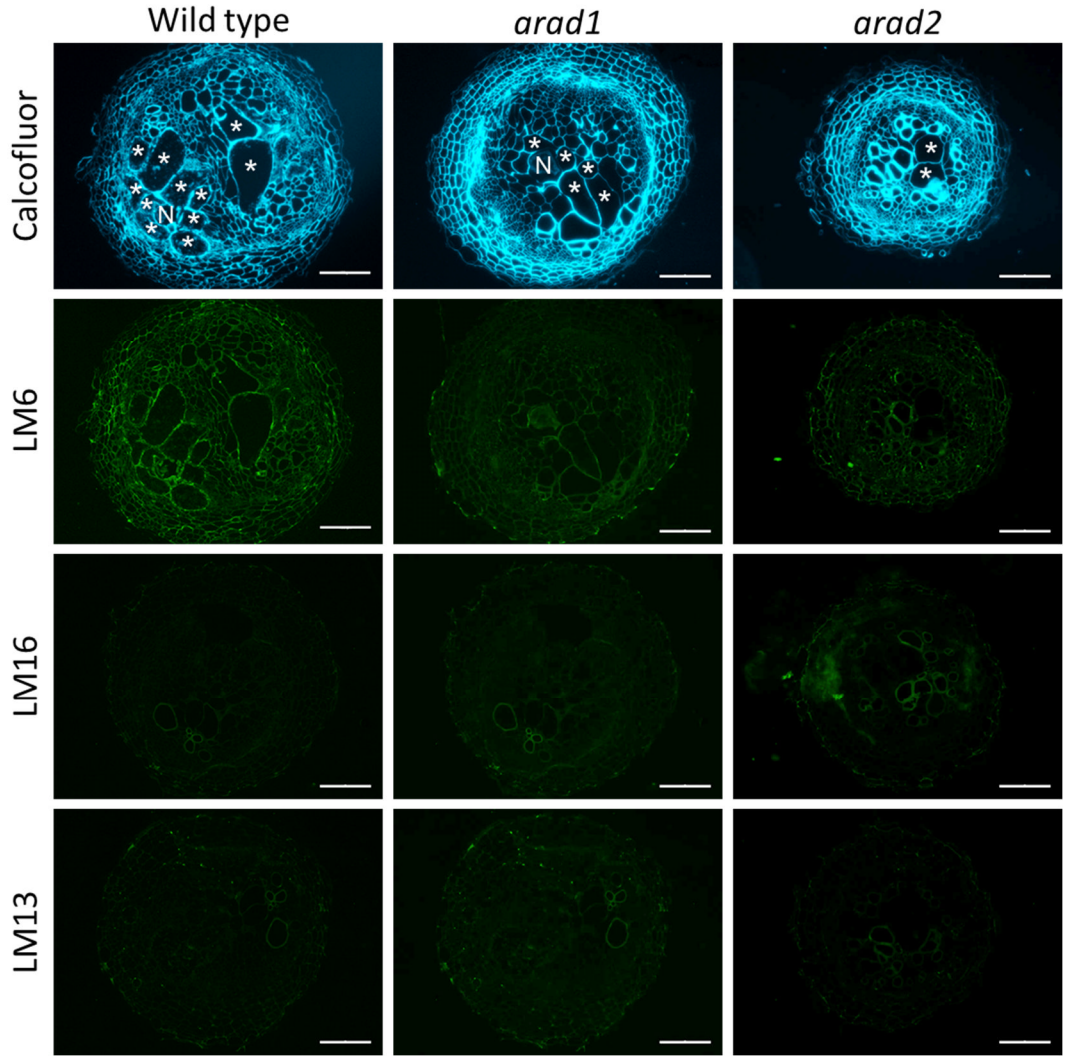

Figure 5.8 Immuno-labelling of arabinan in nematode infected *Arabidopsis thaliana* wild type (Col-0) and *arabinan deficient 1 (arad1)*, *arabinan deficient 2 (arad2)* mutants root sections at 21 dpi. Calcofluor white staining of root sections allows visualisation of all cell walls. LM6, LM16 and LM13 antibodies were applied to reveal the presence and abundance of arabinan, processed arabinan and linearized arabinan, respectively. Asterisks represent giant cells in nematode feeding site; N, nematode; Bars: 100 µm.

5.4.2 Evaluating the impact of the mutant host on nematode development and function

The role of cell wall genes on nematode number (fusiform, total nematode and adult female), nematode size, gall number and gall size was evaluated.

5.4.2.1 Role of hemicellulose-related cell wall genes on nematode development and function

Hemicellulose-related cell wall Arabidopsis mutants *glz1, msr1*and *mur3* were tested to check the role of cell wall genes on nematode development and function. The *PARVUS/GLZ1* gene is involved in glucuronoxylan biosynthesis and therefore has a role in secondary cell wall thickening (Lee et al., 2007a). This xylan-related gene knockout resulted in fewer nematodes, both fusiform and adult female, and reduced nematode size, gall thickness and gall number (Figure 5.9 a). It may be concluded from this result that although xylan is not present in giant cell walls, it is required for the successful broader development and function of the feeding site. The expression of the *GLZ1* gene was not altered in infected tissue of wild type plants compared to uninfected roots. (Table 5.5). This might be surprising given the proliferation of xylem vessels that is observed within galls. However, GLZ1 is clearly important in xylem formation. Therefore the effects of the *glz1* mutant on nematode number, nematode size, gall number and gall size reduced may be related to less solute transportation to the nematode feeding site.

The mutation of mannan-related gene, *msr1* led to a reported 40% reduction of mannosyl residues in the stems of Arabidopsis (Wang et al., 2013). Fewer adult female nematodes were present in roots of *msr1* mutant plants with reduced nematode size, gall thickness and gall number, however no significant differences were observed in fusiform and total nematode number (Figure 5.9 b). Mannan-related gene (*MSR1*) expression analysis showed significant down-regulation at 21 dpi, but there were not significant difference observed in nematode infected roots at 7, 14 and 28 dpi (Table 5.5).

Xyloglucan is involved in formation and function of the cell walls. Lower levels of galactosylated xylose were previously found in the *mur3* mutant (Kong et al., 2015). Expression of the xyloglucan-related gene *MUR3* was up-regulated during the early

stages (7 and 14 dpi) of *M. incognita* infection (Table 5.6). The *mur3* mutant plants supported a reduced number of nematodes but galls were not affected (Figure 5.9c). In general, hemicellulose-related mutants (*glz1, msr1* and *mur3,*) caused the suppression of adult female numbers but had varying effects on nematode size, gall thickness, gall number, fusiform and total nematode number (Figure 5.9). Smaller nematode body size was observed in xylan (*glz1*) and mannan (*msr1*) related mutants but not the *mur3* mutant. Larger female nematodes may produce a higher number of eggs. Smaller size of nematode may also be related to less nutrient flow from plant. The *mur3 and glz1* knockout mutants resulted in decreases in nematode number. Lower nematode numbers could be related to the lower level of early infection of plants or failure to induce a feeding site. The *mur3* and *glz1* mutants also harboured caused fewer and smaller galls (Figure 5.9). Gall size is a representative sign for plant response to the nematode that larger galls may indicate higher level of nutrient flow.

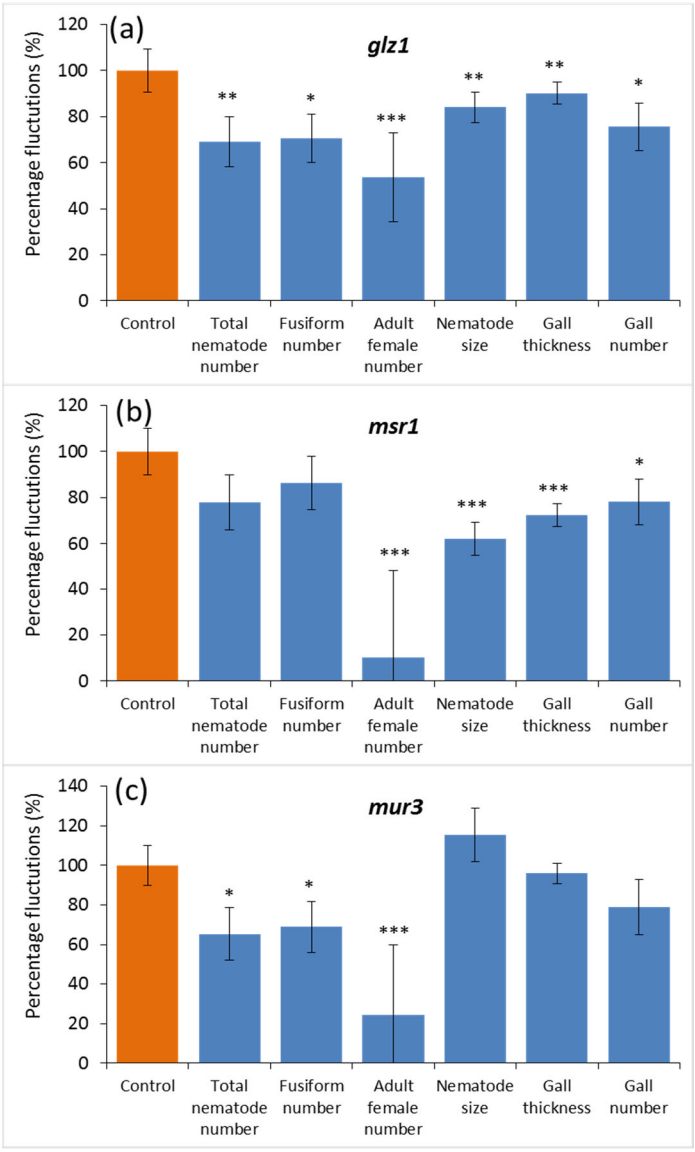

Figure 5.9 The effect of hemicellulose-related cell wall gene knockout on nematode number (total nematode, fusiform, adult female), nematode size, gall thickness and gall number. Nematode and gall parameters in *Arabidopsis thaliana* wild type (Col-0) and cell wall mutants were tested 28 days post infection (dpi) with *M. incognita*. Arabidopsis mutants (blue) were compared to wild type (orange) to calculate percentage fluctuations. Hemicellulose-related gene mutants: (a) *glz1* (xylan-related gene), (b) *msr1* (heteromannan-related gene), (c) *mur3* (xyloglucan-related gene) were represented. Error bars represent standard error of the mean of plants pooled from two independent experiments (n= 33-45 plants for nematode and gall numbers, n= 32 nematodes for measurement of nematode size, n= 30 galls for the measurement of gall thickness). Asterisks characterise statistical significance level: ***P ≤ 0.001; **P ≤ 0.01, *P ≤ 0.05.

5.4.2.2 Role of pectin-related cell wall genes on nematode development and function

Pectin-related cell wall Arabidopsis mutants *qul1, pme31, bgal5, rgxt1, arad1* and *arad2* were tested to check the effect of cell wall genes on nematode development and function. The *pme31* and *qul1* genes have functions related to the homogalacturonan subgroup of pectin but *bgal5, rgxt1, arad1* and *arad2* impact on the rhamnogalacturonan subgroup of pectin. Infection of the *qul1* and *pme31* mutant hosts resulted in no significant changes in any nematode and gall parameters compared to wild type (Figure 5.10 a & b). Similarly, there were no significant differences in *QUL1* and *PME31* gene expression at 7, 14, 21 and 28 dpi based on analysis of the microarray data (Table 5.5). This may suggest that *qul1* and *pme31* genes do not play an important role in nematode development and feeding. Infection of the *bgal5* mutant hosts resulted in a decrease in fusiform and total nematode number, nematode size, gall thickness and gall number but no differences were observed in adult female number (Figure 5.10 c). However, the expression of *bgal5* gene was down-regulated at 21 dpi (Table 5.5).

RHAMNOGALACTURONAN XYLOSYLTRANSFERASE 1 (*RGXT1*) is involved in the biosynthesis of pectic rhamnoglacturonan-II (Egelund et al., 2006). Mutation in the *RGXT1* gene resulted in decrease of adult nematode number, nematode size, gall thickness and gall number but not total or fusiform number (Figure 5.11 a). However, *RGXT1* gene was down-regulated at an early (7 dpi) stage in the nematode feeding site (Table 5.5). The *ARABINAN DEFICIENT 1* gene (*ARAD1*) is involved in arabinan biosynthesis and the mutant plants have reduced arabinose content (Harholt et al., 2006). *ARAD1* and *ARAD2* are localised to the same region of the Golgi (Harholt et al., 2012). The *arad1* and *arad2* mutants each resulted in an increase in total and fusiform nematode numbers, and gall number, however no differences were observed among the adult female number, gall thickness and nematode size (Figure 5.11 b, c). Gene expression analysis of *ARAD1* and *ARAD2* showed them to be up-regulated in nematode-infected roots at 21 dpi and 14 dpi, respectively (Table 5.5).

Overall, there was no consistent pattern in the effects of pectin related mutants on nematode or gall development. Homogalacturonan-related mutants (*qul1* and *pme31*) did not affect either nematode or gall parameters. Galactan and rhamnogalacturonan-

related mutants (*bgal5* and *rgxt1*) had a suppressive effect but gall number was increased in the *arad1* mutant (Figure 5.10 c, 5.11 a, b). The *rgxt1* mutant plants supported fewer female nematodes (Figure 5.11 a) but other pectin-related mutants (*bgal5, qul1, pme31, arad1, arad2*) showed no significant differences in female nematode number compared to wild type plants (Figure 5.10a, b, c and 5.11 b, c). Pectin-related mutants showed both constructive and suppressive effects on gall number. Galactan and rhamnogalacturonan-related mutants (*bgal5* and *rgxt1*) had a suppressive effect on nematode induced gall size and gall number (Figure 5.10 c, 5.11 a).

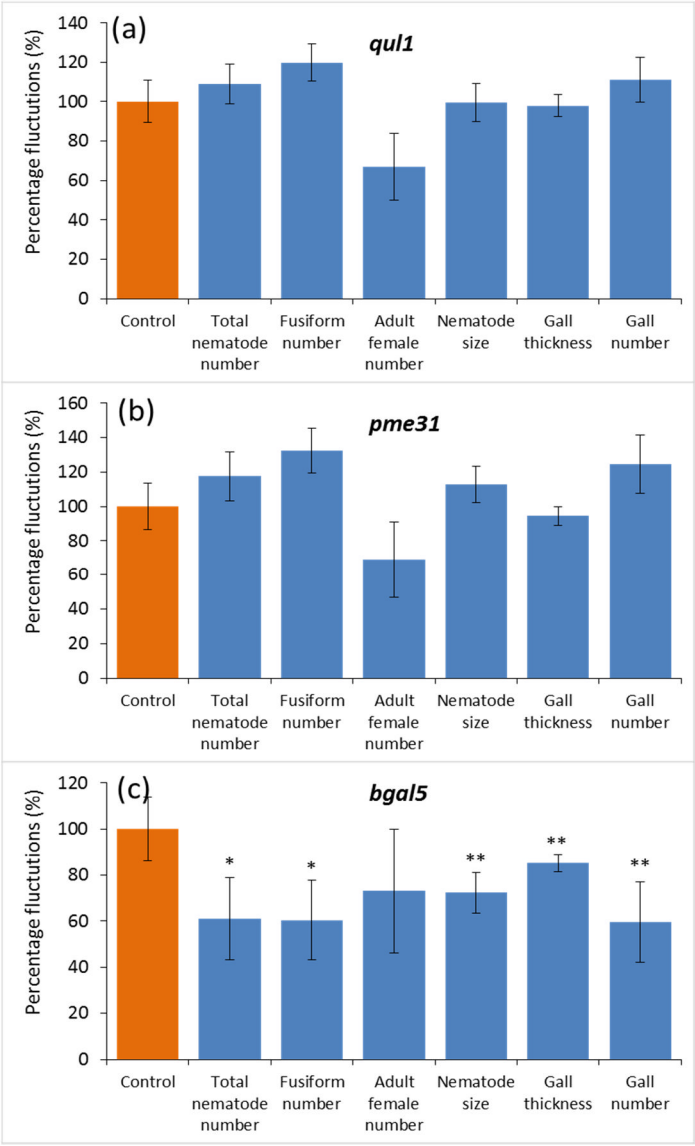

Figure 5.10 The effect of pectin-related cell wall gene knockout on nematode number (total nematode, fusiform, adult female), nematode size, gall thickness and gall number. Nematode and gall parameters in *Arabidopsis thaliana* wild type (Col-0) and cell wall mutants were tested 28 days post infection (dpi) with *M. incognita*. Arabidopsis mutants (blue) were compared to wild type (orange) to calculate percentage fluctuations. Pectin-related gene mutants: (a) *qul1* (homogalacturonan-related gene), (b) *pme31* (pectin methyl esterase-related gene), (c) *bgal5* (galactan-related gene) were represented. Error bars represent standard error of the mean of plants pooled from two independent experiments (n= 39-45 plants for nematode and gall numbers, n= 32 nematodes for measurement of nematode size, n= 30 galls for the measurement of gall thickness). Asterisks characterise statistical significance level: ***P ≤ 0.001; **P ≤ 0.01,*P ≤ 0.05.

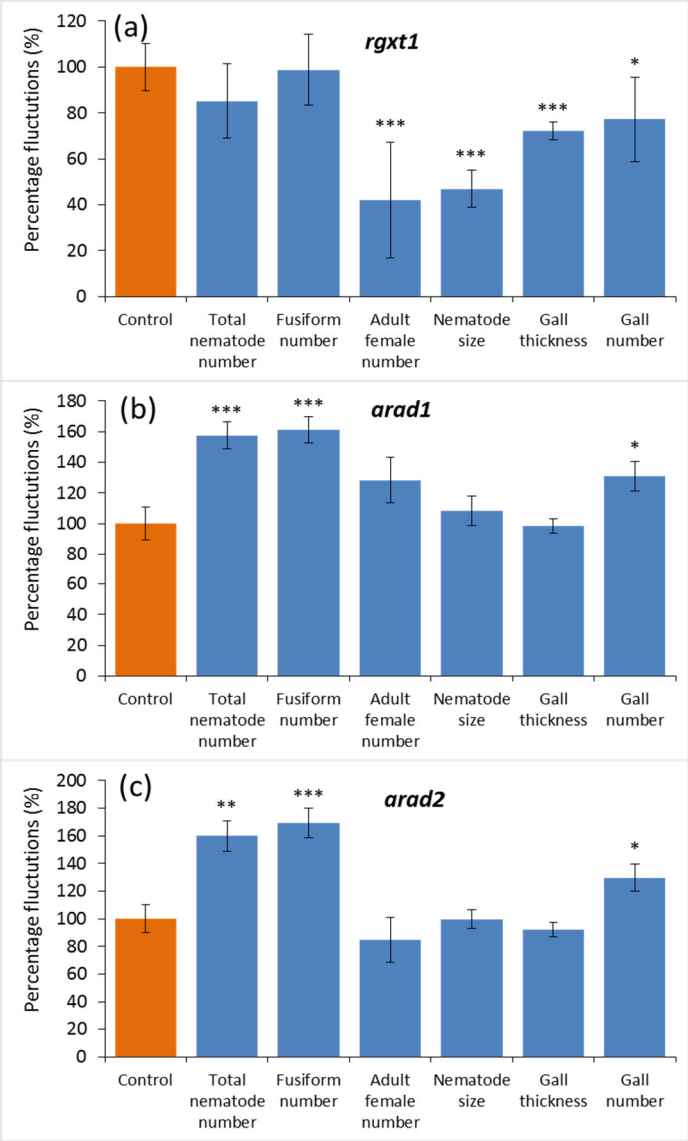

Figure 5.11 The effect of pectin-related cell wall gene knockout on nematode number (total nematode, fusiform, adult female), nematode size, gall thickness and gall number. Nematode and gall parameters in *Arabidopsis thaliana* wild type (Col-0) and cell wall mutants were tested 28 days post infection (dpi) with *M. incognita*. Arabidopsis mutants (blue) were compared to wild type (orange) to calculate percentage fluctuations. Pectin-related gene mutants: (a) *rgxt1* (rhamnogalacturonan-related gene), (b) *arad1* (arabinan-related gene), (c) *arad2* (arabinan-related gene) were represented. Error bars represent standard error of the mean of plants pooled from two independent experiments (n= 44-50 plants for nematode and gall numbers, n= 32 nematodes for measurement of nematode size, n= 30 galls for measurement of gall thickness). Asterisks characterise statistical significance level: ***P ≤ 0.001; **P ≤ 0.01, *P ≤ 0.05.

5.4.2.3 Role of glycoprotein-related cell wall genes in nematode development

Glycoprotein-related cell wall Arabidopsis mutants *agp8, perk10* and *lrx3* were tested to check the effect of these cell wall genes on nematode development. *ARABINOGALACTAN PROTEIN 8* (*AGP8*) encodes an extracellular proteoglycan with a putative role in cell adhesion (Schultz et al., 2000). This AGP-related gene knockout resulted in increased total nematode number, fusiform and adult female number, nematode size and gall number but not gall thickness (Figure 5.12 a). The highest average female number observed in any mutant or wild type plant was in nematode infected *agp8* mutant. The extensin related *perk10* mutant resulted in increased adult female number, nematode size, gall thickness and gall number but no differences were observed in fusiform and total nematode number (Figure 5.12 b). Infection of the mutant *leucine-rich repeat/extensin 3* (*lrx3*) resulted in increase of nematode number (total and fusiform number) but not adult female number, nematode size, gall thickness and gall number (Figure 5.12 c). *AGP8* and *LRX3* genes were both down-regulated at 21 dpi (Table 5.5). Although, the expression of *PROLINE-RICH EXTENSIN-LIKE RECEPTOR KINASE 10* (*PERK10*) was up-regulated in infected roots compared to uninfected root tissues at 14 and 28 dpi (Table 5.5), nematode parameters were also increased (Figure 5.12 b).

In general, glycoprotein-related mutants (*agp8*, *lrx3* and *perk10*) initiated a positive effect on gall number. The *agp8* and perk10 mutants caused a positive effect on nematode size but no significant effect was observed in *lrx3* plants. Adult female numbers were positively affected by the knockout of glycoprotein-related genes but a suppressive effect was found in pectin and hemicellulose-related gene knockouts. Infection of the glycoprotein-related mutants (*agp8* and *perk10*) resulted in increased numbers of adult female but no significant effect was observed in *perk10*. The knockouts of glycoprotein-related mutants (*agp8*, *lrx3* and *perk10*) resulted in no effect on gall thickness (Figure 5.12 a, b, c).

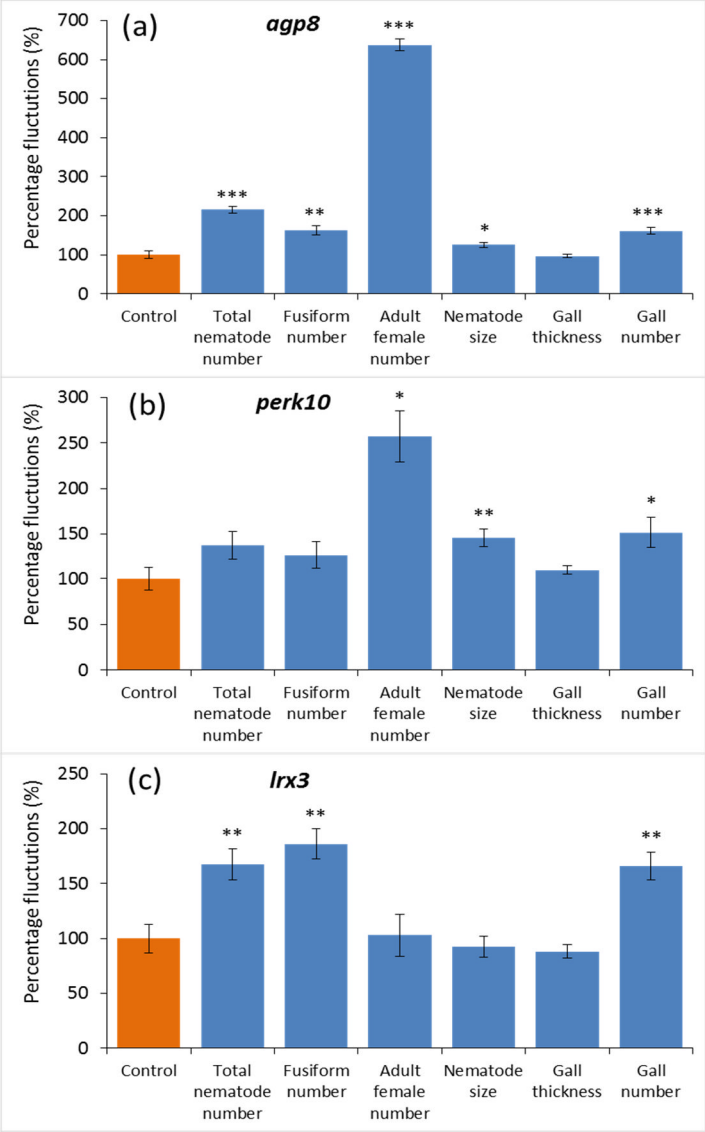

Figure 5.12 The effect of glycoprotein-related cell wall gene knockout on nematode number (total nematode, fusiform, adult female), nematode size, gall thickness and gall number. Nematode and gall parameters in *Arabidopsis thaliana* wild type (Col-0) and cell wall mutants were tested 28 days post infection (dpi) with *M. incognita*. Arabidopsis mutants (blue) were compared to wild type (orange) to calculate percentage fluctuations. Glycoprotein-related gene mutants: (a) *agp8* (arabinogalactan-protein-related gene), (b) *perk10* (extensin-related gene), (c) *lrx3* (extensin-related gene) were represented. Error bars represent standard error of the mean of plants pooled from two independent experiments (n= 39-44 plants for nematode and gall numbers, n= 32 nematodes for measurement of nematode size, n= 30 galls for the measurement of gall thickness). Asterisks characterise statistical significance level: ***$P \leq 0.001$; **$P \leq 0.01$, *$P \leq 0.05$.

Table 5.5 Expression of cell wall genes at 7, 14, 21, 28 days post infection (dpi) and effects of cell wall gene mutants on nematode development and functions

Cell wall components		Cell wall genes	Gene expression*				Nematode, gall numbers and size					
			7 dpi	14 dpi	21 dpi	28 dpi	Female	Fusiform	Total	Nematode size	Gall number	Gall size
Hemicellulose		*GLZ1*	(--)	(--)	(--)	(--)	↓	↓	↓	↓	↓	↓
		MSR1	(--)	(--)	↓	(--)	↓	(--)	(--)	↓	↓	↓
		MUR3	↑	↑	(--)	(--)	↓	↓	↓	(--)	(--)	(--)
Pectin	HG	*QUL1*	(--)	(--)	(--)	(--)	(--)	(--)	(--)	(--)	(--)	(--)
		PME31	(--)	(--)	(--)	(--)	(--)	(--)	(--)	(--)	(--)	(--)
	RG-I	*BGAL5*	(--)	(--)	↓	(--)	(--)	↓	↓	↓	↓	↓
		RGXT1	↓	(--)	(--)	(--)	↓	(--)	(--)	↓	↓	↓
		ARAD1	(--)	(--)	↑	(--)	(--)	↑	↑	(--)	↑	(--)
		ARAD2	(--)	↑	(--)	(--)	(--)	↑	↑	(--)	↑	(--)
Glycoprotein		*AGP8*	(--)	(--)	↓	(--)	↑	↑	↑	↑	↑	(--)
		PERK10	(--)	↑	(--)	↑	↑	(--)	(--)	↑	↑	(--)
		LRX3	(--)	(--)	↓	(--)	(--)	↑	↑	(--)	↑	(--)

(--) Unaffected, ↑ increased, ↓ decreased, RG-I; rhamnogalacturonan-I, HG; homogalacturonan, *; microarray data was taken from Genevestigator and the evaluation was performed based on statistical differences ($P < 0.05$).

5.5 Discussion

5.5.1 Role of cell wall genes in nematode development

5.5.1.1 Hemicellulose-related genes

Glycosyltransferases which are enzymes that establish natural glycosidic linkages are found in plants and play several important roles from polysaccharide synthesis, cell adhesion (Bouton et al., 2002), glycosylation of flavonols (Cui et al., 2016), salicylic acid (Lee and Raskin, 1999) and plant hormones (Indole-3-acetic Acid) (Jackson et al., 2001). The Arabidopsis glycosyltransferase-related gene, *GLZ1,* plays a role in the biosynthesis of xylan and hence cell wall thickening (Lee et al., 2007b). In the present study, infection of the *glz1* mutant resulted in decrease in nematode number, nematode size, gall thickness and gall number (Figure 5.6 a). The *glz1* gene is important for Arabidopsis development and carbohydrate metabolism (Shao et al., 2004).

A linear ß-1,4-linked backbone, mannans are composed of mannosyl residues (Reid, 1985). The mannosyl amount (glucomannans in stems) is decreased by 40% in the *mannan synthesis related 1* (*msr1*) Arabidopsis mutant (Wang et al., 2013). In this study, nematode number, nematode size, gall thickness and gall number were all reduced on the *msr1* mutant plants (Figure 5.6 b). Gene expression was not affected by nematode infection at 7, 14, 28 dpi, however the *MSR1* gene was down-regulated at 21 dpi (Table 5.5). This gene is also down-regulated 48 h after inoculation with *Agrobacterium tumefaciens* (Ditt et al., 2006). The gene expression may be related to compatible plant and nematode interactions.

The disruption of xyloglucan affects cellular processes (Kong et al., 2015). The xyloglucan-related *MUR3* encodes a xyloglucan galactosyltransferase that is evolutionarily conserved amongst plants (Madson et al., 2003). Reactive Oxygen Species (ROS) are involved in abiotic stress and slightly higher levels of ROS are found in *mur3* plants than the wild-type. The increasing level of ROS is related to reducing the cellular damage (Li et al., 2013). The *mur3* mutant also demonstrated resistance against infection with a virulent oomycete pathogen, *Hyaloperonospora parasitica* Noco2 (Tedman-Jones et al., 2008). In this present experiment, xyloglucan-related *mur3* mutant resulted in a decrease in nematode numbers but not nematode size, gall thickness or gall number (Figure 5.6 c). The disruption of cell

wall biosynthesis may trigger plant defence (Tedman-Jones et al., 2008) so decreased nematode numbers may be related to plant defence.
In general, hemicellulose-related gene knockdowns resulted in decreased nematode and gall parameters. This result may be related to the consequence of the disruption of cell wall biosynthesis that may activate plant defence.

5.5.1.2 Pectin-related genes

Pectin consists of a main backbone (galacturonic acid) and can be divided into different groups based on the side chains. Homogalacturonan, rhamnogalacturonan-I, and rhamnogalacturonan-II are sub-groups of pectin in the plant cell wall (Willats et al., 2001b, Harholt et al., 2010, Mohnen, 2008). The pectin-related genes *QUL1* (homogalacturonan related), *PME31* (homogalacturonan related), *BGAL5* (rhamnogalacturonan related), *RGXT1* (rhamnogalacturonan related), *ARAD1* and *ARAD2* (rhamnogalacturonan related) were investigated in this chapter.
Among the sub-groups of pectic polysaccharides, homogalacturonan is a major (65 % of the pectin) component that consists of linear 1,4-linked galacturonic acid backbone (Mohnen, 2008, Harholt et al., 2010). In this study, the *qul1* mutant resulted in no significant changes on nematode and gall parameters. Similarly, *QUL1* gene expression was not affected in nematode infected roots of Arabidopsis at any time point. Pectin methylesterases eliminate methylester groups from homogalacturonan which change cell wall rigidity (Micheli, 2001). The Arabidopsis pectin methylesterase mutant *pme31* had increased susceptibility to *Pseudomonas syringae* (Bethke et al., 2014). However, the *pme31* mutant did not have any impact on nematodes or galls and nematode infection did not alter expression of *PME31*. *PME31* is one of 66 pectin methylesterase genes in Arabidopsis (Louvet et al., 2006). If all 66 genes and mutants could be investigated in relation to *Meloidogyne* infection, that may give a clearer picture of the role of *PME* genes in regulating the high methyl-esterification of pectin found in giant cell walls.
The Arabidopsis gene *BGAL5* encodes a beta-galactosidase (Gantulga et al., 2008) and belongs to the glycoside hydrolase family 35 (Ahn et al., 2007). Seventeen Arabidopsis genes encode putative beta-galactosidases (Chandrasekar and van der Hoorn, 2016). Galactosidases commence RG-I galactan degradation in plant tissues (Willats et al., 2001b). The beta-galactosidase is expressed during stress conditions

in different part of plant organs: root, petiole, rosette, stem, flower, silique and seedlings that may involve in a role of cell wall modification (Gantulga et al., 2008). The protein AtBGAL5 is involved in cell wall changes and trichome development (Albornos et al., 2012). Reduced nematode numbers, nematode size, gall thickness and gall number were observed on *bgal5* mutant plants. Pectic degradation may act as signalling molecules for defence responses (Willats et al., 2001b).

RGXT1 belongs to the glycosyltransferase family-77 in Carbohydrate-Active enZYmes (CAZy). Arabidopsis genes *RGXT1* and *RGXT2* are involved in rhamnogalacturonan synthesis (Egelund et al., 2006). The rhamnogalacturonan-II is a greatly conserved and stable pectic polysaccharide (Willats et al., 2001b). The *rgxt1* mutant resulted in decreased adult female number, nematode size, gall thickness and gall number. *RGXT1* gene expression was down-regulated by nematodes only at 7 dpi but it was not affected at 14, 21 and 28 dpi. These results suggest that rhamnogalacturonan is an important cell wall constituent that contributes to successful nematode development.

Arabinan belongs to the rhamnogalacturonan-I sub-group of pectic polysaccharides. Rhamnogalacturonan-I is a very diverse and complex polysaccharide (Willats et al., 2001b, Caffall and Mohnen, 2009) consisting of a heterogenic structure which carries arabinan and galactan side chains (Caffall and Mohnen, 2009). The *ARAD1* and *ARAD2* genes are involved in arabinan biosynthesis (Harholt et al., 2012). Mutation of the *ARAD1* gene causes reduced arabinose content in leaves and stems (Harholt et al., 2006). Both the *arad1* and *arad2* mutant plants supported higher numbers of nematodes (fusiform and total nematode number). *ARAD1* gene expression (microarray data) was up-regulated at 21 dpi but it was not altered at 7, 14 and 28 dpi whilst *ARAD2* expression was up-regulated only at 14 dpi. The decreasing side-chains of arabinan and galactan in RG-I, and increasing HG-calcium are related to the weakening of the cell wall expansibility and strength. RG-I side chains are also closely related to cell adhesion (Caffall and Mohnen, 2009). The complex arabinan structure affects the mechanical properties in the cell wall during the mechanical stress (Verhertbruggen et al., 2013). In this study, the increased nematode number in arabinan deficient mutants (*arad1* and *arad2*) may be related to nematode-induced altering of cell wall complexity, strength, expansibility and cell adhesion.

In general, pectin-related gene knockdowns resulted in diverse effects on nematode number, gall number, nematode size and gall thickness. This may be related to pectin containing a diverse mixture of side-chains in the different sub-groups of pectic polysaccharides which are involved in changing cell wall structure, either triggering or blocking the signalling plant defence during the nematode infection.

5.5.1.3 Glycoprotein-related genes

Arabinogalactan proteins (AGPs) are complex peptides that consist of protein backbones (short backbones of 10 to 13 amino acid residues) of hydroxyproline, alanine, serine and threonine residues, and are found in the plasma membrane and cell wall (Ellis et al., 2010, Schultz et al., 2000). AGPs are involved in many functions in plants from biotic and abiotic stress, cell death, cell division, cell expansion, plant reproductive and development, cell adhesion (Nothnagel, 1997, Schultz et al., 2000, Schultz et al., 2002, Johnson et al., 2003). Knockout of the *AGP8* gene increased plant susceptibility with increased nematode number, nematode size, gall thickness and gall number. Correspondingly, gene expression was down-regulated at 21 dpi but it was not affected at other time points. The AGPs are triggered in wound-like responses, cell wall thickening and callose synthesis (Guan and Nothnagel, 2004), which may be related to pathogen suppressive effects on nematodes. Therefore, the knockdown of *AGP8* may have resulted in an increase in nematode infection and development due to lack of triggering plant defence.

Extensin-like receptor-like kinases (PERKs) are positively charged with amino acids and found in the external surface of plasma membrane in plant cells (Nakhamchik et al., 2004). The *PERK10* is expressed in roots and negatively affects Arabidopsis root growth (Humphrey et al., 2015). Increased numbers of adult females, nematode size and gall number were observed on *perk10* mutants. However, the gene expression was up-regulated at 14 and 28 dpi. The *PERK1* gene is rapidly induced during wounding in *Brassica napus* (Silva and Goring, 2002). The knock down of *PERK10* gene may result in losing of the signalling for plant defence response. Therefore, *M. incognita* infection was positively affected.

AGPs are involved in root hair development in Arabidopsis (Velasquez et al., 2011). The leucine-rich extensin family is very variable in terms of length and motif organisation. The *LRX3* gene is expressed in all organs of Arabidopsis (Baumberger

et al., 2003) and the *lrx3* mutant resulted in increased fusiform and total nematode number and gall number. However, the gene expression was up-regulated at 21 dpi but it was unaffected at 7, 14 and 28 dpi. It can be concluded from this result that *LRX3,* plays an as yet unidentified role in plant-nematode parasitism.

Extensin is involved in disease and wound responses in which the accumulation of extensin increases (Lamport et al., 2011), and the expression of extensin is induced after pathogen attack (Keller, 1993). Knockdowns of extensin in Arabidopsis may be related to decrease in the plant defence signalling and mechanisms during the nematode infection.

Overall, both extensin and AGP mutants (*agp8*, *perk10* and *lrx3*) resulted in increased plant susceptibility in this study. Cell wall proteins are involved in cell wall extension in Arabidopsis (Irshad et al., 2008). It may be concluded from results of this study that the disruption of cell wall glycoprotein-related genes may be involved in the cell wall extension and signalling of plant defences during the nematode parasitism.

5.6 Overview

- ✓ Microarray data revealed that cell wall genes were differently regulated in nematode infected roots
- ✓ *In situ* analysis revealed that cell wall polysaccharides were less detected in cell walls in the majority of cell wall mutants compared to the Arabidopsis wild type.
- ✓ Cell wall-related mutants of Arabidopsis (*mur3*, *msr1*, *glz1*, *qul1*, *pme31*, *bgal5*, *rgxt1*, *arad1*, *arad2*, *agp8, perk10* and *lrx3*) resulted in increased, decreased and no effect to the nematode number (fusiform, female and total nematode number), nematode size, gall number and gall size.

Chapter 6

General discussion

6 General Discussion

6.1 Pathogen induced galls

Like root-knot nematodes (Perry et al., 2010, Favery et al., 2016a), other plant pathogens including bacteria, fungi (Le Fevre et al., 2015) and insects (Raman, 2011) also cause the formation of galls via hypertrophy and hyperplasia. Galls are abnormally differentiated growths on living organisms (animals or plants) induced by a pathogen or parasite, for their own benefit (Meyer 1987). In this study, abnormal growth in nematode-infected roots of all hosts was observed, although the gall size and gall thickness relative to adjacent root varied on the different host species (aduki bean, maize, Arabidopsis and potato). Pathogen-induced plant galls are often caused by an increase of plant growth hormones, specifically cytokinin and auxin in host cells (Kant and Ramani, 1990). Plant galls which are seen on many plant organs including, roots, shoots, petioles, leaf-blades, flower buds and flowers are induced by different pests and pathogens: bacteria, viruses, fungi, nematodes, insects and mites (Kant and Ramani, 1990). There may be similarities in the structure and formation of galls induced by these different pests and pathogens.

6.2 Plant cell wall interactions with other plant pathogens: fungi, bacteria and insects

Plant pathogens penetrate the plant cell wall either by force, or through wounds and natural openings. Fungi generally enter by natural openings, wounds and forcing, whereas bacteria enter the plant mostly via natural openings (Albersheim et al., 2011). Plant pathogens including insects, bacteria, fungi, nematodes and symbiotic organisms interact first with the cuticle and cell wall (Lionetti and Metraux, 2014). The cuticle consists of cuticular layer and cuticle proper including waxes (aliphatic and cyclic compounds), polyester-type biopolymers and fatty acids (Muller and Riederer, 2005).

6.2.1 Fungal pathogens

Fungi release cutinases and cell-wall degrading enzymes to modify the cuticle and plant cell wall for the production of phytotoxic metabolites which support the fungal penetration (Ferreira et al., 2006). They attack the plant cell wall by releasing the cell wall degrading enzymes (Bellincampi et al., 2014). For example a fungus, *Uromyces*

vicia-fabae (Faba bean rust), releases chitin deacetylase, proteases, acidic celluloses, pectin methylesterases, neutral cellulases, polygalacturonate lyase and amino acid permease during stomatal penetration (Mendgen et al., 1996).

The fungi penetrate the plant cuticle and plant cell wall by an appressorium which is a specialised cell type of fungi used to infect the host (Howard et al., 1991, Ferreira et al., 2006). The penetration stage is crucially important for the successful parasitism of fungi, and they have diverse invasion strategies (Mendgen et al., 1996). Small proteins (Hydrophobins) which are found only in filamentous fungi are secreted from the hyphae and conidial surfaces - they are involved in the interactions between the fungus and its surroundings (Whiteford and Spanu, 2002). More hyphae of *Phytophthora cinnamomi* are found in xylem vessels in secondary cell walls than within primary cell walls in the roots of *Quercus ilex,* and hemibiotrophic parasitism (during the development of haustoria and hyphal accumulations do not give damage to plant cell walls) is seen (Redondo et al., 2015). Our studies show that *M. incognita*-induced giant cell walls lack secondary cell walls (based on lack of xylan binding) and proliferation of xylem vessels was observed surrounding the giant cells in this study (Figure 3.2) – xylem is discrete and not part of the feeding site.

The host plant can respond to fungal infection with changes to its cell walls at the site of invasion. The host constructs a cell wall apposition (CWA) or papilla which is a process of cell wall thickening and it is set in the penetration site of the fungus to be used as a defence line within the cell wall (Collinge, 2009). The papilla consists of many complexes such as phenolic and organic compounds, ROS, callose and protein (Collinge, 2009, Brown et al., 1998) and plays an important resistant role against fungal penetration (Huckelhoven, 2007). However, the role of particular components which are found in the papilla for a successful defence is still uncertain which may be related to the complexity of papilla (Collinge, 2009). There are a number of other cell wall-related aspects of plant defence against fungal pathogens. In addition to CWA, the lignification and thickening of secondary cell walls occur as a plant defence mechanism to fungal penetration (Lionetti and Metraux, 2014). Plants produce inhibitors of the cell wall-degrading enzymes utilised by pathogens, for instance, the xylanase inhibitors TL-XI, TAXI and XIP are produced by the host wheat plant during the release of endoxylanases by a fungal pathogen (Juge, 2006). Cell wall-associated polygalacturonase-inhibiting proteins (PGIPs) counteract the

polygalacturonases (PGs) used by a range of pathogens and insects to degrade homogalacturonan (Spadoni et al., 2006). Damage of the cell wall by the pathogen can trigger signalling pathways to activate the plant defence mechanisms (Bellincampi et al., 2014). This involves the release of oligogalacturonides from partial degradation of homogalacturonan which can then act as elicitors to induce a range of defence responses, probably via recognition by wall-associated kinases (WAKs). The strengthening of plant cell-walls by changes in their composition may be involved in the resistance against plant pathogens, or at least acts to limit the host range among the plant species (Vorwerk et al., 2004, Underwood, 2012). The modifications of polysaccharide components of the cell wall such as remodelling of pectin content/structure, alterations of cell wall result in change in plant resistance to powdery mildew (Vogel et al., 2004, Vogel et al., 2002, Vogel and Somerville, 2000, Schulze-Lefert and Vogel, 2000). Modification of cellular signalling pathways, cell wall strengthening and producing antimicrobial compounds against pathogen secretions are some of the cellular responses during the pathogen attack (Hematy et al., 2009).

6.2.2 Bacterial plant pathogens

Cell walls do not totally isolate cells in that cytoplasmic connections by plasmodesmata, signalling and nutrient exchange occur between them (Lucas et al., 2009). Cell wall local softening occurs during the bacteria attack and softening can involve either cell wall polymer-degradation or cell wall intermolecular interaction-weakening between polysaccharides (Cosgrove, 2000, Rich et al., 2014, Parniske, 2000). They degrade the plant cell wall during infection and growth processes for nutrient uptake (Bellincampi et al., 2014). Bacterial expansins which attach to cellulose and plant cell wall degrading enzymes that solubilise arabinoxylan and homogalacturonan are involved in cell wall loosening (Cosgrove, 2015). We know that homogalacturonan is an important component of *M. incognita* induced giant cell walls and that host expansins play an important role in the formation of the feeding site of a cyst nematode *Heterodera schachtii* (Wieczorek et al., 2006). The genome of *M. incognita* also encodes 20 secreted expansins (Abad et al., 2008) that are likely to play a role in softening the cell wall, maybe to allow easier access to other cell wall hydrolysing enzymes or to facilitate expansion of the giant cells.

Rhizobium spp., which are nitrogen-fixing bacteria termed also root-nodule bacteria result in nodulation in the roots of legumes (*Fabaceae*). The alteration of cell wall molecular architecture and modification of cell morphology accompanies the process of nodule development (Brewin, 2004). The bacteria alter the glycoprotein (arabinogalactan and extensin) glycosylation motifs within the cell walls to induce root nodulations (Brewin, 2004). Similarly, alterations in the amount of AGPs and extensin were observed in the giant cell wall in this study suggesting a similar role for arabinogalactan in host response to a nematode pathogen and a symbiont. The infection thread which is an intracellular tube structure of rhizobial bacteria is embedded in the cell matrix and binds the plant cell wall, and modifies the biosynthesis of the plant cell wall including cellulose or hemicellulose (Brewin, 2004). Similarly, a higher amount of heteromannan (hemicellulose) was observed within the nematode induced galls. Another plant cell wall protein, expansin is involved during the rhizobia inoculation (Giordano and Hirsch, 2004).

Following the pathogen attack, the plant cell wall produces oligosaccharides which trigger plant defences (Hematy et al., 2009). Some Arabidopsis genes necessary for *Agrobacterium tumefaciens* infection have roles related to modification of the synthesis of plant cell wall polysaccharide. For instance, an AGP gene is disrupted in one mutant that displays resistance to bacterial infection and an *Arabidopsis* cellulose synthase-like gene (*CSLA9*) which encodes a putative glycosyltransferase, is also required for infection of *A. tumefaciens* (Zhu et al., 2003). The mechanism behind the observed resistance in the mutants is not known. Knockout of another *AGP* gene in Arabidopsis, *AGP8*, had the opposite effect on nematode infection and increased susceptibility, resulting in a higher infection rate and larger nematodes. This highlights both the variability that can occur in the interactions of different pathogens and the same host plant and also the difficulties in predicting the role of cell-wall related genes when there are large gene families that may have a spectrum of different activities and functions.

Reactive oxygen species (ROS) that are produced by plant cells are involved in several cellular processes, plant-pathogen interactions including plant-bacteria interactions (Baker and Orlandi, 1995). ROS accumulation also occurs during the biotic interactions with symbiotic bacteria (Torres, 2010). The active oxygen induces the strengthening of the plant cell wall during the pathogen infections (Baker and

Orlandi, 1995). Mutations of cellulose synthases (*CESA4*, *CESA7* and *CESA8*) increase the plant resistance to a bacterium *Ralstonia solanacearum* and modify the secondary cell wall (Hernandez-Blanco et al., 2007). The cellulose deficiency enhances the resistance to pathogens including bacteria, and it stimulates Ethylene (ET) and Jasmonic acid (JA) signalling (Hematy et al., 2009).

6.2.3 Insect pests of plants

Some insects species belonging to Diptera, Lepidoptera and Hemiptera (Shorthouse et al., 2005) induce galls that are found on leaves and stems (Maia and Silva, 2016). Insect-induced galls are the result of hyperplasia and hypertrophy that lead to exceptional modifications: abnormal cell wall thickness (thick cell walls in dead cells and thin layered cell walls in living cells) in galls (Raman, 2011). In addition to the cell wall modification, other changes such as developed cytoplasm, uneven vacuoles, hypertrophied nucleus and nucleolus, lavish cell organelles occur within the galls which are the source of increased carbohydrates and lipids, soluble sugars and proteins (Raman, 2011). In this way, the changes induced by the insects are very similar to those induced in nematode feeding cells. Insect infection cause changes in plant cell wall polysaccharide compositions such that pectin and hemicellulose increases but xylose decreases in the gall cell walls induced by *Distylium racemosum* (Konno et al., 2003). Similarly, pectin (homogalacturonan, arabinan, processed arabinan) and hemicellulose (mannan) increased in *M. incognita* induced galls in this study, indicating that pest and pathogens can elicit similar changes in plant cell wall composition. A psyllid *Cardiaspina retator* causes the deformation of cell walls of *Eucalyptus camaldulensis* leaves (Crawford and Zambryski, 2000). The plant cell wall may give a response of strengthening the cell wall via lignification, producing compounds and volatiles as a defence mechanism to inhibit insect feeding (Wielkopolan and Obrepalska-Steplowska, 2016). During the insect attack such as *Daktulosphaira vitifoliae* (Hemiptera: Phylloerida) on *Vitis vinifera*, the plant gives a stress related hypersensitive response including cell apoptosis, increasing of flavonoids and phenolic resources, deteriorated vacuoles, uneven cell walls and irregular cell wall thickening (Raman et al., 2009). Although the exact role of cell wall components is not well understood, some cell wall polysaccharides are involved in plant resistance against pests (Santiago et al., 2013). A resistant cultivar of maize

against *Diatraea grandiosella* and *Spodoptera frugiperda* has a higher level of hemicellulose and fibre in the cell wall, and cellulose amount is negatively correlated with these leaf feeders (Santiago et al., 2013).

In general, findings of this study relating to the modifications of nematode-induced gall and giant cell wall compositions share similarities with the alterations of cell wall compositions induced by other symbionts, pests and pathogens. In relation to plant cell walls there are clearly commonalities across a diverse range of biotrophic interactions with a host plant. These aspects that are shared in many biotrophic interactions that are deleterious to plant health may play an important future role as potential points of action for broad spectrum biotechnological resistance mechanisms.

This work has been conducted with one of the most damaging *Meloidogyne* species, *M. incognita*. This study focussed on developmental changes in the host cell walls due to *Meloidogyne* infection at 21 dpi. The results of this thesis are important for both producing a better understanding of the cell wall composition and related genes are important for the development of nematode feeding sites, as well as their strategic implications: the role they play in nematode resistance may influence biotechnological approaches for future studies.

Determining how *Meloidogyne* species modify cell wall molecular architecture during the development of the feeding site at different time points – induction of giant cells in early infection (1-3 days), and vascularisation of feeding site and nutrient uptake (4-14 days) – would enhance our understanding of giant cell wall development. Furthermore, more than 100 *Meloidogyne* species cause damage in world agriculture and even at the gross morphological level there are differences in the host response to infection. The site of infection in the roots is often different and gall size varies while some *Meloidogyne* species do not lead to the production of galls in the host at all for example, *M. paranaensis* does not cause gall formation in coffee plants (Perry et al., 2010). The false root-knot nematode, *Nacobbus aberrans* produces galls on the roots of their hosts that are similar in appearance to those caused by *Meloidogyne* species, although the actual cells of the feeding site differ in significantly in morphology. Non-nematode plant pathogens also create specialised feeding structures that are similar to those created by *Meloidogyne* – for example root nodules occur on the roots of plants (primarily *Fabaceae*) that associate with

symbiotic nitrogen-fixing bacteria. Therefore, it would be of great interest to reveal the molecular architecture of feeding sites caused by these species as a future study for deeper understanding the functions of cell walls following infection. Such an investigation may point to convergent pathways of evolution and conservation of cell wall alterations across not only genera but of kingdoms.

References

7 References

ABAD, P., FAVERY, B., ROSSO, M. N. & CASTAGNONE-SERENO, P. 2003. Root-knot nematode parasitism and host response: molecular basis of a sophisticated interaction. *Molecular Plant Pathology,* 4**,** 217-224.

ABAD, P., GOUZY, J., AURY, J. M., CASTAGNONE-SERENO, P., DANCHIN, E. G., DELEURY, E., PERFUS-BARBEOCH, L., ANTHOUARD, V., ARTIGUENAVE, F., BLOK, V. C., CAILLAUD, M. C., COUTINHO, P. M., DASILVA, C., DE LUCA, F., DEAU, F., ESQUIBET, M., FLUTRE, T., GOLDSTONE, J. V., HAMAMOUCH, N., HEWEZI, T., JAILLON, O., JUBIN, C., LEONETTI, P., MAGLIANO, M., MAIER, T. R., MARKOV, G. V., MCVEIGH, P., PESOLE, G., POULAIN, J., ROBINSON-RECHAVI, M., SALLET, E., SEGURENS, B., STEINBACH, D., TYTGAT, T., UGARTE, E., VAN GHELDER, C., VERONICO, P., BAUM, T. J., BLAXTER, M., BLEVE-ZACHEO, T., DAVIS, E. L., EWBANK, J. J., FAVERY, B., GRENIER, E., HENRISSAT, B., JONES, J. T., LAUDET, V., MAULE, A. G., QUESNEVILLE, H., ROSSO, M. N., SCHIEX, T., SMANT, G., WEISSENBACH, J. & WINCKER, P. 2008. Genome sequence of the metazoan plant-parasitic nematode *Meloidogyne incognita*. *Nat Biotechnol,* 26**,** 909-15.

AHN, Y. O., ZHENG, M., BEVAN, D. R., ESEN, A., SHIU, S.-H., BENSON, J., PENG, H.-P., MILLER, J. T., CHENG, C.-L., POULTON, J. E. & SHIH, M.-C. 2007. Functional genomic analysis of *Arabidopsis thaliana* glycoside hydrolase family 35. *Phytochemistry,* 68**,** 1510-1520.

ALBERSHEIM, P., AN, J. H., FRESHOUR, G., FULLER, M. S., GUILLEN, R., HAM, K. S., HAHN, M. G., HUANG, J., ONEILL, M., WHITCOMBE, A., WILLIAMS, M. V., YORK, W. S. & DARVILL, A. 1994. Structure and function studies of plant-cell wall polysaccharides. *Biochemical Society Transactions,* 22**,** 374-378.

ALBERSHEIM, P., DARVILL, A., ROBERTS, K., SEDEROFF, R., STAEHELIN, A., ALBERSHEIM, P., DARVILL, A., ROBERTS, K., SEDEROFF, R. & STAEHELIN, A. 2011. *Plant Cell Walls: From Chemistry to Biology*. Garsland Science, New York.

ALBORNOS, L., MARTIN, I., PEREZ, P., MARCOS, R., DOPICO, B. & LABRADOR, E. 2012. Promoter activities of genes encoding beta-galactosidases from Arabidopsis a1 subfamily. *Plant Physiology and Biochemistry,* 60**,** 223-232.

ALONSO, J. M., STEPANOVA, A. N., LEISSE, T. J., KIM, C. J., CHEN, H. M., SHINN, P., STEVENSON, D. K., ZIMMERMAN, J., BARAJAS, P., CHEUK, R., GADRINAB, C., HELLER, C., JESKE, A., KOESEMA, E., MEYERS, C. C., PARKER, H., PREDNIS, L., ANSARI, Y., CHOY, N., DEEN, H., GERALT, M., HAZARI, N., HOM, E., KARNES, M., MULHOLLAND, C., NDUBAKU, R., SCHMIDT, I., GUZMAN, P., AGUILAR-HENONIN, L., SCHMID, M., WEIGEL, D., CARTER, D. E., MARCHAND, T., RISSEEUW, E., BROGDEN, D., ZEKO, A., CROSBY, W. L., BERRY, C. C. & ECKER, J. R. 2003. Genome-wide Insertional mutagenesis of *Arabidopsis thaliana*. *Science,* 301**,** 653-657.

ALTER, O. 2006. Discovery of principles of nature from mathematical modeling of DNA microarray data. *Proceedings of the National Academy of Sciences of the United States of America,* 103**,** 16063-16064.

AREND, M. 2008. Immunolocalization of (1,4)-beta-galactan in tension wood fibers of poplar. *Tree Physiology,* 28**,** 1263-1267.

AZAM, T., HISAMUDDIN, SINGH, S. & ROBAB, M. I. 2011. Effect of different inoculum levels of *Meloidogyne incognita* on growth and yield of *Lycopersicon esculentum*, and internal structure of infected root. *Archives of Phytopathology and Plant Protection,* 44**,** 1829-1839.

BAKER, C. J. & ORLANDI, E. W. 1995. Active oxygen in plant pathogenesis. *Annual Review of Phytopathology,* 33**,** 299-321.

BARTLEM, D. G., JONES, M. G. K. & HAMMES, U. Z. 2014. Vascularization and nutrient delivery at root-knot nematode feeding sites in host roots. *Journal of Experimental Botany,* 65**,** 1789-1798.

BASU, S., OMADJELA, O., GADDES, D., TADIGADAPA, S., ZIMMER, J. & CATCHMARK, J. M. 2016. Cellulose microfibril formation by surface-tethered cellulose synthase enzymes. *Acs Nano,* 10**,** 1896-1907.

BAUMBERGER, N., DOESSEGER, B., GUYOT, R., DIET, A., PARSONS, R. L., CLARK, M. A., SIMMONS, M. P., BEDINGER, P., GOFF, S. A., RINGLI, C. & KELLER, B. 2003. Whole-genome comparison of leucine-rich repeat extensins in Arabidopsis and rice. A conserved family of cell wall proteins form a vegetative and a reproductive clade. *Plant Physiology,* 131**,** 1313-1326.

BELLINCAMPI, D., CERVONE, F. & LIONETTI, V. 2014. Plant cell wall dynamics and wall-related susceptibility in plant-pathogen interactions. *Frontiers in plant science,* 5**,** 228-228.

BERG, R. H., FESTER, T. & TAYLOR, C. G. 2009. Cell Biology of Plant Nematode Parasitism. *In:* BERG, R. H. & TAYLOR, C. G. (eds.) *Cell Biology of Plant Nematode Parasitism.*

BETHKE, G., GRUNDMAN, R. E., SREEKANTA, S., TRUMAN, W., KATAGIRI, F. & GLAZEBROOK, J. 2014. Arabidopsis PECTIN METHYLESTERASEs Contribute to Immunity against *Pseudomonas syringae*. *Plant Physiology,* 164**,** 1093-1107.

BIDHENDI, A. J. & GEITMANN, A. 2016. Relating the mechanics of the primary plant cell wall to morphogenesis. *Journal of Experimental Botany,* 67**,** 449-461.

BIRD, A. F. & BIRD, J. 1991. *The structure of nematodes,* London and New York, Academic Press.

BIRD, D. M. 1996. Manipulation of host gene expression by root-knot nematodes. *Journal of Parasitology,* 82**,** 881-888.

BIRD, D. M. & KALOSHIAN, I. 2003. Are roots special? Nematodes have their say. *Physiological and Molecular Plant Pathology,* 62**,** 115-123.

BIRD, D. M., WILLIAMSON, V. M., ABAD, P., MCCARTER, J., DANCHIN, E. G., CASTAGNONE-SERENO, P. & OPPERMAN, C. H. 2009. The genomes of root-knot nematodes. *Annu Rev Phytopathol,* 47**,** 333-51.

BOUTON, S., LEBOEUF, E., MOUILLE, G., LEYDECKER, M. T., TALBOTEC, J., GRANIER, F., LAHAYE, M., HOFTE, H. & TRUONG, H. N. 2002. Quasimodo1 encodes a putative membrane-bound glycosyltransferase required for normal pectin synthesis and cell adhesion in Arabidopsis. *Plant Cell,* 14**,** 2577-2590.

BOWLES, D. J. & NORTHCOTE, D. H. 1976. Size and distribution of polysaccharides during their synthesis within membrane system of maize root cells. *Planta,* 128**,** 101-106.

BRADLEY, D. J., KJELLBOM, P. & LAMB, C. J. 1992. Elicitor-induced and wound-induced oxidative cross-linking of a proline-rich plant-cell wall protein - a novel, rapid defense response. *Cell,* 70**,** 21-30.

BREWIN, N. J. 2004. Plant cell wall remodelling in the rhizobium-legume symbiosis. *Critical Reviews in Plant Sciences,* 23**,** 293-316.

BRISSON, L. F., TENHAKEN, R. & LAMB, C. 1994. Function of oxidative cross-linking of cell-wall structural proteins in plant-disease resistance. *Plant Cell,* 6**,** 1703-1712.

BROWN, I., TRETHOWAN, J., KERRY, M., MANSFIELD, J. & BOLWELL, G. P. 1998. Localization of components of the oxidative cross-linking of glycoproteins and of callose synthesis in papillae formed during the interaction between non-pathogenic strains of *Xanthomonas campestris* and French bean mesophyll cells. *Plant Journal,* 15**,** 333-343.

BROWN, P. O. & BOTSTEIN, D. 1999. Exploring the new world of the genome with DNA microarrays. *Nature Genetics,* 21**,** 33-37.

BROWN, R. M. 2004. Cellulose structure and biosynthesis: What is in store for the 21st century? *Journal of Polymer Science Part a-Polymer Chemistry,* 42**,** 487-495.

BURKHART, C. N. & BURKHART, C. G. 2005. Assessment of frequency, transmission, and genitourinary complications of enterobiasis (pinworms). *International Journal of Dermatology,* 44**,** 837-840.

CAFFALL, K. H. & MOHNEN, D. 2009. The structure, function, and biosynthesis of plant cell wall pectic polysaccharides. *Carbohydrate Research,* 344**,** 1879-1900.

CAILLAUD, M. C., DUBREUIL, G., QUENTIN, M., PERFUS-BARBEOCH, L., LECORNTE, P., ENGLER, J. D., ABAD, P., ROSSO, M. N. & FAVERY, B. 2008. Root-knot nematodes manipulate plant cell functions during a compatible interaction. *Journal of Plant Physiology,* 165**,** 104-113.

CARPITA, N., TIERNEY, M. & CAMPBELL, M. 2001. Molecular biology of the plant cell wall: searching for the genes that define structure, architecture and dynamics. *Plant Molecular Biology,* 47**,** 1-5.

CARPITA, N. C. 1996. Structure and biogenesis of the cell walls of grasses. *Annual Review of Plant Physiology and Plant Molecular Biology,* 47**,** 445-476.

CASSAB, G. I. 1998. Plant cell wall proteins. *Annual Review of Plant Physiology and Plant Molecular Biology,* 49**,** 281-309.

CAVALIER, D. M., LEROUXEL, O., NEUMETZLER, L., YAMAUCHI, K., REINECKE, A., FRESHOUR, G., ZABOTINA, O. A., HAHN, M. G., BURGERT, I., PAULY, M., RAIKHEL, N. V. & KEEGSTRA, K. 2008. Disrupting two *Arabidopsis thaliana* xylosyltransferase genes results in plants deficient in xyloglucan, a major primary cell wall component. *Plant Cell,* 20**,** 1519-1537.

CHANDRASEKAR, B. & VAN DER HOORN, R. A. L. 2016. Beta galactosidases in Arabidopsis and tomato - a mini review. *Biochemical Society Transactions,* 44**,** 150-158.

CHANLIAUD, E., DE SILVA, J., STRONGITHARM, B., JERONIMIDIS, G. & GIDLEY, M. J. 2004. Mechanical effects of plant cell wall enzymes on cellulose/xyloglucan composites. *Plant Journal,* 38**,** 27-37.

CHRISTIAENS, S., VAN BUGGENHOUT, S., VANDEVENNE, E., JOLIE, R., VAN LOEY, A. M. & HENDRICKX, M. E. 2011. Towards a better understanding of the pectin structure-function relationship in broccoli during processing: Part II - Analyses with anti-pectin antibodies. *Food Research International,* 44**,** 2896-2906.

CLAUSEN, M. H., RALET, M. C., WILLATS, W. G. T., MCCARTNEY, L., MARCUS, S. E., THIBAULT, J. F. & KNOX, J. P. 2004. A monoclonal antibody to feruloylated-(1 -> 4)-beta-D-galactan. *Planta,* 219**,** 1036-1041.

CLAUSEN, M. H., WILLATS, W. G. T. & KNOX, J. P. 2003. Synthetic methyl hexagalacturonate hapten inhibitors of antihomogalacturonan monoclonal antibodies LM7, JIM5 and JIM7. *Carbohydrate Research,* 338**,** 1797-1800.

COLLINGE, D. B. 2009. Cell wall appositions: the first line of defence. *Journal of Experimental Botany,* 60**,** 351-352.

CONSORTIUM, C. E. S. 1998. Genome sequence of the nematode *C-elegans*: A platform for investigating biology. *Science,* 282**,** 2012-2018.

COSGROVE, D. J. 1998. Cell wall loosening by expansins. *Plant Physiology,* 118**,** 333-339.

COSGROVE, D. J. 2000. Loosening of plant cell walls by expansins. *Nature,* 407**,** 321-326.

COSGROVE, D. J. 2005. Growth of the plant cell wall. *Nature Reviews Molecular Cell Biology,* 6**,** 850-861.

COSGROVE, D. J. 2014. Re-constructing our models of cellulose and primary cell wall assembly. *Current Opinion in Plant Biology,* 22**,** 122-131.

COSGROVE, D. J. 2015. Plant expansins: diversity and interactions with plant cell walls. *Current Opinion in Plant Biology,* 25**,** 162-172.

COSGROVE, D. J. & JARVIS, M. C. 2012. Comparative structure and biomechanics of plant primary and secondary cell walls. *Frontiers in Plant Science,* 3.

COTTON, J. A., LILLEY, C. J., JONES, L. M., KIKUCHI, T., REID, A. J., THORPE, P., TSAI, I. J., BEASLEY, H., BLOK, V., COCK, P. J. A., EVES-VAN DEN AKKER, S., HOLROYD, N., HUNT, M., MANTELIN, S., NAGHRA, H., PAIN, A., PALOMARES-RIUS, J. E., ZAROWIECKI, M., BERRIMAN, M., JONES, J. T. & URWIN, P. E. 2014. The genome and life-stage specific transcriptomes of *Globodera pallida* elucidate key aspects of plant parasitism by a cyst nematode. *Genome Biology,* 15.

CRAWFORD, K. M. & ZAMBRYSKI, P. C. 2000. Subcellular localization determines the availability of non-targeted proteins to plasmodesmatal transport. *Current Biology,* 10**,** 1032-1040.

CUI, L. L., YAO, S. B., DAI, X. L., YIN, Q. G., LIU, Y. J., JIANG, X. L., WU, Y. H., QIAN, Y. M., PANG, Y. Z., GAO, L. P. & XIA, T. 2016. Identification of UDP-glycosyltransferases involved in the biosynthesis of astringent taste compounds in tea (*Camellia sinensis*). *Journal of Experimental Botany,* 67**,** 2285-2297.

CURTIS, R. H. C. 2008. Plant-nematode interactions: Environmental signals detected by the nematode's chemosensory organs control changes in the surface cuticle and behaviour. *Parasite-Journal De La Societe Francaise De Parasitologie,* 15**,** 310-316.

CURTIS, R. H. C., ROBINSON, A. F. & PERRY, R. N. 2010. Hatch and Host Location. *Root-Knot Nematodes***,** 139-162.

DAVIES, L. J., LILLEY, C. J., KNOX, J. P. & URWIN, P. E. 2012. Syncytia formed by adult female *Heterodera schachtii* in *Arabidopsis thaliana* roots have a distinct cell wall molecular architecture. *New Phytologist,* 196**,** 238-246.

DAVIS, E. L., HUSSEY, R. S. & BAUM, T. J. 2004. Getting to the roots of parasitism by nematodes. *Trends in Parasitology,* 20**,** 134-141.

DE ALMEIDA ENGLER, J. & GHEYSEN, G. 2013. Nematode-induced endoreduplication in plant host cells: why and how? *Molecular plant-microbe interactions : MPMI,* 26**,** 17-24.

DE SMET, I., LAU, S., VOSS, U., VANNESTE, S., BENJAMINS, R., RADEMACHER, E. H., SCHLERETH, A., DE RYBEL, B., VASSILEVA, V., GRUNEWALD, W., NAUDTS, M., LEVESQUE, M. P., EHRISMANN, J. S., INZE, D., LUSCHNIG, C., BENFEY, P. N., WEIJERS, D., VAN MONTAGU, M. C. E., BENNETT, M. J., JUERGENS, G. & BEECKMAN, T. 2010. Bimodular auxin response controls organogenesis in Arabidopsis. *Proceedings of the National Academy of Sciences of the United States of America,* 107**,** 2705-2710.

DECRAEMER, W. & GERAERT, E. 2006. Ectoparasitic Nematodes. *Plant Nematology***,** 153-184.

DECRAEMER, W. & HUNT, D. J. 2006. Structure and Classification. *Plant Nematology***,** 3-32.

DEEPAK, S., SHAILASREE, S., KINI, R. K., MUCK, A., MITHOFER, A. & SHETTY, S. H. 2010. Hydroxyproline-rich Glycoproteins and Plant Defence. *Journal of Phytopathology,* 158**,** 585-593.

DIOGO, R. V. C. & WYDRA, K. 2007. Silicon-induced basal resistance in tomato against Ralstonia solanacearum is related to modification of pectic cell wall polysaccharide structure. *Physiological and Molecular Plant Pathology,* 70**,** 120-129.

DITT, R. F., KERR, K. F., DE FIGUEIREDO, P., DELROW, J., COMAI, L. & NESTER, E. W. 2006. The Arabidopsis thaliana transcriptome in response to *Agrobacterium tumefaciens*. *Molecular Plant-Microbe Interactions,* 19**,** 665-681.

DRAEGER, C., FABRICE, T. N., GINEAU, E., MOUILLE, G., KUHN, B. M., MOLLER, I., ABDOU, M.-T., FREY, B., PAULY, M., BACIC, A. & RINGLI, C. 2015. Arabidopsis leucine-rich repeat extensin (LRX) proteins modify cell wall composition and influence plant growth. *Bmc Plant Biology,* 15.

DUNCAN, L. W. & MOENS, M. 2006. Migratory Endoparasitic Nematodes. *Plant Nematology***,** 123-152.

EGELUND, J., PETERSEN, B. L., MOTAWIA, M. S., DAMAGER, I., FAIK, A., OLSEN, C. E., ISHII, T., CLAUSEN, H., ULVSKOV, P. & GESHI, N. 2006. Arabidopsis thaliana RGXT1 and RGXT2 encode Golgi-localized (1,3)-alpha-D-xylosyltransferases involved in the synthesis of pectic rhamnogalacturonan-II. *Plant Cell,* 18**,** 2593-2607.

ELLING, A. A. 2013. Major emerging problems with minor *Meloidogyne* species. *Phytopathology,* 103**,** 1092-1102.

ELLIS, M., EGELUND, J., SCHULTZ, C. J. & BACIC, A. 2010. Arabinogalactan-Proteins: Key regulators at the cell surface? *Plant Physiology,* 153**,** 403-419.

ENDO, B. Y. & WERGIN, W. P. 1973. Ultrastructural investigation of clover roots during early stages of infection by root-knot nematode, *Meloidogyne-incognita*. *Protoplasma,* 78**,** 365-379.

ENGVALL, E. & PERLMANN, P. 1972. Enzyme-linked immunosorbent assay, elisa .3. Quantitation of specific antibodies by enzyme-labeled anti-immunoglobulin in antigen-coated tubes. *Journal of Immunology,* 109**,** 129.

EO, J., NAKAMOTO, T. N., OTOBE, K. & MIZUKUBO, T. M. 2007. The role of pore size on the migration of *Meloidogyne incognita* juveniles under different tillage systems. *Nematology,* 9**,** 751-758.

ESQUERRETUGAYE, M. T., LAFITTE, C., MAZAU, D., TOPPAN, A. & TOUZE, A. 1979. Cell-surfaces in plant-microorganism interactions .2. Evidence for the accumulation of hydroxyproline-rich glycoproteins in the cell-wall of diseased plants as a defense-mechanism. *Plant Physiology,* 64**,** 320-326.

FAVERY, B., QUENTIN, M., JAUBERT-POSSAMAI, S. & ABAD, P. 2016. Gall-forming root-knot nematodes hijack key plant cellular functions to induce multinucleate and hypertrophied feeding cells. *J Insect Physiol,* 84**,** 60-9.

FERREIRA, R. B., MONTEIRO, S., FREITAS, R., SANTOS, C. N., CHEN, Z. J., BATISTA, L. M., DUARTE, J., BORGES, A. & TEIXEIRA, A. R. 2006. Fungal pathogens: The battle for plant infection. *Critical Reviews in Plant Sciences,* 25**,** 505-524.

FORBES, L. B. 2000. The occurrence and ecology of Trichinella in marine mammals. *Veterinary Parasitology,* 93**,** 321-334.

FORTNUM, B. A., KASPERBAUER, M. J., HUNT, P. G. & BRIDGES, W. C. 1991. Biomass partitioning in tomato plants infected with *Meloidogyne incognita*. *Journal of Nematology,* 23**,** 291-297.

FOSU-NYARKO, J., NICOL, P., NAZ, F., GILL, R. & JONES, M. G. K. 2016. Analysis of the Transcriptome of the Infective Stage of the Beet Cyst Nematode, *H. schachtii*. *PLoS One,* 11.

FUENTES, S., PIRES, N. & OSTERGAARD, L. 2010. A clade in the QUASIMODO2 family evolved with vascular plants and supports a role for cell wall composition in adaptation to environmental changes. *Plant Molecular Biology,* 73**,** 605-615.

FULLER, V. L., LILLEY, C. J., ATKINSON, H. J. & URWIN, P. E. 2007. Differential gene expression in Arabidopsis following infection by plant-parasitic nematodes *Meloidogyne incognita* and *Heterodera schachtii*. *Molecular Plant Pathology,* 8**,** 595-609.

GANTULGA, D., TURAN, Y., BEVAN, D. R. & ESEN, A. 2008. The Arabidopsis At1g45130 and At3g52840 genes encode beta-galactosidases with activity toward cell wall polysaccharides. *Phytochemistry,* 69**,** 1661-1670.

GAO, M. G. & SHOWALTER, A. M. 1999. Yariv reagent treatment induces programmed cell death in Arabidopsis cell cultures and implicates arabinogalactan protein involvement. *Plant Journal,* 19**,** 321-331.

GESHI, N., JORGENSEN, B. & ULVSKOV, P. 2004. Subcellular localization and topology of beta(1 -> 4)galactosyltransferase that elongates beta(1 -> 4)galactan side chains in rhamnogalacturonan I in potato. *Planta,* 218**,** 862-868.

GHEYSEN, G. & MITCHUM, M. G. 2009. Molecular Insights in the Susceptible Plant Response to Nematode Infection. *In:* BERG, R. H. & TAYLOR, C. G. (eds.) *Plant Cell Monographs.*

GINZINGER, D. G. 2002. Gene quantification using real-time quantitative PCR: An emerging technology hits the mainstream. *Experimental Hematology,* 30**,** 503-512.

GIORDANO, W. & HIRSCH, A. M. 2004. The expression of MaEXP1, a Melilotus alba expansin gene, is upregulated during the sweetclover-Sinorhizobium meliloti interaction. *Molecular Plant-Microbe Interactions,* 17**,** 613-622.

GIRAULT, R., HIS, I., ANDEME-ONZIGHI, C., DRIOUICH, A. & MORVAN, C. 2000. Identification and partial characterization of proteins and proteoglycans encrusting the secondary cell walls of flax fibres. *Planta,* 211**,** 256-264.

GIRON, D., HUGUET, E., STONE, G. N. & BODY, M. 2016. Insect-induced effects on plants and possible effectors used by galling and leaf-mining insects to manipulate their host-plant. *Journal of Insect Physiology,* 84**,** 70-89.

GLAZER, I., ORION, D. & APELBAUM, A. 1983. Interrelationships between ethylene production, gall formation, and root-knot nematode development in tomato plants infected with *Meloidogyne javanica*. *Journal of Nematology,* 15**,** 539-544.

GLICKMANN, E., GARDAN, L., JACQUET, S., HUSSAIN, S., ELASRI, M., PETIT, A. & DESSAUX, Y. 1998. Auxin production is a common feature of most pathovars of *Pseudomonas syringae*. *Molecular Plant-Microbe Interactions,* 11**,** 156-162.

GLUSHKA, J. N., TERRELL, M., YORK, W. S., O'NEILL, M. A., GUCWA, A., DARVILL, A. G., ALBERSHEIM, P. & PRESTEGARD, J. H. 2003. Primary structure of the 2-O-methyl-alpha-L-fucose-containing side chain of the pectic polysaccharide, rhamnogalacturonan II. *Carbohydrate Research,* 338**,** 341-352.

GOETHALS, K., VEREECKE, D., JAZIRI, M., VAN MONTAGU, M. & HOLSTERS, M. 2001. Leafy gall formation by *Rhodococcus fascians*. *Annual Review of Phytopathology,* 39**,** 27-52.

GORSHKOVA, T. A., MIKSHINA, P. V., IBRAGIMOVA, N. N., MOKSHINA, N. E., CHERNOVA, T. E., GURJANOV, O. P. & CHEMIKOSOVA, S. B. 2009. Pectins in secondary cell walls: modifications during cell wall assembly and maturation. *Pectins and Pectinases***,** 149-165.

GUAN, Y. & NOTHNAGEL, E. A. 2004. Binding of arabinogalactan proteins by Yariv phenylglycoside triggers wound-like responses in Arabidopsis cell cultures. *Plant Physiology,* 135**,** 1346-1366.

GUILLEMIN, F., GUILLON, F., BONNIN, E., DEVAUX, M. F., CHEVALIER, T., KNOX, J. P., LINERS, F. & THIBAULT, J. F. 2005. Distribution of pectic epitopes in cell walls of the sugar beet root. *Planta,* 222**,** 355-371.

HAEGEMAN, A., MANTELIN, S., JONES, J. T. & GHEYSEN, G. 2012. Functional roles of effectors of plant-parasitic nematodes. *Gene,* 492**,** 19-31.

HAMANN, T. 2015. The plant cell wall integrity maintenance mechanism - A case study of a cell wall plasma membrane signaling network. *Phytochemistry,* 112**,** 100-109.

HAMMES, U. Z., SCHACHTMAN, D. P., BERG, R. H., NIELSEN, E., KOCH, W., MCINTYRE, L. M. & TAYLOR, C. G. 2005. Nematode-induced changes of transporter gene expression in Arabidopsis roots. *Molecular Plant-Microbe Interactions,* 18**,** 1247-1257.

HARHOLT, J., JENSEN, J. K., SORENSEN, S. O., ORFILA, C., PAULY, M. & SCHELLER, H. V. 2006. ARABINAN DEFICIENT 1 is a putative arabinosyltransferase involved in biosynthesis of pectic arabinan in Arabidopsis. *Plant Physiology,* 140**,** 49-58.

HARHOLT, J., SUTTANGKAKUL, A. & SCHELLER, H. V. 2010. Biosynthesis of pectin. *Plant Physiology,* 153**,** 384-395.

HARHOLT, J., JENSEN, J. K., VERHERTBRUGGEN, Y., SOGAARD, C., BERNARD, S., NAFISI, M., POULSEN, C. P., GESHI, N., SAKURAGI, Y., DRIOUICH, A., KNOX, J. P. & SCHELLER, H. V. 2012. ARAD proteins associated with pectic arabinan biosynthesis form complexes when transiently overexpressed in planta. *Planta,* 236**,** 115-128.

HAYASHI, T. 1989. Xyloglucans in the primary-cell wall. *Annual Review of Plant Physiology and Plant Molecular Biology,* 40**,** 139-168.

HEMATY, K., CHERK, C. & SOMERVILLE, S. 2009. Host-pathogen warfare at the plant cell wall. *Current Opinion in Plant Biology,* 12**,** 406-413.

HEREDIA, A., JIMENEZ, A. & GUILLEN, R. 1995. Composition of plant-cell walls. *Zeitschrift Fur Lebensmittel-Untersuchung Und-Forschung,* 200**,** 24-31.

HERNANDEZ-BLANCO, C., FENG, D. X., HU, J., SANCHEZ-VALLET, A., DESLANDES, L., LLORENTE, F., BERROCAL-LOBO, M., KELLER, H., BARLET, X., SANCHEZ-RODRIGUEZ, C., ANDERSON, L. K., SOMERVILLE, S., MARCO, Y. & MOLINA, A. 2007. Impairment of cellulose synthases required for Arabidopsis secondary cell wall formation enhances disease resistance. *Plant Cell,* 19**,** 890-903.

HERNANDEZ-GOMEZ, M. C., RUNAVOT, J.-L., GUO, X., BOUROT, S., BENIANS, T. A. S., WILLATS, W. G. T., MEULEWAETER, F. & KNOX, J. P. 2015. Heteromannan and Heteroxylan Cell Wall Polysaccharides Display Different Dynamics During the Elongation and Secondary Cell Wall Deposition Phases of Cotton Fiber Cell Development. *Plant and Cell Physiology,* 56**,** 1786-1797.

HERVÉ, C., MARCUS, S. E. & KNOX, J. P. 2011. Monoclonal Antibodies, Carbohydrate-binding modules, and the detection of polysaccharides in plant cell walls. *In:* POPPER, Z. A. (ed.) *Plant Cell Wall: Methods and Protocols.*

HEWEZI, T., HOWE, P., MAIER, T. R., HUSSEY, R. S., MITCHUM, M. G., DAVIS, E. L. & BAUM, T. J. 2008. Cellulose binding protein from the parasitic nematode *Heterodera schachtii* interacts with arabidopsis pectin methylesterase: Cooperative cell wall modification during parasitism. *Plant Cell,* 20**,** 3080-3093.

HIRSINGER, C., PARMENTIER, Y., DURR, A., FLECK, J. & JAMET, E. 1997. Characterization of a tobacco extensin gene and regulation of its gene family in healthy plants and under various stress conditions. *Plant Molecular Biology,* 33**,** 279-289.

HIRST, S. I. & STAPLEY, L. A. 2000. Parasitology: The dawn of a new millennium. *Parasitology Today,* 16**,** 321-321.

HOFMANN, J., YOUSSEF-BANORA, M., DE ALMEIDA-ENGLER, J. & GRUNDLER, F. M. W. 2010. The role of callose deposition along plasmodesmata in nematode feeding sites. *Molecular Plant-Microbe Interactions,* 23**,** 549-557.

HOPE, I. A. 1999. *C. elegans A Practical Approach,* Oxford, Oxford University press, Oxford.

HOWARD, R. J., FERRARI, M. A., ROACH, D. H. & MONEY, N. P. 1991. Penetration of hard substrates by a fungus employing enormous turgor pressures. *Proceedings of the National Academy of Sciences of the United States of America,* 88**,** 11281-11284.

HRUBA, P., HONYS, D., TWELL, D., CAPKOVA, V. & TUPY, J. 2005. Expression of beta-galactosidase and beta-xylosidase genes during microspore and pollen development. *Planta,* 220**,** 931-940.

HUCKELHOVEN, R. 2007. Cell wall - Associated mechanisms of disease resistance and susceptibility. *Annual Review of Phytopathology.*

HUMPHREY, T. V., HAASEN, K. E., ALDEA-BRYDGES, M. G., SUN, H., ZAYED, Y., INDRIOLO, E. & GORING, D. R. 2015. PERK-KIPK-KCBP signalling negatively regulates root growth in Arabidopsis thaliana. *Journal of Experimental Botany,* 66**,** 71-83.

HUTANGURA, P., MATHESIUS, U., JONES, M. G. K. & ROLFE, B. G. 1999. Auxin induction is a trigger for root gall formation caused by root-knot nematodes in white clover and is associated with the activation of the flavonoid pathway. *Australian Journal of Plant Physiology,* 26**,** 221-231.

IRSHAD, M., CANUT, H., BORDERIES, G., PONT-LEZICA, R. & JAMET, E. 2008. A new picture of cell wall protein dynamics in elongating cells of Arabidopsis thaliana: Confirmed actors and newcomers. *Bmc Plant Biology,* 8.

ITO, S., SUZUKI, Y., MIYAMOTO, K., UEDA, J. & YAMAGUCHI, I. 2005. AtFLA11, a fasciclin-like arabinogalactan-protein, specifically localized in screlenchyma cells. *Bioscience Biotechnology and Biochemistry,* 69**,** 1963-1969.

JACKSON, R. G., LIM, E. K., LI, Y., KOWALCZYK, M., SANDBERG, G., HOGGETT, J., ASHFORD, D. A. & BOWLES, D. J. 2001. Identification and biochemical characterization of an Arabidopsis indole-3-acetic acid glucosyltransferase. *Journal of Biological Chemistry,* 276**,** 4350-4356.

JAMET, E., CANUT, H., BOUDART, G. & PONT-LEZICA, R. F. 2006. Cell wall proteins: a new insight through proteomics. *Trends in Plant Science,* 11**,** 33-39.

JOHNSON, K. L., JONES, B. J., BACIC, A. & SCHULTZ, C. J. 2003. The fasciclin-like arabinogalactan proteins of arabidopsis. A multigene family of putative cell adhesion molecules. *Plant Physiology,* 133**,** 1911-1925.

JONES, J. T., HAEGEMAN, A., DANCHIN, E. G. J., GAUR, H. S., HELDER, J., JONES, M. G. K., KIKUCHI, T., MANZANILLA-LOPEZ, R., PALOMARES-RIUS, J. E., WESEMAEL, W. M. L. & PERRY, R. N. 2013. Top 10 plant-parasitic nematodes in molecular plant pathology. *Molecular Plant Pathology,* 14**,** 946-961.

JONES, L., MILNE, J. L., ASHFORD, D. & MCQUEEN-MASON, S. J. 2003. Cell wall arabinan is essential for guard cell function. *Proceedings of the National Academy of Sciences of the United States of America,* 100**,** 11783-11788.

JONES, L., SEYMOUR, G. B. & KNOX, J. P. 1997. Localization of pectic galactan in tomato cell walls using a monoclonal antibody specific to (1->4)-beta-D-galactan. *Plant Physiology,* 113**,** 1405-1412.

JONES, M. G. K. 1981. Host-cell responses to endo-parasitic nematode attack - structure and function of giant-cells and syncytia. *Annals of Applied Biology,* 97**,** 353-&.

JONES, M. G. K. & GOTO, D. B. 2011. Root-knot Nematodes and Giant Cells. *Genomics and Molecular Genetics of Plant-Nematode Interactions***,** 83-100.

JONES, M. G. K. & PAYNE, H. L. 1978. Early stages of nematode-induced giant-cell formation in roots of *Impatiens balsamina*. *Journal of Nematology,* 10**,** 70-84.

JOSE-ESTANYOL, M. & PUIGDOMENECH, P. 2000. Plant cell wall glycoproteins and their genes. *Plant Physiology and Biochemistry,* 38**,** 97-108.

JUGE, N. 2006. Plant protein inhibitors of cell wall degrading enzymes. *Trends in Plant Science,* 11**,** 359-367.

KACZKOWSKI, J. 2003. Structure, function and metabolism of plant cell wall. *Acta Physiologiae Plantarum,* 25**,** 287-305.

KANT, U. & RAMANI, V. 1990. Insect induced plant galls in tissue-culture. *Proceedings of the Indian Academy of Sciences-Animal Sciences,* 99**,** 257-265.

KARSEN, G., WESEMAEL, W. & MOENS, M. 2013. Root-knot nematodes. *In:* PERRY, R.N. & MOENS, M. (eds) *Plant Nematology.* Oxfordshire, UK: CAB International.

KARSSEN, G. & MOENS, M. 2006. Root-knot nematodes. *In:* ERRY, R.N. & MOENS, M. (eds) *Plant Nematology.*

KARSSEN, G., WASEMAEL, W. & MOENS, M. 2013. Root-knot nematodes. *In:* PERRY, R. M., M. (ed.) *Plant Nematology.* Oxfordshire, UK: CABI.

KAUL, S., KOO, H. L., JENKINS, J., RIZZO, M., ROONEY, T., TALLON, L. J., FELDBLYUM, T., NIERMAN, W., BENITO, M. I., LIN, X. Y., TOWN, C. D., VENTER, J. C., FRASER, C. M., TABATA, S., NAKAMURA, Y., KANEKO, T., SATO, S., ASAMIZU, E., KATO, T., KOTANI, H., SASAMOTO, S., ECKER, J. R., THEOLOGIS, A., FEDERSPIEL, N. A., PALM, C. J., OSBORNE, B. I., SHINN, P., CONWAY, A. B., VYSOTSKAIA, V. S., DEWAR, K., CONN, L., LENZ, C. A., KIM, C. J., HANSEN, N. F., LIU, S. X., BUEHLER, E., ALTAFI, H., SAKANO, H., DUNN, P., LAM, B., PHAM, P. K., CHAO, Q., NGUYEN, M., YU, G. X., CHEN, H. M., SOUTHWICK, A., LEE, J. M., MIRANDA, M., TORIUMI, M. J., DAVIS, R. W., WAMBUTT, R., MURPHY, G., DUSTERHOFT, A., STIEKEMA, W., POHL, T., ENTIAN, K. D., TERRYN, N., VOLCKAERT, G., SALANOUBAT, M., CHOISNE, N., RIEGER, M., ANSORGE, W., UNSELD, M., FARTMANN, B., VALLE, G., ARTIGUENAVE, F., WEISSENBACH, J., QUETIER, F., WILSON, R. K., DE LA BASTIDE, M., SEKHON, M., HUANG, E., SPIEGEL, L., GNOJ, L., PEPIN, K., MURRAY, J., JOHNSON, D., HABERMANN, K., DEDHIA, N., PARNELL, L., PRESTON, R., HILLIER, L., CHEN, E., MARRA, M., MARTIENSSEN, R., MCCOMBIE, W. R., MAYER, K., WHITE, O., BEVAN, M., LEMCKE, K., CREASY, T. H., BIELKE, C., HAAS, B., HAASE, D., MAITI, R., RUDD, S., PETERSON, J., SCHOOF, H., FRISHMAN, D., MORGENSTERN, B., et al. 2000. Analysis of the genome sequence of the flowering plant *Arabidopsis thaliana*. *Nature,* 408**,** 796-815.

KELLER, B. 1993. Structural cell-wall proteins. *Plant Physiology,* 101**,** 1127-1130.

KIDO, N., YOKOYAMA, R., YAMAMOTO, T., FURUKAWA, J., IWAI, H., SATOH, S. & NISHITANI, K. 2015. The Matrix Polysaccharide (1;3,1;4)-beta-D-Glucan is Involved in Silicon-Dependent Strengthening of Rice Cell Wall (vol 56, pg 268, 2015). *Plant and Cell Physiology,* 56**,** 1679-1679.

KIELISZEWSKI, M. J., ONEILL, M., LEYKAM, J. & ORLANDO, R. 1995. Tandem mass-spectrometry and structural elucidation of glycopeptides from a hydroxyproline-rich plant-cell wall glycoprotein indicate that contiguous hydroxyproline residues are the major sites of hydroxyproline o-arabinosylation. *Journal of Biological Chemistry,* 270**,** 2541-2549.

KIEMLE, S. N., ZHANG, X., ESKER, A. R., TORIZ, G., GATENHOLM, P. & COSGROVE, D. J. 2014. Role of (1,3)(1,4)-beta-Glucan in Cell Walls: Interaction with Cellulose. *Biomacromolecules,* 15**,** 1727-1736.

KLEIN, D. 2002. Quantification using real-time PCR technology: applications and limitations. *Trends in Molecular Medicine,* 8**,** 257-260.

KLJUN, A., BENIANS, T. A. S., GOUBET, F., MEULEWAETER, F., KNOX, J. P. & BLACKBURN, R. S. 2011. Comparative Analysis of Crystallinity Changes in Cellulose I Polymers Using ATR-FTIR, X-ray Diffraction, and Carbohydrate-Binding Module Probes. *Biomacromolecules,* 12**,** 4121-4126.

KNOCH, E., DILOKPIMOL, A. & GESHI, N. 2014. Arabinogalactan proteins: focus on carbohydrate active enzymes. *Frontiers in Plant Science,* 5.

KNOX, J. P. 1992. Molecular probes for the plant-cell surface. *Protoplasma,* 167**,** 1-9.

KNOX, J. P. 1997. The use of antibodies to study the architecture and developmental regulation of plant cell walls. *In:* JEON, K. W. (ed.) *International Review of Cytology - a Survey of Cell Biology, Vol 171.*

KNOX, J. P. 2008. Revealing the structural and functional diversity of plant cell walls. *Current Opinion in Plant Biology,* 11**,** 308-313.

KNOX, J. P. 2012. In situ detection of cellulose with carbohydrate-binding modules. *In:* GILBERT, H. J. (ed.) *Cellulases.*

KNOX, J. P., DAY, S. & ROBERTS, K. 1989. A set of cell-surface glycoproteins forms an early marker of cell position, but not cell type, in the root apical meristem of *Daucus carota* L. *Development,* 106**,** 47-56.

KNOX, J. P., LINSTEAD, P. J., PEART, J., COOPER, C. & ROBERTS, K. 1991. Developmentally regulated epitopes of cell-surface arabinogalactan proteins and their relation to root-tissue pattern-formation. *Plant Journal,* 1**,** 317-326.

KNOX, J. P., PEART, J. & NEILL, S. J. 1995. Identification of novel cell, surface epitopes using a leaf epidermal-strip assay system. *Planta,* 196**,** 266-270.

KOENNING, S. R., KIRKPATRICK, T. L., STARR, J. L., WRATHER, J. A., WALKER, N. R. & MUELLER, J. D. 2004. Plant-parasitic nematodes attacking cotton in the United States - Old and emerging production challenges. *Plant Disease,* 88**,** 100-113.

KONG, Y., PENA, M. J., RENNA, L., AVCI, U., PATTATHIL, S., TUOMIVAARA, S. T., LI, X., REITER, W.-D., BRANDIZZI, F., HAHN, M. G., DARVILL, A. G., YORK, W. S. & O'NEILL, M. A. 2015. Galactose-depleted xyloglucan is dysfunctional and leads to dwarfism in Arabidopsis. *Plant Physiology,* 167**,** 1296-U294.

KONNO, H., NAKATO, T. & TSUMUKI, H. 2003. Altered matrix polysaccharides in cell walls of pocket galls formed by an aphid on *Distylium racemosum* leaves. *Plant Cell and Environment,* 26**,** 1973-1983.

KORAYEM, A. M., EL-BASSIOUNY, H. M. S., ABD EL-MONEM, A. A. & MOHAMED, M. M. M. 2012. Physiological and biochemical changes in different sugar beet genotypes infected with root-knot nematode. *Acta Physiologiae Plantarum,* 34**,** 1847-1861.

KUBISTA, M., ANDRADE, J. M., BENGTSSON, M., FOROOTAN, A., JONAK, J., LIND, K., SINDELKA, R., SJOBACK, R., SJOGREEN, B., STROMBOM, L., STAHLBERG, A. & ZORIC, N. 2006. The real-time polymerase chain reaction. *Molecular Aspects of Medicine,* 27**,** 95-125.

KUMADA, Y. 2014. Site-specific immobilization of recombinant antibody fragments through material-binding peptides for the sensitive detection of antigens in enzyme immunoassays. *Biochimica Et Biophysica Acta-Proteins and Proteomics,* 1844**,** 1960-1969.

KUMAR, M., CAMPBELL, L. & TURNER, S. 2016. Secondary cell walls: biosynthesis and manipulation. *Journal of Experimental Botany,* 67**,** 515-531.

KYNDT, T., GOVERSE, A., HAEGEMAN, A., WARMERDAM, S., WANJAU, C., JAHANI, M., ENGLER, G., DE ALMEIDA ENGLER, J. & GHEYSEN, G. 2016. Redirection of auxin flow in Arabidopsis thaliana roots after infection by root-knot nematodes. *Jornal of Experimental Bot*any, 67, 4559-4570.

KYNDT, T., VIEIRA, P., GHEYSEN, G. & DE ALMEIDA-ENGLER, J. 2013. Nematode feeding sites: unique organs in plant roots. *Planta,* 238**,** 807-818.

LAMPORT, D. T. A., KIELISZEWSKI, M. J., CHEN, Y. N. & CANNON, M. C. 2011. Role of the Extensin Superfamily in Primary Cell Wall Architecture. *Plant Physiology,* 156**,** 11-19.

LAO, N. T., LONG, D., KIANG, S., COUPLAND, G., SHOUE, D. A., CARPITA, N. C. & KAVANAGH, T. A. 2003. Mutation of a family 8 glycosyltransferase gene alters cell wall carbohydrate composition and causes a humidity-sensitive semi-sterile dwarf phenotype in Arabidopsis. *Plant Molecular Biology,* 53**,** 687-701.

LE FEVRE, R., EVANGELISTI, E., REY, T. & SCHORNACK, S. 2015. Modulation of Host Cell Biology by Plant Pathogenic Microbes. *In:* SCHEKMAN, R. (ed.) *Annual Review of Cell and Developmental Biology, Vol 31.*

LEE, C., ZHONG, R., RICHARDSON, E. A., HIMMELSBACH, D. S., MCPHAIL, B. T. & YE, Z.-H. 2007a. The PARVUS gene is expressed in cells undergoing secondary wall thickening and is essential for glucuronoxylan biosynthesis. *Plant and Cell Physiology,* 48**,** 1659-1672.

LEE, C. H., ZHONG, R. Q., RICHARDSON, E. A., HIMMELSBACH, D. S., MCPHAIL, B. T. & YE, Z. H. 2007b. The *PARVUS* gene is expressed in cells undergoing secondary wall thickening and is essential for glucuronoxylan biosynthesis. *Plant and Cell Physiology,* 48**,** 1659-1672.

LEE, H. & RASKIN, I. 1999. Purification, cloning, and expression of a pathogen inducible UDP-glucose: Salicylic acid glucosyltransferase from tobacco. *Journal of Biological Chemistry,* 274**,** 36637-36642.

LEE, K. J. D., MARCUS, S. E. & KNOX, J. P. 2011. Cell Wall Biology: Perspectives from cell wall imaging. *Molecular Plant,* 4**,** 212-219.

LEROUX, O., LEROUX, F., BAGNIEWSKA-ZADWORNA, A., KNOX, J. P., CLAEYS, M., BALS, S. & VIANE, R. L. L. 2011. Ultrastructure and composition of cell wall appositions in the roots of Asplenium (Polypodiales). *Micron,* 42**,** 863-870.

LEROUX, O., SORENSEN, I., MARCUS, S. E., VIANE, R. L. L., WILLATS, W. G. T. & KNOX, J. P. 2015. Antibody-based screening of cell wall matrix glycans in ferns reveals taxon, tissue and cell-type specific distribution patterns. *Bmc Plant Biology,* 15.

LI, S. X. & SHOWALTER, A. M. 1996. Cloning and developmental/stress-regulated expression of a gene encoding a tomato arabinogalactan protein. *Plant Molecular Biology,* 32**,** 641-652.

LI, W., GUAN, Q., WANG, Z.-Y., WANG, Y. & ZHU, J. 2013. A Bi-Functional Xyloglucan Galactosyltransferase Is an Indispensable Salt Stress Tolerance Determinant in Arabidopsis. *Molecular Plant,* 6**,** 1344-1354.

LI, Y., FESTER, T. & TAYLOR, C. G. 2009. Transcriptomic Analysis of Nematode Infestation. *In:* BERG, R. H. & TAYLOR, C. G. (eds.) *Cell Biology of Plant Nematode Parasitism.*

LIEPMAN, A. H., WIGHTMAN, R., GESHI, N., TURNER, S. R. & SCHELLER, H. V. 2010. Arabidopsis - a powerful model system for plant cell wall research. *Plant Journal,* 61**,** 1107-1121.

LIONETTI, V. & METRAUX, J. P. 2014. Plant cell wall in pathogenesis, parasitism and symbiosis. *Frontiers in Plant Science,* 5.

LOUVET, R., CAVEL, E., GUTIERREZ, L., GUENIN, S., ROGER, D., GILLET, F., GUERINEAU, F. & PELLOUX, J. 2006. Comprehensive expression profiling of the pectin methylesterase gene family during silique development in Arabidopsis thaliana. *Planta,* 224**,** 782-791.

MADSON, M., DUNAND, C., LI, X. M., VERMA, R., VANZIN, G. F., CALPLAN, J., SHOUE, D. A., CARPITA, N. C. & REITER, W. D. 2003. The MUR3 gene of Arabidopsis encodes a xyloglucan galactosyltransferase that is evolutionarily related to animal exostosins. *Plant Cell,* 15**,** 1662-1670.

MAIA, V. C. & SILVA, L. O. 2016. Insect galls of Restinga de Marambaia (Barra de Guaratiba, Rio de Janeiro, RJ). *Brazilian journal of biology = Revista brasleira de biologia,* 76**,** 787-95.

MANFIELD, I. W., BERNAL, A. J., MOLLER, I., MCCARTNEY, I., RIESS, N. P., KNOX, J. P. & WILLATS, W. G. T. 2005. Re-engineering of the PAM1 phage display monoclonal antibody to produce a soluble, versatile anti-homogalacturonan scFv. *Plant Science,* 169**,** 1090-1095.

MANGEON, A., JUNQUEIRA, R. M. & SACHETTO-MARTINS, G. 2010. Functional diversity of the plant glycine-rich proteins superfamily. *Plant signaling & behavior,* 5**,** 99-104.

MARCUS, S. E., BLAKE, A. W., BENIANS, T. A. S., LEE, K. J. D., POYSER, C., DONALDSON, L., LEROUX, O., ROGOWSKI, A., PETERSEN, H. L., BORASTON, A., GILBERT, H. J., WILLATS, W. G. T. & KNOX, J. P. 2010. Restricted access of proteins to mannan polysaccharides in intact plant cell walls. *Plant Journal,* 64**,** 191-203.

MARCUS, S. E., VERHERTBRUGGEN, Y., HERVÉ, C., ORDAZ-ORTIZ, J. J., FARKAS, V., PEDERSEN, H. L., WILLATS, W. G. T. & KNOX, J. P. 2008. Pectic homogalacturonan masks abundant sets of xyloglucan epitopes in plant cell walls. *Bmc Plant Biology,* 8, 60.

MAROWA, P., DING, A. & KONG, Y. 2016. Expansins: roles in plant growth and potential applications in crop improvement. *Plant Cell Reports,* 35**,** 949-965.

MARTIN, I., HERNANDEZ-NISTAL, J., ALBORNOS, L., LABRADOR, E. & DOPICO, B. 2013. beta III-Gal is Involved in Galactan Reduction During Phloem Element Differentiation in Chickpea Stems. *Plant and Cell Physiology,* 54**,** 960-970.

MCCARTNEY, L., MARCUS, S. E. & KNOX, J. P. 2005. Monoclonal antibodies to plant cell wall xylans and arabinoxylans. *Journal of Histochemistry & Cytochemistry,* 53**,** 543-546.

MCCARTNEY, L., STEELE-KING, C. G., JORDAN, E. & KNOX, J. P. 2003. Cell wall pectic (1 -> 4)-beta-D-galactan marks the acceleration of cell elongation in the Arabidopsis seedling root meristem. *Plant Journal,* 33**,** 447-454.

MCFARLANE, H. E., DORING, A. & PERSSON, S. 2014. The Cell Biology of Cellulose Synthesis. *In:* MERCHANT, S. S. (ed.) *Annual Review of Plant Biology, Vol 65.* Palo Alto: Annual Reviews.

MCNEIL, M., DARVILL, A. G., FRY, S. C. & ALBERSHEIM, P. 1984. Structure and function of the primary-cell walls of plants. *Annual Review of Biochemistry,* 53**,** 625-663.

MEIKLE, P. J., HOOGENRAAD, N. J., BONIG, I., CLARKE, A. E. & STONE, B. A. 1994a. A (1- 3,1- 4)-beta-glucan-specific monoclonal-antibody and its use in the quantitation and immunocyto-chemical location of (1- 3,1- 4)-beta-glucans. *Plant Journal,* 5**,** 1-9.

MEIKLE, P. J., HOOGENRAAD, N. J., BONIG, I., CLARKE, A. E. & STONE, B. A. 1994b. A (1-]3,1-]4)-Beta-Glucan-Specific Monoclonal-Antibody and Its Use in the Quantitation and Immunocyto-Chemical Location of (1-]3,1-]4)-Beta-Glucans. *Plant Journal,* 5**,** 1-9.

MELLEROWICZ, E. J. & SUNDBERG, B. 2008. Wood cell walls: biosynthesis, developmental dynamics and their implications for wood properties. *Current Opinion in Plant Biology,* 11**,** 293-300.

MELLEROWICZ, E. J., BAUCHER, M., SUNDBERG, B. & BOERJAN, W. 2001. Unravelling cell wall formation in the woody dicot stem. *Plant Molecular Biology,* 47**,** 239-274.

MENDGEN, K., HAHN, M. & DEISING, H. 1996. Morphogenesis and mechanisms of penetration by plant pathogenic fungi. *Annual Review of Phytopathology,* 34**,** 367-386.

MICHELI, F. 2001. Pectin methylesterases: cell wall enzymes with important roles in plant physiology. *Trends in Plant Science,* 6**,** 414-419.

MIKSHINA, P. V., PETROVA, A. A. & GORSHKOVA, T. A. 2015. Functional diversity of rhamnogalacturonans I. *Russian Chemical Bulletin,* 64**,** 1014-1023.

MITREVA-DAUTOVA, M., ROZE, E., OVERMARS, H., DE GRAAFF, L., SCHOTS, A., HELDER, J., GOVERSE, A., BAKKER, J. & SMANT, G. 2006. A symbiont-independent endo-1,4-beta-xylanase from the plant-parasitic nematode *Meloidogyne incognita*. *Molecular Plant-Microbe Interactions,* 19**,** 521-529.

MOENS, M., PERRY, R. N. & STARR, J. L. 2010. *Meloidogyne* Species - a Diverse Group of Novel and Important Plant Parasites. *Root-Knot Nematodes***,** 1-17.

MOHNEN, D. 2008. Pectin structure and biosynthesis. *Curr Opin Plant Biol,* 11**,** 266-77.

MOLLER, I., MARCUS, S. E., HAEGER, A., VERHERTBRUGGEN, Y., VERHOEF, R., SCHOLS, H., ULVSKOV, P., MIKKELSEN, J. D., KNOX, J. P. & WILLATS, W. 2008. High-throughput screening of monoclonal antibodies against plant cell wall glycans by hierarchical clustering of their carbohydrate microarray binding profiles. *Glycoconjugate Journal,* 25**,** 37-48.

MOLLER, S. G., URWIN, P. E., ATKINSON, H. J. & MCPHERSON, M. J. 1998. Nematode-induced expression of atao1, a gene encoding an extracellular diamine oxidase associated with developing vascular tissue. *Physiological and Molecular Plant Pathology,* 53**,** 73-79.

MOORE, J. P., FARRANT, J. M. & DRIOUICH, A. 2008. A role for pectin-associated arabinans in maintaining the flexibility of the plant cell wall during water deficit stress. *Plant Signaling & Behavior,* 3**,** 102-4.

MULLER, C. & RIEDERER, M. 2005. Plant surface properties in chemical ecology. *Journal of Chemical Ecology,* 31**,** 2621-2651.

MUNOZ-BERTOMEU, J. & LORENCES, E. P. 2014. Changes in xyloglucan endotransglucosylase/hydrolase (XTHs) expression and XET activity during apple fruit infection by Penicillium expansum Link. A. *European Journal of Plant Pathology,* 138**,** 273-282.

MURUGESAN, Y. K., PASINI, D. & REY, A. D. 2015. Self-assembly Mechanisms in Plant Cell Wall Components. *Journal of Renewable Materials,* 3**,** 56-72.

MUTWIL, M., DEBOLT, S. & PERSSON, S. 2008. Cellulose synthesis: a complex complex. *Current Opinion in Plant Biology,* 11**,** 252-257.

NAKHAMCHIK, A., ZHAO, Z. Y., PROVART, N. J., SHIU, S. H., KEATLEY, S. K., CAMERON, R. K. & GORING, D. R. 2004. A comprehensive expression analysis of the Arabidopsis proline-rich extensin-like receptor kinase gene family using bioinformatic and experimental approaches. *Plant and Cell Physiology,* 45**,** 1875-1881.

NGUEMA-ONA, E., COIMBRA, S., VICRE-GIBOUIN, M., MOLLET, J. C. & DRIOUICH, A. 2012. Arabinogalactan proteins in root and pollen-tube cells: distribution and functional aspects. *Annals of Botany,* 110**,** 383-404.

NGUEMA-ONA, E., VICRE-GIBOUIN, M., CANNESAN, M.-A. & DRIOUICH, A. 2013. Arabinogalactan proteins in root-microbe interactions. *Trends in Plant Science,* 18**,** 440-9.

NICHOLAS, W. L. 1984. *The Biology of Free Living Nematodes*, Clarendon press, Oxford.

NOBRE, M. J. G. & EVANS, K. 1998. Plant and nematode surfaces: Their structure and importance in host-parasite interactions. *Nematologica,* 44**,** 103-124.

NORTHCOTE, D. H., DAVEY, R. & LAY, J. 1989. Use of antisera to localize callose, xylan and arabinogalactan in the cell-plate, primary and secondary walls of plant-cells. *Planta,* 178**,** 353-366.

NOTHNAGEL, E. A. 1997. Proteoglycans and related components in plant cells. *In:* JEON, K. W. (ed.) *International Review of Cytology - a Survey of Cell Biology, Vol 174.*

O'NEILL, M. A., ISHII, T., ALBERSHEIM, P. & DARVILL, A. G. 2004. Rhamnogalacturonan II: Structure and function of a borate cross-linked cell wall pectic polysaccharide. *Annual Review of Plant Biology,* 55**,** 109-139.

PABST, M., FISCHL, R. M., BRECKER, L., MORELLE, W., FAULAND, A., KOFELER, H., ALTMANN, F. & LEONARD, R. 2013. Rhamnogalacturonan II structure shows variation in the side chains monosaccharide composition and methylation status within and across different plant species. *Plant Journal,* 76**,** 61-72.

PATOVA, O. A., GOLOVCHENKO, V. V. & OVODOV, Y. S. 2014. Pectic polysaccharides: structure and properties. *Russian Chemical Bulletin,* 63**,** 1901-1924.

PATTATHIL, S., AVCI, U., BALDWIN, D., SWENNES, A. G., MCGILL, J. A., POPPER, Z., BOOTTEN, T., ALBERT, A., DAVIS, R. H., CHENNAREDDY, C., DONG, R. H., O'SHEA, B., ROSSI, R., LEOFF, C., FRESHOUR, G., NARRA, R., O'NEIL, M., YORK, W. S. & HAHN, M. G. 2010. A Comprehensive Toolkit of Plant Cell Wall Glycan-Directed Monoclonal Antibodies. *Plant Physiology,* 153**,** 514-525.

PAULY, M., GILLE, S., LIU, L., MANSOORI, N., DE SOUZA, A., SCHULTINK, A. & XIONG, G. 2013. Hemicellulose biosynthesis. *Planta,* 238**,** 627-642.

PAULY, M. & KEEGSTRA, K. 2016. Biosynthesis of the Plant Cell Wall Matrix Polysaccharide Xyloglucan. *In:* MERCHANT, S. S. (ed.) *Annual Review of Plant Biology, Vol 67.*

PEDERSEN, H. L., FANGEL, J. U., MCCLEARY, B., RUZANSKI, C., RYDAHL, M. G., RALET, M.-C., FARKAS, V., VON SCHANTZ, L., MARCUS, S. E., ANDERSEN, M. C. F., FIELD, R., OHLIN, M., KNOX, J. P., CLAUSEN, M. H. & WILLATS, W. G. T. 2012. Versatile High Resolution Oligosaccharide Microarrays for Plant Glycobiology and Cell Wall Research. *Journal of Biological Chemistry,* 287.

PENNELL, R. I., KNOX, J. P., SCOFIELD, G. N., SELVENDRAN, R. R. & ROBERTS, K. 1989. A family of abundant plasma-membrane associated glycoproteins related to the arabinogalactan proteins is unique to flowering plants. *Journal of Cell Biology,* 108**,** 1967-1977.

PEREIRA, A. M., PEREIRA, L. G. & COIMBRA, S. 2015. Arabinogalactan proteins: rising attention from plant biologists. *Plant Reproduction,* 28**,** 1-15.

PEREZ, S., RODRIGUEZ-CARVAJAL, M. A. & DOCO, T. 2003. A complex plant cell wall polysaccharide: rhamnogalacturonan II. A structure in quest of a function. *Biochimie,* 85**,** 109-121.

PERRY, R. N. & CLARKE, A. J. 1981. Hatching mechanisms of nematodes. *Parasitology,* 83**,** 435-449.

PERRY, R. N. & MOENS, M. 2013. Plant nematology. *Plant Nematology 2nd edition***,** 542-542. Oxfordshire, UK: CAB International.

PERRY, R. N., MOENS, M. & STARR, J. L. 2010. Root-knot Nematodes *Root-Knot Nematodes***,** Oxfordshire, UK: CAB International.

PERRY, R. N. & WESEMAEL, W. M. L. 2008. Host plant effects on hatching of root-knot nematodes. *Russian Journal of Nematology,* 16**,** 1-5.

PILARSKA, M., KNOX, J. P. & KONIECZNY, R. 2013. Arabinogalactan-protein and pectin epitopes in relation to an extracellular matrix surface network and somatic embryogenesis and callogenesis in *Trifolium nigrescens* Viv. *Plant Cell Tissue and Organ Culture,* 115**,** 35-44.

PLANCOT, B., SANTAELLA, C., JABER, R., KIEFER-MEYER, M. C., FOLLET-GUEYE, M. L., LEPRINCE, J., GATTIN, I., SOUC, C., DRIOUICH, A. & VICRE-GIBOUIN, M. 2013. Deciphering the Responses of Root Border-Like Cells of Arabidopsis and Flax to Pathogen-Derived Elicitors. *Plant Physiology,* 163**,** 1584-1597.

PLOEG, A. T. & MARIS, P. C. 1999. Effects of temperature on the duration of the life cycle of a *Meloidogyne incognita* population. *Nematology,* 1**,** 389-393.

PROT, J. C. & VAN GUNDY, S. D. 1981. Effect of soil texture and the clay component on migration of *Meloidogyne incognita* 2nd-stage juveniles. *Journal of Nematology,* 13**,** 213-217.

PUHLMANN, J., BUCHELI, E., SWAIN, M. J., DUNNING, N., ALBERSHEIM, P., DARVILL, A. G. & HAHN, M. G. 1994. Generation of monoclonal-antibodies against plant cell-wall polysaccharides .1. Characterization of a monoclonal-antibody to a terminal alpha-(1- 2)-linked fucosyl-containing epitope. *Plant Physiology,* 104**,** 699-710.

QIN, L., KUDLA, U., ROZE, E. H. A., GOVERSE, A., POPEIJUS, H., NIEUWLAND, J., OVERMARS, H., JONES, J. T., SCHOTS, A., SMANT, G., BAKKER, J. & HELDER, J. 2004. Plant degradation: A nematode expansin acting on plants. *Nature,* 427**,** 30-30.

QUIST, C. W., SMANT, G. & HELDER, J. 2015. Evolution of Plant Parasitism in the Phylum Nematoda. *In:* VANALFEN, N. K. (ed.) *Annual Review of Phytopathology, Vol 53.* Palo Alto: Annual Reviews.

RADONIC, A., THULKE, S., MACKAY, I. M., LANDT, O., SIEGERT, W. & NITSCHE, A. 2004. Guideline to reference gene selection for quantitative real-time PCR. *Biochemical and Biophysical Research Communications,* 313**,** 856-862.

RAMAN, A. 2011. Morphogenesis of insect-induced plant galls: facts and questions. *Flora,* 206**,** 517-533.

RAMAN, A., BEIDERBECK, R. & HERTH, W. 2009. Early subcellular responses of susceptible and resistant Vitis taxa to feeding by grape phylloxera Daktulosphaira vitifoliae. *Botanica Helvetica,* 119**,** 31-39.

RASMANN, S., ALI, J. G., HELDER, J. & VAN DER PUTTEN, W. H. 2012. Ecology and Evolution of Soil Nematode Chemotaxis. *Journal of Chemical Ecology,* 38**,** 615-628.

RASOOLY, A. & HEROLD, K. E. 2008. Food microbial pathogen detection and analysis using DNA microarray technologies. *Foodborne Pathogens and Disease,* 5**,** 531-550.

REDONDO, M. A., PEREZ-SIERRA, A., ABAD-CAMPOS, P., TORRES, L., SOLLA, A., REIG-ARMINANA, J. & GARCIA-BREIJO, F. 2015. Histology of *Quercus ilex* roots during infection by *Phytophthora cinnamomi.* *Trees-Structure and Function,* 29**,** 1943-1957.

REID, J. S. G. 1985. Cell-wall storage carbohydrates in seeds - biochemistry of the seed gums and hemicelluloses. *Advances in Botanical Research Incorporating Advances in Plant Pathology,* 11**,** 125-155.

REIS, D. & VIAN, B. 2004. Helicoidal pattern in secondary cell walls and possible role of xylans in their construction. *Comptes Rendus Biologies,* 327**,** 785-790.

REITER, W. D. 2002. Biosynthesis and properties of the plant cell wall. *Current Opinion in Plant Biology,* 5**,** 536-542.

REITER, W. D., CHAPPLE, C. & SOMERVILLE, C. R. 1997. Mutants of *Arabidopsis thaliana* with altered cell wall polysaccharide composition. *Plant Journal,* 12**,** 335-345.

RENNIE, E. A. & SCHELLER, H. V. 2014. Xylan biosynthesis. *Current Opinion in Biotechnology,* 26**,** 100-107.

RIDLEY, B. L., O'NEILL, M. A. & MOHNEN, D. A. 2001. Pectins: structure, biosynthesis, and oligogalacturonide-related signaling. *Phytochemistry,* 57**,** 929-967.

ROBERTS, K. & SHIRSAT, A. H. 2006. Increased extensin levels in Arabidopsis affect inflorescence stem thickening and height. *Journal of Experimental Botany,* 57**,** 537-545.

RODRIGUEZ-GACIO, M. D. C., IGLESIAS-FERNANDEZ, R., CARBONERO, P. & MATILLA, A. J. 2012. Softening-up mannan-rich cell walls. *Journal of Experimental Botany,* 63**,** 3975-3988.

SANTIAGO, R., BARROS-RIOS, J. & MALVAR, R. A. 2013. Impact of Cell Wall Composition on Maize Resistance to Pests and Diseases. *International Journal of Molecular Sciences,* 14**,** 6960-6980.

SANTNER, A. & ESTELLE, M. 2009. Recent advances and emerging trends in plant hormone signalling. *Nature,* 459**,** 1071-1078.

SCHELLER, H. V., JENSEN, J. K., SORENSEN, S. O., HARHOLT, J. & GESHI, N. 2007. Biosynthesis of pectin. *Physiologia Plantarum,* 129**,** 283-295.

SCHELLER, H. V. & ULVSKOV, P. 2010. Hemicelluloses. *In:* MERCHANT, S., BRIGGS, W. R. & ORT, D. (eds.) *Annual Review of Plant Biology, Vol 61.*

SCHULTZ, C. J., JOHNSON, K. L., CURRIE, G. & BACIC, A. 2000. The classical arabinogalactan protein gene family of arabidopsis. *Plant Cell,* 12**,** 1751-1767.

SCHULTZ, C. J., RUMSEWICZ, M. P., JOHNSON, K. L., JONES, B. J., GASPAR, Y. M. & BACIC, A. 2002. Using genomic resources to guide research directions. The arabinogalactan protein gene family as a test case. *Plant Physiology,* 129**,** 1448-1463.

SCHULZE-LEFERT, P. & VOGEL, J. 2000. Closing the ranks to attack by powdery mildew. *Trends in Plant Science,* 5**,** 343-348.

SEIFERT, G. J. & ROBERTS, K. 2007. The biology of arabinogalactan proteins. *Annual Review of Plant Biology.*

SENECHAL, F., WATTIER, C., RUSTERUCCI, C. & PELLOUX, J. 2014. Homogalacturonan-modifying enzymes: structure, expression, and roles in plants. *Journal of Experimental Botany,* 65**,** 5125-5160.

SEVERGNINI, M., CREMONESI, P., CONSOLANDI, C., DE BELLIS, G. & CASTIGLIONI, B. 2011. Advances in DNA microarray technology for the detection of foodborne pathogens. *Food and Bioprocess Technology,* 4**,** 936-953.

SHAO, M. H., ZHENG, H. Q., HU, Y., LIU, D. H., JANG, J. C., MA, H. & HUANG, H. 2004. The GAOLAOZHUANGREN1 gene encodes a putative glycosyltransferase that is critical for normal development and carbohydrate metabolism. *Plant and Cell Physiology,* 45**,** 1453-1460.

SHORTHOUSE, J. D., WOOL, D. & RAMAN, A. 2005. Gall-inducing insects - Nature's most sophisticated herbivores. *Basic and Applied Ecology,* 6**,** 407-411.

SHOWALTER, A. M. 1993. Structure and function of plant-cell wall proteins. *Plant Cell,* 5**,** 9-23.

SHOWALTER, A. M. 2001. Arabinogalactan-proteins: structure, expression and function. *Cellular and Molecular Life Sciences,* 58**,** 1399-1417.

SHOWALTER, A. M., KEPPLER, B., LICHTENBERG, J., GU, D. Z. & WELCH, L. R. 2010. A bioinformatics approach to the identification, classification, and analysis of hydroxyproline-rich glycoproteins. *Plant Physiology,* 153**,** 485-513.

SILVA, N. F. & GORING, D. R. 2002. The proline-rich, extensin-like receptor kinase-1 (PERK1) gene is rapidly induced by wounding. *Plant Molecular Biology,* 50**,** 667-685.

SLABAUGH, E., DAVIS, J. K., HAIGLER, C. H., YINGLING, Y. G. & ZIMMER, J. 2014. Cellulose synthases: new insights from crystallography and modeling. *Trends in Plant Science,* 19**,** 99-106.

SMALLWOOD, M., BEVEN, A., DONOVAN, N., NEILL, S. J., PEART, J., ROBERTS, K. & KNOX, J. P. 1994. Localization of cell-wall proteins in relation to the developmental anatomy of the carrot root apex. *Plant Journal,* 5**,** 237-246.

SMALLWOOD, M., MARTIN, H. & KNOX, J. P. 1995. An epitope of rice threonine-rich and hydroxyproline-rich glycoprotein is common to cell-wall and hydrophobic plasma-membrane glycoproteins. *Planta,* 196**,** 510-522.

SMALLWOOD, M., YATES, E. A., WILLATS, W. G. T., MARTIN, H. & KNOX, J. P. 1996. Immunochemical comparison of membrane-associated and secreted arabinogalactan-proteins in rice and carrot. *Planta,* 198**,** 452-459.

SNYDER, D. W., OPPERMAN, C. H. & BIRD, D. M. 2006. A method for generating *Meloidogyne incognita* males. *Journal of Nematology,* 38**,** 192-194.

SPADONI, S., ZABOTINA, O., DI MATTEO, A., MIKKELSEN, J. D., CERVONE, F., DE LORENZO, G., MATTEI, B. & BELLINCAMPI, D. 2006. Polygalacturonase-inhibiting protein interacts with pectin through a binding site formed by four clustered residues of arginine and lysine. *Plant Physiology,* 141**,** 557-564.

STACEY, N. J., ROBERTS, K. & KNOX, J. P. 1990. Patterns of expression of the jim4 arabinogalactan-protein epitope in cell-cultures and during somatic embryogenesis in *Daucus carota* L. *Planta,* 180**,** 285-292.

STRANGE, K. 2006. *C. elegans* - Methods and applications - Preface. *In:* STRANGE, K. (ed.) *Methods in Molecular Biology.*

TATTERSALL, F. H., NOWELL, F. & SMITH, R. H. 1994. A review of the endoparasites of wild house mice *Mus domesticus*. *Mammal Review,* 24**,** 61-71.

TAYLOR, C. M., KARUNARATNE, C. V. & XIE, N. 2012. Glycosides of hydroxyproline: Some recent, unusual discoveries. *Glycobiology,* 22**,** 757-767.

TAYLOR, N. G. 2008. Cellulose biosynthesis and deposition in higher plants. *New Phytologist,* 178**,** 239-252.

TEDMAN-JONES, J. D., LEI, R., JAY, F., FABRO, G., LI, X., REITER, W.-D., BREARLEY, C. & JONES, J. D. G. 2008. Characterization of Arabidopsis mur3 mutations that result in constitutive activation of defence in petioles, but not leaves. *Plant Journal,* 56**,** 691-703.

TENG, X. K. & XIAO, H. S. 2009. Perspectives of DNA microarray and next-generation DNA sequencing technologies. *Science in China Series C-Life Sciences,* 52**,** 7-16.

THE ARABIDOPSIS INFORMATION, R. 2011. Arabidopsis assembly project. *European Nucleotide Archive*.

TORRES, M. A. 2010. ROS in biotic interactions. *Physiologia Plantarum,* 138**,** 414-429.

TRIANTAPHYLLOU, A. 1973. Environmental sex differentiation of nematodes in relation to pest management. *Annual Review of Phytopathology,* 11**,** 441-462.

TRUDGILL, D. L. & BLOK, V. C. 2001. Apomictic, polyphagous root-knot nematodes: Exceptionally successful and damaging biotrophic root pathogens. *Annual Review of Phytopathology,* 39**,** 53-77.

TURNER, S. J. & ROWE, J. A. 2006. Cyst Nematodes. *Plant Nematology***,** 91-122.

UNDERWOOD, W. 2012. The plant cell wall: a dynamic barrier against pathogen invasion. *Frontiers in Plant Science,* 3.

VALLARINO, J. G. & OSORIO, S. 2012. Signaling role of oligogalacturonides derived during cell wall degradation. *Plant Signaling & Behavior,* 7**,** 1447-9.

VARNER, J. E. & LIN, L. S. 1989. Plant-cell wall architecture. *Cell,* 56**,** 231-239.

VEGA-SANCHEZ, M. E., VERHERTBRUGGEN, Y., SCHELLER, H. V. & RONALD, P. C. 2013. Abundance of mixed linkage glucan in mature tissues and secondary cell walls of grasses. *Plant Signaling & Behavior,* 8**,** e23143-e23143.

VELASQUEZ, S. M., RICARDI, M. M., DOROSZ, J. G., FERNANDEZ, P. V., NADRA, A. D., POL-FACHIN, L., EGELUND, J., GILLE, S., HARHOLT, J., CIANCIA, M., VERLI, H., PAULY, M., BACIC, A., OLSEN, C. E., ULVSKOV, P., PETERSEN, B. L., SOMERVILLE, C., IUSEM, N. D. & ESTEVEZ, J. M. 2011. O-glycosylated cell wall proteins are essential in root hair growth. *Science,* 332**,** 1401-1403.

VERHERTBRUGGEN, Y., MARCUS, S. E., CHEN, J. & KNOX, J. P. 2013. Cell wall pectic arabinans influence the mechanical properties of *Arabidopsis thaliana* inflorescence stems and their response to mechanical stress. *Plant and Cell Physiology,* 54**,** 1278-1288.

VERHERTBRUGGEN, Y., MARCUS, S. E., HAEGER, A., ORDAZ-ORTIZ, J. J. & KNOX, J. P. 2009a. An extended set of monoclonal antibodies to pectic homogalacturonan. *Carbohydrate Research,* 344**,** 1858-1862.

VERHERTBRUGGEN, Y., MARCUS, S. E., HAEGER, A., VERHOEF, R., SCHOLS, H. A., MCCLEARY, B. V., MCKEE, L., GILBERT, H. J. & KNOX, J. P. 2009b. Developmental complexity of arabinan polysaccharides and their processing in plant cell walls. *Plant Journal,* 59**,** 413-425.

VIDAL, S., DOCO, T., WILLIAMS, P., PELLERIN, P., YORK, W. S., O'NEILL, M. A., GLUSHKA, J., DARVILL, A. G. & ALBERSHEIM, P. 2000. Structural characterization of the pectic polysaccharide rhamnogalacturonan II: evidence for the backbone location of the aceric acid-containing oligoglycosyl side chain. *Carbohydrate Research,* 326**,** 277-294.

VIGLIERCHIO, D.R. 1971. Nematodes and other pathogens in auxin-related plant-growth disorders. *Botanical Review,* 37**,** 1-21.

VOGEL, J. 2008. Unique aspects of the grass cell wall. *Current Opinion in Plant Biology,* 11**,** 301-307.

VOGEL, J. & SOMERVILLE, S. 2000. Isolation and characterization of powdery mildew-resistant Arabidopsis mutants. *Proceedings of the National Academy of Sciences of the United States of America,* 97**,** 1897-1902.

VOGEL, J. P., RAAB, T. K., SCHIFF, C. & SOMERVILLE, S. C. 2002. PMR6, a pectate lyase-like gene required for powdery mildew susceptibility in Arabidopsis. *Plant Cell,* 14**,** 2095-2106.

VOGEL, J. P., RAAB, T. K., SOMERVILLE, C. R. & SOMERVILLE, S. C. 2004. Mutations in PMR5 result in powdery mildew resistance and altered cell wall composition. *Plant Journal,* 40**,** 968-978.

VON MENDE, N. 1997. Migration behavior of root-knot nematodes in roots. *Journal of Nematology,* 29**,** 611-611.

VORWERK, S., SOMERVILLE, S. & SOMERVILLE, C. 2004. The role of plant cell wall polysaccharide composition in disease resistance. *Trends in Plant Science,* 9**,** 203-209.

VOVLAS, N., RAPOPORT, H. F., JIMENEZ DIAZ, R. M. & CASTILLO, P. 2005. Differences in Feeding sites induced by root-knot nematodes, *Meloidogyne* spp., in chickpea. *Phytopathology,* 95**,** 368-75.

WANG, M., HEIMOVAARADIJKSTRA, S., VANDERMEULEN, R. M., KNOX, J. P. & NEILL, S. J. 1995. The monoclonal-antibody jim19 modulates abscisic-acid action in barley aleurone protoplasts. *Planta,* 196**,** 271-276.

WANG, Y., MORTIMER, J. C., DAVIS, J., DUPREE, P. & KEEGSTRA, K. 2013. Identification of an additional protein involved in mannan biosynthesis. *Plant Journal,* 73**,** 105-117.

WEFERS, D., TYL, C. E. & BUNZEL, M. 2014. Novel arabinan and galactan oligosaccharides from dicotyledonous plants. *Frontiers in chemistry,* 2**,** 100-100.

WEI, H., XU, Q., TAYLOR, L. E., II, BAKER, J. O., TUCKER, M. P. & DING, S.-Y. 2009. Natural paradigms of plant cell wall degradation. *Current Opinion in Biotechnology,* 20**,** 330-338.

WESEMAEL, W. M. L., PERRY, R. N. & MOENS, M. 2006. The influence of root diffusate and host age on hatching of the root-knot nematodes, *Meloidogyne chitwoodi* and *M.fallax*. *Nematology,* 8**,** 895-902.

WHITEFORD, J. R. & SPANU, P. D. 2002. Hydrophobins and the interactions between fungi and plants. *Molecular Plant Pathology,* 3**,** 391-400.

WIECZOREK, K., GOLECKI, B., GERDES, L., HEINEN, P., SZAKASITS, D., DURACHKO, D. M., COSGROVE, D. J., KREIL, D. P., PUZIO, P. S., BOHLMANN, H. & GRUNDLER, F. M. W. 2006. Expansins are involved in the formation of nematode-induced syncytia in roots of *Arabidopsis thaliana*. *Plant Journal,* 48**,** 98-112.

WIELKOPOLAN, B. & OBREPALSKA-STEPLOWSKA, A. 2016. Three-way interaction among plants, bacteria, and coleopteran insects. *Planta,* 244**,** 313-332.

WIGGERS, R. J., STARR, J. L. & PRICE, H. J. 1990. DNA content and variation in chromosome-number in plant-cells affected by *Meloidogyne incognita* and *M. arenaria*. *Phytopathology,* 80**,** 1391-1395.

WILLATS, W. G. T., GILMARTIN, P. M., MIKKELSEN, J. D. & KNOX, J. P. 1999. Cell wall antibodies without immunization: generation and use of de-esterified homogalacturonan block-specific antibodies from a naive phage display library. *Plant Journal,* 18**,** 57-65.

WILLATS, W. G. T., MARCUS, S. E. & KNOX, J. P. 1998. Generation of a monoclonal antibody specific to (1 -> 5)-alpha-L-arabinan. *Carbohydrate Research,* 308**,** 149-152.

WILLATS, W. G. T., MCCARTNEY, L. & KNOX, J. P. 2001a. In-situ analysis of pectic polysaccharides in seed mucilage and at the root surface of *Arabidopsis thaliana*. *Planta,* 213**,** 37-44.

WILLATS, W. G. T., MCCARTNEY, L., MACKIE, W. & KNOX, J. P. 2001b. Pectin: cell biology and prospects for functional analysis. *Plant Molecular Biology,* 47**,** 9-27.

WILLATS, W. G. T., MCCARTNEY, L., STEELE-KING, C. G., MARCUS, S. E., MORT, A., HUISMAN, M., VAN ALEBEEK, G. J., SCHOLS, H. A., VORAGEN, A. G. J., LE GOFF, A., BONNIN, E., THIBAULT, J. F. & KNOX, J. P. 2004. A xylogalacturonan epitope is specifically associated with plant cell detachment. *Planta,* 218**,** 673-681.

WILLATS, W. G. T., STEELE-KING, C. G., MCCARTNEY, L., ORFILA, C., MARCUS, S. E. & KNOX, J. P. 2000. Making and using antibody probes to study plant cell walls. *Plant Physiology and Biochemistry,* 38**,** 27-36.

WILLIAMSON, V. M. & GLEASON, C. A. 2003. Plant-nematode interactions. *Current Opinion in Plant Biology,* 6**,** 327-333.

WOLF, S., MOUILLE, G. & PELLOUX, J. 2009. Homogalacturonan Methyl-Esterification and Plant Development. *Molecular Plant,* 2**,** 851-860.

WYSS, U. & GRUNDLER, F. M. W. 1992. Feeding-behavior of sedentary plant parasitic nematodes. *Netherlands Journal of Plant Pathology,* 98**,** 165-173.

XUE, J., BOSCH, M. & KNOX, J. P. 2013. Heterogeneity and Glycan Masking of Cell Wall Microstructures in the Stems of *Miscanthus giganteus*, and Its Parents *M. sinensis* and *M. sacchariflorus*. *Plos One,* 8.

YAN, A., WU, M. J., YAN, L. M., HU, R., ALI, I. & GAN, Y. B. 2014. AtEXP2 Is Involved in Seed Germination and Abiotic Stress Response in Arabidopsis. *PLoS One,* 9.

YATES, E. A., VALDOR, J. F., HASLAM, S. M., MORRIS, H. R., DELL, A., MACKIE, W. & KNOX, J. P. 1996. Characterization of carbohydrate structural features recognized by anti-arabinogalactan-protein monoclonal antibodies. *Glycobiology,* 6**,** 131-139.

YONG, W. D., LINK, B., O'MALLEY, R., TEWARI, J., HUNTER, C. T., LU, C. A., LI, X. M., BLEECKER, A. B., KOCH, K. E., MCCANN, M. C., MCCARTY, D. R., PATTERSON, S. E., REITER, W. D., STAIGER, C., THOMAS, S. R., VERMERRIS, W. & CARPITA, N. C. 2005. Genomics of plant cell wall biogenesis. *Planta,* 221**,** 747-751.

YOO, S. M. & LEE, S. Y. 2008. Diagnosis of pathogens using DNA microarray. *Recent patents on biotechnology,* 2**,** 124-9.

YOUSIF, G. M. 1979. Histological responses of 4 leguminous crops infected with M*eloidogyne incognita*. *Journal of Nematology,* 11**,** 395-401.

YU, Z., KANG, B., HE, X., LV, S., BAI, Y., DING, W., CHEN, M., CHO, H.-T. & WU, P. 2011. Root hair-specific expansins modulate root hair elongation in rice. *Plant Journal,* 66**,** 725-734.

ZABOTINA, O. A., AVCI, U., CAVALIER, D., PATTATHIL, S., CHOU, Y.-H., EBERHARD, S., DANHOF, L., KEEGSTRA, K. & HAHN, M. G. 2012. Mutations in multiple xxt genes of arabidopsis reveal the complexity of xyloglucan biosynthesis. *Plant Physiology,* 159**,** 1367-1384.

ZANDLEVEN, J., SORENSEN, S. O., HARHOLT, J., BELDMAN, G., SCHOLS, H. A., SCHELLER, H. V. & VORAGEN, A. J. 2007. Xylogalacturonan exists in cell walls from various tissues of *Arabidopsis thaliana*. *Phytochemistry,* 68**,** 1219-1226.

ZHANG, Z.-Q. 2013. Animal biodiversity: An update of classification and diversity in 2013. *Zootaxa,* 3703**,** 5-11.

ZHAO, M.-R., HAN, Y.-Y., FENG, Y.-N., LI, F. & WANG, W. 2012. Expansins are involved in cell growth mediated by abscisic acid and indole-3-acetic acid under drought stress in wheat. *Plant Cell Reports,* 31**,** 671-685.

ZHU, Y., PETTOLINO, F., MAU, S. L. & BACIC, A. 2005. Characterization of cell wall polysaccharides from the medicinal plant *Panax notoginseng*. *Phytochemistry,* 66**,** 1067-1076.

ZHU, Y. M., NAM, J., CARPITA, N. C., MATTHYSSE, A. G. & GELVIN, S. B. 2003. Agrobacterium-mediated root transformation is inhibited by mutation of an Arabidopsis cellulose synthase-like gene. *Plant Physiology,* 133**,** 1000-1010.